THE MOLECULAR MECHANISMS OF ORGANOPHOSPHORUS COMPOUND-INDUCED CYTOTOXICITY

Kent Richard Carlson

**Dissertation submitted to the Faculty of the
Virginia Polytechnic Institute and State University in
partial fulfillment of the requirements for the degree of**

DOCTOR OF PHILOSOPHY

in

Veterinary Medical Sciences

**Marion Ehrich, Co-Chairperson
Bernard S. Jortner, Co-Chairperson
Brad Klein
Jeff Bloomquist
Mitzi Nagarkatti**

**May 19th, 2000
Blacksburg, Virginia**

Keywords: Organophosphorus, SH-SY5Y, cytotoxicity, apoptosis

THE MOLECULAR MECHANISMS OF ORGANOPHOSPHORUS COMPOUND-INDUCED CYTOTOXICITY

Kent Richard Carlson

(ABSTRACT)

Certain organophosphorus compounds have the ability to induce a delayed neuropathic condition in sensitive species termed organophosphorus compound-induced delayed neurotoxicity (OPIDN). Esteratic changes associated with OPIDN have been successfully modeled *in vitro*. The physical characteristics of lesion development in OPIDN including the mode of nerve cell death, cytotoxic initiator and effector molecules, and cytoskeletal involvement have received little *in vitro* investigation. This dissertation evaluated the mode of cell death (apoptosis versus oncotic-necrosis), and cell cycle, cytoskeletal, nuclear, and mitochondrial alterations induced by OP compounds in SH-SY5Y cultures, an *in vitro* human neuroblastoma model. The distribution of *in vivo* neural degeneration in white Leghorn hen models was also assessed as a prelude to validating the mode of OP compound-induced *in vivo* neural cell death. These endpoints were evaluated by utilizing flow cytometry, spectrophotometry, gel electrophoresis, immunohistochemistry, light, and electron microscopy. Initial data gathered on culture parameters revealed that the mitotic status, basal rates of cell death, and total culture density were dependent on the condition of the media and the initial seeding density. Subsequent *in vitro* investigations used standardized culture conditions with OP compounds (diisopropylphosphorofluoridate (DFP), paraoxon, parathion, phenyl saligenin phosphate (PSP), tri-ortho-tolyl phosphate (TOTP), and triphenyl phosphite (TPPi); 1μM - 1mM). These studies revealed that OP compounds altered the cell cycle phase, decreased the amount of intracellular f-actin, altered the mitochondrial membrane potential, and induced caspase-3 activation and nuclear partitioning characteristic of apoptosis. The amount of change in these parameters was strongly dependent on the OP compound, the length of incubation time, and the presence of modulators of cytotoxicity such as phenylmethylsulfonyl fluoride (PMSF), carbachol, Ac-DEVD-CHO, Ac-IETD-CHO, and cyclosporin A. Preliminary *in vivo* experiments designed to validate *in vitro* results revealed neural degeneration involving fibers, terminals, and cell soma in spinal cord and brain tissue of PSP- and TPPi- exposed hens. The distribution and magnitude of these changes were contingent on the OP compound and length of time post-exposure. Subsequent experiments designed to evaluate the mode of cell death in these tissues revealed little evidence of either necrosis or apoptosis. These results, therefore, did not support or refute *in vitro* observations. Many OP compound-induced subcellular alterations have been demonstrated in our *in vitro* SH-SY5Y neuroblastoma model. Even though the mode of cell death observed in SH-SY5Y cells was not validated in *in vivo* experiments, *in vitro* observations nonetheless provide stimulating areas to further research the mechanisms of OPIDN and OP compound-induced cell death.

Funding for the research involved in this dissertation was provided by a Novartis - Society of Toxicology graduate student fellowship, US EPA grant R825356, and the Virginia-Maryland Regional College of Veterinary Medicine.

ACKNOWLEDGMENTS

I would like to express my sincerest gratitude to my advisors, Dr. Marion Ehrich and Dr. Bernard Jortner. Both have exhibited extreme patience, provided economic support, and taken the time to review critically all manuscripts and ideas associated with this project.

I would also like to thank other members of my committee, Dr. Jeff Bloomquist, Dr. Brad Klein, and Dr. Mitzi Nagarkatti for their guidance during proposal writing and for continual encouragement during my Ph.D. candidacy.

Finally, I would like to thank the Virginia-Maryland Regional College of Veterinary Medicine for funding (Departmental and US EPA R825356), technical support, and the liberty to work when and how I chose.

DECLARATION OF WORK PERFORMED

I declare that I, Kent Richard Carlson, performed all of the work reported in this dissertation except that which is reported below.

Cells for flow cytometry were collected and prepared by me and then given to Joan Kalnitsky for processing through the flow cytometer (Flow Cytometry Laboratory). Cells destined for ultrastructural observations were collected and fixed by me and then given to Kathy Lowe and Virginia Viers for embedding and sectioning (Ultrastructure Laboratory). Hen nervous system tissue destined for immunohistopathology was harvested by me, Linda Correll, and Jason Hunt (Toxicology Laboratory) and embedded and sectioned by Jill Songer (Histopathology Laboratory).

TABLE OF CONTENTS

i. ABSTRACT..... *ii*
ii. ACKNOWLEDGMENTS..... *iii*
iii. DECLARATION OF WORK PERFORMED..... *iv*
iv. TABLE OF CONTENTS..... *v*
v. LIST OF FIGURES..... *ix*
vi. LIST OF TABLES..... *xiv*
vii. ABBREVIATIONS..... *xvi*

PART I HYPOTHESIS

HYPOTHESIS

Hypothesis..... 2

PART II LITERATURE REVIEW

Chapter 1 LITERATURE REVIEW

A. History of Organophosphorus (OP) Compounds..... 9

B. Importance of OP Compounds in Our Daily Lives 10

C. Proposed Mechanisms of Toxicity Associated with OP Compounds

1. Cellular Toxicity Studies
Putative Serine Substrates..... 11
Viability..... 12
Nuclear Structure and Function..... 12
Mitochondrial Structure and Function..... 13
Enzyme Activity..... 14
Cytostructural Components..... 15
Summary..... 16

2. Whole Animal Studies
Acutely Toxic Effects..... 17
Delayed Neuropathic Effects..... 18
Chickens (*Gallus domesticus*)..... 19

Embryonic and Juvenile Chicks (*Gallus domesticus*)..... 22
Japanese Quail (*Coturnix coturnix*), Bobwhites (*Colinus virginianus*), Mallard Ducks (*Anas platyrhychos*), or Ring-necked Pheasants (*Phasianus colchicus*)..... 23
Summary..... 25

D. *In Vitro* SH-SY5Y Human Neuroblastoma Model
1. Morphology and Background..... 25
2. Receptors and Cell Signaling..... 26
3. Enzymes and Neurotransmitters..... 26
4. Nuclear Considerations..... 27
5. Cytoskeleton..... 27
6. Growth and Death..... 27
7. Differentiation..... 29
Summary..... 30

PART III MATERIALS AND METHODS

Chapter 2 Experimental Methods and Protocols..... 32

PART IV RESULTS

Chapter 3 Human Neuroblastoma Cell Viability and Growth are Affected by Altered Culture Conditions

Abstract..... 37
Introduction..... 38
Experimental Methods..... 40
Results 42
Discussion..... 46
References..... 50

Chapter 4 Organophosphorus Compounds Alter the Cell Cycle Phase of SH-SY5Y Human Neuroblastoma Cells

Abstract..... 62
Introduction..... 63
Experimental Methods..... 65
Results 66

Discussion..... 70
References..... 74

Chapter 5 Organophosphorus Compound-induced Modification of SH-SY5Y Human Neuroblastoma Mitochondrial Transmembrane Potential

Abstract..... 96
Introduction..... 97
Experimental Methods..... 99
Results 101
Discussion..... 104
References..... 108

Chapter 6 Organophosphorus Compounds Alter Intracellular F-actin Concentrations in SH-SY5Y Human Neuroblastoma Cells

Abstract..... 122
Introduction..... 123
Experimental Methods..... 124
Results 126
Discussion..... 128
References..... 131

Chapter 7 Organophosphorus Compound-induced Apoptosis in SH-SY5Y Human Neuroblastoma Cells

Abstract..... 143
Introduction..... 144
Experimental Methods..... 146
Results 149
Discussion..... 152
References..... 157

Chapter 8 The Distribution of Degenerating Neurons in Organophosphorus Compound-induced Delayed Neuropathy (OPIDN) in White Leghorn Hens as Assessed by Fluoro-Jade

Abstract..... 179
Introduction..... 180
Experimental Methods..... 182
Results 184
Discussion..... 186
References..... 190

Chapter 9 The Mode of Cell Death (Apoptosis versus Oncotic Necrosis) in Organophosphorus Compound-induced Delayed Neuropathy (OPIDN) in White Leghorn Hens

Abstract..... 202
Introduction..... 203
Materials and Methods..... 204
Results 207
Discussion..... 208
References..... 210

PART V DISCUSSION

Chapter 10 DISCUSSION..... 214

CONCLUSIONS..... 232

PART VI GENERAL REFERENCES

REFERENCES..... 235

PART VII APPENDICES AND VITA

Appendix A - Representative flow cytometry histograms for propidium iodide labeling of DNA content..... 249

Appendix B - Representative flow cytometry histograms for rhodamine 123 labeling of mitochondrial DY..... 255

Appendix C - Representative flow cytometry histograms for FITC labeling of f-actin content..... 263

Appendix D - Representative flow cytometry histograms for phycoerythrin labeling of active caspase-3..... 271

VITA..... 274

LIST OF FIGURES

Hypothesis

Figure 0.1. Flow chart diagramming the endpoints assessed in this study and their hypothetical position of effect following exposure to OP compounds..... 3

Figure 0.2. Molecular structures of the six OP compounds (DFP, paraoxon, parathion, PSP, TOTP, and TPPi) used in this dissertation.....4

Figure 0.3. Potential OP compound-induced molecular interactions in the nucleus. The diagram depicts hypothetical molecular interactions initiated by OP compound-induced damage (nuclear/genetic) or aberrant phosphorylation (p53, Bcl-2, pRb, c-Jun, c-Fos). Darkly encircled areas represent potential initiation, execution, or cell death endpoints assessed in this dissertation..... 5

Figure 0.4. Potential OP compound-induced molecular interactions in the mitochondria. The diagram depicts hypothetical molecular interactions initiated by OP compound-induced damage (mitochondrial/genetic), membrane integration, or aberrant phosphorylation (Bcl-2, Ca^{2+} ATPase, CAM Kinase II). Darkly encircled areas represent potential initiation, execution, or cell death endpoints assessed in this dissertation.....6

Figure 0.5. Potential OP compound-induced molecular interactions in the cytoskeleton and potential cytoskeletal cleavage sites for caspase and calpain proteases. The diagram depicts hypothetical sites on the cytoskeleton where OP compounds may aberrantly phosphorylate (actin microfilaments, lamin filaments, spectrin heterodimers, and vimentin intermediate filaments). Cleavage sites for caspase and calpain proteases are also detailed (band 3, band 4.1, ankyrin, adducin, actin microfilaments, lamin filaments, spectrin heterodimers, and vimentin intermediate filaments). Darkly encircled areas represent potential initiation or execution sites assessed in this dissertation..... 7

Chapter 3

Figure 3.1. Percent confluency (cell coverage of plastic substrate) of SY5Y-B cultures with different initial seeding densities over time. Fig. 3.1a, cultures without media changes; Fig. 3.1b, cultures with 67% of their media changed daily..... 54

Figure 3.2. Total cell number over time in SY5Y-B cultures. Fig. 3.2a, cultures without media changes; Fig. 3.2b, cultures with 67% of their media changed daily..... 55

Figure 3.3. Plasma membrane integrity of SY5Y-B cells over time. Fig. 3.3a, cultures without media changes; Fig. 3.3b, cultures with 67% of their media changed daily..... 56

Figure 3.4. Percent of SY5Y-B cells in G_0/G_1 phase of the cell cycle over time. Fig. 3.4a, cultures without media changes; Fig. 3.4b, cultures with 67% of their media changed daily..... 57

Figure 3.5. Percent of SY5Y-B cells in S phase of the cell cycle over time. Fig. 3.5a, cultures without media changes; Fig. 3.5b, cultures with 67% of their media changed daily..... 58

Figure 3.6. Percent of SY5Y-B cells in G_2/M phase of the cell cycle over time. Fig. 3.6a, cultures without media changes; Fig. 3.6b, cultures with 67% of their media changed daily..... 59

Figure 3.7. Percent of SY5Y-B cells with subG_1 amounts of DNA over time. Fig. 3.7a, cultures without media changes; Fig. 3.7b, cultures with 67% of their media changed daily..... 60

Chapter 4

Figure 4.1. SH-SY5Y cells exposed to diisopropylphosphorofluoridate (DFP; 10µM, 100µM, and 1mM). Fig. 4.1a, cells in G_0/G_1 phase; Fig. 4.1b, cells in S phase; Fig. 4.1c, cells in G_2/M phase; Fig. 4.1d, cells with subG_1 (fragmented) DNA..... 80-81

Figure 4.2. SH-SY5Y cells exposed to paraoxon (10µM, 100µM, and 1mM). Fig. 4.2a, cells in G_0/G_1 phase; Fig. 4.2b, cells in S phase; Fig. 4.2c, cells in G_2/M phase; Fig. 4.2d, cells with subG_1 (fragmented) DNA..... 82-83

Figure 4.3. SH-SY5Y cells exposed to parathion (100µM and 1mM). Fig. 4.3a, cells in G_0/G_1 phase; Fig. 4.3b, cells in S phase; Fig. 4.3c, cells in G_2/M phase; Fig. 4.3d, cells with subG_1 (fragmented) DNA..... 84-85

Figure 4.4. SH-SY5Y cells exposed to phenyl saligenin phosphate (PSP; 1µM, 10µM, 100µM, and 1mM). Fig. 4.4a, cells in G_0/G_1 phase; Fig. 4.4b, cells in S phase; Fig. 4.4c, cells in G_2/M phase; Fig. 4.4d, cells with subG_1 (fragmented) DNA..... 86-87

Figure 4.5. SH-SY5Y cells exposed to tri-ortho-tolyl phosphate (TOTP; 10µM, 100µM, and 1mM). Fig. 4.5a, cells in G_0/G_1 phase; Fig. 4.5b, cells in S phase; Fig. 4.5c, cells in G_2/M phase; Fig. 4.5d, cells with subG_1 (fragmented) DNA..... 88-89

Figure 4.6. SH-SY5Y cells exposed to triphenylphosphite (TPPi; 10µM, 100µM, and 1mM). Fig. 4.6a, cells in G_0/G_1 phase; Fig. 4.6b, cells in S phase; Fig. 4.6c, cells in G_2/M phase; Fig. 4.6d, cells with subG_1 (fragmented) DNA..... 90-91

Figure 4.7. SH-SY5Y cells exposed to phenylmethylsulfonyl fluoride (PMSF; 1nM, 10nM, 100nM, 1µM, 10µM, 100µM, and 1mM). Fig. 4.7a, cells in G_0/G_1 phase; Fig. 4.7b, cells in S phase; Fig. 4.7c, cells in G_2/M phase..... 92-93

Figure 4.8. SubG_1 (fragmented) DNA in SH-SY5Y cells treated with PMSF before (-12 to -6 hr), at the same time, and after (+6 to +12 hr), exposure to OP compounds (1mM paraoxon, PSP, TOTP, and TPPi; 100µM TOTP) and 150mM NaCl..... 94

Chapter 5

Figure 5.1. Mitochondrial fluorescence in SH-SY5Y cells..... 114

Figure 5.2. OP compound-induced changes in cellular transmembrane potential. Figure 5.2a, TOTP alone (n=6); Figure 5.2b, TOTP effects after carbachol pretreatment (1mM, 30 hr, n=6); Figure 5.2c, TPPi alone (n=9); Figure 5.2d, parathion alone (n=3); Figure 5.2e, parathion effects after cyclosporin A pretreatment (500nM, 30 hr, n=3)..... 115-117

Figure 5.3. TPPi-induced changes in transmembrane potential as assessed by flow cytometry..... 118

Figure 5.4. OP compound-induced changes in transmembrane potential ($\Delta\Psi$), substrate adhesion (SA), and DNA fragmentation (DNAF). Figure 5.4a, TOTP; Figure 5.4b, PSP; Figure 5.4c, TPPi; Figure 5.4d, parathion..... 119-120

Chapter 6

Figure 6.1. F-actin fluorescence in SH-SY5Y cells. Fig. 6.1a, 1% ethanol (1440 min); Fig. 6.1b, 1mM parathion (720 min); Fig. 6.1c, 1mM parathion (1440 min); Fig. 6.1d, 1mM TPPi (1440 min)..... 134-137

Figure 6.2. The relative amount of f-actin in SH-SY5Y cells. Fig. 6.2a, Parathion (100µM and 1mM); Fig. 6.2b, PSP and TOTP (100µM and 1mM); Fig. 6.2c, TPPi (100µM and 1mM)..... 138-139

Figure 6.3. The total concentration of protein (as a percent of control) in SH-SY5Y cells. Fig. 6.3a, DFP and TPPi (100µM and 1mM); Fig. 6.3b, Paraoxon and Parathion (100µM and 1mM); Fig. 6.3c, PSP and TOTP (100µM and 1mM)..... 140-141

Chapter 7

Figure 7.1. Nuclear fluorescence in SH-SY5Y cells. Fig. 7.1a is 1% ethanol incubation for 1440 min; Fig. 7.1b is cells incubated with 1mM parathion for 1440 min; Fig. 7.1c is cells incubated with 1mM TOTP for 1440 min; Fig. 7.1d is a 500nM staurosporine treatment for 1440 min (positive control)..... 167-168

Figure 7.2. OP compound-induced changes in nuclear fragmentation. Fig. 7.2a, 1mM paraoxon, 1mM parathion, and 500nM staurosporine; Fig. 7.2b, 1mM PSP, 1mM TOTP, and 1mM TPPi..... 169

Figure 7.3. OP compound-induced changes in nuclear fragmentation following 30 hr pretreatment with 1mM carbachol or 500nM cyclosporin A. Fig. 7.3a, 1mM parathion and 1mM TOTP; Fig. 7.3b, 1mM paraoxon and 1mM TPPi..... 170

Figure 7.4. OP compound-induced DNA fragmentation as viewed by gel electrophoresis..... 171

Figure 7.5. OP compound-induced changes in caspase-3 activation. Fig. 7.5a, 1mM paraoxon and 1mM parathion; Fig. 7.5b, 1mM PSP, 1mM TOTP, and 1mM TPPi..... 172

Figure 7.6. OP compound-induced changes in caspase-3 activation following pretreatment with 500nM cyclosporin A (CsA, 30h). Fig. 7.6a, 1mM paraoxon and 1mM parathion; Fig. 7.6b, 1mM TOTP and 1mM TPPi..... 173

Figure 7.7. OP compound-induced changes in caspase-3 activation following 8h pretreatment with 25µM Ac-DEVD-CHO (DEVD), 25µM Ac-IETD-CHO (IETD), or 1mM phenylmethylsulfonyl fluoride (PMSF). Fig. 7.7a, 1mM parathion (PTH); Fig. 7.7b, 1mM PSP; Fig. 7.7c, 1mM TOTP; Fig. 7.7d, 1mM TPPi..... 174-175

Figure 7.8. Electron micrographs of SH-SY5Y cell ultrastructure. Fig. 7.8a shows 1% ethanol treated cells; Fig. 7.8b and 7.8c show degenerate morphology of cells exposed to 1mM PSP or TOTP, respectively (1290 min.)..... 176-177

Chapter 8

Figure 8.1. Clinical neurologic dysfunction assessed on a scale from 0 (no effect) to 6 (severe paralysis)..... 193

Figure 8.2. Fluoro-Jade fluorescence in control and TPPi-exposed spinal cord (SC) sections from postexposure day 21. Fig. 8.2a, DMSO-exposed longitudinal section of cervical SC (200X); Fig. 8.2b, TPPi-exposed longitudinal section of cervical SC (200X); Fig. 8.2c, DMSO-exposed transverse section of spinocerebellar tracts (100X); Fig. 8.2d, TPPi-exposed transverse section of spinocerebellar tracts (100X); Fig. 8.2e, DMSO-exposed transverse section of medial-pontine tracts (100X); Fig. 8.2f, TPPi-exposed transverse section of medial-pontine tracts (100X)..... 194-196

Figure 8.3. Composite drawings of OP compound-induced neuron terminal (stipples), cell body (stipples), and tract (dashes) degeneration in parasaggital views of the brain and optic tectum, and coronal sections of the lumbar spinal cord of a hen. Fig. 8.3a, PSP, parasagittal section of the brain; Fig. 8.3b, PSP, parasagittal section of the forebrain and optic tectum; Fig. 8.3c, PSP, transverse section of the lumbar spinal cord; Fig. 8.3d, TPPi, parasagittal section of the brain; Fig. 8.3e, TPPi, parasagittal section of the optic tectum; Fig. 8.3f, TPPi, transverse section of the lumbar spinal cord..... 197-200

LIST OF TABLES

Chapter 5

Table 5.1. Contribution of the mitochondrial membrane potential to the total change in transmembrane potential induced by OP compounds..... 114

Chapter 10

Table 10.1. Summary table for DFP-induced changes in mitochondrial transmembrane potential (TMP), f-actin concentration (FA), substrate adhesion (SA), caspase activation (CA), DNA fragmentation (DNAF), nuclear fragmentation (NUCF), the proportion of cells in G_0/G_1 phase of the cell cycle (GO/G1), the proportion of cells in S phase of the cell cycle (S), the proportion of cells in G_2/M phase of the cell cycle (G2/M), and the total protein concentration (PROT). Table 10.1a, 1mM DFP; Table 10.1b, 100µM DFP; Table 10.1c, 10µM DFP..... 215-216

Table 10.2. Summary table for paraoxon-induced changes in mitochondrial transmembrane potential (TMP), f-actin concentration (FA), substrate adhesion (SA), caspase activation (CA), DNA fragmentation (DNAF), nuclear fragmentation (NUCF), the proportion of cells in G_0/G_1 phase of the cell cycle (GO/G1), the proportion of cells in S phase of the cell cycle (S), the proportion of cells in G_2/M phase of the cell cycle (G2/M), and the total protein concentration (PROT). Table 10.2a, 1mM paraoxon; Table 10.2b, 100µM paraoxon; Table 10.2c, 10µM paraoxon..... 218-219

Table 10.3. Summary table for parathion-induced changes in mitochondrial transmembrane potential (TMP), f-actin concentration (FA), substrate adhesion (SA), caspase activation (CA), DNA fragmentation (DNAF), nuclear fragmentation (NUCF), the proportion of cells in G_0/G_1 phase of the cell cycle (GO/G1), the proportion of cells in S phase of the cell cycle (S), the proportion of cells in G_2/M phase of the cell cycle (G2/M), and the total protein concentration (PROT). Table 10.3a, 1mM parathion; Table 10.3b, 100µM parathion; Table 10.3c, 10µM parathion..... 221-222

Table 10.4. Summary table for PSP-induced changes in mitochondrial transmembrane potential (TMP), f-actin concentration (FA), substrate adhesion (SA), caspase activation (CA), DNA fragmentation (DNAF), nuclear fragmentation (NUCF), the proportion of cells in G_0/G_1 phase of the cell cycle (GO/G1), the proportion of cells in S phase of the cell cycle (S), the proportion of cells in G_2/M phase of the cell cycle (G2/M), and the total protein

concentration (PROT). Table 10.4a, 1mM PSP; Table 10.4b, 100µM PSP; Table 10.4c, 10µM PSP..... 224-225

Table 10.5. Summary table for TOTP-induced changes in mitochondrial transmembrane potential (TMP), f-actin concentration (FA), substrate adhesion (SA), caspase activation (CA), DNA fragmentation (DNAF), nuclear fragmentation (NUCF), the proportion of cells in G_0/G_1 phase of the cell cycle (GO/G1), the proportion of cells in S phase of the cell cycle (S), the proportion of cells in G_2/M phase of the cell cycle (G2/M), and the total protein concentration (PROT). Table 10.5a, 1mM TOTP; Table 10.5b, 100µM TOTP; Table 10.5c, 10µM TOTP..... 227-228

Table 10.6. Summary table for TPPi-induced changes in mitochondrial transmembrane potential (TMP), f-actin concentration (FA), substrate adhesion (SA), caspase activation (CA), DNA fragmentation (DNAF), nuclear fragmentation (NUCF), the proportion of cells in G_0/G_1 phase of the cell cycle (GO/G1), the proportion of cells in S phase of the cell cycle (S), the proportion of cells in G_2/M phase of the cell cycle (G2/M), and the total protein concentration (PROT). Table 10.6a, 1mM TPPi; Table 10.6b, 100µM TPPi; Table 10.6c, 10µM TPPi..... 230-231

ABBREVIATIONS

ACh - Acetylcholine

AChE - Acetylcholinesterase

BuChE - Butyrylcholinesterase

CBxE - Carboxylesterase

DFP - Diisopropylphosphorofluoridate

EPA - Environmental Protection Agency

NTE - Neurotoxic Esterase, Neuropathy Target Esterase

OP - Organophosphorus

PI - Propidium Iodide

PMSF - Phenylmethylsulfonyl Fluoride

PSP - Phenyl Saligenin Phosphate

PTP - Permeability Transition Pore

TCP - Tricresyl Phosphate

TOCP - Tri-ortho Cresyl Phosphate (=TOTP)

TOTP - Tri-ortho Tolyl Phosphate

TPPi - Triphenyl Phosphite

$\Delta\Psi_m$ - Mitochondrial Transmembrane Potential

$\Delta\Psi_p$ - Plasma Membrane Potential

PART I

HYPOTHESIS

HYPOTHESIS

Organophosphorus (OP) compounds are utilized in a variety of household, agricultural, and industrial processes. They are primarily sold as pesticides, but have secondary markets as industrial plasticizers, fuel additives, and chemical warfare agents.

OP compounds used as pesticides induce acute *in vivo* physiological toxicity by phosphorylating acetylcholinesterase (AChE), an enzyme that degrades the neurotransmitter acetylcholine after it is released into the neural synaptic cleft. Phosphorylation inhibits AChE and results in an accumulation of acetylcholine in the synapse. In mammals, this results in clinical signs ranging from mild salivation to convulsions or death. Other sequela that follow exposure to certain OP compounds include a form of central and peripheral neuropathic degeneration termed OP compound-induced delayed neurotoxicity (OPIDN). Most of the subcellular mechanisms involved in OPIDN have yet to be determined.

SH-SY5Y human neuroblastoma cultures have been used successfully *in vitro* to model OP compound-induced alterations in esteratic enzymes, lysosomal function, Ca^{2+} flux, and other subcellular conditions involved in OPIDN. Investigation into the physical characteristics of OPIDN lesion development such as the mode of neural cell death (apoptosis versus oncotic necrosis) and the mechanisms involved in its initiation and execution have not, however, undergone extensive experimentation *in vitro*.

OP compound-induced subcellular effects in various organelles and structures (Fig. 0.1) were investigated in the immortal human neuroblastoma cell line SH-SY5Y following exposure to two non-neuropathic OP compounds (paraoxon and parathion) and four other OP compounds that induce OPIDN *in vivo* (DFP, PSP, TOTP, and TPPi; Fig. 0.2). *In vitro* studies were undertaken because they provided the necessary clarity to determine potential mechanisms involved in OP compound-induced cell death, and hence by extrapolation, the development of lesions in OPIDN.

The following research tested one primary and 4 secondary hypotheses. The **fundamental hypothesis** was that **OP compounds induced cytotoxicity via activation of apoptotic pathways**. Secondary hypotheses included: **1)** OP compound-induced cytotoxicity involved changes in nuclear structure and function (Fig. 0.3), **2)** OP compound-induced cytotoxicity involved changes in mitochondrial function (Fig. 0.4), **3)** OP compound-induced cytotoxicity involved changes in cytosolic caspase proteases (Fig. 0.5), and **4)** OP compound-induced cytotoxicity resulted in degradation of cytostructural elements (Fig. 0.5).

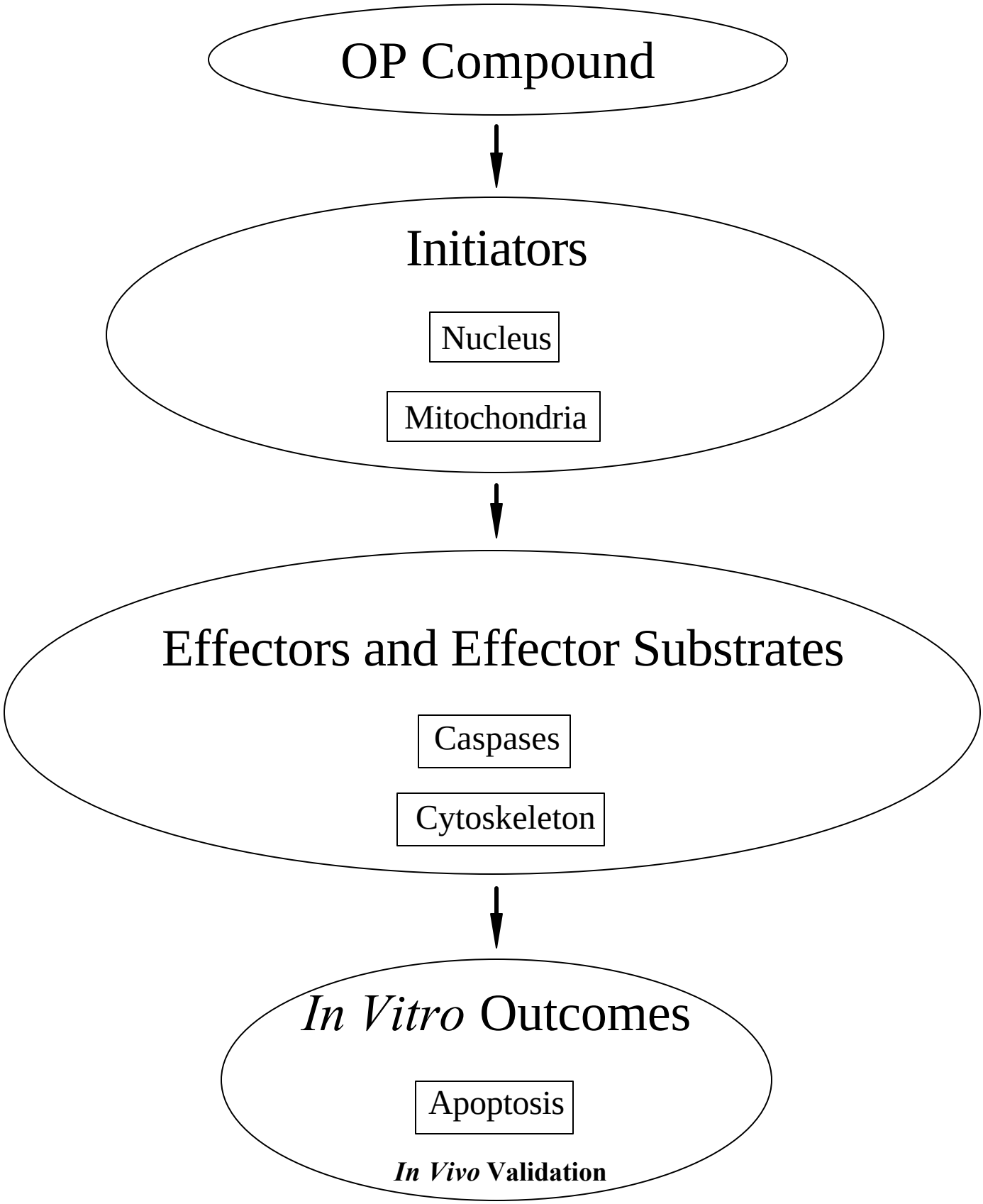

Figure 0.1 Flow chart diagramming the endpoints assessed in this study and their hypothetical position of effect following exposure to OP compounds

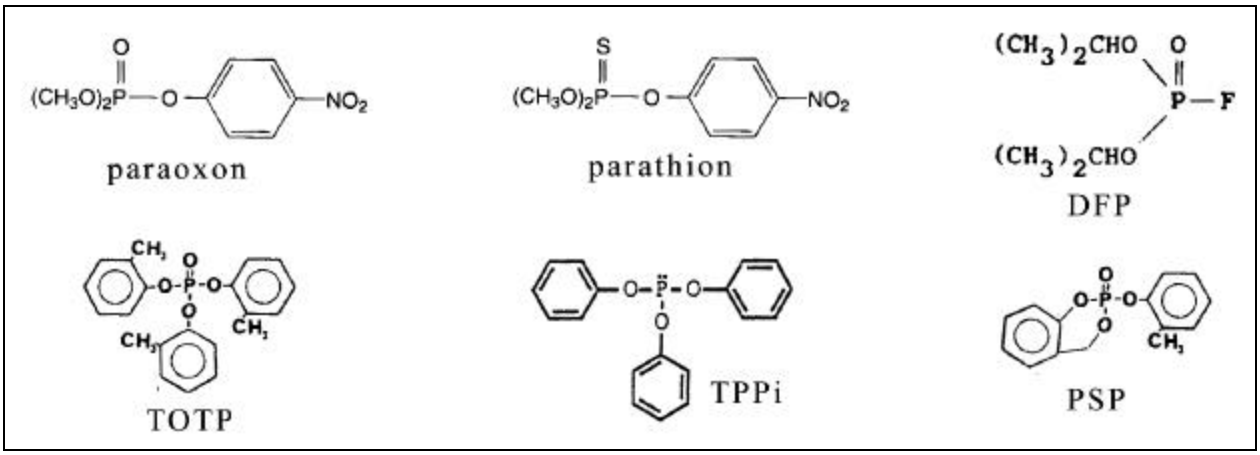

Figure 0.2 Molecular structures of the six OP compounds
(DFP, paraoxon, parathion, PSP, TOTP, and TPPi) used in this dissertation

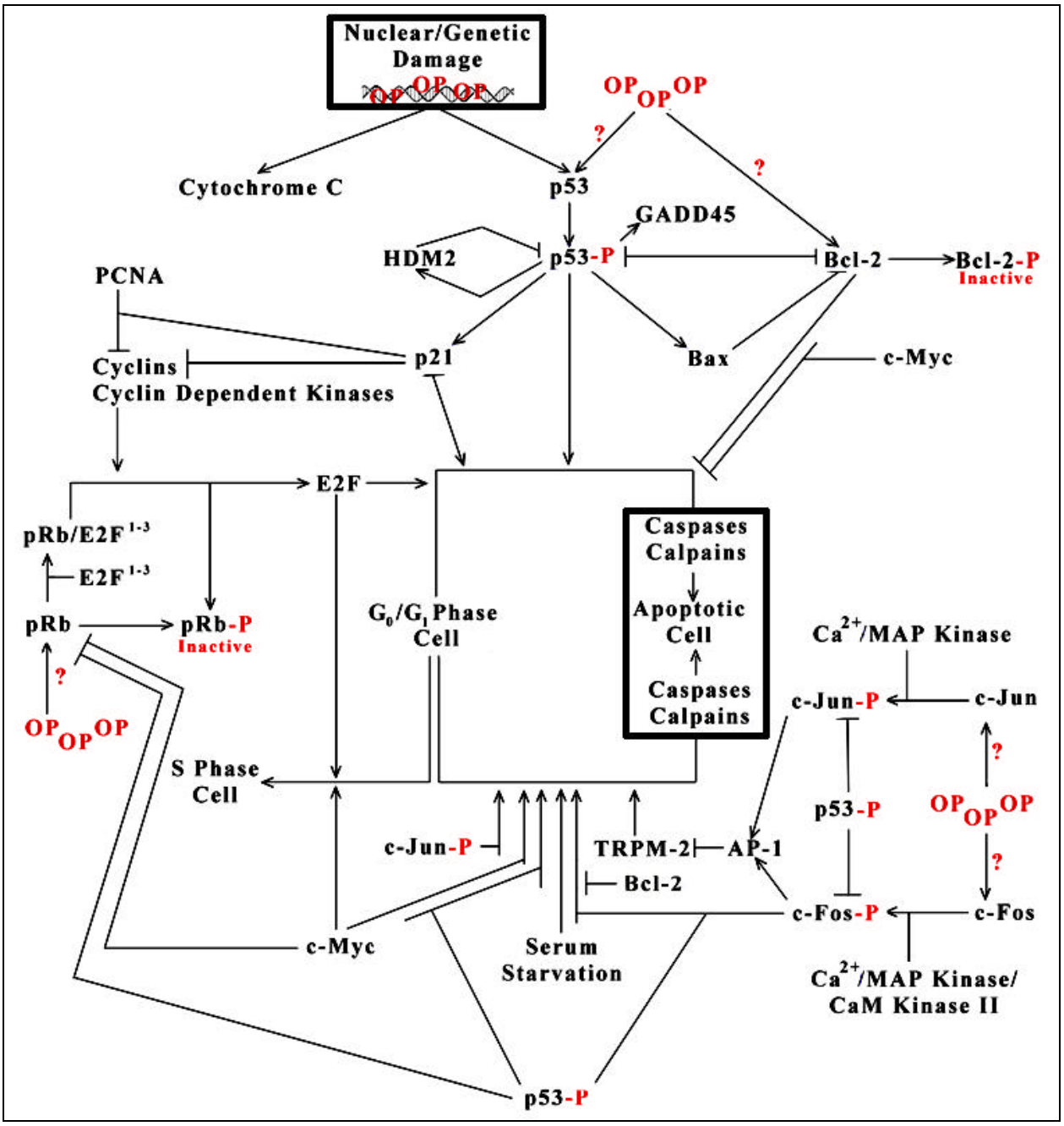

Figure 0.3 Potential OP compound-induced molecular interactions in the nucleus. The diagram depicts hypothetical molecular interactions initiated by **OP** compound-induced damage (nuclear/genetic) or aberrant phosphorylation (p53, Bcl-2, pRb, c-Jun, c-Fos). Darkly encircled areas represent potential initiation, execution, or cell death endpoints assessed in this dissertation.

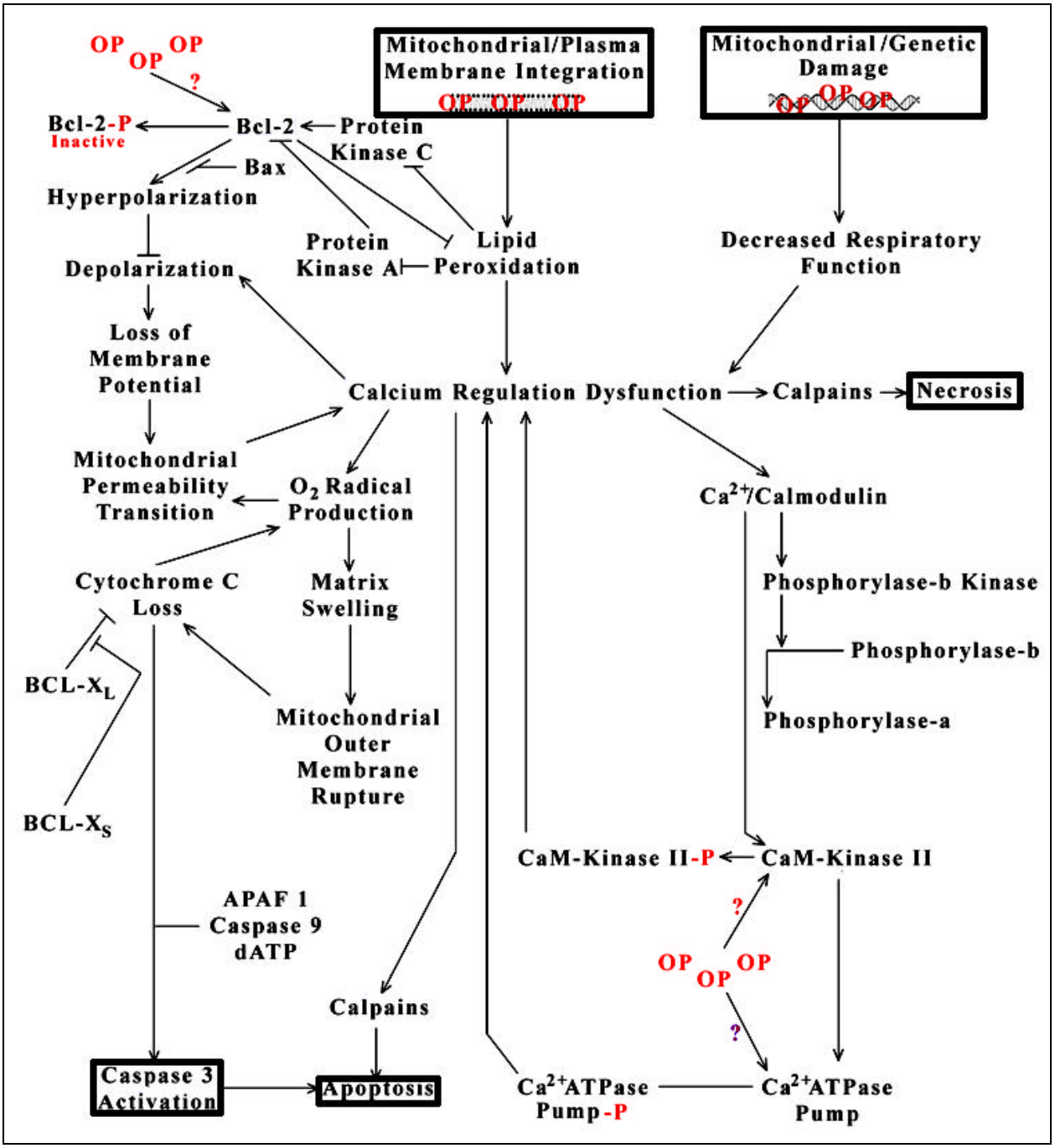

Figure 0.4 Potential OP compound-induced molecular interactions in the mitochondria. The diagram depicts hypothetical molecular interactions initiated by **OP** compound-induced damage (mitochondrial/genetic), membrane integration, or aberrant phosphorylation (Bcl-2, Ca^{2+} ATPase, CaM Kinase II). Darkly encircled areas represent potential initiation, execution, or cell death endpoints assessed in this dissertation.

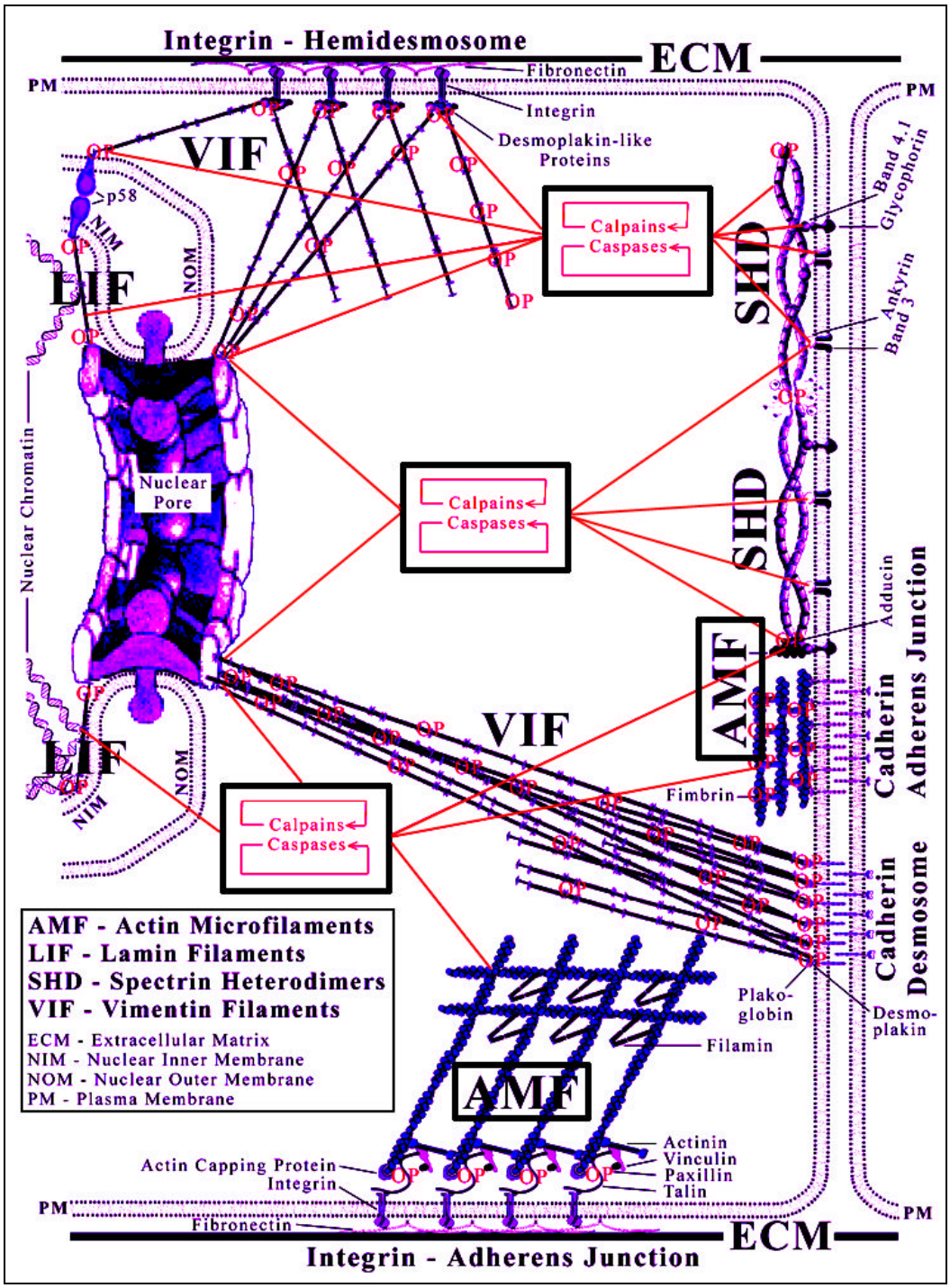

Figure 0.5 Potential OP compound-induced molecular interactions in the cytoskeleton and potential cytoskeletal cleavage sites for caspase and calpain proteases. The diagram depicts hypothetical sites on the cytoskeleton where **OP** compounds may aberrantly phosphorylate (actin microfilaments, lamin filaments, spectrin heterodimers, and vimentin intermediate filaments). Caspase and calpain protease cleavage sites are also detailed (band 3, band 4.1, ankyrin, adducin, actin microfilaments, lamin filaments, spectrin heterodimers, and vimentin intermediate filaments). Darkly encircled areas represent potential initiation or execution sites assessed in this dissertation.

PART II

LITERATURE REVIEW

Chapter 1

LITERATURE REVIEW

A. History of Organophosphorus (OP) Compounds

The first OP compound, tetraethylpyrophosphate (TEPP) was synthesized by Phillipe de Clermont in 1854. The utility of this compound was not realized at the time so the product was largely ignored. Seventy-eight years later in 1932, dimethyl- and diethylphosphorofluoridate were synthesized. Vapors created during synthesis were reported to have induced chest tightness, choking, and diminished vision in the researchers (Koelle, 1994). These unfortunate side effects led Gerhard Schraeder, a German researcher, to later evaluate these OP compounds for their pesticidal activity. Shortly thereafter during World War II, two other OP compounds of military relevance, tabun and sarin, were synthesized by the Germans but fortunately never used (Sidell, 1994). In 1946 after the war, Germany re-introduced TEPP as the first organophosphorous insecticide for agricultural use. This was followed quickly by the introduction of ethyl parathion in 1947, methyl parathion in 1949, and malathion in 1950 (Ware, 1994). During these early years many additional aliphatic, phenyl-derivative, and heterocyclic-derivative OP compounds were created.

Currently, over 400 OP compound formulations have been registered with the EPA for use in a variety of situations. The most popular use for OP compounds has been as pesticides. Overall, malathion has been most heavily applied in the United States. It was used extensively to control the Mediterranean fruit fly in Florida, Texas, Los Angeles, and other locations in California (Ware, 1994). In other countries parathion has been used instead of malathion because of its relatively inexpensive production costs (Koelle, 1994).

The largest quantity of insecticidal OP compounds have been used in agricultural endeavors. Approximately 19 to 29 million pounds of OP compounds (primarily chlorpyrifos, terbufos, and parathion) were used in agricultural crop production in 1995. This represented 21 to 32 percent of the total insecticide use for that year. Private and commercial pesticide applicators also used a large volume of OP compounds in 1995. Fourteen to 20 million pounds of OP compounds (chlorpyrifos, diazinon, and malathion) were used as insecticidal applications to residential, commercial, and government buildings and properties. Applicators in this sector were more dependent on OP compounds as insecticides than those in agriculture. Approximately 48 to 69 percent of the insecticides used by these professional applicators were OP compounds. Domestic home and garden applicators used the lowest proportion of OP compounds in 1995. Approximately 4 to 8 million pounds of OP compounds (chlorpyrifos and diazinon) were used by homeowners during this period. As with professional applicators, homeowners also relied heavily on OP compounds for insecticidal activity. Twenty-three to 47 percent of all of the insecticides in home and garden applications in 1995 were OP compounds (Aspelin, 1997).

Overall in 1995, 37 to 57 million pounds of OP compounds were used in pest management situations in the United States. OP compounds represented 21 to 69% of all pesticides used in 1995. The actual volume of OP compounds used was undoubtedly much higher, as these figures did not consider utilization in medicinal, industrial, or military processes. The volume of OP compounds used as insecticides was nonetheless a large one and garnered over 1 billion dollars for their respective industries per year.

Industrial and military processes have also historically utilized many OP compounds. Tricresyl phosphate and triphenyl phosphate have been used as industrial flame retardants and plasticizers for polyvinylchloride plastic materials (Cavalleri and Cosi, 1979; Mochida *et al.*, 1988). Triphenyl phosphite was also used as an antioxidant additive in the rubber and plastics industry (Katoh *et al.*, 1990). Trixylenyl phosphate and trialkyl phosphate were also used as hydraulic fluids (Mortensen and Ladefoged, 1992). Other OP compounds not registered for commercial sale by the EPA, such as sarin, tabun, soman, and VX have been reserved for use by the military as chemical anti-cholinesterase "nerve gas" weapons (Maxwell and Koplovitz, 1990, Langenberg *et al.*, 1996, Lallemont *et al.*, 1997).

B. Importance of OP Compounds in Our Daily Lives

Virtually every sector of society utilizes organophosphorus compounds to some extent. OP compounds are primarily used as insecticides in domestic situations but also have secondary roles in medicine.

OP compounds have diverse and numerous applications as pesticides. Insecticidal applications increase both large-scale monoculture crop and smaller-scale domestic garden and orchard yields by destroying herbivorous insect pests such as weevils and moths. Usage of OP compounds also destroys insects that would decrease the aesthetic value of home landscapes (Japanese beetles, Gypsy moths), the structural stability of human residences (termites, carpenter ants), and the quality of interior home-life (cockroaches, silverfish). OP pesticides are additionally been used in public health applications to control insect vectors that might cause pathogenic changes in a host species. For example, veterinarians use many of these OP compounds as anthelmintics and anti-flea and tick treatments (Booth and McDonald, 1982).

OP compounds are also used in medicinal applications. Ecothiophate iodide and isofluorophate can relieve the intraocular pressure associated with glaucoma. Following application of these compounds to the conjunctiva of the eye, constriction of the ciliary and iris muscle decreases and allows intraocular aqueous to be resorbed more efficiently at the canal of Schlemm, thus reducing the intraocular pressure (Koelle, 1994). Investigations into various human neuropathies also benefit from the use of OP compounds. Administration of these compounds to animal models generates a substantial amount of information on axonal transport, their interaction with cytoskeletal elements, and their implications in neurodegeneration.

Concerns regarding OP compounds' effects on human physiology are commented on by the U.S. EPA's Gene-Tox Program (Preston *et al.*, 1981), proponents of the Food Quality Protection Act

of 1996 (Mileson *et al.*, 1998), and others affiliated with infant (Schilter *et al.*, 1996) and adult exposure situations (Al-Shatti *et al.*, 1997; de Ratt *et al.*, 1997; Joksic *et al.*, 1997). Their concerns are addressed to a limited extent in this dissertation by evaluating OP compound-induced effects on novel intracellular targets.

C. Proposed Mechanisms of Toxicity Associated with OP Compounds

1. Cellular Toxicity Studies

This dissertation primarily evaluated the mode of OP compound-induced *in vitro* cytotoxicity (apoptosis versus oncotic necrosis). Secondary hypotheses investigated potential mechanistic pathways involved in the initiation, execution, and final stages of OP compound-induced cell death. Conclusions from the *in vitro* model of neural cell death were then evaluated in *in vivo* settings.

In the following sections, hypothetical substrates for OP compounds and alterations in viability are briefly discussed before the potential targets (nucleus, mitochondria, enzymes, cytoskeleton) of OP compound-induced cytotoxicity.

Putative Serine Substrates

Putative serine substrates for phosphorylation abound in the cell. Enzymes that degrade neurotransmitters or other esters such as acetylcholinesterase (AChE), butyrylcholinesterase (BuChE), carboxylesterase (CBxE), and neuropathy target esterase (NTE) all have serine residues that can be phosphorylated. Other molecules involved in ion regulation, such as Bcl-2 (Haldar, 1995), and neuromodulin (Liu and Storm, 1989), or cell cycle progression and transcription such as cyclin dependent kinases (Alberts *et al.*, 1994), p53 (Ko and Prives, 1996), pRb (Fahraeus *et al.*, 1996), Histone H3 (Waring *et al.*, 1997), IκB (Barkett *et al.*, 1997; Whiteside and Israël, 1997), c-Jun (Pulverer *et al.*, 1991), and c-Fos (Barber and Verma, 1987) can also be phosphorylated on active serine residues. The regulation of intermediate filaments such as GFAP, vimentin, desmin, keratin, α-internexin, NF-L and nuclear lamin is highly dependent on serine phosphorylation (Takai *et al.*, 1996). Cell signaling through proteins such as phosphatidylinositol 3′-kinase/pp76 (Cengel *et al.*, 1998), and insulin receptors (Strack *et al.*, 1997), cell adhesion as modulated by syndecan-1 (Oh *et al.*, 1997), and cell metabolism via phosphorylase kinase (Cohen, 1982) are also regulated by phosphorylation of serine residues.

OP compound-induced phosphorylation of active serine residues on proteins other than AChE, BuChE, CBxE, or NTE are not currently being investigated to any extent. Theoretically, if these other proteins have binding consensus sequences and adjacent molecular environments similar to esterases, OP compounds may be able to induce such diverse effects as aberrant mitosis, calcium dysregulation, intermediate filament disassembly, transcriptional activation, receptor inhibition, chromosomal condensation, and/or a loss of substrate adhesion. Any one of these could precipitate cellular cytotoxicity in a variety of manners (Fig 0.3, 0.4, and 0.5).

Viability

Viability is decreased in cells following exposure to most OP compounds. OP compound-induced changes in viability are assessed primarily through the application of three methods; neutral red staining of lysosomes, trypan blue dye exclusion, and cytosolic fluorochrome retention. The first method extrapolates lysosomal integrity to cell viability. The second two assess plasma membrane integrity and the exclusion or retention of cellular stains, respectively. These methods are used to generate percent of control viability as well as half-maximal inhibitory concentrations or doses (IC_{50}/ID_{50}) following exposure to various OP compounds (Harvey and Sharma, 1980; Mochida *et al.*, 1988; Veronesi and Ehrich, 1993a, 1993b; Ehrich *et al.*, 1997; Veronesi *et al.*, 1997). Interestingly, concentrations of OP compounds that decrease viability are 100 to 1000X greater than those used to inhibit AChE activity (Rowles *et al.*, 1995).

Exposure to some OP compounds results in increased viability rather than cytotoxicity. Exposure to diazinon (1μM) increases IEC-6 and human colonic epithelial cell proliferation and viability (Greenman *et al.*, 1997). Similarly, treatment with low concentrations of dicrotophos (900μM) or TOTP (8μM) causes proliferation of neuroblastoma 2-A cells (Harvey and Sharma, 1980). The dose dependent differences between proliferation and death suggest that multiple pathways and substrates are being affected by exposure to OP compounds.

Nuclear Structure and Function

Nuclear structure is altered by exposure to OP compounds. Knoth-Anderson *et al.* (1992) report structural alterations in the bovine adrenomedullary chromaffin cell nuclear membranes following 24 hr exposure to 100μ M TPPi. Specifically, exposure to TPPi results in indentation of the nuclear membrane and the formation of a perinuclear band of translucent material. Twenty-four hour exposure to similar concentrations of DFP and paraoxon also induces the formation of abnormally crenylated nuclei, but to a much lesser extent.

Changes in nuclear function also occur following exposure to OP compounds. Malathion exposure (50-70μg/ml) for 24 hr decreases nucleic acid synthesis (RNA and DNA) and increases chromosomal gaps and breaks in human lymphocytes. In contrast, similar exposures with 10μg/ml malathion increases DNA and RNA synthesis (Walter *et al.*, 1980). The incorporation of tritiated thymidine into nuclear DNA is also reduced in a dose dependent manner after exposing PC12 pheochromocytoma cells for 72 hr to tricresyl phosphate (TCP, 1-1000μg/ml), TPPi (10-1000μg/ml), and paraoxon (100-1000μg/ml) (Flaskos *et al.*, 1994). Similar decreases in DNA, RNA, and protein synthesis are reported in c1300 neuroblastoma cells following exposure to 1mg/ml DFP for 24, 48 and 72 hr (Hong *et al.*, 1995). Treatment with hexamethonium, a ganglionic blocker, and hemicholinium, a choline reuptake blocker, reverses the DFP-mediated DNA inhibition but not RNA inhibition (Hong *et al.*, 1995).

Changes in nuclear function may relate to the ability of OP compounds to induce genetic anomalies. TOTP, a protoxicant, is mutagenic following metabolic activation in the Ames test using

Salmonella typhimurium. In further tests, the primary cyclic metabolite of TOTP (2-phenoxy-4H-1,3,2-benzodioxaphosphorin 2-oxide) also forms adducts in calf thymus DNA (Mentzschel *et al.*, 1993). Dichlorvos, trichlorfon, paraoxon, and methylazinphos are able to induce mutagenicity in the forward mutation test system *ade6* of the yeast *Schizosaccharomyces pombe* (Gilot-Delhalle, 1983). Synergistic effects in toxicity and mutagenicity are observed in this test when trichlorfon is combined with malathion, methylparathion, or methylazinphos.

Increases in sister chromatid exchange frequencies (SCE, a correlate of point mutations) occur in lymphoid cell lines following 48 hr exposure to OP compounds (0.02-20μg/ml) such as azodrin, diazinon (with metabolic activation), dichlofenthion, dimethoate, chlorpyrifos, malathion, parathion, phorate, phosdrin, R1303, and viozene (Sobti *et al.*, 1982). Similar results are reported by Herath *et al.* (1989) and Nishio and Uyeki (1981) following investigations into the genetic effects of malathion (20-50μg/ml; 4 hr) on human lymphocytes, and the genetic effects of dichlorvos, dicrotophos, malathion, parathion, leptophos, diazoxon, malaoxon, paraoxon, and leptophos-oxon (0.03-1mM; 38 hr) in chinese hamster ovary (CHO) cells, respectively. They suggest, as did Sobti *et al.* (1982), that increased rates of chromosomal aberrations and SCE frequencies are directly related to OP compound exposure. Nishio and Uyeki (1981) also add that the oxon analogs of the test OP compounds have the highest SCE frequencies and greater antiproliferative effects than the sulfur analogs.

Similar changes are seen following exposure to other OP compounds. Chen *et al.* (1981) describe increases in SCE frequencies in V79 (CHO) cells following exposure to methylparathion, demeton, trichlorfon, dimethoate, methidathion, and malathion (10-160μg/ml; 28-34 hr). Some of the same OP compounds, in addition to oxydemeton methyl and fenthion, increase SCE frequencies in V79 cells in the presence of S-9 metabolic activating systems. All of these compounds, except oxydemeton methyl, induce a cell cycle delay, but no correlation could be found to SCE frequencies.

Mitochondrial Structure and Function

Mitochondrial structure and function in cellular models change following exposure to OP compounds. Exposure of chick dorsal root ganglia (DRG) primary explant cultures to 1μM paraoxon (144 hr) results in mitochondrial swelling and a loss of cristae structure. Exposure to 1 to 10μM fenthion results in no changes, however, to the mitochondrial structure of DRGs in this study (Tuler and Bowen, 1989). Mitochondrial swelling and loss of cristae in bovine adrenomedullary chromaffin cells are also observed following 24 hr 100μM TPPi exposures (Knoth-Anderson *et al.*, 1992).

Functional changes in mitochondria occur following exposure to OP compounds. Holmuhamedov *et al.* (1996) demonstrate that exposure to ethaphos (8.5-100μg/mg mitochondrial protein; 3-4 min) uncouples mitochondrial respiration and inhibits mitochondrial dehydrogenases that participate in the oxidation of succinate, α-glycerophosphate, and pyruvate+malate. This compound does not interfere, however, in the regulation of inner membrane permeability, cytochrome activity, or mitochondrial ATPase activity. Knoth-Anderson *et al.* (1992) report that TPPi exposures have an additional effect on ATP generation, since 100μM exposures (1-24 hr) inhibited 90% of the incorporation of adenosine into ATP. OP compound-induced inhibition of ATP generation is not a

universal event however, since subsequent exposures to 100μM paraoxon or DFP did not affect adenosine incorporation.

Others also report changes in mitochondrial respiration following OP compound exposure. Sitkiewicz *et al.* (1980) demonstrates that changes in respiration occur after treatment with structural analogs of ethaphos (Dipterex, DDVP, Ronnel, and its oxygen analog; 5-500μM; 3-5 min). This study reports that Ronnel's oxygen analog also inhibits cytochrome *c* oxidase and NADH:cytochrome *c* reductase, while Ronnel-itself only inhibits cytochrome *c* oxidase. The inhibition of oxidative phosphorylation by the oxygen analog of Ronnel is shown to act in a time, concentration, and animal age related fashion (Skonieczna *et al.*, 1980).

Enzyme Activities

OP compounds alter the activity of enzymes such as AChE, CBxE, and NTE following OP compound administration. These three enzymes are of primary importance in OP compound-induced physiological toxicity and OP compound-induced delayed neurotoxicity (OPIDN). Inhibition of AChE can induced *in vivo* physiological toxicity, CBxE can serve as an esteratic sink for highly toxic OP compounds, and inhibition of NTE is correlated with the development of OPIDN. These three are routinely assessed in cell culture models designed to mimic toxic and neuropathic conditions even though their activity may not actually be critical for cell survival (Flaskos *et al.*, 1994).

AChE can be inhibited to a great extent following incubation with some OP compounds but not others. Fifteen minute incubation of soman (GD; 5.5μM) with superior cervical ganglion cells decreases AChE levels to <1% of untreated cellular controls (Yourick *et al.*, 1991) . The AChE activity gradually reappears over a 20 hour period ($t_{½}$ of 10 hours) and is not affected by the administration of glycyl-L-glutamine, a neurotrophic factor thought to be responsible for the maintenance of AChE content in some tissues. Other studies observe a dose-dependent inhibition of AChE by VX, Soman, GF, DFP, and to a much lesser extent, their phosphonylated oximes in mouse embryo neurons (Sawyer *et al.*, 1991). Mipafox and paraoxon (50μM) inhibit SH-SY5Y AChE within 10 minutes after administration (Nostrandt and Ehrich, 1992). Similar findings for mipafox are reported by Rowles *et al.* (1995) who observes that AChE levels are largely inhibited after 10 minute and 2 hour incubations with 10μM and 100μM mipafox, respectively. In other studies, DFP (IC_{50} = 0.093μM) , malaoxon (IC_{50} = 0.0097μM), mipafox (IC_{50} = 13μM) , PSP (IC_{50} = 0.26μM) , and paraoxon (IC_{50} = 0.004μM) also inhibit AChE well (Ehrich *et al.*, 1994; Veronesi *et al.*, 1997; Ehrich and Correll, 1998), in contrast to TOTP (IC_{50} = >1000μM) , malathion (IC_{50} = 50μM) , and parathion (IC_{50} = 600μM) (Veronesi *et al.*, 1997).

Carboxylesterase (CBxE) can also be inhibited to a great extent following exposure to OP compounds. Veronesi and Ehrich (1993b) report that CBxE appears to bind OP compounds faster and with greater affinity than AChE in some cell culture systems. They also comment that CBxE shows little structural preference for one OP compound over another. CBxE is inhibited well by OP compounds such as PSP (IC_{50} = 0.068μM), mipafox (IC_{50} = 84μM), and DFP (IC_{50} = 1.7μM), but not very well

by compounds such as malaoxon (IC_{50} = 500μM) or paraoxon (IC_{50} = 380μM) (Ehrich *et al.*, 1995b; Ehrich and Correll, 1998).

A variety of OP compounds can inhibit *in vitro* NTE activity. N1E-115 neuroblastoma cell NTE is inhibited well by leptophos-oxon and DFP, but poorly by EPN and leptophos (Fedalei and Nardone, 1983). In addition, SH-SY5Y cell NTE is inhibited well by mipafox but not by paraoxon or parathion (Rowles *et al.*, 1995). Interestingly, mipafox-mediated inhibition of NTE decreases after preincubation with verapamil (100nM) or carbamates such as aldicarb (Nostrandt and Ehrich, 1993). Bovine adrenal chromaffin cell NTE is also inhibited significantly following 4 hr exposure to 100μM TPPi and DFP (Knoth-Anderson and Abou-Donia, 1993). PSP (IC_{50} = 0.03μM), TSP (IC_{50} = 0.043μM), mipafox (IC_{50} = 14μM), and DFP (IC_{50} = 1μM) inhibit completely SH-SY5Y NTE. This is in contrast to the marginal inhibition displayed by protoxicants or compounds that didn't elicit *in vivo* OPIDN such as paraoxon (IC_{50} = >1000μM), parathion (IC_{50} = >1000μM), malaoxon (IC_{50} = 740μM), and malathion (IC_{50} = >1000μM) (Veronesi and Ehrich, 1993a, Ehrich *et al.*, 1994).

Other enzymes can also be affected by OP compound treatment. Increases in the activity of phosphorylase-a, an enzyme that breaks down muscle glycogen into glucose, occur following exposure to DFP, VX, soman, sarin, and tabun treatments (1μM to 1mM; 2 to 10 min) in rat pheochromocytoma PC12 cells and isolated hepatocytes (Kauffman *et al.*, 1990). Exposure to TPPi (100μM; 24 hr) also results in a cytosolic glycogen buildup in bovine adrenal chromaffin cells. This is thought to result from disrupted metabolism, because both creatinine kinase and succinate dehydrogenase activity are simultaneously reduced in the mitochondria of these cells 24 to 48 hours after dosing (Knoth-Anderson *et al.*, 1992).

Cytostructural Components

Cytostructural components such as the cell's plasma membrane are affected by OP compound administration. Parathion and azinphos (100μM) (and not malathion) interact with the polar head groups of short chain lipid compounds and interfere with interactions between membrane lipids and cholesterol. This interaction results in a gross disorder in lipid packing and restriction of the motion of the phospholipid hydrocarbon chains. This in turn weakens fatty acid interactions and decreases lipid adhesion. Ultimately, this increases the permeability of the lipid membrane to nonelectrolytes and to ion-ionophore complexes while not disrupting the membrane integrity (Antunes-Madeira *et al.*, 1980).

Certain OP compounds also reduce neurite extension and maintenance. Dose-dependent (100nM-50μM) TOCP-induced reductions in neurite outgrowth are observed in differentiated C-6 rat brain glioma and N-18 mouse brain neuroblastoma cells following 14 day exposures (Henschler *et al.*, 1992). Flaskos *et al.* (1994) demonstrate similar events in PC12 pheochromocytoma cells following 72 hr exposure to paraoxon and TPPi (10-1000μg/ml). Twenty-four hour exposures to TOTP and DFP (8μM-1.3mM) and TPPi (100μM) also reduces neurites in N-2a neuroblastoma cells (Harvey and Sharma, 1980) and bovine adrenomedullary chromaffin cells (Knoth-Anderson *et al.*, 1992), respectively. Lower concentration exposures induce the formation of shrunken, rough, irregular, and swollen neurites, in contrast to neurite "spikes" which predominate at higher concentrations (Harvey and

Sharma 1980). Mipafox treatments (10μM; 72 hr) induce the formation of plasma membrane blebs, abnormal growth cones, and shrunken and irregularly swollen neurites (Nostrandt and Ehrich, 1992). Fenthion (1-10μM; 72 hr) treatment also induces neuritic lesions in chick dorsal root ganglia primary explant cultures. These lesions are characterized by vacoulization (0.5-1 to 5-10μm), a loss of tubular structures, retraction of pseudopodia, cell membrane disruption at growth cone, a loss of neurofilaments, disruption of the microtubules, lipid accumulations in the cytoplasm, and a fragmentation of the plasma membrane (Tuler and Bowen, 1989).

In many cells, loss of the neurites precedes rounding up and detachment from the plate. Nostrandt and Ehrich (1992) document that paraoxon (50μM) exposure for 3-7 hours results in cellular rounding and detachment.

Summary

OP compounds affect *in vitro* cellular viability in a concentration-dependent manner. High concentrations of OP compounds exposures are cytotoxic. Low concentrations, on the other hand, may encourage proliferation. Until recently, *in vivo* viability studies have historically labeled OP compound-induced cytotoxic events in tissue as necrotic. The overwhelming consensus that these mechanisms were necrotic was because all of the viability protocols used in these studies assessed necrotic, not apoptotic, cell death. In fact, only a few studies have assessed whether OP compounds elicit an apoptotic or necrotic mode of cell death. Since the mode of cell death for OP compound-induced *in vitro* cytotoxicity and OPIDN have yet to be described, this presents an area of primary importance for research.

OP compounds also affect nuclear structure and function. OP compounds elicit increases in DNA adducts, aberrant sister chromatid exchange frequencies, mutagenicity, cell cycle delay, and decreases in DNA and RNA synthesis. No publications have delineated OP compound-induced temporal changes in nuclear morphology. Similarly, investigation into OP compound-induced functional changes in the nucleus (e.g. cell cycle control) has received only limited investigation.

Mitochondrial structure and function are also affected following OP compound exposure. Respiratory enzymes such as creatinine kinase, succinate dehydrogenase, cytochrome c oxidase, and NADH:cytochrome c reductase can be impaired following exposure to certain OP compounds. Likewise, direct changes are seen in the ATP-generating capability of cells following OP compound exposure. OP compound-induced alterations in intact mitochondria have received little study and deserves more attention. Publications evaluating OP compound-induced changes in mitochondrial function (e.g. ionic homeostasis) have also received minimal attention.

Cytosolic and membrane bound enzymes such as AChE, NTE, CBxE, and phosphorylase-a are affected following exposure to OP compounds. OP compound-induced enzyme activity has attracted the most attention in cellular studies as a diagnostic tool for modeling rather than as a potential stimulus or effector of cell death. The activation of other enzymes that may assist in cell death (e.g. caspases) have not been discussed in literature.

Membrane and cytostructural alterations are also common following exposure to OP compounds. Increases in membrane permeability and decreases in neurite extension and maintenance are frequently observed following exposure. The cytoskeletal proteins (e.g. f-actin) involved in these have not been investigated and may additionally play a role in the final stages of OP compound-induced cytotoxicity.

Overall, the above studies suggest that OP compounds detrimentally affect the viability of exposed *in vitro* culture systems. The mechanisms behind OP compound-induced cytotoxicity, however, have not yet been linked discretely to any one target system or cell death pathway. As shown, there is ample documentation of OP compound induced changes in multiple cellular targets such as genetic integrity, mitochondrial function, enzyme activity, and cytostructural integrity. Further investigation into these areas may clarify discrete initiation points, effector pathways, and effector substrates for OP compound-induced cytotoxic reactions.

2. Whole Animal Studies

This dissertation primarily evaluated the mode of OP compound-induced *in vitro* cytotoxicity (apoptosis versus oncotic necrosis). Secondary hypotheses investigated potential mechanistic pathways involved in the initiation, execution, and final stages of OP compound-induced cell death. Conclusions from the *in vitro* model of neural cell death were then evaluated in *in vivo* settings.

In the following section, the history of OPIDN and text on the distribution and extent of OP compound-induced neuropathic degeneration are discussed prior to any *in vivo* evidence relating to a mode of cell death. This pattern is thought to reflect an experimental approach, since the question of "where is the neuropathy" has to be evaluated before "what kind cell death is occurring in the neuropathy". *In vivo* investigations were designed to validate conclusions generated by modeling in SH-SY5Y human neuroblastoma cells.

Acutely Toxic Effects

OP pesticides inhibit acetylcholinesterase (AChE; EC 3.1.1.7) in invertebrates (Escartin and Porte, 1996) and vertebrates such as humans and chickens (Abou-Donia, 1995). Carboxylesterase (CBxE; EC 3.1.1.1), butyrylcholine esterase (BuChE; EC 3.1.1.8), and other less specific serine esterases in mammals and avians are also inhibited by OP compounds (Ehrich *et al.*, 1995a; Ehrich, 1996; Ehrich *et al.*, 1997). Inhibition of AChE induces an acute *in vivo* toxicity, while inhibition of the other enzymes has no known physiological sequelae.

AChE is an enzyme that degrades the neurotransmitter acetylcholine (ACh) after it is released into synaptic cleft. Inhibition of the AChE enzyme results in an accumulation of ACh in synapses within the neuromuscular junctions, parasympathetic postganglionic terminals, autonomic ganglia, and other cholinergic sites within the mammalian CNS (Hatch, 1982; Koelle, 1994). Excess ACh stimulates muscarinic, and nicotinic receptors and leads to clinical signs that include excessive salivation and

lacrimation, polyuria, miosis, diarrhea, tremors, hypothermia, and convulsions (Fernando *et al.*, 1985; Kunimatsu *et al.*, 1996; Lallemont *et al.*, 1997; Raveh *et al.*, 1997). Nociceptive pathways are also affected by acute OP compound poisoning (Chemnitius *et al.*, 1989) as are M_2 muscarinic receptors in the heart. OP compound interactions with these receptors are thought to result in abnormalities in cardiac rhythm following OP compound poisoning (Silveira *et al.*, 1990). OP compound-induced CNS depression, diaphragmatic paralysis, and respiratory failure can lead to death in overdose situations (Sidell, 1994, Saunders and Harper, 1994).

Delayed Neuropathic Effects

One of two forms of a progressive central and peripheral neuropathy can be induced in animals following exposure to certain OP compounds. These are termed organophosphorus compound-induced delayed neurotoxicity / polyneuropathy (OPIDN/OPIDP Type I or II). In OPIDN, a focal chemical transection of susceptible axons results in Wallerian degeneration-like changes and subsequent secondary demyelination (Bouldin and Cavanagh, 1979a, 1979b; Abou-Donia, 1995).

Type-I and Type-II neuropathies differ in their areas of affliction, time of onset, and display of clinical signs and symptoms. In many cases, acute cholinergic toxicity and inhibition of esterases are metabolically resolved by the time of clinical onset. In severe poisonings, clinical recovery from the paralytic effects of OPIDN is negligible (Abou-Donia, 1995).

Clinical onset of OPIDN is correlated to the inhibition and aging of a carboxylesterase termed NTE (neuropathy target esterase, neurotoxic esterase). Sixty to seventy percent irreversible inhibition of this enzyme following OP compound exposure invariably results in the development of OPIDN in sensitive species (Bursian *et al.*, 1983; McCain *et al.*, 1996). This enzyme is not, however, the definitive etiologic agent behind OPIDN (Ehrich, 1996).

Clinical cases of human OPIDN were first recorded in the late 1800's in France. The neuropathies seen in these cases have been attributed retrospectively to the administration of creosote oil as a treatment for pulmonary tuberculosis. The primary ingredients in this phospho-creosote oil are phosphoric acid esters and coal tar phenols (Davis and Richardson, 1980).

Tri-ortho cresyl phosphate (TOCP, tri-ortho tolyl phosphate, TOTP) is the first OP compound specifically identified as an inducer of OPIDN in humans. In the 1930s, consumption of TOCP-tainted drinking alcohol resulted in numerous incidences described as "ginger" or "Jake leg" paralysis in the mid- and southwestern United States (Abou-Donia, 1995). TOCP was implicated in another incident in 1958, where nine shoe factory workers in Italy acquired polyneuropathic symptoms similar to OPIDN. These symptoms involved motor nerves but pyramidal signs were evident in workers for 2 to 10 years after diagnosis. Unlike "ginger" paralysis, the causative agent was never precisely determined. TOCP was heavily used in this workplace, however, and thought to be the etiologic agent in this case and in at least 400 other subsequent cases (Cavalleri and Cosi, 1980). TOCP was also involved in the development of over ten thousand cases of OPIDN in Morocco in 1959. In this incident, imported cooking oil was found to be contaminated with high levels of TOCP. TOCP has been determined to be

the etiologic agent in at least 16 other occurrences of OPIDN from 1925 to 1988. World-wide, tens of thousands of people are thought to have been involved in these incidents (Abou-Donia, 1995).

Other OP compounds have also been implicated as causative agents for OPIDN in humans. In 1951, people working for an organophosphorus pesticide manufacturing laboratory in England reported OPIDN-like symptoms. Three people in this incident had initial neuropathic symptoms progress to include complete paralysis of the legs and partial paralysis of the hands and arms. One OP compound, mipafox, was thought to be the responsible agent in this case (Abou-Donia, 1995). Leptophos, another OP compound, was thought to have caused paralysis in hundreds of Egyptian water buffalo. Six people working at the same site also developed OPIDN-like symptoms and were found to have high levels of leptophos in their tissues (El-Sebae, 1977).

Currently, adult domestic laying hens are used to screen OP compounds for neuropathic potential (EPA, 1996). In hens, gait and posture are observed clinically to assess the initial severity of OPIDN prior to hematological or pathological exam. Other researchers utilize neurological functional observational batteries (FOBs) to assess the degree of clinical impairment elicited by OPIDN causing compounds. These tests, however, are not as sensitive as assessing plasma, RBC, or brain NTE inhibition and do not give any indication of cumulative toxicity (Sheets *et al.*, 1997).

A variety of avian species have been exposed to neuropathic OP compounds in order to induce OPIDN. Because animals differ in their sensitivity and reactions to OP compounds, the following pages will discuss OP compound-induced neuropathic effects by species type.

Chickens (*Gallus domesticus*)

The EPA requires that all OP compounds intended for registration be tested for clinical signs indicative of OPIDN in adult domestic laying hens between the ages of 8 and 14 months (EPA, 1996). Hens are currently the most sensitive model for screening OP compounds in that they closely approximate OP compound-induced physiological changes seen in humans. The hen model is not without its own flaws, however. Intraspecies differences in hen genetics (Dunnington *et al.*, 1989; Ehrich *et al.*, 1986, 1993a) and immunological status (Jortner and Ehrich, 1987) affect the development of OPIDN, so must also be considered when testing for compounds that induce OPIDN.

Administration of many OPIDN-inducing OP compounds to hens may initially elicit an acute cholinergic response. For example, exposure to DFP and mipafox, excellent inhibitors of AChE, induce cholinergic crisis and other side effects such as muscular weakness (Barnes and Denz, 1953; Tanaka *et al.*, 1990; Ehrich *et al.*, 1995a). EPN and coumaphos are also acutely toxic. Dermal or oral exposure to these compounds can result in cholinergic poisoning in spite of preventive atropine sulfate administration. Interestingly, the acute signs of EPN and coumaphos lessen after repeated doses (Abou-Donia *et al.*, 1982; Abou-Donia *et al.*, 1983). In contrast, other OPIDN-inducing OP compounds such as DEF, PSP, and TOTP are weak inhibitors of hen AChE and do not elicit many cholinergic signs following administration (Barnes and Denz, 1953; Abou-Donia *et al.*, 1983; Abou-Donia, 1993; Jortner and Ehrich, 1987; Ehrich *et al.*, 1995a).

The temporal development of clinical OPIDN in hens is OP compound- and dose-dependent. Type I OPIDN compounds typically elicit clinical changes 5 to 21 days after administration. Of these, PSP induces some of the earliest changes. McCain *et al.* (1996) and Jortner and Ehrich (1987) report that hens treated with PSP are reluctant to move and display a mild ataxia after only 6 to 10 days post administration. TOCP, coumaphos and mipafox induce the onset of OPIDN at similar time frames such as 9 to 12, 9 to 13, and 10 to 14 days post exposure, respectively. Hens exposed to DFP do not show any clinical signs such as ataxia by day 7 but demonstrate severe ataxia and paralysis by days 14 and 21, respectively (Tanaka *et al.*, 1990). EPN-induced ataxia and paralysis can occur even later than this, at some 17 to 41 days after exposure (Barnes and Denz, 1953; Abou-Donia *et al.*, 1982; Abou-Donia *et al.*, 1983; Ehrich *et al.*, 1986).

Most Type I OPIDN-eliciting neurotoxicants induce similar and specific degenerative patterns in the hen model. Jortner and Ehrich (1987) describe the elements of OPIDN as including bilateral degeneration of axons in the cerebellum, medulla and pons, spinal cord, and the peripheral nervous system. The induced degeneration is primarily axonal with secondary myelinic involvement.

Few changes in neural tissue are seen early after exposure to OP compounds. Minimal axonal and terminal degeneration in the brainstem and cerebellum; scattered degeneration in fibers of the external cuneate nucleus; and punctate terminal degeneration in descending vestibular and deep cerebellar nuclei occur by 7 days post-dosing. TOTP administration induces comparatively more axonal and terminal degeneration in the vestibular and deep cerebellar nuclei than DFP at this period in some studies (Tanaka *et al.*, 1990). In other studies exposure to TOTP and PSP elicits no obvious degeneration by day 7 (Jortner and Ehrich, 1987).

Denser terminal and axonal degeneration is seen in all areas by 14 days following OP compound exposure. Moderate degeneration is observed in the axons and terminals of the cervical lateral nucleus and the fasciculis gracilis. Lighter degeneration is seen in the external cuneate nucleus and the lateral reticular nucleus. At this time minimal degeneration also occurs in fibers of the dorsal spinocerebellar tract; the white matter of folia I; and the medial portions of the deep cerebellar nuclei (Tanaka *et al.*, 1990).

The greatest amount of axonal degeneration is noted at 21 days after OP compound exposure. Dense axonal degeneration is observed at cervical levels in the fasciculis gracilis dorsal spinocerebellar tracts, and at lumbar levels in the anterior and postero-lateral columns (Barnes and Denz, 1953; Jortner and Ehrich, 1987). At caudal medullary levels, axons of smaller diameter that terminate in the external cuneate, inferior olivary nuclei, and the surrounding lateral reticular formation undergo terminal degeneration. Rostral medullary terminal degeneration during this period is also seen in the spinal lemniscus, lateral paragigantocellular reticular nucleus, and the nucleus tractus solitarius, as well as in axons comprising the intramedullary portions of glossopharyngeal and vagus nerves. At rostral levels of the pons there is small diameter axonal degeneration in the ventral spinocerebellar tract, while at the pons-midbrain junction there is only light degeneration in the nucleus isthmo-opticus. In the cerebellum, degeneration is recorded in the mossy fibers in the granular layers of folia I-Vb. Here, the degeneration

is densest in folia IV and V. Light degeneration in the deep cerebellar nuclei is also present at this time (Tanaka *et al.*, 1990; Ehrich *et al.*, 1995a).

Ultrastructural changes induced by most Type-I compounds are also similar. Most lesions are initiated in the larger myelinated axons. Swelling precedes a breakdown of the axonal integrity which then precipitates a "multifocal loss of myelin" (Jortner and Ehrich, 1987). Intramyelinic and intraaxonal vacoulation, intra-axonal collections of normal and abnormal mitochondria, dense and lamellar bodies, and granular degeneration of the neurofilaments, as well as axonal and myelin debris within macrophages and neutrophils are observed subsequently (Bouldin and Cavanagh, 1979b; Abou-Donia *et al.*, 1982; Abou-Donia *et al.*, 1983; Jortner and Ehrich, 1987; Dyer *et al.*, 1992; Ehrich *et al.*, 1995a).

OP compound-induced peripheral nerve degeneration also results in focal intra-axonal collections of mitochondria, dense bodies, and small multilamellar membranous figures, and increases in smooth endoplasmic reticulum-like tubules. A breakdown of axonal neurofilaments within focal "clear" areas follow these changes. Over time, the clear areas expand to involve the entire axon and are associated with focal swelling and the deposition of fine granular material, "flocculent debris", degenerated mitochondria, and dense bodies. Fibers with this amount of damage undergo segmentation and phagocytosis by macrophages and Schwann cells. Schwann cells accomplish this task by migrating into the endoneurial tube left by the degenerating axon. The Schwann cells filling the endoneurial tube (Bands of Bungner) later participate in axonal regeneration as well (Jortner and Ehrich, 1987).

The administration of TPPi or any of its Type-II OPIDN-eliciting structural relatives (tri-o-cresyl phosphite, tri-m-cresyl phosphite, tri-p-cresyl phosphite), results in clinical and pathologic changes in the hen that have some similarity to those elicited by Type I compounds (Carrington *et al.*, 1988; Tanaka *et al.*, 1992). The clinical onset for TPPi-induced OPIDN is approximately 5 days. By 7 days post exposure, hens display mild to moderate ataxia which progresses to severe ataxia and paralysis by 21 days (Carrington *et al.*, 1988; Tanaka *et al.*, 1992). As with Type-I compounds, TPPi initiates degeneration in the spinal cord and brainstem. Unlike Type-I compounds however, TPPi also induces degeneration in other forebrain structures such as the higher-order centers responsible for processing and integrating sensorimotor, visual, and auditory information.

The first TPPi-induced degenerative changes occur by days 5 to 7 post-dosing. Following exposure, swollen axons are seen in the nuclei of the caudal medulla (lateral cervical and lateral reticular nuclei) and the medial portion (gray matter) of the ventral horn of the spinal cord. No lesions are evident before this time. By day 14 an increasing number of brain and spinal cord axons start to degenerate. Swollen axons in the gray matter and peripheral nerves become more evident at this time (Carrington *et al.*, 1988; Tanaka *et al.*, 1992).

The patterns of degeneration are similar on day 14 or 21 post-exposure. Degeneration on day 21 is much denser, however, than day 14 post-exposure tissues. Both spinal cord and peripheral nerve axons and terminals show degeneration and swelling all along their lengths. Specifically, there is dense degeneration in the fasciculis gracilis at cervical levels; moderate to dense degeneration in the

spinocerebellar and medial pontine-spinal tracts at all levels; scattered degeneration in the lateral and ventral funiculi; and terminal degeneration at all levels of the spinal cord, with increased densities in Laminae VII and VIII (Carrington *et al.*, 1988; Tanaka *et al.*, 1992).

Axonal and terminal degeneration are also seen in the medulla and cerebellum at 14 days after TPPi exposure. Axonal degeneration is observed in the spinocerebellar tract; the ventral part of medial longitudinal fasciculus; the spinal lemniscus; the reticular formation; and the fascicles of cranial nerves IX and X. Dense terminal degeneration is also present in the gracile-cuneate, lateral cervical, external cuneate, and lateral paragigantocellular reticular nuclei. The lateral vestibular nucleus is unique in that it contains degenerating axons, terminals, and cell soma. Dense cerebellar degeneration also occurs primarily in the granule cell layers of foliae I-VI by 21 days post-TPPi dosing. Lighter degeneration is additionally seen in the deep nuclei and white matter foliae VII-IX (Carrington *et al.*, 1988; Tanaka *et al.*, 1992).

Midbrain and forebrain involvement make TPPi different from Type-I OPIDN-inducing neurotoxicants. At the peak effect of TPPi, there is heavy axonal degeneration in the paleostriatum primitivum (consistent with the human globus pallidus); ansa lenticularis; lateral spiriform nucleus; and the tegmental nucleus. Moderate axonal degeneration is also seen in the paleostriatum; ansa lenticularis; dorsal intermediate thalamic nucleus (consistent with the human ventral lateral thalamic nucleus); lateral spiriform nucleus; pedunculo-pontine tegmentum (consistent with the human substantia nigra pars compacta); lateral mesencephalic nuclei pars dorsalis; and the deeper layers of optic tectum (Carrington *et al.*, 1988; Tanaka *et al.*, 1992).
Since TPPi exposure affects supplementary midbrain and forebrain structures Carrington *et al.* (1988) postulates that there are "two distinct mechanisms (that) underlie the neurotoxicity of TPPi".

Ultrastructurally, TPPi elicits damage in both perikarya and axons. Perikaryal damage manifests itself as nuclear debris, karyorrhexis, and chromatolysis. Additional TPPi-induced damage in the hindbrain, spinal cord, and peripheral nerve is similar to that caused by Type-I neurotoxicants.

In the adult chicken, perikaryal damage suggestive of neural cell death is only described following exposure to the Type-II OPIDN compound, TPPi. This damage is termed a "neuronal necrosis" by Carrington *et al.* (1988) but the actual mode of cell death (apoptosis or oncotic necrosis) has not been determined. Ultrastructural observations support either mode of cell death.

Embryonic and Juvenile Chicks (*Gallus domesticus*)

The development of clinical OPIDN is strongly dependent on age and species of the test subject. Age susceptibility is explored to its greatest extent in the embryo and juvenile chick model.

Treatment of chick embryos with TOCP results in no clinical signs of OPIDN upon hatching or at subsequent periods. High doses of TOCP do inhibit hatching, however, and increase chick mortality slightly (9%) (Bursian *et al.*, 1982). As with other species, signs that might be attributed to cholinergic toxicity such as diarrhea, generalized muscle weakness, and an inability to stand are also observed after

hatching. These symptoms are coupled to the impairment of leg motor function (Sheets *et al.*, 1987). Leg motor functional impairment is observed in both TOCP and desbromoleptophos treated chicks and is due to altered innervation and damage to the chick leg muscles (Sheets and Norton, 1985; Farage-Elawar *et al.*, 1991). Time of OP compound administration is important for chick embryo development. Desbromoleptophos administration before organogenesis results in structural malformations while administration afterwards only elicits post-hatching paresis (Farage-Elawar *et al.*, 1991).

Treatment of juvenile post-hatch chicks (less than two weeks old) with DFP results in few clinical signs indicative of OPIDN (Peraica *et al.*, 1993). This finding is in contrast to DFP-treated 10 week-old chicks which, at 7 days, develop an ataxia that progresses to paralysis. DFP-treated 10 week-old chicks also develop severe spinal cord lesions after 7 days which correlates to the onset of ataxia (Funk *et al.*, 1994a). Comparable results are obtained in 40 day old chicks. These chicks develop ataxia after a single high dose of DFP. The effects of this treatment are potentiated when PMSF is given after DFP, but ameliorated when given before (Peraica *et al.*, 1993).

Structural and ultrastructural changes in chick sensitive age groups parallel those seen in adult hens. Bilaterally symmetric DFP-induced lesions occur first in the spinal cord gray and white matter and then proceed to the PNS. Specifically, degeneration is found in cervical dorsal column, spinocerebellar, and mid-lateral caudal white matter tracts, and lumbar ventral white matter tracts. In particular, "a higher incidence of neuronal necrosis and chromatolysis" is also found in ventral horn motor neurons of the spinal cord gray matter and in dorsal root ganglia of DFP-exposed groups (Funk *et al.*, 1994a).

As with adult OPIDN, the pathological changes involved in the development of chick OPIDN are described as a "neuronal necrosis". This conclusion implies perikaryal degeneration, but has not been evaluated experimentally. In the chick, OPIDN-inducing OP compounds produce early ultrastructural changes such as chromatolytic neurons with eccentrically located nuclei and abnormally distributed Nissl substance, vacoulation in the white matter and axonal degeneration without astrocytic response in the PNS, centrally placed spheroids with accumulations of neurofilaments and microtubules, increased numbers of mitochondria, and slight swelling and loss of cristae in combination with thinned axonal sheaths. Advanced ultrastructural changes also include abundant tubulovesicular profiles with lamellar vacoules, macrophages containing numerous cytoplasmic vacoules and lamellated membrane, swollen vacoulated mitochondria and rough endoplasmic reticulum, multiple vacoules within the axoplasm, irregularly dispersed neurofilaments, and condensed cytoplasmic filaments and organelles (Funk *et al.*, 1994a). Overall, these observations are supportive of either apoptotic or necrotic modes of cell death.

Japanese Quail (*Coturnix coturnix*), Bobwhites (*Colinus virginianus*), Mallard Ducks (*Anas platyrhychos*), or Ring-necked Pheasants (*Phasianus colchicus*)

Very few studies examine the neuropathic effects of OP compounds on avian wildlife. In one study, Bursian *et al.* (1983) attempts to correlate NTE inhibition with neuropathic effects after oral TOTP administration to four avian species, the quail, bobwhite, mallard duck, and ring-necked

pheasant. Clinical neuropathy is seen in only the ring-necked pheasants, even though whole brain extracts from all species show NTE inhibition of 61 to 70%. The lack of clinical signs in quail following exposure to oral TOTP is administration-route dependent and confirmed by other studies (Varghese *et al.*, 1995b). Dermally administered TOTP elicits mild ataxia in quails after 4 to 10 days. This ataxia later progresses to paralysis (Kinebushi *et al.*, 1993). In contrast, oral dosing of TOTP induces no clinical effects. Interestingly, slight degeneration of the white matter of the cerebellum (cerebellar foliae III-V) is seen upon necropsy of these birds (Varghese *et al.*, 1995b).

Type II OPIDN-eliciting compounds also have neuropathic effects in quails. Dermally administered TPPi results in gross ataxia or paralysis by day 1 or 2 post dosing. These symptoms either completely resolve or result in quail morbidity (Kinebushi *et al.*, 1993). In contrast to this, two studies performed by Varghese *et al.* (1995a, 1995b), report that subcutaneous administration of TPPi results in a slightly later onset of 4 to 7 days.

Specifically, TPPi elicits diffuse axonal and terminal degeneration in the external cuneate nucleus; the gigantocellular, parvocellular, paragigantocellular, and lateral reticular nuclei; the medial, descending, superior, and lateral vestibular nuclei; the red nucleus; the pedunculopontine tegmental nucleus pars compacta; and the lateral spiriform nucleus of the quail. Dense axonal degeneration is also observed in the brachium conjunctivum and brachium conjunctivum descendens; the medial longitudinal fasciculus; the spinal lemniscus; and the ansa lenticularis regions of the brain (Varghese *et al.*, 1995a, 1995b).

Degeneration is present in forebrain visual and auditory tracts. Anterograde degeneration is observed in the nuclei and tracts related to the visual tectofugal system; the brachium of the superior colliculus; the nucleus rotundus; pretectal nucleus; the ectostriatum; and the visuomotor control nuclei. Axonal and terminal degeneration is additionally noted in the lateral mesencephalic nucleus; the nucleus ovidalis; and the area L. of Rose in the caudal neostriatum. These areas are important in the transmission and processing of higher order visuomotor, visual sensory, and auditory sensory information. Qualitative estimates of degeneration reveal that the auditory system is more sensitive to the degenerative effects of TPPi than the visual system (Varghese *et al.*, 1995a, 1995b).

Cerebellar areas are also affected by exposure to TPPi. Dense degeneration occurs in axons and terminals in the white matter and granule cell layers of all cerebellar foliae. Dense terminal and perikaryal degeneration is also observed in the medial and intermediate deep cerebellar nuclei. Lighter degeneration is present in the lateral cerebellar nucleus following exposure (Varghese *et al.*, 1995a, 1995b).

TPPi-induced degeneration of cell perikarya is observed in the lateral and medial cerebellar nuclei; the lateral and medial vestibular nucleus; the ovoid nucleus; the lateral reticular paragigantocellular nucleus; the pedunculopontine tegmental nucleus; and the rotund nucleus in exposed quail (Varghese *et al.*, 1995b). The authors did not assess the mode of neuronal cell death in these areas, however, to qualify somatic degeneration as apoptotic or necrotic.

Summary

Certain OP compounds induce a delayed neurotoxic syndrome (OPIDN) in sensitive species such as chickens and humans. Affected axons undergo a Wallerian-like distal-but-not-terminal degeneration. Neural terminals and perikarya are also affected in some areas of the CNS.

The distribution of degeneration depends on the type of OP compound. Pentavalent OP compounds that induce OPIDN (Type-I) affect peripheral nerves, the spinal cord, the cerebellum, and tracts and nuclei in the medulla and pons. Trivalent OP compounds that induce OPIDN (Type-II) affect additional tracts and nuclei in the midbrain and forebrain.

Perikaryal degeneration is observed following exposure to both Type-I and Type-II compounds. This degeneration has been termed a "neuronal necrosis" even though the actual mode of cell death (apoptosis or oncotic necrosis) has not been determined. Ultrastructural observations support either mode of cell death.

Overall, the above studies suggest that OP compounds detrimentally affect the viability of exposed neural tissues *in vivo*. As with *in vitro* studies, the mechanism behind OPIDN (OP compound-induced cytotoxicity), however, has not yet been linked discretely to any one target system or cell death pathway. Further investigation into these areas may clarify the mechanisms involved.

D. *In Vitro* SH-SY5Y Human Neuroblastoma Model

1. Morphology and Background

SH-SY5Y human neuroblastoma cells are utilized as the *in vitro* model for determining OP-induced cytotoxic effects. The use of neuroblastoma cell lines in describing OP-induced toxicity is supported by previous research (Veronesi and Ehrich, 1993a, 1993b; Ehrich *et al.*, 1994). In addition, others assert that *in vitro* systems can be used to test potential prophylactic OP compound treatments before progressing to *in vivo* models (Hong *et al.*, 1995).

SH-SY5Y cells are derived from a subclone of the SK-N-SH cell line, a primary culture of sympathetic adrenal origin isolated from a bone marrow tumor excised from a 4 year old girl (Baker *et al.*, 1989). Three distinct subtypes of SH-SY5Y cells are described on the basis of morphological differences; a small, rounded, loosely adherent, neuroblast-like form with numerous neuritic processes (N-type), a flattened and highly substrate adherent epithelial-like form (S-type), and an intermediate form (I-type) (Biedler *et al.*, 1988; Hartley, 1996). All three forms can transdifferentiate into each other without chemical stimuli (Ross *et al.*, 1983; Biedler *et al.*, 1988). Sadee *et al.* (1987) report that all three forms have different cytoskeletal structure, second messenger systems, and receptor compositions, but no differences in clathrin subunit composition.

2. Receptors and Cell Signaling

SH-SY5Y cells have approximately 20,000 to 30,000 M_3 muscarinic receptors (Sorenson *et al.*, 1997) per N-type cell (Sadee *et al.*, 1987) in addition to lesser concentrations of M_1 and M_2 muscarinic receptors (Ehrich *et al.*, 1994). These receptors can be stimulated by ACh or muscarinic agonists such as carbachol to activate phosphoinositide-specific phospholipase C (PLC) pathways. Muscarinic activation of these pathways induces an increase in inositol 1,4,5-trisphosphate (IP_3) formation, binding to type-1 and -2 IP_3 receptors, and a biphasic increase in calcium from both extracellular and non-mitochondrial intracellular sources. This reaction is strongly dependent on previous muscarinic receptor activation (which can lead to downregulation of IP_3 receptors) and calcium fill state in the cell (Wilcox *et al.*, 1996). Muscarinic activation is also associated with a minuscule change in current (depolarization). This indicates that extracellular calcium influx is not mediated through L- and N-type voltage sensitive calcium channels (Forsythe *et al.*, 1992). Excessive muscarinic activation leads to clathrin protein-mediated receptor internalization and receptor inactivation (Sorenson *et al.*, 1997).

Veronesi *et al.* (1997) reports that SH-SY5Y cells also possess nicotinic receptors. When stimulated, these depolarize cell membranes and activate voltage dependent Na^+ and K^+ channels but produced little change in calcium levels (Forsythe *et al.*, 1992). Depolarization of cell membranes in both circumstances is similar in differentiated and undifferentiated cells. Perez-Polo *et al.* (1979) report no electrical activity, however, in undifferentiated cell membranes following veratridine stimulation.

SH-SY5Y cells express a variety of other receptor types. Mu- and δ- opioid receptors are present in SH-SY5Y cells (Sadee *et al.*, 1987). Approximately 600 low-affinity nerve growth factor (NGF) receptors are also present per SH-SY5Y cell (Baker *et al.*, 1989), but high affinity NGF (TrkA) and brain-derived neurotrophic factor (BDNF - Trk B) receptors have yet to be elucidated (Itano *et al.*, 1996).

3. Enzymes and Neurotransmitters

SH-SY5Y cells also possess similar biochemical attributes as differentiated neurons. The cells have high levels of dopamine-β hydroxylase (Biedler and Spengler, 1976; Perez-Polo *et al.*, 1979), tyrosine hydroxylase (Ross *et al.*, 1983; Biedler *et al.*, 1988), and ATP synthase (Itano, 1995), enzymes important in creating the neurotransmitters dopamine, norepinephrine, and ATP, respectively. All cell types also express focal adhesion kinase, a molecule important in substrate attachment (Lambert *et al.*, 1994), carboxylesterase, A-esterase, OP-oxidase, and AChE (Ehrich *et al.*, 1995b; Ehrich and Correll, 1998), neurotoxic esterase (Nostrandt and Ehrich, 1992; Ehrich *et al.*, 1995b), and ornithine decarboxylase (Pope *et al.*, 1995), but little monoamine oxidase A or B (Lai, 1997). Specific subpopulations of these cells also express tyrosinase, a melanocyte marker (S-type; Lambert *et al.*, 1994) and reuptake transporters for exocytosed catecholamines such as norepinephrine (N- and I-type; Sadee *et al.*, 1987; Biedler *et al.*, 1988).

4. Nuclear Considerations

SH-SY5Y cells possess many nuclear characteristics that enable them to be a good model for discriminating OP-induced apoptosis. The cells are chromosomally stable and nearly diploid (Perez-Polo *et al.*, 1979). Biedler and Spengler (1976) also note that the cells do not have any chromosomal anomalies (homogeneously staining regions) that are associated with increased enzyme production or drug resistance. Maintenance of stable diploid cultures is important for this dissertation because the primary method for determining nuclear effects is extrapolated from data on diploid DNA quantity. Cells with more than 4N (G_2/M phase cells) DNA content are considered "multiple events" and not included ("gated out") in the data analysis. Analyzing data would have been difficult, therefore, if OP compounds act in a similar manner to microtubule polymerizers such as docetaxal and paclitaxel. These compounds inhibit cytokinesis and lead to increased tetraploidy (8N) and octaploidy (16N) (Riccardi *et al.*, 1995).

5. Cytoskeleton

SH-SY5Y cells have a significant amount of their cytoskeleton determined. Taylor *et al.* (1995) report the presence of intermediate filaments such as vimentin, microtubule associated protein 2 (MAP 2, which functions as an interconnecting bridge between microtubules and neurofilaments), and neurofilaments in undifferentiated SH-SY5Y cells. Five to seven different isoforms of microtubule associated tau protein are also observed (Song and Ehrich, 1997) as well as fodrin, MAP 1 (Shea *et al.* 1995), and actin and β-actin (Sadee *et al.*, 1987; Davidoff *et al.*, 1992). SH-SY5Y cells also have microtubular bundles. Interestingly, these are of similar size and disposition as in *in vivo* neurons (Perez-Polo *et al.*, 1979).

6. Growth and Death

Mattsson *et al.* (1986) and Martin *et al.* (1992) describe that dividing N- and I-type cells were able to express type-I and -II insulin-like growth factor (IGF) receptors. Stimulation of type-I IGF receptors can induce an increase in the growth and metabolic activity in cells (Matthews and Feldman, 1996). Stimulation also initiates a 3 to 5 fold decrease in c-myc expression (Sumantran and Feldman, 1993), an increase in ornithine decarboxylase activity (Mattsson *et al.*, 1986), and a decrease in apoptosis induced by hyperosmotic conditions (150mM sodium chloride media) or metabolic stressors such as serum starvation (Matthews and Feldman, 1996, Singleton *et al.*, 1996). In comparison, stimulation of type-II IGF receptors by autocrines increases the rate of DNA synthesis, cell division, cell growth, and neurite extension (Martin and Feldman, 1993).

Sadee *et al.* (1987) and Hammerling *et al.* (1987) also describe the expression of the intermediate early genes *n-myc* and *c-myc*, and *c-fos* expression, respectively in SH-SY5Y cells. These genes are important in cell proliferation and growth. Levels for *n-myc* expression are not amplified in these cells (Baker *et al.*, 1989) and in some cells *c-myc* regulation is not affected by retinoic acid (RA) differentiation (Lasorella *et al.*, 1995). Amplification of *n-myc* in tumors is associated with increased drug resistance and a poor survival prognosis (Baker *et al.*, 1989).

SH-SY5Y cells also express many regulators of cell death pathways. SH-SY5Y constitutively expresses the anti-cell death, Ced-3 homologue protein, Bcl-2 (Hockenbery *et al.*, 1990; Kromer, 1997). RA- or TPA-induced differentiation or exposure to carbachol, a muscarinic acetylcholine agonist, also induces Bcl-2 levels. In contrast, Bcl-2 expression is reduced by dibutyryl cAMP, forskolin, or cholera toxin treatments. This suggests that positive regulation of Bcl-2 is mediated via protein kinase C while negative regulation is mediated through protein kinase A second messenger pathways (Lasorella *et al.*, 1995; Itano *et al.*, 1996).

Functional proteins involved in DNA repair such as p53 and p21, are also characterized in SH-SY5Y cells (Davidoff *et al.*, 1992; Poluha *et al.*, 1996; Ronca *et al.*, 1997). SH-SY5Y p53 protein has a greater half-life ($t_{1/2}$ of >6 hours versus 15 minutes), however, than in other cell models (Davidoff *et al.*, 1992). These proteins (p53 and p21) are described as switches, in that when DNA damage occurs, they can either elicit an apoptotic response or stop mitosis in order to allow time for DNA repair.

A variety of studies describe the apoptotic or oncotic/necrotic death of SH-SY5Y cells. Cece *et al.* (1995) and Copani *et al.* (1995) report that exposure of SH-SY5Y cells to apoptosis-inducing drugs such as cisplatin, an antineoplastic drug, or the β-amyloid peptide (βAP), a molecule associated with accumulation of amyloid plaques in Alzheimer's Disease, respectively, results in cell death. Hypercondensation of the chromatin adjacent to the intact nuclear membrane, a loss of substrate attachment, shrinking and margination of the nucleus, membrane blebbing, and finally plasma membrane, nuclear membrane, and cytoplasmic disintegration is observed following these exposures (Lambert *et al.*, 1994; Tredici *et al.*, 1995; Ronca *et al.*, 1997). Cisplatin treatment also forces the cells to arrest in the G_2/M phase of the cell cycle before dying (Cece *et al.*, 1995). Interestingly, differentiated SH-SY5Y cells resist cisplatin induced apoptosis (Lasorella *et al.*, 1995). Exposure to βAP induces cells to undergo antigenic modification and upregulate tau epitopes in addition to the above morphological changes. Apoptosis induced by βAP can be blocked by endonuclease inhibitors such as aurintricarboxylic acid but not free radical scavengers such as ascorbate, β-mercaptoethanol, catalase, vitamin E, and neopterin (Li *et al.*, 1996) and the apoptotic mechanism is tentatively linked to irregularities in calcium homeostasis (Copani *et al.*, 1995) and p75 nerve growth factor receptor ($p75^{NGFR}$) expression (Rabizadeh *et al.*, 1994).

SH-SY5Y cells can also be induced to undergo apoptosis by exposure to 2-methoxyestradiol, an endogenous estradiol metabolite, and colchicine, both inhibitors of microtubule polymerization. Both forms of apoptosis are dependent on protein synthesis (Nakagawa-Yagi, 1996; Nakagawa-Yagi, 1994). The former is also dependent on apopain activation and the latter on protein kinase A activity, mRNA synthesis, and CaM II kinase activation.

Other compounds such as MPP^+ (1-methyl-4-phenyl-pyridinium), an active metabolite of MPTP (1-methyl-4-phenyl-1,2,3,6-tetrahydropyridine) which induces Parkinsonian-like symptoms (Itano and Nomura 1995), staurosporine, and H7, both protein kinase inhibitors (Ronca *et al.*, 1997), are able to induce apoptosis in SH-SY5Y cultures. Following exposure, cells undergoing apoptosis have morphological changes comparable to those induced by cisplatin or βAP. MPP^+-induced

apoptosis is different, however, in that it is a mitochondrial respiratory chain inhibitor and does not require any mRNA or protein synthesis (Itano and Nomura 1995).

7. Differentiation

SH-SY5Y cells differentiated by various treatments have biochemical and morphological characters that can be distinct from undifferentiated cells. While differentiation in itself is not important for this study, it can reveal molecular capabilities of the cell. Three primary chemicals are utilized to induce SH-SY5Y differentiation; nerve growth factor (NGF), retinoic acid (RA), and 12-O-tetradecanoyl-phorbol-13-acetate (TPA).

Treatment of naive SH-SY5Y cells with NGF for an extended period of time induces neurite extension, a loss of mitotic ability, increased protein synthesis, and cellular aggregation (Perez-Polo *et al.*, 1979). NGF also induces the upregulation of microtubule-associated protein, ornithine decarboxylase, c-fos, intermediate filament protein, and c-jun as well as the enzymatic activities of DNA polymerase α, DNA methylase, and AP endonuclease. HLA-A, HLA-B, and β2-microglobulin levels are upregulated during NGF differentiation (Jensen *et al.*, 1992). In some cases, differentiation encourages the development of a potential for membrane depolarization and resistance to cell death induced by certain chemicals such as 6-hydroxydopamine (Perez-Polo *et al.*, 1979). Cellular differentiation by the combination treatment NGF and amphidicolin (an inhibitor of DNA polymerases α and δ) increases expression of p21/Waf1, an inhibitor of cyclin-E dependent protein kinases (cdk2 and cdk4) (Poluha *et al.*, 1996). Increased expression of this protein may explain the loss of mitotic ability in differentiated cells, since these kinases and cyclins A, D1, D2, D3, and E are required for the G_1-S transition in the cell cycle. Withdrawal of NGF after terminal differentiation also induces a form of cellular apoptosis not modulated by changes in Bcl-2 or p53 proteins (Jensen *et al.*, 1992).

Exposure of SH-SY5Y cells to RA also results in biochemical and morphological changes. RA induces the elaboration of neurites and increased vacoulation, cellular rounding, and cellular fragmentation. RA-differentiated cells also increases the expression of vimentin and MAP2c (Taylor *et al.*, 1995), an electrically excitable membrane (Forsythe *et al.* 1992), and a 20 to 40 fold increase in *bcl-2* expression (Lasorella *et al.*, 1995). RA differentiation downregulates the expression of *c-myc*, *n-myc*, and *c-fos* in some investigations (Hammerling *et al.*, 1987, Baker *et al.*, 1989) but not in others (Lasorella *et al.*, 1995). In contrast to NGF differentiation, RA-induced *c-myc* downregulation may account for SH-SY5Y cellular differentiation (a loss in mitotic activity). The *c-myc* gene encodes a nuclear transcription factor necessary to trigger the cell into S phase of the cell cycle.

Combination treatments such as RA and low serum (1%) levels are also used to differentiate SH-SY5Y cells. Combination differentiation increases the expression of the high molecular weight neurofilament NF-H, the microtubule associated protein tau (the smallest form of tau), MAP 1-B, and the synaptic vesicle associated protein, synapsin I (Hartley *et al.*, 1996).

SH-SY5Y cells treated with TPA reveal morphological and biochemical changes indicative of differentiation. SH-SY5Y cells develop neurites and cytoplasmic neurosecretory granules, show a 2 fold

increase in the activity of neuron-specific enolase, and a 30 to 40 fold increase in noradrenaline and adrenaline concentrations following TPA exposure (Påhlman *et al.*, 1981). Downregulation of *c-* and *n-myc*, upregulation of *c-fos* expression (Hammerling *et al.*, 1987), and upregulation of Bcl-2 (Itano *et al.*, 1996) also occurs during TPA differentiation. In addition, Mattsson *et al.* (1986) reveals that differentiation of SH-SY5Y cell with TPA abolishes the mitogenic response to IGF I and II.

Summary

SH-SY5Y cells are used as an *in vitro* model for numerous disease processes associated with the nervous system. These investigations reveal subcellular information (nuclear function and mitotic effects, enzyme activities, receptor densities, cytoskeletal construction, membrane and second messenger systems) which assist in explaining pathological effects for many of these processes. Exhaustive description of these factors is necessary because of the breath of secondary hypotheses in this dissertation. Secondary hypotheses cover the entire process of cell death including initiation, execution, and potential terminal substrates. Much of the information above undoubtedly contributes to such processes.

Investigations involving SH-SY5Y cells also demonstrate that numerous cell death pathways can be activated in different manners. This is of principal importance for this dissertation, since the primary hypothesis involves determining the mode of cell death (apoptosis versus necrosis) induced by OP compounds.

PART III

MATERIALS AND METHODS

Chapter 2

EXPERIMENTAL METHODS AND PROTOCOLS

Methods for both *in vitro* and *in vivo* experiments were utilized in this dissertation. They tested the hypothesis that cytotoxic concentrations of OP compounds induce an apoptotic form of cell death. Secondary hypotheses investigating the involvement of subcellular organelles or structures in the initiation and execution of cytotoxicity were also tested in the following studies:

Chapter 3. This study established baseline culture parameters such as seeding density and media changes for SH-SY5Y and IMR-32 human neuroblastoma cell lines. Standardization of culture parameters allowed background cytotoxicity to be minimized and experimental variation to be reduced. Four endpoints were assessed: culture confluency, total cell number, membrane integrity, and DNA content.

1) Culture confluency, or the relative amount of occupied space on the culture dish, was estimated by phase contrast microscopy.

2) Total cell number was microscopically assessed by utilizing Trypan blue and a coverslipped hemocytometer.

3) Membrane integrity was microscopically assessed by utilizing Trypan blue and a coverslipped hemocytometer.

4) DNA composition was evaluated by using propidium iodide and flow cytometric techniques. Data files were subsequently processed through Multicycle DNA Cell Cycle Analysis Software (version 3.11 - Phoenix Flow Systems, Inc., San Diego, CA).

Chapter 4. This study established OP compound-induced cell cycle effects in SH-SY5Y human neuroblastoma cells. Evaluating alterations in the cell cycle allowed nuclear function to be assessed. One method was used to estimate the relative amount of DNA in cells following exposure.

1) DNA composition was evaluated by using propidium iodide and flow cytometric techniques. Data files were subsequently processed through Multicycle DNA Cell Cycle Analysis Software (version 3.11 - Phoenix Flow Systems, Inc., San Diego, CA).

Chapter 5. This study established OP compound-induced alterations in SH-SY5Y human neuroblastoma mitochondria, DNA, and substrate adherence. Evaluating these parameters allowed mitochondrial function, genetic integrity, and plasma membrane perturbations to be determined. Methods were used to assess structural changes in mitochondria, alterations in the mitochondrial transmembrane potential, DNA fragmentation, and substrate adherence.

1) Structural changes in mitochondria were observed by utilizing rhodamine 123 and fluorescence microscopy.

2) Alterations in the mitochondrial transmembrane potential were assessed by utilizing rhodamine 123, fluorescence microplate spectrophotometry, and flow cytometric techniques.

3) DNA composition was evaluated by using propidium iodide and flow cytometric techniques. Data files were subsequently processed through Multicycle DNA Cell Cycle Analysis Software (version 3.11 - Phoenix Flow Systems, Inc., San Diego, CA).

4) Substrate adherence was determined by using a hemocytometer and light microscope to count cells in OP compound-exposed plates (adherent cells) and plates with wash media (non-adherent cells). The percent of adherent cells was then calculated using the formula: [adherent cells/(adherent cells+non-adherent cells)] x 100.

Chapter 6. This study established OP compound-induced alterations in SH-SY5Y human neuroblastoma cell f-actin and total protein. Evaluating these parameters allowed cytoskeletal disturbances to be revealed. Methods were used to assess structural changes in f-actin, alterations in the concentration of f-actin, and the concentration of total protein.

1) Structural changes in f-actin were observed by utilizing Alexa™ 488 phalloidin and fluorescence microscopy.

2) Alterations in the f-actin concentration were assessed by utilizing Alexa™ 488 phalloidin and flow cytometric techniques. Data files generated by the flow cytometer were then processed through Epics XL Flow Cytometry Workstation software.

3) Protein concentrations were determined by staining with a dye that has an affinity for protein and spectrophotometry. SOFTmax PRO software was used to normalized samples to mg/ml of protein.

Chapter 7. This study established OP compound-induced modes of cell death in SH-SY5Y human neuroblastoma cells. Evaluating the mode of cell death allowed changes in nuclear morphology, DNA integrity, and protease activation to be resolved. Methods were used to assess structural changes in nuclei, nuclear fragmentation, DNA fragmentation, caspase-3 activation, and ultrastructural alterations.

1) Structural changes in nuclei were observed by utilizing Hoechst 33342 and fluorescence microscopy.

2) Alterations in DNA fragmentation were assessed by agarose gel electrophoresis. Banding patterns of propidium iodide labeled DNA were then visualized with a UV transilluminator.

3) Caspase-3 activation was determined by fixing OP compound exposed cells with a Cytofix/Cytoperm™ Kit, staining with fluorescently labeled anti-active caspase-3 antibodies, and analyzing using flow cytometric techniques.

4) Ultrastructural alterations were determined by using techniques associated with transmission electron microscopy.

Chapter 8. This study established the distribution and extent of OP compound-induced neurodegeneration in white Leghorn hen brain and spinal cord tissues. Evaluating these parameters allowed confirmation that OPIDN occurs. It also prioritized neuropathic regions for a subsequent study involved in assessing the mode of cell death. Methods were used to assess clinical deficits and the distribution and extent of histopathological alterations following exposure to OP compounds.

1) Clinical deficits were estimated by utilizing a simple 7 point scoring technique derived from Stumpf *et al.* (1989). Deficits ranged from none to severe leg paralysis.

2) Histopathological alterations were discerned by utilizing Fluoro-Jade, a stain for degenerating neurons, and fluorescence microscopy.

Chapter 9. This study established the mode of cell death (apoptosis versus oncotic necrosis) in white Leghorn hen brain and spinal cord tissues. Evaluating the mode of cell death allowed previous *in vitro* investigations to be validated. Methods were used to assess the type and distribution of histopathological alterations following exposure to OP compounds.

1) Histopathological sections were stained with the TdT-FragEL™ DNA fragmentation kit in order to detect apoptotic and necrotic cells by light microscopy.

2) Histopathological sections were stained with a monoclonal antibody to single-stranded DNA (F7-26) in order to detect apoptotic cells by light microscopy.

3) Histopathological sections were stained with Hoechst 33342 dye in order to detect apoptotic morphological changes in nuclei by fluorescence microscopy.

Statistics. Statistical validity of quantitative *in vitro* data points ($p<0.05$) was determined by utilizing PC-SAS software (version 6.1) to perform an analysis of variance (ANOVA) followed by Duncan's Multiple Range Test.

PART IV

RESULTS

Chapter 3

Human Neuroblastoma Cell Viability and Growth are Affected by Altered Culture Conditions

Kent Carlson and Marion Ehrich

Submitted to In Vitro Toxicology

Virginia-Maryland Regional College of Veterinary Medicine,
Blacksburg, Virginia, 24061

ABSTRACT

The effects of differing culture parameters are seldom investigated, even though they influence the way immortalized cells grow and die. In this study, the changes in total cell number, confluency, membrane permeability, and DNA content were evaluated in SH-SY5Y and IMR-32 human neuroblastoma cells following culture at different seeding densities and media consistencies. These four endpoints were determined using a hemocytometer, phase-contrast microscope, trypan blue (0.4% v/v), and propidium iodide (50μg/ml), respectively. Both cell lines (SH-SY5Y and IMR-32) responded in a similar manner to changing culture conditions, even though baseline values for all four endpoints were different. Significant seeding density-dependent changes in all four parameters were observed over time in both cell lines ($p<0.05$), with the largest effects being observed in confluency and total cell number. Daily media changes also significantly altered the four assay endpoints in a time-dependent fashion ($p<0.05$). DNA content (percent of cells in G_0/G_1, S, and G_2/M phase) was primarily affected by media changes. Results suggest that environmental culture conditions greatly affect cellular mitosis and death. This information may be of particular relevance in the investigation of compounds that act on specific cell cycle stages, such as antineoplastic agents.

INTRODUCTION

In vitro toxicity testing offers a wide range of scenarios for toxicant exposure and a large variety of available species and tissue type cells to test when compared to *in vivo* alternatives (Costa, 1998). As with *in vivo* studies, the response of toxicant and cell type depends largely on the conditions of exposure. Uniformity of exposure conditions enables toxicant-induced changes to be discerned from background events.

Two conditions of primary importance in maintaining exposure uniformity in cell cultures are the initial amount of cells per well, termed the seeding density, and the condition of the media. These two factors affect cell-to-cell contact and communication, and cell metabolism, growth, and division, respectively. Alterations in seeding density can change cellular response to toxicants (Hunter *et al.,* 1993). Changing media conditions can also alter the cytotoxic sensitivity of cells (Pissiotis and Spangberg, 1993). Seeding density- and conditioned media-induced effects on SH-SY5Y and IMR-32 human neuroblastoma cell lines are reported primarily as they relate to the production of secreted factors (Meghani *et al.*, 1993; Hirose *et al.*, 1994; Babajko *et al.*, 1997; Cedazo-Minguez *et al.*, 1999), cell survival (Kamio et al., 1989; Yu and Zuo, 1997), or morphological changes (Sonnenfeld and Ishii, 1982). Other information on the mitotic status of these cells under varying culture conditions has not been published. These cell types (human) do not have *in vivo* alternatives for testing toxicological endpoints, so it is important to assess the effect of seeding density and media condition in these model cell cultures prior to initiating experimentation.

The effect of exposure conditions on cell growth and viability can be evaluated on a cellular or subcellular basis. Evaluations at the cellular level include total cell counts and estimations of cell confluency (Cook and Mitchell, 1989). Determination of these can illustrate cell reproductive patterns and the potential effects of cell-to-cell contact. Alterations at the subcellular level can be determined by observing changes in membrane permeability or DNA content (Abdulla and Campbell, 1997). Both parameters can be used as estimates of viability. Estimation of DNA content also indicates culture-induced cell cycle effects, which is of importance when screening compounds that act on a specific cell cycle stage such as antineoplastic drugs (Riccardi *et al.,* 1995). In any case, utilization of both cellular and subcellular criteria enable an accurate description of culture environment-induced alterations.

Cultured cell lines such as SH-SY5Y and IMR-32 are used to model the toxicological mechanisms underlying *in vivo* cancers and neurodegenerative processes. Both SH-SY5Y and IMR-32 cell lines are derived from human neuroblastoma tissue. SH-SY5Y clonal cells are roughly diploid and genetically stable (Perez-Polo *et al.,* 1979). IMR-32 cells are also diploid but possess abnormal homogeneously staining regions on their chromosomes (Biedler and Spengler, 1976). These two cell lines have been used to examine mechanisms associated with Alzheimer's disease (Morelli *et al.,* 1999; Zhong *et al.,* 1999), Parkinson's disease (Cassarino *et al.,* 1997; Fall and Bennett, 1999), and amyotrophic lateral sclerosis (Carri *et al.,* 1997). They have also been utilized to define subcellular changes associated with exposure to environmental neurotoxicants such as organophosphorus compounds (Veronesi and Ehrich, 1993; Carlson and Ehrich, 1999). This versatility has prompted

some to recommend *in vitro* systems for routine use in neurotoxicant screening batteries (Veronesi, 1992).

This study evaluated changes in SH-SY5Y and IMR-32 human neuroblastoma cell number, confluency, membrane permeability, and DNA content following exposure to variable culture conditions. Culture-induced effects of toxicological importance such as cell cycle shifts, increased morbidity, or cell contact inhibition could be estimated in this manner. Culture factors with methodological relevance such as total cell number per well or confluency over time could also be evaluated using these methods. This information is important because it illustrates that culture factors of seemingly little consequence can grossly affect the outcome of endpoints typically assayed in *in vitro* toxicological testing or screening batteries.

EXPERIMENTAL METHODS

Chemicals. Hoechst 33342 and propidium iodide (PI) were acquired from Molecular Probes (Eugene, OR). Trypan blue was purchased from Sigma Chemical Co. (St. Louis, MO).

Cell Culture. IMR-32 (ATCC; Rockville, VA) and SH-SY5Y human neuroblastoma cells from two sources (gifts from Dr. J. Biedler (SY5Y-B), Sloan-Kettering Memorial Cancer Center, NY, and Dr. K. Perez-Polo (SY5Y-KT), University of Texas, Galveston) were cultured as described by Ehrich *et al.* (1995). All three cell types (passages 52-57, 51-57, and 41-46, respectively) were grown in Hams F12 medium (Sigma) supplemented with fetal bovine serum (FBS - 15% v/v) supplied by Gibco (Grand Island, NY) in order to maintain predominately neuroblast morphologies. Prior to confluency, cells were harvested using 0.25% trypsin (Sigma) and seeded onto plastic 96 well microtiter plates (Corning; Corning, NY) or 8 well Labtek multichamber glass slides (Nunc; Rochester, NY) at 1, 2, 4, or $8x10^5$ cells/ml (4800, 9600, 19200, and 38400 cells/cm^2). The cells were then allowed to grow at 37°C and 5% CO_2 for 1-7 days prior to fixation. Half of the samples had 67% of their media exchanged daily.

Culture Confluency. Culture confluency, or the relative amount of occupied space on the culture dish, was estimated at daily intervals by phase contrast microscopy. Observations were made at 200X with a Nikon Diaphot TMD inverted microscope.

Total Cell Number and Trypan Blue Dye Exclusion Evaluation of Membrane Integrity. Following incubation, cells were harvested and dissociated using 0.25% trypsin (Sigma). Trypan blue (Sigma) was then added (0.4% v/v), mixed, and the cell suspension was subsequently pipetted onto a coverslipped hemocytometer. Live and dead cells were counted for each sample, with dead cells being discriminated by the incorporation of trypan blue. Percent of cells with membrane impairment were calculated by the equation: [cells with trypan blue cytoplasm / (cells with trypan blue cytoplasm + cells with bright cytoplasm)] X 100.

Flow Cytometric Evaluation of DNA Content. DNA composition was evaluated by using PI and the cell culture methods described above. Following incubation, the treatment media were replaced by 75µl each of a PI buffer (PBS containing 50µg/ml PI, 1% FBS, and 0.1% sodium azide) and Vindelov's reagent (0.01M Tris, 10mM NaCl, 700U RNAse A (Sigma), 50µg/ml PI, and 0.1% of Igepal-40 (Sigma)). The microtiter plates were incubated overnight at 4°C to allow cellular DNA to saturate with fluorochrome (Robinson *et al.,* 1993). A Coulter Epics XL-MCL flow cytometer was then utilized to analyze these samples (excitation 535nm - emission 617nm). Listmode files generated by the flow cytometer were processed through Multicycle DNA Cell Cycle Analysis Software (version 3.11 - Phoenix Flow Systems, Inc., San Diego, CA) to generate objective estimates of DNA content. Initial incubation points were used as standards to assign software parameters. Cell cycle status was determined by evaluating the content of DNA per cell (Robinson *et al.*, 1993). Representative flow cytometry histograms for propidium iodide can be seen in Appendix A.

Statistics. Each quantitative experiment had between 3 and 16 normalized data points (percentages) for each time and OP concentration. Data were converted into the percent of control and then graphed

as the mean ± the standard deviation. Statistical significance ($p<0.05$) was determined by utilizing PC-SAS software (version 6.1) to perform an analysis of variance (ANOVA) followed by Duncan's Multiple Range Test.

RESULTS

Culture Confluency.

Culture confluency was estimated in order to qualify the effects of cell-to-cell contact in differing culture conditions. Cultures without media changes initially underwent a seeding density-dependent increase in confluency (Fig. 3.1a). Cultures with high seeding densities (19200 and 38400 cells/cm^2) declined in confluency following 7200 minutes of incubation. The decline in confluency was accompanied by a qualitative increase in floating cells and debris. Cultures with daily media changes also increased confluency in a seeding density-dependent manner (Fig. 3.1b). No decline in confluency was seen after these cells reached maximal levels, however.

Statistically significant differences in confluency were observed in SY5Y-B cultures when comparing different seeding densities (Fig. 3.1a and 3.1b; $p<0.05$). Similar seeding density-dependent changes in confluency were seen in SY5Y-KT and IMR-32 cultures (data not shown).

Daily media changes significantly increased SY5Y-B confluency at later incubation periods (>7200 min) and in low seeding density (4800 cells/cm^2) cultures when compared to those with no media changes (Fig 3.1a and 3.1b; $p<0.05$). Daily media changes also significantly increased confluency in SY5Y-KT cultures at incubation periods >2880 min (19200, 9600, and 4800 cells/cm^2 seeding densities) and following long incubations (10080 min) in cultures with large initial seeding densities (38400 cells/cm^2) (data not shown; $p<0.05$). In contrast, changing the media in IMR-32 cultures induced significant changes in confluency only at the highest (38400 cells/cm^2) and lowest (4800 cells/cm^2) seeding densities at incubation periods >5760 min (data not shown; $p<0.05$).

Total Cell Number and Trypan Blue Dye Exclusion Evaluation of Membrane Integrity.

Total cell number was determined in order to evaluate the kinetics of culture growth. In cultures without media changes, the total number of cells initially increased, peaked, and then decreased over time for all seeding densities (Fig. 3.2a). Changing two-thirds of the media every day delayed or abolished peaks and induced a progressive increase in cell number in most circumstances (Fig. 3.2b).

Statistically significant differences in total cell number were observed solely between cultures with the highest seeding densities (Fig. 3.2a and 3.2b, $p<0.05$). Cultures with high seeding densities (38400 cells/cm^2) also reached peak growth earlier and had 2.53X (IMR-32), 3.60X (SY5Y-KT), or 4.16X (SY5Y-B) more cells per well at maximum than those with the lowest initial seeding density (4800 cells/cm^2).

Interestingly, the maximal cell numbers per cell type also differed. IMR-32 had consistently more cells (1.09-1.62X) per well at peak density than SY5Y-KT, which in turn outnumbered SY5Y-B (1.25-1.72X). Although daily media changes did increase the total number of cells per well, IMR-32 still had more cells (0.75-1.48X) than SY5Y-KT, which in turn had more cells (1.38-1.50X) than SY5Y-B.

Daily media changes significantly increased the total number of SY5Y-B cells in cultures seeded at high density (38400 and 19200 cells/cm^2) at incubations >7200 min when compared to cultures with no media changes ($p<0.05$). Fresh media also significantly increased the number of SY5Y-KT cells per well in cultures seeded at lower density (19200, 9600, 4800 cells/cm^2) or high density (38400 cells/cm^2) at incubation periods >8640 min, and >5760 min, respectively (data not shown; $p<0.05$). IMR-32 cultures with high initial seeding densities (38400 and 19200 cells/cm^2) significantly increased in number at incubations >7200 min following daily media changes (data not shown, $p<0.05$).

Cell membrane integrity was utilized as an estimate of culture viability. Gradual decreases in membrane integrity were seen in all culture types in a seeding density-dependent manner (Fig. 3.3a and 3.3b). Cultures with daily media changes increased the retention of membrane integrity only in the highest density culture at later incubation periods.

Seeding density-dependent differences in membrane integrity were present only between high density cultures seeded at 19200 and 38400 cells/cm^2 following 10080 min incubations (Fig. 3.3a; $p<0.05$). Daily media changes significantly improved membrane integrity for SY5Y-B cultures seeded at high density (38400 cells/cm^2) at incubations > 8640 min ($p<0.05$). Fresh media also improved membrane integrity for SY5Y-KT cells seeded at high density (38400 cells/cm^2) at incubations >7200 min, and IMR-32 cells seeded at all densities (38400, 19200, 9600, 4800 cells/cm^2) for incubations >7200 min (data not shown; $p<0.05$).

Flow Cytometric Evaluation of DNA Content.

Flow cytometric estimation of cellular DNA content was used in order to observe changes in the distribution of cells in various cell cycle stages (G_0/G_1, S, G_2/M). The determination of cells with "subG_1" or fragmented DNA also was evaluated in order to complement trypan blue estimates of viability.

SY5Y-B cultures without media changes underwent a density-dependent increase in G_0/G_1 stage cells (Fig. 3.4a). For SY5Y-B, the number of G_0/G_1 stage cells plateaued at 2880 to 7200 min and subsequently declined. In contrast, daily media changes reduced the number of G_0/G_1 stage cells of SY5Y-B cultures in a density-dependent manner (Fig. 3.4b). Following a minimum at 2880 min, the amount of G_0/G_1 cells in these cultures increased gradually.

Seeding density-induced significant differences in the number of G_0/G_1 cells were intermittently observed in SY5Y-B cultures with and without media changes (Fig. 3.4a and 3.4b; $p<0.05$). Daily media changes significantly decreased the number of G_0/G_1 phase cells in all SY5Y-B cultures at incubations >2880 min ($p<0.05$). Media changes also significantly decreased the number of G_0/G_1 phase SY5Y-KT and IMR-32 cells in cultures seeded at higher densities (38400, 19200, 9600 cells/cm^2) at incubations > 4320 min, and in cultures seeded at lower density (4800 cells/cm^2) following incubations for >8640 min (data not shown; $p<0.05$).

The number of S phase cells declined in a seeding density-dependent manner in cultures without media changes (Fig. 3.5a). For SY5Y-B cultures of all seeding densities, this trend continued until approximately 4320 min, whereupon the number of S phase cells gradually started increasing. Media changes, in contrast, induced an initial increase in S phase cells in SY5Y-B cultures (Fig. 3.5b). After reaching a maximum, the number of S phase cells decreased for cultures seeded at lower densities (9600 and 4800 cells/cm^2) but changed only marginally for others.

Significant seeding density-induced changes in the number of S phase SY5Y-B cells were observed at irregular intervals in cultures with and without media changes (Fig. 3.5a and 3.5b; $p<0.05$). Changing the media significantly increased the number of S phase cells at all seeding densities in SY5Y-B cultures between 2880 and 5760 min ($p<0.05$). Media changes also significantly increased the number of S phase SY5Y-KT cells in high seeding density cultures (38400 and 19200 cells/cm^2) at incubations >2880 min and in lower seeding density cultures (9600 and 4800 cells/cm^2) at incubations >5760 min (data not shown; $p<0.05$). In addition, changing the media significantly increased the number of S phase IMR-32 cells seeded at high density (38400 cells/cm^2) when incubating >2880 min and in low seeding density IMR-32 cultures (9600 and 4800 cells/cm^2) at incubations >4320 min (data not shown; $p<0.05$).

The proportion of G_2/M phase cells in SY5Y-B cultures decreased in number following incubation for >2880 min without media changes (Fig. 3.6a). The amount of G_2/M phase cells in lower seeding density SY5Y-B cultures (4800, 9600, 19200 cells/cm^2) subsequently achieved a minimal plateau. In contrast, SY5Y-B cultures seeded initially at 38400 cells/cm^2 continued to decline in the number of G_2/M phase cells. The number of G_2/M phase cells in SY5Y-B cultures with daily media changes remained elevated and fairly constant (Fig. 3.6b). Marginal increases in the number of G_2/M phase cells were seen in higher seeding density (38400 cells/cm^2) SY5Y-B cultures with media changes.

Seeding density did not induce any significant changes to the number of G_2/M phase SY5Y-B cells. Daily media changes, however, significantly increased the number of G_2/M phase SY5Y-B cells at incubations >2880 min ($p<0.05$). Daily media changes also significantly increased the number of G_2/M phase cells in SY5Y-KT cultures initially seeded at high density (38400 and 19200 cells/cm^2) between 2880 and 7200 min and those seeded at low density (9600 and 4800 cells/cm^2) at later incubations (10080 min) (data not shown; $p<0.05$). Changing the media daily had a less significant effect on the proportion of G_2/M phase IMR-32 cells. Media changes induced significant differences for IMR-32 cultures at all seeding densities only at incubations >7200 min (data not shown; $p<0.05$).

Seeding density-dependent changes in the proportion of subG_1 phase cells were seen in cultures with and without media changes. The number of subG_1 cells in SY5Y-B cultures without media changes initially stayed the same in cultures seeded at high density (38400 and 19200 cells/cm^2) or decreased in cultures seeded at low density (9600 and 4800 cells/cm^2) to a minimal level by 4320 minutes (Fig. 3.7a). The proportion of subG_1 cells subsequently increased in all density SY5Y-B cultures at incubations >7200 min The number of subG_1 cells in cultures with media changes initially paralleled seeding density-dependent relationships seen in cultures without media changes (Fig. 3.7b).

Comparatively, the proportion of subG$_1$ cells in SY5Y-B cultures with media changes increased only marginally following 7200 min, however.

Seeding density significantly affected the number of subG$_1$ cells in SY5Y-B cultures at incubation periods <2880 min (Fig. 3.7a and 3.7b; $p<0.05$). Daily media changes, however, only had marginal effects on altering the proportion of subG$_1$ cells. Fresh media induced significant decreases in the number of subG$_1$ cells in SY5Y-B cultures at all seeding densities only in incubations >8640 min ($p<0.05$). Changing the media in SY5Y-KT and IMR-32 cultures significantly decreased the proportion of subG$_1$ cells in cultures seeded at high density (38400 cells/cm^2) at the latest (8640 and 10080 min) and earliest (2880 min) time points (data not shown; $p<0.05$). In addition, changing the media in low seeding density SY5Y-KT cultures (4800 cells/cm^2) significantly decreased the number of subG$_1$ cells in early (1440 and 2880 min) and late (8640 min) incubations (data not shown; $p<0.05$).

DISCUSSION

Culture conditions influence the growth and death of cells in all *in vitro* models and hence, are important to assess prior to initiating drug screening or toxicological testing. The present study evaluates the effects of changing culture conditions (seeding density and media changes) on the confluency, number, membrane integrity, and DNA content of SH-SY5Y and IMR-32 human neuroblastoma cell lines.

Daily media changes significantly affected a majority of the investigated parameters. Both SY5Y and IMR-32 cell lines responded to changes in media by increasing the total cell number per well, increasing the confluency and membrane integrity in high density cultures, and by increasing the proportion of cells in reproductive phases of the cell cycle. The mechanisms behind these increases are not known, but induction of these conditions in other cultures has been shown to be related to nutrient (glutamine) load or the accumulation of inhibitory substances such as ammonia (Butler, 1985).

The number of SY5Y or IMR-32 cells in a particular cell cycle stage (G_0/G_1, S, G_2/M) were most obviously affected by media changes. Changing the media decreased the proportion of G_0/G_1 cells and increased the amount of those in S and G_2/M phase of the cell cycle. The proportion of cells in each phase in cultures with media changes remained similar over time, even following total culture confluency (saturation). This suggested that the cells in all phases had become quiescent (Drewinko *et al.,* 1984) or had been released from contact inhibition and were forming multilayer matrices. Microscopic observations revealed limited multilayer formation in SY5Y and hence led credence to both ideas.

Cell cycle information could be critical when testing compounds such as anti-cancer agents or environmental pollutants. The cytotoxic activity of many of these compounds are restricted to cells in a particular phase of the cell cycle. For example, Bruno *et al.* (1992) reported that DNA topoisomerase I (camptothecin) or II (teniposide) selectively killed G_0 phase thymocytes. Others using the same compounds in HL-60 cultures observed a selective elimination of S, G_2, or M phase cells (Del Bino *et al.,* 1991). In addition, Riccardi *et al.* (1995) and Ponce *et al.* (1994) demonstrated that the cytotoxicity of chemotherapeutic agents such as taxanes or the environmental pollutant, methyl mercury, were dependent on the proportion of G_2/M phase cells. By extrapolation, the cell cycle-selective cytotoxicity of these compounds in SY5Y or IMR-32 cultures would therefore be critically dependent on media changes.

The effects of media condition are typically not controlled well in many studies and hence, could induce situations in which unexpected results are generated. This may be the situation in Spengler *et al.* (1986), who reported variable efficacy with chemotherapeutic agents in neuroblast cells, but attributed the responses to differences in cellular differentiation or morphology. The variations reported may have been related to media conditions, because our data show that alteration of the media strongly influences the distribution of cells in the cell cycle without respect for cell type or seeding density.

Seeding density also had a large effect on culture growth and death. Altering the initial culture density primarily affected the time to culture confluency, the total number of cells per well, and the

plasma membrane integrity. The differentiation of neural cells (Kitani *et al.,* 1997), fidelity of DNA replication (Boesen *et al.,* 1994), and the expression of various proteins such as myofibrils and actin (Campbell *et al.,* 1989), and erythropoetin (Hagiwara *et al.,* 1984) have also been show to be dependent on culture seeding density.

The time to confluency was most affected by seeding density. As in other studies (Hagiwara *et al.,* 1984), cultures with higher initial seeding densities reached confluency earlier than those of low density. This relation was initially independent of media condition. As time in culture progressed, however, this status changed to media dependent, with higher seeding density cultures being affected by "stationary phase aging" and death to a greater extent that low seeding density cultures (Liu, 1999).

Total cell number was affected predominately by seeding density as well. It was also strongly influenced by media changes and was independent of culture confluency at latter time points. This suggested that cell-to-cell contact inhibition was not an important factor governing culture growth for these cell lines. As mentioned previously, this conclusion was supported by light microscopic observations of multilayer SY5Y cells and focal multilayers (towers) of IMR-32 cells.

The seeding density also greatly affected the culture doubling time, as estimated by the total cell number. Similar circumstances have been described for aortic endothelial cells (Duthu and Smith, 1980). Doubling estimates calculated from different seeding density groups for the first three days in culture (SY5Y-B, 36-43.2 hr; SY5Y-KT, 20.1-25.4 hr; IMR-32, 16.3 - 27 hr) bracketed earlier estimates (SK-N-SH, 36 hr; IMR-32, 26 hr) reported by Seeger *et al.* (1977). Daily media changes marginally decreased doubling time (SY5Y-B, 30.9-45.5 hr; SY5Y-KT, 19.6-28.8 hr; IMR-32, 16.6-24.7 hr) but had little effect on the seeding density-doubling time relation in log phase cells. A slight decrease in doubling time was not unexpected because increases in proliferation have been shown to occur in other hematopoetic (McAdams *et al.,* 1996) and neural stem (Kallos and Behie, 1999) cell cultures following media changes.

The proportion of cells in each cell cycle phase were affected to a lessor extent by seeding density. The highest density cultures had the largest proportion of cells in G_0/G_1 phase and the lowest proportion of cells in S and G_2/M phase. In cultures without media changes, the number of G_0/G_1 phase cells increased and S and G_2/M phase cells decreased as 100% confluency was achieved. Daily media changes preserved the seeding density relationship but maintained the cultures in reproductive phase, namely a smaller proportion of G_0/G_1 cells, and higher proportions of S and G_2/M phase cells. This relationship continued after 100% confluency was achieved indicating that cell-to-cell contact was less important than media condition in determining reproductive potential for these cells. Seeding density-induced alteration of the proportion of cells in a cell cycle phase could affect the outcome of *in vitro* testing with drugs such as antineoplastics.

Seeding density also affected culture viability to a greater extent than media changes when observing propidium iodide data. Low density cultures exhibited a significant amount of cell death initially after plating. Higher density cultures, in contrast, had a greater proportion of dying cells after extended culture. Low density cell death may be related to lower oxygen tolerances of low density

cultures (Balin *et al.,* 1984), a lack of cell-to-cell contact, or a lack of cell-produced trophic factors. Because media changes exacerbated early death in these low density cultures, autologous trophic factor production may be the more likely explanation. In any case, the use of cell cultures under low density conditions could exaggerate the estimation of toxicant-induced cell death.

Trypan blue estimates of viability in low density cultures contradicted those that were generated from propidium iodide in the initial time points (<4320 min). Conflicting viability data may represent genuine differences or result from methodological problems. Discrimination of cell death by using trypan blue relies on diffusive penetration of the dye through compromised membranes. This measure of viability therefore underrepresents cell death in which primarily intracellular damage is occurring (Cook and Mitchell, 1989; Thajeb *et al.,* 1997). In contrast, when using flow cytometric DNA cell cycle analysis techniques, the resolution of DNA-bound propidium iodide can occur long before membranes are compromised.

The fragmentation of DNA prior to membrane integrity occurs predominately in apoptotic forms of cell death and is often seen as a consequence of cell senescence (Barrett and Preston, 1994). The loss of membrane integrity in apoptotic cells doesn't occur until after the cell has partitioned into membrane-bound particles (Majno and Joris, 1995; McCarthy and Evan, 1998). These particles are typically overlooked when counting cells via trypan blue. Therefore, results suggest that immediately after plating, a complement of neuroblast cells die via apoptotic mechanisms.

It is necessary to assess culture parameters that affect cell growth and death prior to using the model for drug screening or toxicological testing. This study suggests that culture density and daily media changes significantly affect total cell numbers, confluency, viability, and the proportion of SH-SY5Y and IMR-32 cells in various stages of the cell cycle. The strong correlation between media condition and cell cycle phase especially warrants attention from investigators identifying, testing, and describing mechanisms for new cancer chemotherapeutic agents.

ACKNOWLEDGMENTS

We wish to thank Joan Kalnitsky for flow cytometric assistance. This work was supported by EPA grant R825356 and funds from the Virginia-Maryland Regional College of Veterinary Medicine.

REFERENCES

Abdulla, E.M. and Campbell, I.C. (1997). Chapter 7, Studies of neurotoxicity in cellular models, in: *In Vitro Methods in Pharmaceutical Research*. Academic Press, Ltd.: NY, pp. 155-180.

Babajko, S., Leneuve, P., Loret, C., and Binoux, M. (1997). IGF-binding protein-6 is involved in growth inhibition in SH-SY5Y human neuroblastoma cells: its production is both IGF- and cell density-dependent. *J. Endocrinol.* 152, 221-227.

Balin, A.K., Fisher, A.J., and Carter, D.M. (1984). Oxygen modulates growth of human cells at physiologic partial pressures. *J. Exp. Med.* 160, 152-166.

Barret, J.C. and Preston, G. (1994). Apoptosis and cellular senescence: Forms of irreversible growth arrest, in: *Apoptosis II: The Molecular Basis of Apoptosis in Disease.* L.D. Tomei and F.O. Cope (eds.) Cold Spring Harbor Laboratory Press: NY, pp. 253-281.

Biedler, J.L. and Spengler, B.A. (1976). A novel chromosome abnormality in human neuroblastoma and antifolate-resistant Chinese hamster cell lives in culture. *J. Natl. Cancer Inst.* 57, 683-695.

Boesen, J.J., Niericker, M.J., Dieteren, N., and Simons, J.W. (1994). How variable is a spontaneous mutation rate in cultured mammalian cells? *Mutat. Res.* 307, 121-129.

Bruno, S., Lassota, P., Giaretti, W., and Darzynkiewicz, Z. (1992). Apoptosis of rat thymocytes triggered by prednisolone, camptothecin, or teniposide is selective to G_0 cells and is prevented by inhibitors of proteases. *Oncol. Res.* 4, 29-35.

Butler, M. (1985). Growth limitations in high density microcarrier cultures. *Dev. Biol. Stand.* 60, 269-280.

Campbell, J.H., Kocher, O., Skalli, O., Gabbiani, G., and Campbell, G.R. (1989). Cytodifferentiation and expression of alpha-smooth muscle actin mRNA and protein during primary culture of aortic smooth muscle cells. Correlation with cell density and proliferative state. *Arteriosclerosis* 9, 633-643.

Carlson, K. and Ehrich, M. (1999). Organophosphorus compound-induced modification of SH-SY5Y human neuroblastoma mitochondrial transmembrane potential. *Toxicol. Appl. Pharmacol.* 160, 33-42.

Carri, M.T., Ferri, A., Battistoni, A., Famhy, L., Gabbianelli, R., Poccia, F., and Rotilio, G. (1997). Expression of Cu,Zn superoxide dismutase typical of familial amyotrophic lateral sclerosis induces mitochondrial alteration and increase of cytosolic Ca^{2+} concentration in transfected neuroblastoma SH-SY5Y cells. *FEBS Lett.* 414, 365-368.

Cassarino, D.S., Fall, C.P., Swedlow, R.H., *et al.* (1997). Elevated reactive oxygen species and antioxidant enzyme activities in animal and cellular models of Parkinson's disease. *Biochim. Biophys. Acta* 1362, 77-86.

Cedazo-Minguez, A., Bonecchi, L., Winblad, B., Post, C., Wong, E.H., Cowburn, R.F., and Benatti, L. (1999). Nicergoline stimulates protein kinase c mediated α-secretase processing of the amyloid precursor protein in cultured human neuroblastoma SH-SY5Y cells. *Neurochem. Int.* 35, 307-315.

Cook, J.A. and Mitchell, J.B. (1989). Viability measurements in mammalian systems. *Analyt. Biochem.* 179, 1-7.

Costa, L.G. (1998). Neurotoxicity testing: A discussion of *in vitro* alternatives. *Environ. Health. Perspect.* 106, 505-510.

Del Bino, G., Skierski, J.S., and Darzynkiewicz, Z. (1991). The concentration-dependent diversity of effects of DNA topoisomerase I and II inhibitors on the cell cycle of HL-60 cells. *Exper. Cell Res.* 195, 485-491.

Drewinko, B., Yang, L.Y., Barlogie, B., and Trujillo, J.M. (1984). Cultured human tumor cells may be arrested in all stages of the cycle during stationary phase: demonstration of quiescent cells in G_1, S, and G_2 phase. *Cell Tissue Kinet.* 17, 453-463.

Duthu, G.S. and Smith, J.R. (1980). In vitro proliferation and lifespan of bovine aorta endothelial cells: effect of culture conditions and fibroblast growth factor. *J. Cell Physiol.* 103, 385-392.

Ehrich, M., Correll, L., Carlson, K., Wilcke, J., and Veronesi, B. (1995). Examination of culture conditions on esterase activities in human and mouse neuroblastoma cells. *In Vitro Toxicol.* 8, 199-207.

Fall, C.P. and Bennet JR., J.P. (1999). Characterization and time course of MPP+-induced apoptosis in human SH-SY5Y neuroblastoma cells. *J. Neurosci. Res.* 55, 620-628.

Hagiwara, M., Chen, I.L., and Fisher, J.W. (1984). Erythropoetin production in long-term cultures of human renal carcinoma cells. The role of cell population density. *Exp. Cell Res.* 154, 619-624.

Hirose, Y., Imai, Y., Nakajima, K., Takemoto, N., Toya, S., and Kohsaka, S. (1994). Glial conditioned medium alters the expression of amyloid precursor protein in SH-SY5Y neuroblastoma cells. *Biochem. Biophys. Res. Commun.* 28, 504-509.

Hunter, J., Hirst, B.H., and Simmons, N.L. (1993). Transepithelial secretion, cellular accumulation and cytotoxicity of vinblastine in defined MDCK cell strains. *Biochim. Biophys. Acta* 1179, 1-10.

Kallos, M.S. and Behie, L.A. (1999). Inoculation and growth conditions for high-cell-density expansion of mammalian neural stem cells in suspension bioreactors. *Biotechnol. Bioeng.* 63, 473-483.

Kamio, Y., Kato, H., Kishikawa, T., Toda, T., Sasaki, S., Ito, J., Kato, T., and Tanaka, R. (1989). Enhancement of both intracellular uptake and antitumor action of cisplatinum on human neuroblastoma cells by encapsulation in liposomes. *Jpn. J. Cancer Res.* 80, 787-793.

Kitani, H., Ikeda, H., Atsumi, T., and Wantanabe, R. (1997). Efficiency of neural differentiation of mouse P19 embryonal carcinoma cells is dependent on the seeding density. *Cell Transplant* 6, 521-525.

Liu, P. (1999). Analysis of correlation between some parameters depending on cell proliferation and life span of "stationary phase aging" cultures and maximum life span of mammals. *Tsitologiia* 41, 900-913.

McAdams, T.A., Miller, W.M., and Papoutsakis, E.T. (1996). Hematopoetic cell culture therapies (Part I): Cell culture considerations. *Trends Biotechnol.* 9, 341-349.

McCarthy, N.J. and Evan, G.I. (1998). Methods for detecting and quantifying apoptosis. *Cur. Top. Devel. Biol.* 36, 259-278.

Meghani, M.A., Martin, D.M., Singleton, J.R., and Feldman, E.L. (1993). Effects of serum and insulin-like growth factors on human neuroblastoma cell growth. *Regul. Pept.* 48, 217-224.

Morelli, L., Prat, M.I., and Castano, E.M. (1999). Differential accumulation of soluble amyloid beta peptides 1-40 and 1-42 in human monocytic and neuroblastoma cell lines. Implications for cerebral amyloidogenesis. *Cell Tissue Res.* 298, 225-232.

Perez-Polo, J.R., Werbach-Perez, K., and Tiffany-Castiglioni, E. (1979). A human clonal cell line model of differentiating neurons. *Dev. Biol.* 71, 341-355.

Pissiotis, E. and Spangberg, L. (1993). The importance of culture medium on human dental pulp cell attachment. *Arch. Oral Biol.* 38, 641-647.

Ponce, R.A., Kavanagh, T.J., Mottet, N.K., Whittaker, S.G., and Faustman, E.M. (1994). Effects of methyl mercury on the cell cycle of primary rat CNS cells *in vitro*. *Toxicol. Appl. Pharmacol.* 127, 83-90.

Riccardi, A., Servidei, T., Tornesello, A., Puggioni, P., Mastrangelo, S., Rumi, C., and Riccardi, R. (1995). Cytotoxicity of paclitaxel and docetaxel in human neuroblastoma cell lines. *Eur. J. Cancer* 4, 494-499.

Robinson, J.P., Darzynkiewicz, Z., and Dean, P. (1993). DNA cell cycle analysis: Propidium iodide procedure, in: *Handbook of Flow Cytometry Methods*. John Wiley and Sons, Inc.: NY, p. 97.

Seeger, R.C., Rayner, S.A., Banerjee, A., Chung, H., Laug, W.E., Neustein, H.B., and Benedict, W.F. (1977). Morphology, growth, chromosomal pattern, and fibrinolytic activity of two new human neuroblastoma cell lines. *Cancer Res.* 37, 1364-1371.

Sonnenfeld, K.H. and Ishii, D.N. (1982). Nerve growth factor effects and receptors in cultured human neuroblastoma cell lines. *J. Neurosci. Res.* 8, 375-391.

Spengler, B.A., Ross, R.A., and Biedler, J.L. (1986). Differential drug sensitivity of human neuroblastoma cells. *Cancer Treat. Rep.* 8, 959-965.

Veronesi, B. (1992). In vitro screening batteries for neurotoxicants. *Neurotoxicol.* 13, 185-196.

Veronesi, B. and Ehrich, M. (1993). Using neuroblastoma cell lines to examine organophosphate neurotoxicity. *In Vitro Toxicol.* 6, 57-65.

Yu, P.H. and Zuo, D.M. (1997). Enhanced tolerance of neuroblastoma cells towards the neurotoxin 6-hydroxydopamine following specific cell-cell interaction with primary astrocytes. *Neuroscience* 78, 903-912.

Zhong, J., Iqbal, K., and Grundke-Iqbal, I. (1999). Hyperphosphorylated tau in SY5Y cells: similarities and dissimilarities to abnormally hyperphosphorylated tau from Alzheimer disease brain. *FEBS Lett.* 453, 224-228.

(*a*)

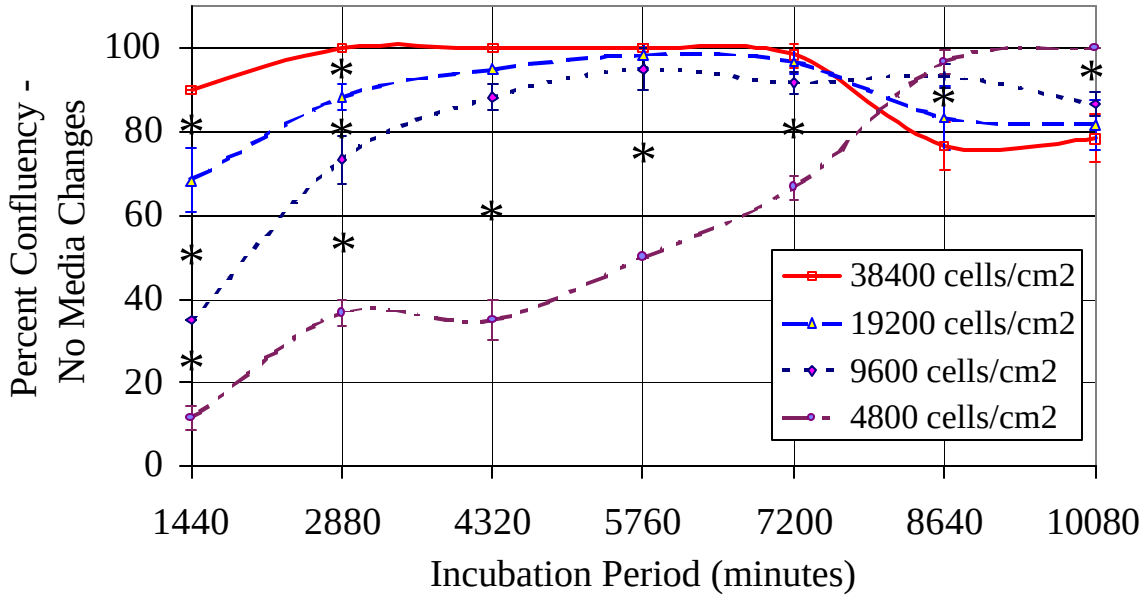

(*b*)

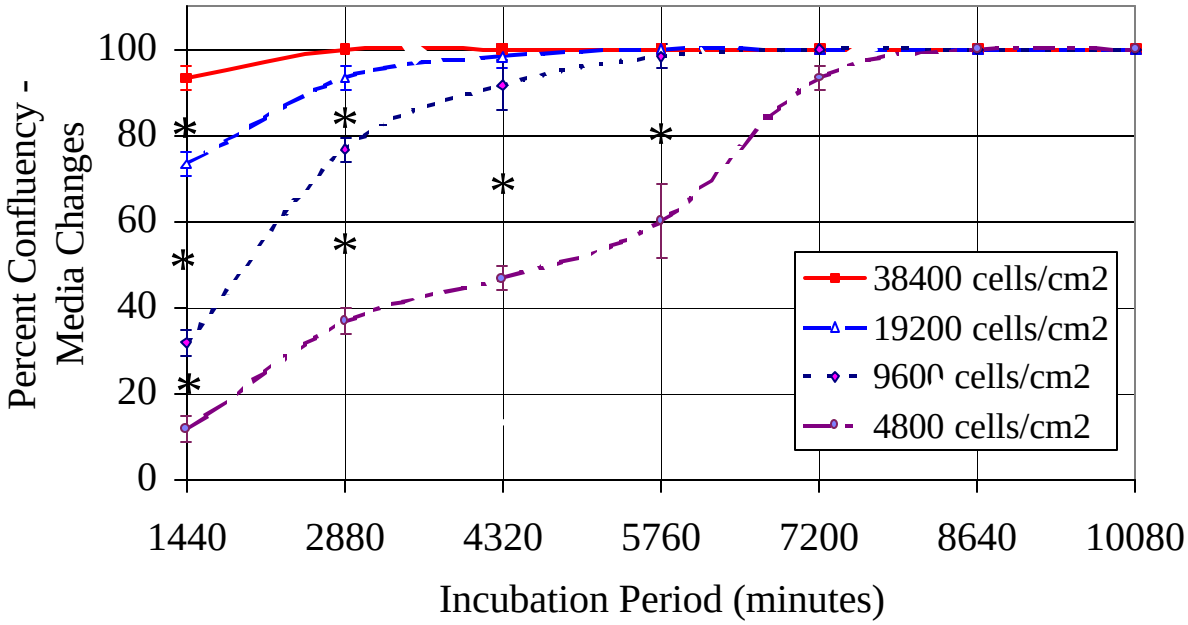

Figure 3.1 Percent confluency (cell coverage of plastic substrate) of SY5Y-B cultures with different initial seeding densities over time. Values are the mean of 3 normalized data points (percentages) ± the standard deviation. Statistical significance of a seeding density when compared to the seeding density depicted in the nearest line are displayed ($P<0.05$, ∗). Fig. 3.1a, cultures without media changes; Fig. 3.1b, cultures with 67% of their media changed daily.

(*a*)

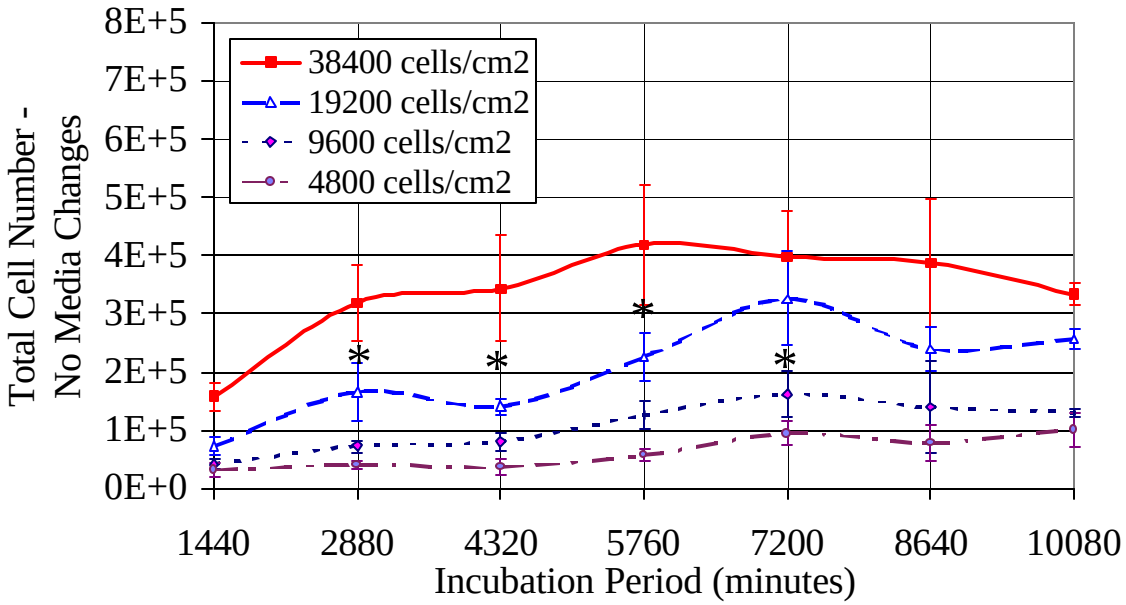

(*b*)

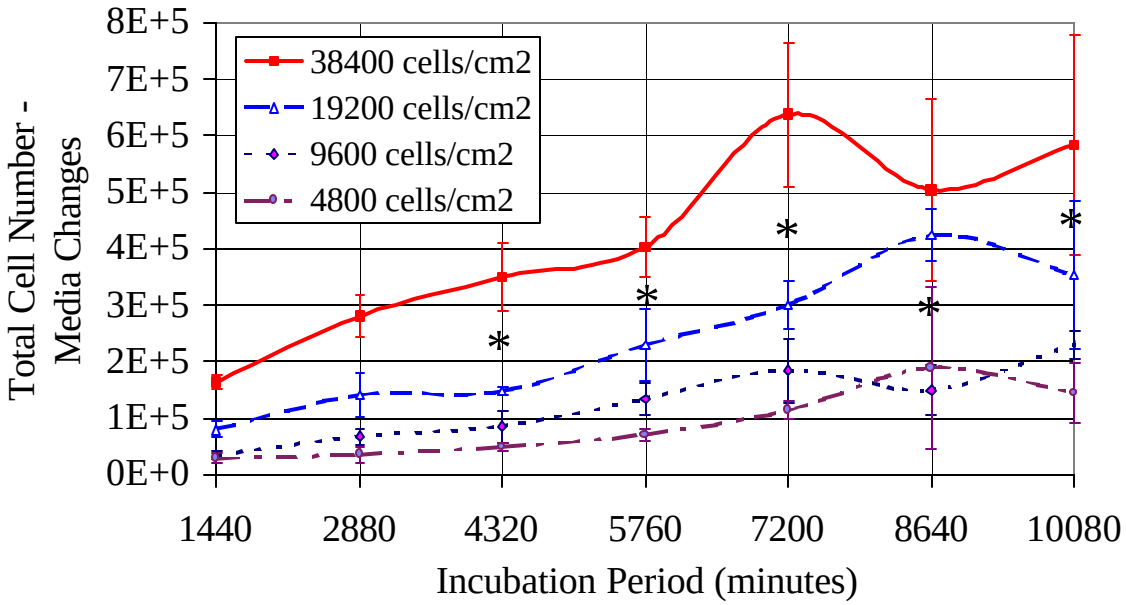

Figure 3.2 Total cell number over time in SY5Y-B cultures. Values (1E+5 = 100,000) are the mean of 3 normalized data points (percentages) ± the standard deviation. Statistical significance of a seeding density when compared to the seeding density depicted in the nearest line are displayed ($P<0.05$, ∗). Fig. 3.2a, cultures without media changes; Fig. 3.2b, cultures with 67% of their media changed daily.

(*a*)

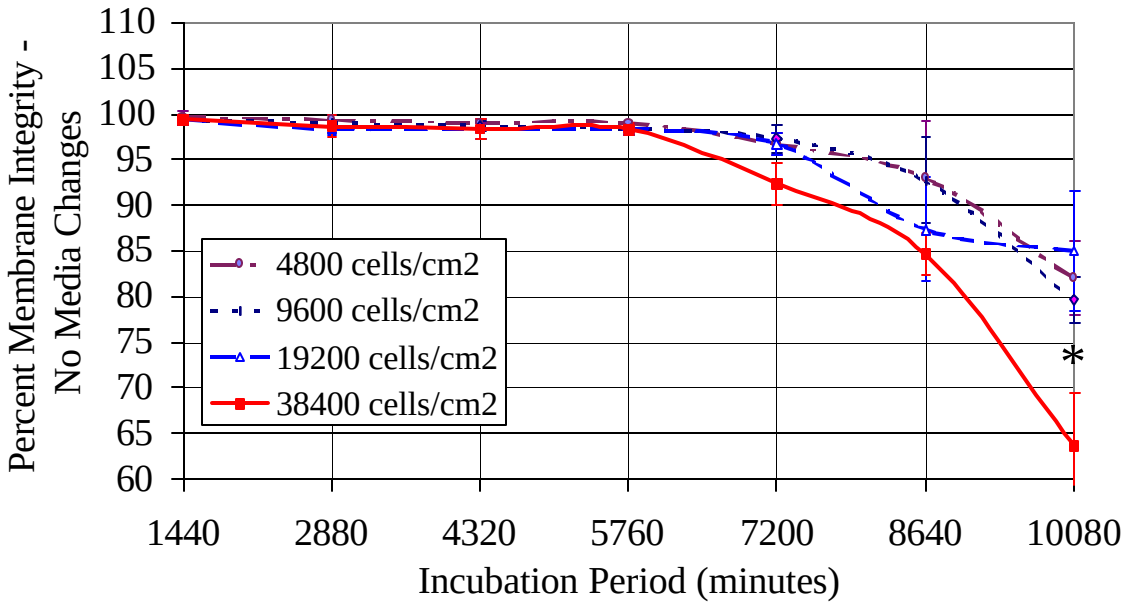

(*b*)

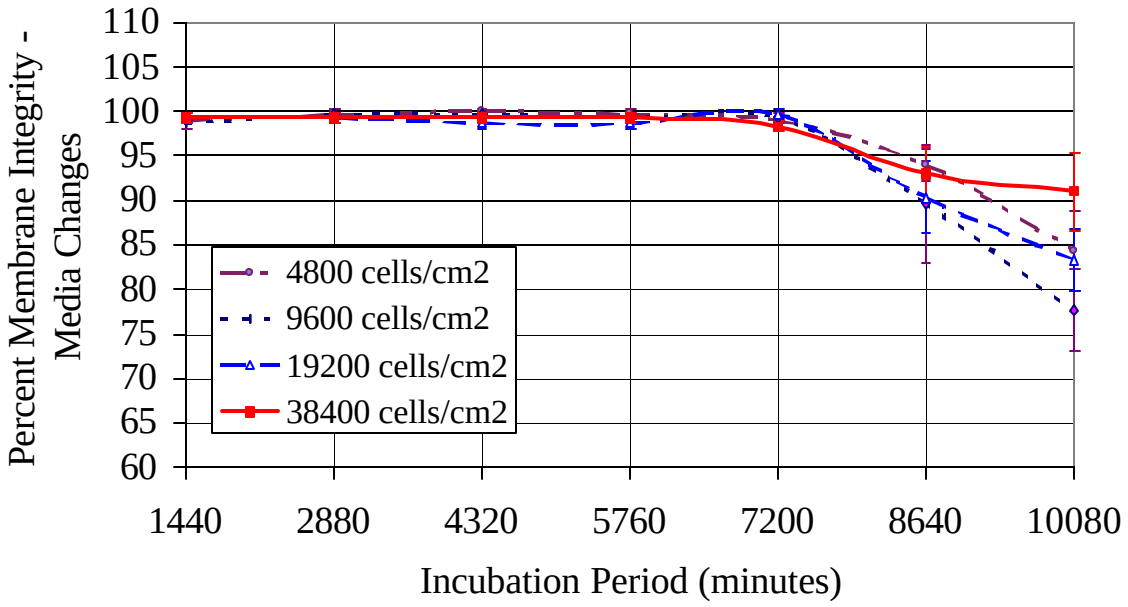

Figure 3.3. Plasma membrane integrity of SY5Y-B cells over time. Values are the mean of 3 normalized data points (percentages) ± the standard deviation. Statistical significance of a seeding density when compared to the seeding density depicted in the nearest line are displayed ($P<0.05$, ∗).

Fig. 3.3a, cultures without media changes; Fig. 3.3b, cultures with 67% of their media changed daily.

(*a*)

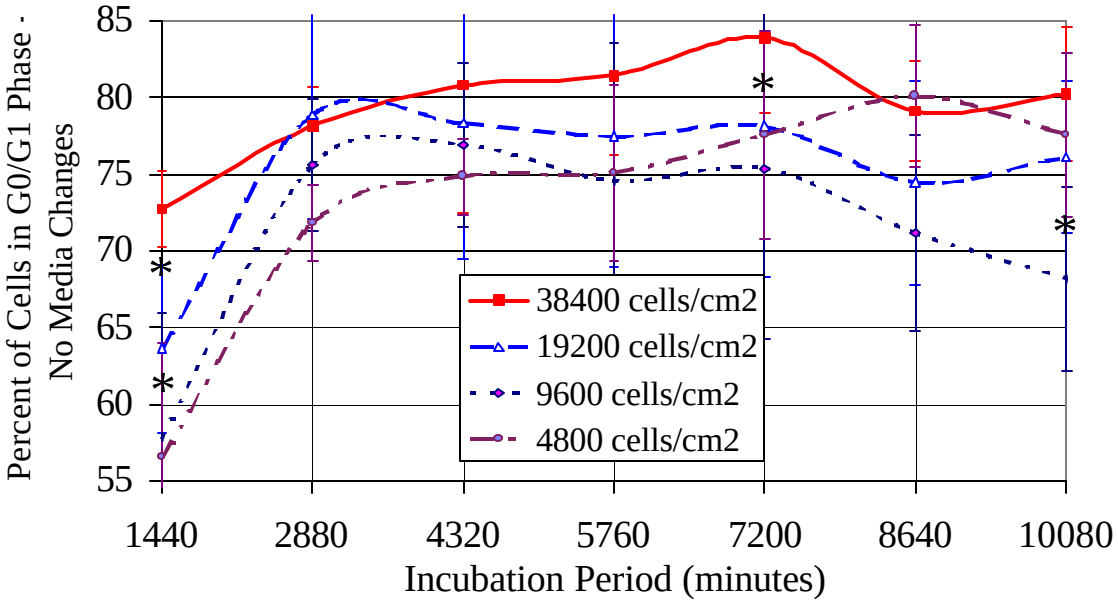

(*b*)

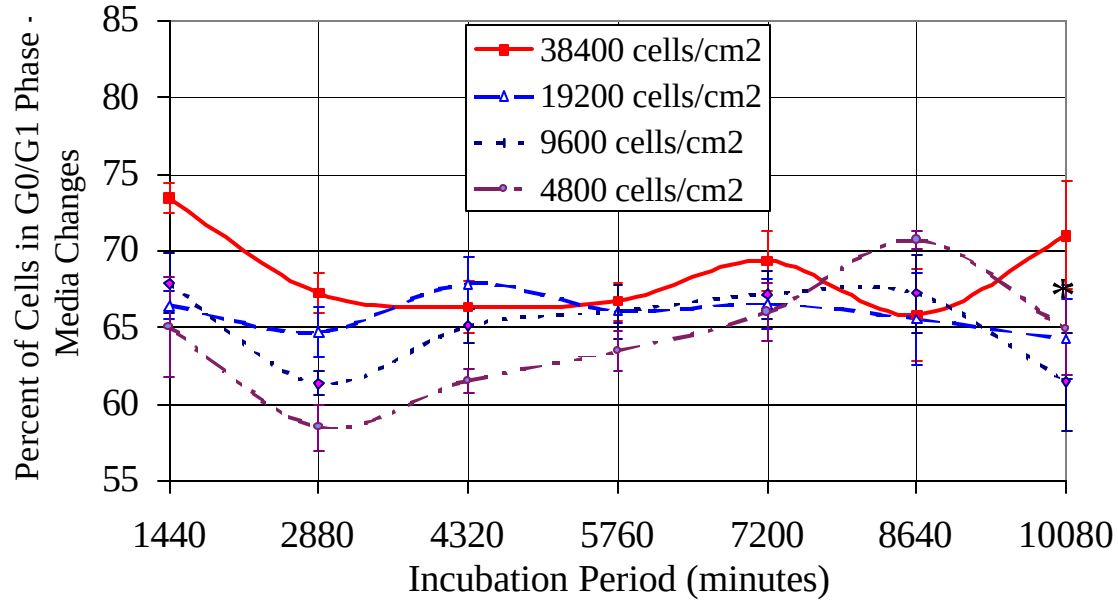

Figure 3.4. Percent of SY5Y-B cells in G_0/G_1 phase of the cell cycle over time. Values are the mean of 3 normalized data points (percentages) ± the standard deviation. Statistical significance of a seeding density when compared to the seeding density depicted in the next nearest line are displayed ($P<0.05$, ∗). Fig. 3.4a, cultures without media changes; Fig. 3.4b, cultures with 67% of their media changed daily.

(*a*)

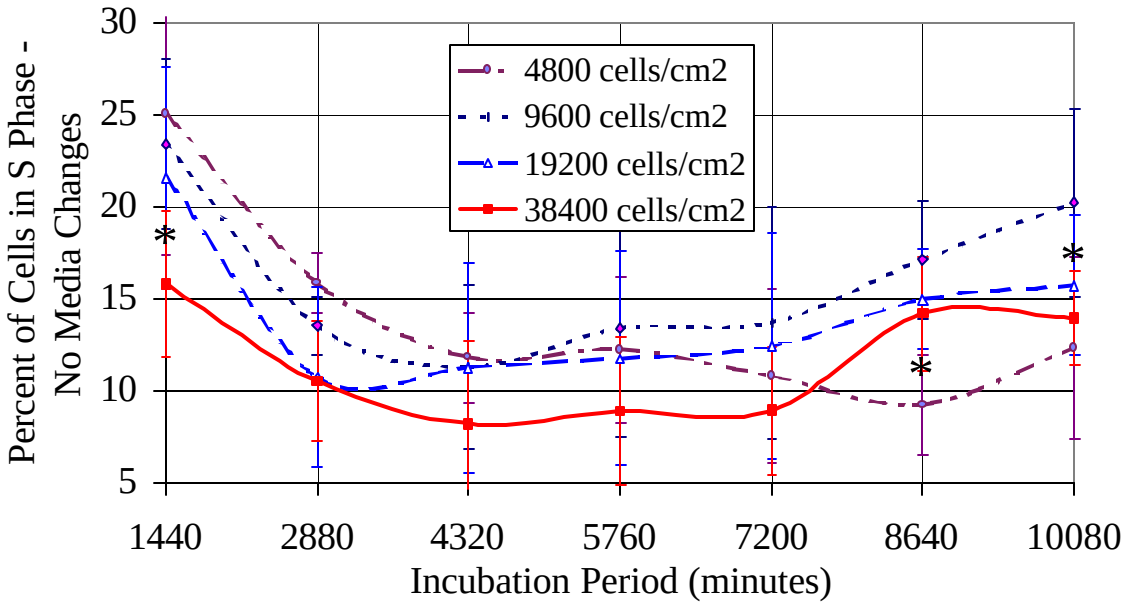

(*b*)

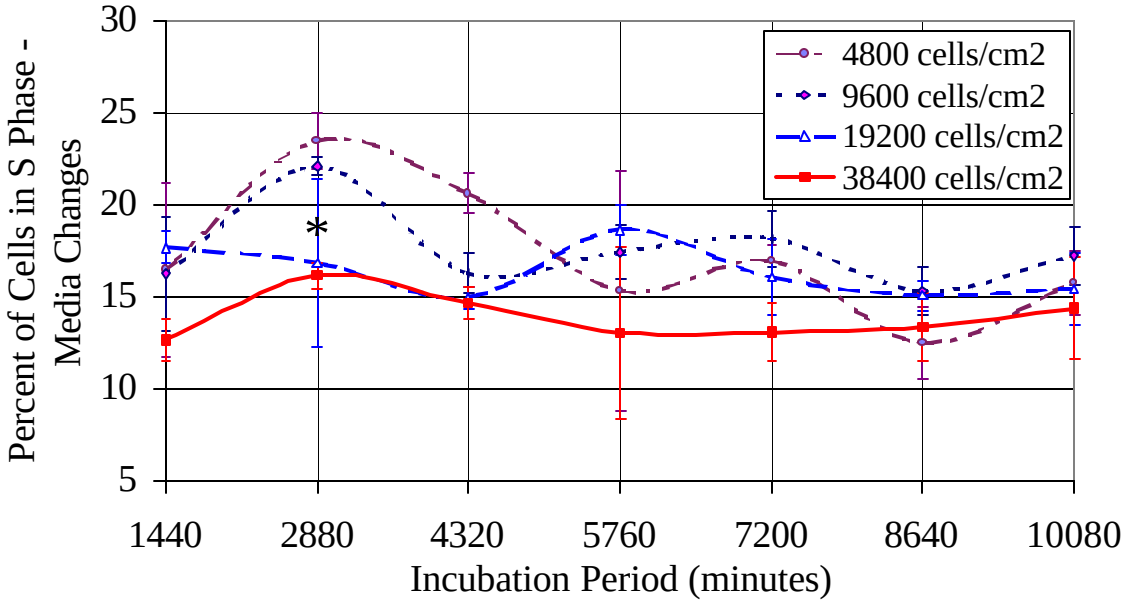

Figure 3.5. Percent of SY5Y-B cells in S phase of the cell cycle over time. Values are the mean of 3 normalized data points (percentages) ± the standard deviation. Statistical significance of a seeding density when compared to the seeding density depicted in the nearest line are displayed ($P<0.05$, ∗). Fig. 3.5a, cultures without media changes; Fig. 3.5b, cultures with 67% of their media changed daily.

(*a*)

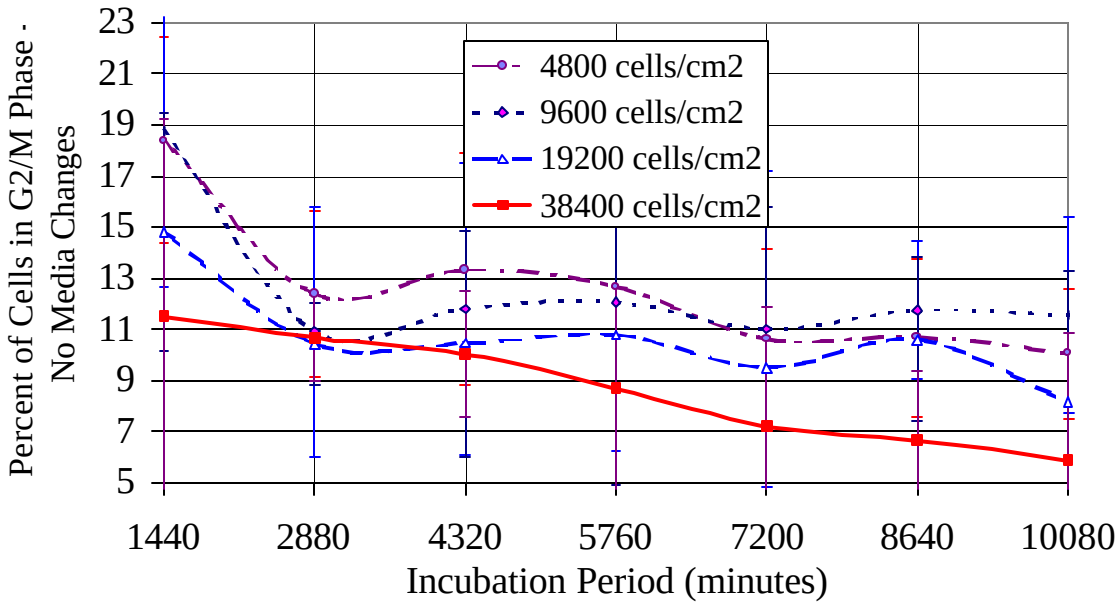

(*b*)

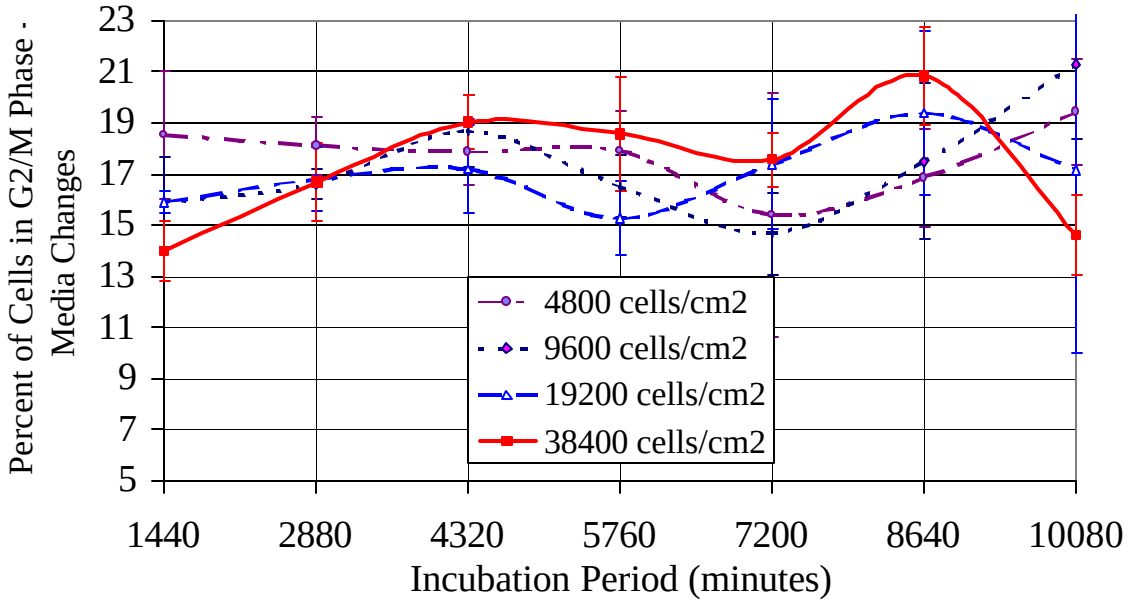

Figure 3.6. Percent of SY5Y-B cells in G_2/M phase of the cell cycle over time. Values are the mean of 3 normalized data points (percentages) ± the standard deviation. Statistical significance of a seeding density when compared to the seeding density depicted in the nearest line are displayed ($P<0.05$, ∗). Fig. 3.6a, cultures without media changes; Fig. 3.6b, cultures with 67% of their media changed daily.

(*a*)

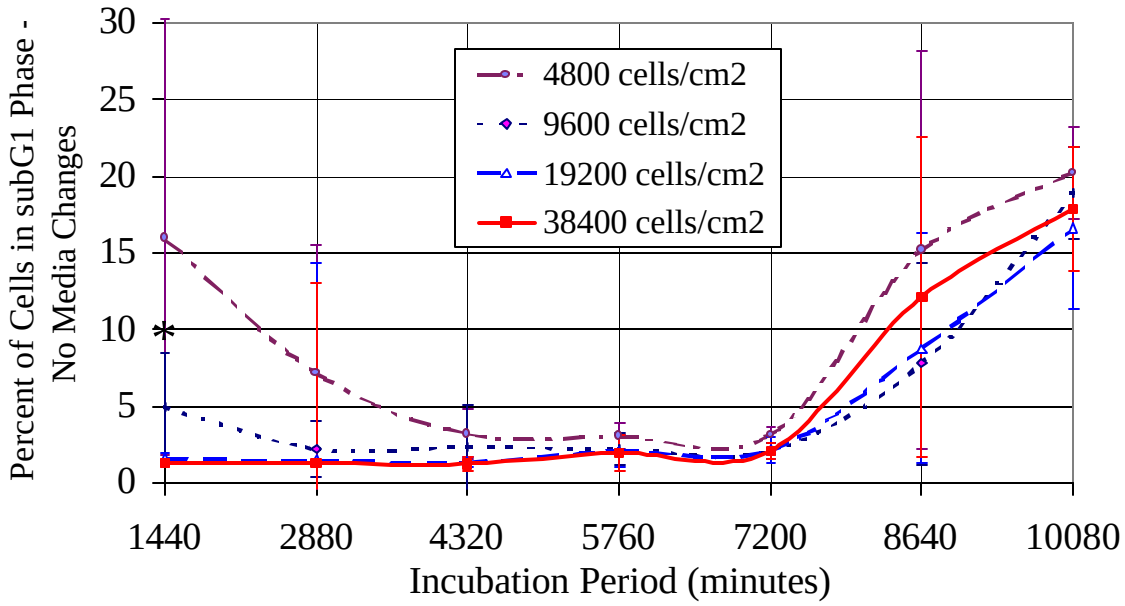

(*b*)

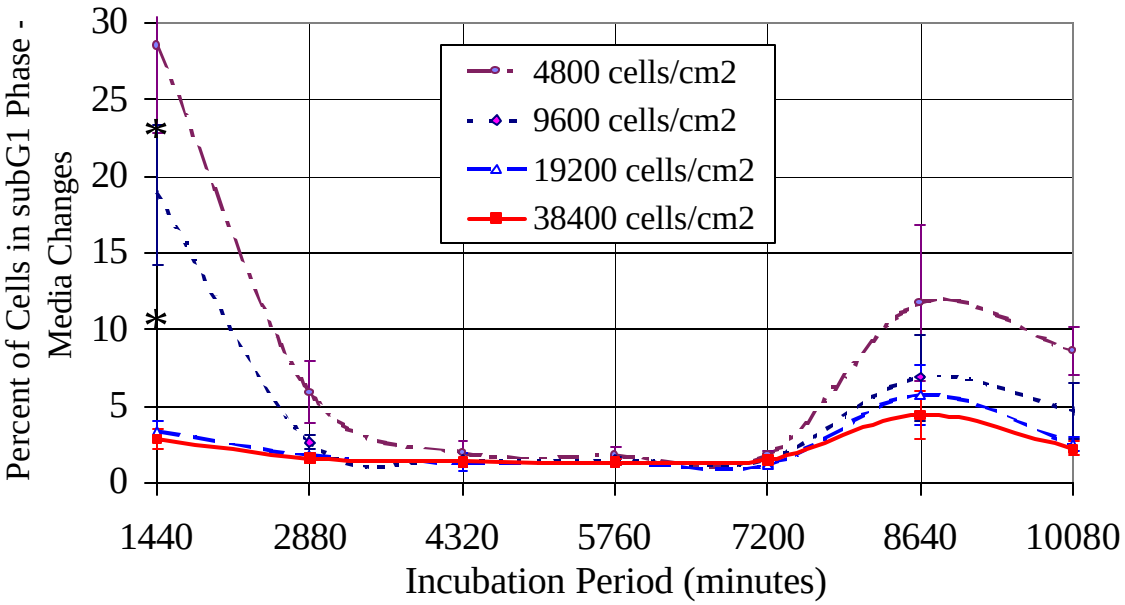

Figure 3.7. Percent of SY5Y-B cells with subG$_1$ amounts of DNA over time. Values are the mean of 3 normalized data points (percentages) ± the standard deviation. Statistical significance of a seeding density when compared to the seeding density depicted in the nearest line are displayed ($P<0.05$, ∗).

Fig. 3.7a, cultures without media changes; Fig. 3.7b, cultures with 67% of their media changed daily.

Chapter 4

Organophosphorus Compounds Alter the Cell Cycle Phase of SH-SY5Y Human Neuroblastoma Cells

Kent Carlson and Marion Ehrich

Virginia-Maryland Regional College of Veterinary Medicine,
Blacksburg, Virginia, 24061

ABSTRACT

In vitro exposure to certain organophosphorus (OP) compounds induces undifferentiated cells to die via a predominately apoptotic process. Many neuronal apoptotic processes have been linked to toxicant-induced alterations in nuclear function such as the cell cycle status. Our objective was to evaluate OP compound-induced alterations in cell cycle status (G_0/G_1, S, and G_2/M) in an *in vitro* model, SH-SY5Y human neuroblastoma cells, in order to determine the relationship between apoptosis and nuclear function (the stage of the cell cycle). Mitotic cell cycle phase was assessed by flow cytometry following exposure to OP compounds (diisopropyl-phosphorofluoridate (DFP), paraoxon, parathion, phenyl saligenin phosphate (PSP), tri-ortho-tolyl phosphate (TOTP), and triphenyl phosphite (TPPi)) in concentrations of 10µM to 1mM for periods of 0-7200 min. Phenylmethylsulfonyl fluoride (PMSF; 1mM, 8 hr), a serine protease inhibitor, was also evaluated for its ability to modulate OP compound-induced cell cycle changes. Exposure to concentrations of OP compounds (10µM DFP, 100µM DFP, 10µM paraoxon, 100µM parathion, 1µM PSP, and 10µM TPPi) that did not increase the amount of cells with subG_1 DNA fragmentation (an indicator of cytotoxicity) significantly increased the accumulation of cells in $G_0/G_1$and G_2/M phase of the cell cycle. Exposure to cytotoxic concentrations of OP compounds (1mM paraoxon, 1mM parathion, 100µM PSP, 1mM PSP, 100µM TOTP, 1mM TOTP, 1mM TPPi) significantly decreased the amount of cells in G_0/G_1 phase after long incubation periods (1440 to 7200 minutes). The proportion of cells in G_2/M phase of the cell cycle also decreased following lengthy incubations with 1mM paraoxon, 100µM PSP, 1mM PSP, 100µM TOTP, and 1mM TOTP, but increased following exposure to 1mM parathion and 1mM TPPi. Increases in S phase cells were also observed following exposure to 1mM parathion, 1mM TOTP and 1mM TPPi. Treatment with PMSF alone induced negligible amounts of DNA fragmentation (0.8%-4.4%) and influenced the cells to become less mitotically active. Pre- and post-treatment of cells with PMSF significantly potentiated the amount of subG_1 DNA fragmentation induced by OP compounds. As the length of PMSF incubation time increased, the amount of fragmentation within each treatment also increased. Overall, the *in vitro* data suggested that OP compounds stimulated cells to increase DNA synthesis and mitotic cycling. Changes in cell cycle did not correlate well to the induction of *in vitro* cytotoxicity, however, implying that the two are not directly linked.

INTRODUCTION

The mechanisms involved in organophosphorus (OP) compound-induced cell death are relatively unknown. A variety of authors describe mitochondrial (Carlson and Ehrich, 1999), enzymatic (Ehrich *et al.*, 1997), cytoskeletal (Tuler and Bowen, 1989), proteolytic (Carlson *et al.*, 2000), and plasma membrane (Antunes-Madeira *et al.*, 1994) alterations following exposure to these compounds. OP compound-induced changes in nuclear or genetic systems such as sister chromatid exchange or cell cycle delay (Chen *et al.*, 1981; Chen *et al.*, 1982; Sobti *et al.*, 1982; Singh *et al.*, 1984; Rupa *et al.*, 1989; De Ferrari *et al.*, 1991; Balaji and Sasikala, 1993; Wilson *et al.*, 1994; Lieberman *et al.*, 1998), binucleation and polyploidization (Lakomy *et al.*, 1984; Moore *et al.*, 1984), chromosomal aberration (Azatian and Voskanian, 1987; Das and John, 1999), colony formation (Gallicchio *et al.*, 1987), single strand DNA breaks (Slamenova *et al.*, 1992), cell proliferation (Flaskos *et al.*, 1994; Cunningham *et al.*, 1993; 1994), spindle aberration (Yin *et al.*, 1998), and micronucleus generation (Titenko-Holland *et al.*, 1997) have also been described. Many of these changes in nuclear function impact cell cycle progression or stasis. This aspect of OP compound-induced modifications has not been explored in detail for OP compounds that induce neuropathic sequelae (*in vivo* cell death).

The mode of cell death (apoptosis versus oncotic necrosis) is described in limited fashion for cells exposed to OP compounds. *In vitro* exposure to neuropathic, non-neuropathic, protoxicant, and actively toxic forms of OP compounds elicits a predominately apoptotic response in neuronal cultures (Carlson *et al.*, 2000). Apoptosis is also induced following *in vivo* exposure of epididymal tissue to phosphamidon (Akbarsha and Sivasamy, 1997), or teleost embryo tissue to diazinon (Hamm *et al.*, 1998).

Apoptosis is correlated to changes in the cell cycle in a variety of models. The overproduction of cell cycle progression proteins c-myc and cyclin A induces apoptosis in fibroblast cultures (Evan *et al.*, 1992; Hoang *et al.*, 1994). Apoptosis is also elevated in neuronal cells following the removal of G1/S phase blockers or cyclin-dependent kinase (CDK) inhibitors (Park *et al.*, 1997). Inhibition of cell cycle progression in mouse L cells, rat thymocytes, and rat astrocytes, also induces apoptosis (Barbiero *et al.*, 1995; Bruno *et al.*, 1992; Morris and Geller, 1996). Apoptosis is additionally initiated when differentiated neurons attempt to re-enter the mitotic cycle (Kranenburg *et al.*, 1996; Giardina *et al.*, 1998; Nuydens *et al.*, 1998).

Examination of the subcellular targets of many OP compounds lends additional credence to the hypothesis that OP compounds may affect the cell cycle status of exposed cells. OP compounds inhibit acetylcholinesterase, carboxylesterase, and neurotoxic esterase by phosphorylating active serine residues on these enzymes (Viana *et al.*, 1988; Ehrich *et al.*, 1995, 1997; Ehrich 1996; Ehrich *et al.*, 1997; Ehrich and Correll, 1998). Proteins related to cell cycle progression and transcription such as cyclin-dependent protein kinases (Cdk), p53, pRb, histone H3, IκB, c-Jun, and c-Fos possess similar serine active sites that are regulated by phosphorylation (Alberts *et al.*, 1994; Ko and Prives, 1996; Weinburg, 1995; Waring *et al.*, 1997; Barkett *et al.*, 1997 and Whiteside and Israel, 1997; Pulverer *et al.*, 1991; and Barber and Verma, 1987; respectively). If these molecules have binding consensus

sequences and adjacent molecular environments similar to esterases, these processes could be interrupted by exposure to OP compounds, leading to alterations in cell cycle progression.

SH-SY5Y human neuroblastoma cells have been used successfully *in vitro* to identify many of the subcellular changes associated with exposure to OP compounds. OP compound-induced mitochondrial alterations (Carlson and Ehrich, 1999), protease activation and the mode of cell death (Carlson *et al.*, 2000), and esteratic enzyme status (Veronesi *et al.*, 1997; Ehrich and Correll, 1998; Ehrich *et al.*, 1994, 1997) have been described in detail for this model. In the work presented here, we utilized this model to evaluate the effect of OP compounds on nuclear function by determining the distribution of cells in three cell cycle phases (G_0/G_1, S, G_2/M). Cellular responses to OP compounds were modulated by phenylmethylsulfonyl fluoride (PMSF), an inhibitor of serine proteases (Sarin *et al.*, 1993).

EXPERIMENTAL METHODS

Chemicals. Diisopropylphosphorofluoridate (DFP; 98% pure), paraoxon (98.5% pure), parathion (99% pure), tri-ortho-tolyl phosphate (TOTP; 98% pure), and triphenyl phosphite (TPPi; 98% pure) were purchased from Chem Service, Inc. (West Chester, PA). Phenyl saligenin phosphate (PSP; 99% pure) was synthesized by Lark Enterprises (Webster, MA). Stock solutions (100mM in ethanol) of these OP compounds were made and stored in the dark at -20ºC for no longer than 2 weeks prior to use. Phenylmethylsulfonyl fluoride (PMSF) was obtained from Sigma Chemical Co. (St. Louis, MO). Propidium iodide (PI) was acquired from Molecular Probes (Eugene, OR).

Cell Culture. SH-SY5Y human neuroblastoma cells were cultured primarily as described by Carlson and Ehrich (2000). SH-SY5Y cells (passage 56-58) were grown in Hams F12 medium (Sigma) supplemented with fetal bovine serum (FBS - 15% v/v) supplied by Summit Biotech, Inc. (Fort Collins, CO). Prior to confluency, cells were harvested using 0.25% trypsin (Sigma) and seeded onto plastic 96 well microtiter plates at $4x10^5$ cells/ml. The cells were then allowed to grow at 37°C and 5% CO_2 for 3-4 days prior to exposure to OP compounds (1nM to 1mM, 0 to 7200 min) or other chemical modifiers. Sixty seven percent of the media (with and without treatment compounds) was exchanged daily before and after exposure to compounds.

Flow Cytometric Evaluation of DNA Content. DNA composition was evaluated by using PI and the cell culture methods described above. Following incubation, the treatment media were replaced by 75µl each of a PI buffer (PBS containing 50µg/ml PI, 1% FBS, and 0.1% sodium azide) and Vindelov's reagent (0.01M Tris, 10mM NaCl, 700U RNAse A (Sigma), 50µg/ml PI, and 0.1% of Igepal-40 (Sigma)). The microtiter plates were then incubated overnight at 4°C to allow cellular DNA to saturate with fluorochrome (Robinson *et al.*, 1993) and then pipetted into flow cytometry tubes. Five thousand cell events were subsequently analyzed on a Coulter Epics XL-MCL flow cytometer (excitation 535nm - emission 617nm). Listmode files generated by the flow cytometer were processed through Multicycle DNA Cell Cycle Analysis Software (version 3.11 - Phoenix Flow Systems, Inc., San Diego, CA) to generate objective estimates of DNA concentration and, therefore, the proportion of cells in each cell cycle phase (G_0/G_1, S, G_2/M). Representative flow cytometry histograms for propidium iodide can be seen in Appendix A.

Statistics. Each quantitative experiment had between 3 and 17 normalized data points (percentages) for each time and OP concentration. Data were converted into the percent of control and then graphed as the mean ± the standard deviation. Statistical significance ($p<0.05$) was determined by utilizing PC-SAS software (version 6.1) to perform an analysis of variance (ANOVA) followed by Duncan's Multiple Range Test.

RESULTS

Distribution and Elimination of SH-SY5Y Cells in the Cell Cycle Following Exposure to OP Compounds

OP compounds affect a variety of nuclear systems that can impact the cell cycle status of exposed cultures. Because altered cell cycle status has been observed in many neuronal cultures undergoing apoptosis, we evaluated the correlation between changes in OP compound-induced DNA fragmentation (interpreted as apoptosis) and changes in the distribution of cells in the cell cycle (phase accumulation), and which cell cycle phase was predominately being affected.

We had to analyze late time point data (≥480 min) when looking for changes in cell cycle progression such as phase accumulation or toxicity. This was because SH-SY5Y cells used in this study had a 38 hr doubling time in cultures with media changes (Carlson and Ehrich, 2000). Approximately 15 to 20% of these cells were in S phase of the cell cycle (and would undergo mitosis), therefore, it would have taken 4 to 5 cycles to double the number of cells. Thus, to see a 15 to 20% change in the number of cells in a particular phase, we had to analyze data from time points 7.6 to 9.5 hours (≥480 min) after dosing.

In order to determine OP compound-induced selective elimination of cells in a particular phase of the cell cycle we also had to calculate the relative rates of increase or decrease over time for each phase in circumstances in which there were and were not cytotoxic responses. By comparing the rates of change of G_0/G_1, S, and G_2/M phase cells during cytotoxicity (the time interval in which cells with subG_1 amounts of DNA were increased) one could directly see if one cell cycle phase was being preferentially deleted.

Ethanol treated control cells remained relatively similar in phase distribution over all incubation periods. Fifty-two to 72 percent of the control cells were in G_0/G_1 phase of the cell cycle. Eight to 27 and 13 to 26 percent of the control cells were in S and G_2/M phase of the cell cycle, respectively. One to 12 percent of the control cells had their DNA fragmented as well.

Dose dependent alterations in cell cycle status were observed following exposure to all OP compounds. Significant differences from ethanol controls occurred predominately at later incubation periods. Exposure to 1mM DFP significantly decreased the number of G_0/G_1 and increased the proportion of S and G_2/M phase cells at 7200 min time points (Fig. 4.1a, 4.1b, and 4.1c; $p<0.05$). Exposure to 100μM DFP, in contrast, significantly increased the proportion of G_0/G_1 phase cells at 5760 min (Fig. 4.1a; $p<0.05$) and the number of S and G_2/M phase cells following exposure for 7200 min (Fig. 4.1b and 4.1c; $p<0.05$). Alterations in the proportion of cells in each cell cycle phase following exposure to 10μM of DFP were similar to that of 100μM exposures. No significant increases were seen in the proportion of cells with subG_1 amounts of DNA following exposure to any concentration of DFP at any time point (Fig. 4.1d).

High concentration (1mM) exposures to paraoxon significantly decreased the proportion of cells in G_0/G_1, S, and G_2/M phases of the cell cycle at time points greater than 4320 min (Fig. 4.2a, 4.2b, and 4.2c, $p<0.05$). Significant increases in the number of cells with subG_1 amounts of DNA were seen at these time points as well (Fig. 4.2d; $p<0.05$). Cells in G_2/M phase of the cell cycle were affected to a greater extent than the other phases ($G_2/M > S > G_0/G_1$) when comparing the rates of change following exposures that induced the formation of subG_1 amount of DNA (2880 to 7200 min). Exposure to lower concentrations (10µM and 100µM) of paraoxon, in contrast, significantly increased the number of G_0/G_1 (10µM; Fig. 4.2a; $p<0.05$) and S and G_2/M phase cells (100µM; Fig. 4.2b and 4.2c; $p<0.05$) following 7200 min incubations. Significant increases in the proportion of cells with subG_1 amounts of DNA were not seen following 10µM exposures. One hundred micromolar exposures, however, significantly increased the number of cells with subG_1 amounts of DNA following 7200 min incubations (Fig. 4.2d; $p<0.05$).

Parathion (1mM) significantly decreased the number of G_0/G_1 and increased the proportion of S phase cells following 4320 min exposures (Fig. 4.3a and 4.3b; $p<0.05$). No significant changes in the number of G_2/M phase cells or cells with subG_1 amounts of DNA were seen following similar exposures because of variability, although mean values for both did increase (Fig. 4.3c and 4.3d; $p<0.05$). Cells in G_0/G_1 phase of the cell cycle were deleted to a greater extent than the other phases ($G_0/G_1 > G_2/M > S$) when comparing the rates of change following exposures that induced the formation of subG_1 amount of DNA (1440 to 4320 min). Lower concentration parathion exposures (100µM) did not significantly effect the distribution of cells in any phase of the cell cycle.

High concentrations of PSP induced a significant, precipitous decrease in the number of G_0/G_1, S, and G_2/M cells following 2880 min (100µM and 1mM), 2880 min (1mM) and 5760 min (100µM), and 4320 min of exposure, respectively (Fig. 4.4a, 4.4b, and 4.4c; $p<0.05$). Similar concentrations of PSP induced significant DNA (subG_1) fragmentation after 1440 min of exposure (Fig. 4.4d; $p<0.05$). Lower concentration (10µM) exposures to PSP significantly decreased the proportion of G_0/G_1 and increased the number of S and G_2/M phase cells following 4320 min, 7200 min, and 4320 min, respectively (Fig. 4.4a, 4.4b, and 4.4c; $p<0.05$). No significant changes in the amount of cells with subG_1 DNA levels were observed following exposure to 100µM PSP, even though fragmentation increased > 600% (Fig. 4.4d, $p<0.05$). G_2/M phase cells were deleted to a greater extent than the other phases ($G_2/M > G_0/G_1 > S$) when comparing the rates of change following 1mM PSP exposures that induced the formation of subG_1 amount of DNA (960 to 7200 min). In contrast, lower concentration (100µM) exposures selectively affected G_0/G_1 phase cells to a greater extent ($G_0/G_1 > G_2/M > S$). Exposure to the lowest test concentration of PSP (1µM) significantly increased the proportion of G_0/G_1, S, and G_2/M phase cells following 5760 min, 1440 min, and 4320 min incubations, respectively (Fig. 4.4a, 4.4b, and 4.4c; $p<0.05$). The number of S phase cells subsequently declined over exposure time and was significantly lower than controls by 5760 min (Fig. 4c; $p<0.05$). The number of cells with subG_1 amounts of DNA did not significantly change over time for this concentration of PSP (Fig. 4.4d; $p<0.05$).

TOTP exposure (1mM) significantly decreased the proportion of G_0/G_1, increased the number of S, and decreased the amount of G2/M phase cells following 2880 min, 2880 min, and 4320 min

incubations, respectively (Fig. 4.5a, 4.5b, and 4.5c; $p<0.05$). Although initially elevated, the number of S phase cells was significantly less than controls by 5760 min incubations (Fig. 4.5b, $p<0.05$). The number of cells with subG_1 DNA fragmentation also increased following 960 min of incubation with 1mM TOTP (Fig. 4.5d; $p<0.05$). Exposure to 100μM TOTP significantly decreased the number of cells in G_0/G_1, S, and G_2/M phase cells following 4320 min, 5760 min, and 5760 min of incubations, respectively (Fig. 4.5a, 4.5b, and 4.5c; $p<0.05$). These decreases coincided with significant increases by 4320 min in the number of cells with subG_1 amounts of DNA (Fig. 4.5d; $p<0.05$). As observed with paraoxon, exposure to 1mM TOTP affected G_2/M phase cells to a greater extent than the other phases ($G_2/M > S > G_0/G_1$) when comparing the rates of change following cytotoxic exposures between 480 and 7200 min Lower concentration (100μM) TOTP exposures, however, selectively deleted G_0/G_1 phase cells to a greater extent ($G_0/G_1 > G_2/M > S$) than others. Lowest concentration TOTP exposures (10μM) significantly increased the number of G_0/G_1 phase cells following 5760 min incubations (Fig. 4.5d; $p<0.05$). No other significant differences in the proportion of cells in cell cycle phases were seen for 10μM exposures.

High concentration (1mM) TPPi exposures significantly decreased the number of G_0/G_1 stage cells and increased the number of S and G_2/M phase cells at 4320 min (Fig 4.6a, 4.6b, and 4.6c; $p<0.05$). The proportion of S phase cells subsequently declined and was significantly less than controls by 5760 min (Fig. 4.6b; $p<0.05$). Changes in the number of cells in relative cell cycle phases were preceded by a significant increase in the number of cells with subG_1 amounts of DNA (Fig. 4.6d; $p<0.05$). Exposure to 1mM TPPi preferentially induced cytotoxicity in G_0/G_1 phase cells ($G_0/G_1 > G_2/M > S$) when comparing the rates of change following exposures between 1440 and 7200 min. Exposure to lower concentrations of TPPi (100μM) significantly increased the number of G_0/G_1 and decreased the number cells with subG_1 amounts of DNA following 5760 min exposures (Fig 4.6a and 4.6d; $p<0.05$). The lowest concentration exposure of TPPi (10μM) significantly increased the number of G_2/M phase cells at 4320 min incubations (Fig 4.6c; $p<0.05$).

PMSF-induced Alterations in SH-SY5Y Cell Cycle Phases

Cells were treated with 1nm to 1mM concentrations of PMSF, a serine protease inhibitor, in order to evaluate cell cycle changes elicited by this compound. PMSF treatment induced cells to change the relative proportion of cells within each cell cycle phase. Baseline values following PMSF administration alone revealed that approximately 50 to 80% of cells were in G_0/G_1, 10 to 25% in S, and 8 to 23% in G_2/M phase of the cell cycle following 1440 to 7200 minute incubations. PMSF treatment increased the percent of G_0/G_1 phase cells over time (Fig. 4.7a). Associated decreases in the proportion of S and G_2/M phase cells were also seen over time (Fig. 4.7b and 4.7c respectively).

PMSF-induced Changes in the Cell Cycle Phase in SH-SY5Y Cells Altered From Exposure to OP Compounds

PMSF was administered pre- and post- OP compound in order the evaluate its ability to inhibit or potentiate OP compound-induced changes in cell cycle status or DNA content. *In vivo* administration of PMSF prior to OP compound exposure can mitigate neuropathic lesions in OPIDN,

while post-OP compound administration potentiates OPIDN (Lotti *et al.*, 1991; Massicotte *et al.*, 1999). Media with increased sodium chloride concentration (NaCl; 150mM) was used as a positive control to induce cytotoxicity (apoptosis).

Treatment with PMSF in combination with 1mM TOTP, PSP, TPPi, or NaCl significantly increased the proportion of cells with subG_1 (fragmented) amounts of DNA when compared to exposures of PMSF-alone or OP compound-alone (Fig. 4.8; $p<0.05$). Time-dependent increases in cytotoxicity were also observed following 1mM paraoxon and 100μM TOTP exposures. In general, as the length of PMSF incubation time increased, the amount of fragmentation within each treatment also increased. The increased amount of DNA fragmentation in combination treatments was greater than the sum of PMSF-alone and compound-alone induced fragmentation, suggesting that PMSF had a potentiating effect on DNA fragmentation at this concentration.

DISCUSSION

The present study evaluated the effects of OP compounds on SH-SY5Y human neuroblastoma cell cycle status. PMSF was used as a cytotoxic modifier to determine important parameters of cell cycle control and to emulate *in vivo* investigations involving protease inhibition.

Flow cytometric data was able to determine OP compound-induced accumulation of cells in particular phases of the cell cycle. In order to evaluate phase accumulation, noncytotoxic OP compound exposures, identified as time points in which no significant subG_1 DNA fragmentation occurred, were compared. Without cytotoxicity, changes in the proportion of cells in each cycle phase could be directly related to the influence of the OP compound.

Overall, the data suggested that OP compounds with little or no cytotoxic potential (DFP) affected the distribution of G_0/G_1 and S phase cells differently from noncytotoxic concentrations of other OP compounds (paraoxon, parathion, PSP, TOTP, and TPPi).

Exposure to noncytotoxic concentrations of all OP compounds uniformly increased the proportion of G_2/M phase cells with one exception, 10µM TOTP. Increased proportions of G_2/M phase cells could be due to accumulation of cells in the secondary gap phase (G_2) or continued upregulated mitosis (M). Accumulation of cells in G_2/M phase would effectively delay completion of the cell cycle and decrease proliferation. These effects are reported following noncytotoxic administration of other OP compounds (Greenman *et al.*, 1997; Balaji and Sasikala, 1993). OP compound-induced cell cycle delay has also been demonstrated by Chen *et al.* (1981).

Accumulation in G_2 or G_2/M phase of the cell cycle is also described following exposure to chemicals such as methyl mercury, which interferes with mitotic spindle performance (Ponce *et al.*, 1994), DNA topoisomerase inhibitors (Del Bino *et al.*, 1991), and other stimuli which induce DNA damage and consequently upregulate the activity and concentration of a 53 kDa nuclear phosphoprotein termed p53 (Ko and Prives, 1996; Pellegata *et al.*, 1996). OP compound-induced spindle damage has been observed by Yin *et al.* (1998). Other OP compound-induced DNA damage such as sister chromatid exchanges or chromosome aberrations (Chen *et al.*, 1981; Das and John, 1999; Lieberman *et al.*, 1998; Wilson *et al.*, 1994), single DNA strand breaks (Slamenova *et al.*, 1992), and micronucleus formation (Titenko-Holland *et al.*, 1997) have also been documented.

Upregulated mitosis (M) as indicated by cellular proliferation is also reported following exposure to low concentrations of OP compounds. Harvey and Sharma (1980) noted that noncytotoxic concentrations of TOTP, DFP and dicrotophos stimulated proliferation of neuroblastoma 2-A cells. Greenman *et al.* (1997) observed similar proliferation in rat intestinal and human colonic cell lines exposed to diazinon.

Given that proliferation, spindle inhibition, or DNA damage were not assessed in this study, cellular delay in G_2 phase or upregulated continuation through M phase may account for the accumulation of cells in this stage of the cell cycle following exposure to noncytotoxic concentrations of

OP compounds. In future studies, administration of specific cell cycle blockers such as desferoxamine and mimosine (G_1/S; Park *et al.*, 1997) or teniposide (G_2/M; Del Bino *et al.*, 1991) may be able to define further these effects.

Flow cytometric data also determined if cells were being selectively eliminated (by apoptosis) in a particular phase of the cell cycle. This determination required that the relative rates of increase or decrease over time were known for circumstances in which there was and was not a cytotoxic response. By comparing the rates of change during cytotoxicity one could directly see if one cell cycle phase was being preferentially deleted.

Exposure to 1mM paraoxon, PSP, and TOTP (cytotoxic concentrations) predominately eliminated cells in G_2/M phase of the cell cycle. In contrast, exposure to parathion (1mM), PSP (100µM), TOTP (100µM), and TPPi (1mM) selectively deleted cells in G_0/G_1 phase. These effects were not correlated to the fragmentation of nuclei or the rapidity of cytotoxic insult, but did follow a similar trend as caspase-3 activation (Carlson *et al.*, 2000). In that study, caspase activation for 1mM paraoxon, PSP, and TOTP occurred before activation by other compounds or concentrations.

G_2/M phase arrest leading to cell death have been observed following stimuli that interfere with DNA integrity, such as *in vitro* exposure to methyl mercury or colchicine (Ponce *et al.*, 1994), VP-16 (Barbiero *et al.*, 1995), or camptothecin, teniposide, and 4′-(9-acridynylamino-3-methanesulfon-m-anisidide (Del Bino *et al.*, 1991). Selective G_0/G_1 phase toxicity has also been reported following exposure to similar DNA-damaging compounds (Bruno *et al.*, 1992). This is the first report of such an effect with OP compounds.

Exposure to PMSF alone was not cytotoxic to SH-SY5Y cells at concentrations from 1nM to 1mM and incubation times up to 7200 min. Similar findings have been reported for HL60 cells (Drexler, 1997). Exposure to PMSF at concentrations from 1nM to 1mM increased the proportion of G_0/G_1, and decreased the proportion of S and G_2/M phase cells as the length of incubation time increased. The decrease in mitotic cycling occurred whether each cell cycle phase was expressed as percent of cells (G_0/G_1 + S + G_2/M = 100%) or percent of solvent control. PMSF-induced events such as this have not been previously reported.

The trends reported here may have resulted from the inhibition of proteases important to cell cycle control. Ross (1996) and Kato (1999) reported that degradation of specific cell cycle proteins such as cyclins were necessary for mitotic progression. Although suggested (Zhu *et al.*, 1995), PMSF-induced inhibition of ubiquination-proteosome pathways has not been observed following numerous investigations (Hua *et al.*, 1996; Kobayashi *et al.*, 1996; Drexler, 1997) which indicates that other proteolytic pathways related to cell cycle progression may be involved in PMSF-induced mitotic inhibition.

OP compound-induced *in vivo* cell death (neuropathy) can be inhibited or promoted by the application of PMSF before or after OP compound exposure, respectively (Lotti *et al.*, 1991; Massicotte *et al.*, 1999). Similar PMSF-elicited differences in *in vitro* cell death were not observed in

this study. Pretreatment with PMSF potentiated the formation of subG_1 DNA (DNA fragmentation). As the total length of PMSF treatment increased, so did DNA fragmentation, and hence cytotoxicity. Compounds with the best ability to induce apoptosis (NaCl) were potentiated to the greatest extent. PMSF-induced potentiation of cytotoxic insults has been reported (Zhu *et al.*, 1995), but was not expected in this study, because others had documented PMSF-induced inhibition of cytotoxicity at similar concentrations (Suffys *et al.*, 1988; Sarin *et al.*, 1993). PMSF-potentiated cytotoxicity prevented analysis of its effects on OP compound-induced accumulation of G_2/M phase cells.

Overall, the data suggest that OP compounds alter the cell cycle status of undifferentiated SH-SY5Y human neuroblastoma cells. Increases in the proportion of G_2/M phase cells were consistently seen following exposure to DFP, paraoxon, parathion, PSP, TOTP, and TPPi. Less consistent increases in G_0/G_1 phase cells were also seen. Exposure to PMSF also altered the cell cycle distribution by increasing the proportion of G_0/G_1 and decreasing S and G_2/M phase cells. Alterations in the cell cycle control may provide a mechanism for OP compound-induced *in vivo* neuropathy and explain why PMSF can inhibit this development. Further investigations into this area will clarify these issues.

ACKNOWLEDGMENTS

We wish to thank Joan Kalnitsky for flow cytometric assistance. This work was supported by EPA grant R825356 and funds from the Virginia-Maryland Regional College of Veterinary Medicine.

REFERENCES

Alberts, B., Bray, D., Lewis, J., Raff, M., Roberts, K., and Watson, J.D. (1994). Chapter 16: The cytoskeleton. In *Molecular Biology of the Cell*, pp. 821-861. Garland Publishing, Inc., New York.

Antunes-Madeira, M.C., Videira, R.A., and Madeira, V.M.C. (1994). Effects of parathion on membrane organization and its implications for the mechanisms of toxicity. *Biochim. Biophys. Acta.* 1190, 149-154.

Akbarsha, M.A. and Sivasamy, P. (1998). Male reproductive toxicity of phosphamidon: Histopathological changes in epididymis. *Ind. J. Exp. Biol.* 36, 34-38.

Azatian, R.A. and Voskanian, A.Z. (1987). Cytogenetic activity of various organophosphorus insecticides. *Tsitol. Genet.* 21, 226-227.

Balaji, M. and Sasikala, K. (1993). Cytogenetic effect of malathion in *in vitro* cultures of human peripheral blood. *Mutat. Res.* 301, 13-17.

Barber, J.R. and Verma, I.M. (1987). Modification of fos proteins: Phosphorylation of c-fos, but not v-fos is stimulated by 12-tetradecanoyl-phorbol-13-acetate and serum. *Mol. Cell Biol.* 7, 2201-2211.

Barbiero, G., Duranti, F., Bonelli, G., Amenta, J.S., and Baccino, F.M. (1995). Intracellular ionic variations in the apoptotic death of L cells by inhibitors of cell cycle progression. *Exp. Cell Res.* 217, 410-418.

Barkett, M., Xue, D., Horvitz, H.R., and Gilmore, T.D. (1997). Phosphorylation of IκB-α inhibits its cleavage by caspase CPP32 *in vitro*. *J. Biol. Chem.* 272, 29419-29422.

Bruno, S., Lassota, P., Giaretti, W., and Darzynkiewicz, Z. (1992). Apoptosis of rat thymocytes triggered by prednisolone, camptothecin, or teniposide is selective to G_0 cells and is prevented by inhibitors of proteases. *Oncol. Res.* 4, 29-35.

Carlson, K. and Ehrich, M. (1999). Organophosphorus compound-induced modification of SH-SY5Y human neuroblastoma mitochondrial transmembrane potential. *Toxicol. Appl. Pharmacol.* 160, 33-42.

Carlson, K. and Ehrich, M. (2000). Human neuroblastoma cell viability and growth are affected by altered culture conditions. *In Vitro Toxicol.* submitted.

Carlson, K., Jortner, B., and Ehrich, M. (2000). Organophosphorus compound-induced apoptosis in SH-SY5Y human neuroblastoma cells. *Toxicol. Appl. Pharmacol.* submitted.

Chen, H.H., Hsueh, J.L., Sirianni, S.R., and Huang, C.C. (1981). Induction of sister-chromatid exchanges and cell cycle delay in cultured mammalian cells treated with eight organophosphorous pesticides. *Mutat. Res.* 88, 307-316.

Chen, H.H., Sirianni, S.R., and Huang, C.C. (1982). Sister chromatid exchanges in Chinese hamster cells treated with seventeen organophosphorus compounds in the presence of a metabolic activation system. *Environ. Mut.* 4, 621-624.

Cunningham, M.L., Elwell, M.R., and Matthews, H.B. (1994). Relationship of carcinogenicity and cellular proliferation induced by mutagenic noncarcinogens vs carcinogens. III. Organophosphate pesticides vs. tris(2,3-dibromopropyl)phosphate. *Fundam. Appl. Toxicol.* 23, 363-369.

Cunningham, M.L., Elwell, M.R., and Matthews, H.B. (1993). Site specific cell proliferation in renal tubular cells by the renal tubular carcinogen tris(2,3-dibromopropyl)phosphate. *Environ. Health Perspect.* 101, 253-257.

Das, P. and John, G. (1999). Induction of sister chromatid exchanges and chromosome aberrations in vivo in Etroplus suratensis (Bloch) following exposure to organophosphorus pesticides. *Toxicol. Lett.* 104, 111-116.

De Ferrari, M., Artuso, M., Bonassi, S., Bonatti, S., Cavalieri, Z., Pescatore, D., Marchini, E., Pisano, V., and Abbondandolo, A. (1991). Cytogenetic biomonitoring of an Italian population exposed to pesticides: chromosome aberration and sister-chromatid exchange analysis in peripheral blood lymphocytes. *Mutat. Res.* 260, 105-113.

Del Bino, G., Skierski, J.S., and Darzynkiewicz, Z. (1991). The concentration-dependent diversity of effects of DNA topoisomerase I and II inhibitors on the cell cycle of HL-60 cells. *Exp. Cell Res.* 195, 485-491.

Drexler, H.C.A. (1997). Activation of the cell death program by inhibition of proteasome function. *Proc. Nat. Acad. Sci. USA* 94, 855-860.

Ehrich, M. (1996). Neurotoxic esterase inhibition: Predictor of potential for organophosphorus-induced delayed neuropathy. *Biomark. Agrochem. Tox.* Sub. 643, 79-93.

Ehrich, M., Correll, L., and Veronesi, B. (1994). Neuropathy target esterase inhibition by organophosphorus esters in human neuroblastoma cells. *Neurotoxicology* 15, 309-314.

Ehrich, M., Correll, L., Carlson, K., Wilcke, J., and Veronesi, B. (1995). Examination of culture conditions on esterase activities in human and mouse neuroblastoma cells. *In Vitro Toxicol.* 8, 199-207.

Ehrich, M., Correll, L., and Veronesi, B. (1997). Acetylcholinesterase and neuropathy target esterase inhibitions in neuroblastoma cells to distinguish organophosphorus compounds causing acute and delayed neurotoxicity. *Fundam. Appl. Toxicol.* 38, 1-9.

Ehrich, M. and Correll, L. (1998). Inhibition of carboxylesterases in SH-SY5Y human and NB41A3 mouse neuroblastoma cells by organophosphorus esters. *J. Toxicol. Environ. Health*, Part A 53, 101-115.

Evan, G.I., Wyllie, A.H., Gilbert, C.S., Littlewood, T.D., Land, H., Brooks, M., Waters, C.M., Penn, L.Z., and Hancock, D.C. (1992). Induction of apoptosis in fibroblasts by c-myc protein. *Cell* 69, 119-128.

Flaskos, J., McLean, W.G., and Hargreaves, A.J. (1994). The toxicity of organophosphate compounds towards cultured PC12 cells. *Toxicol. Lett.* 70, 71-76.

Gallichio, V.S., Casale, G.P., and Watts, T. (1987). Inhibition of human bone marrow-derived stem cell colony formation (CFU-E, BFU-E, and CFU-GM) following *in vitro* exposure to organophosphates. *Exp. Hematol.* 15, 1099-1102.

Giardina, S.F., Cheung, N.S., Reid, M.T., and Beart, P.M. (1998). Kainate-induced apoptosis in cultured murine cerebellar granule cells elevates expression of the cell cycle gene cyclin D1. *J. Neurochem.* 71, 1325-1328.

Greenman, S.B., Rutten, M.J., Fowler, W.M., Scheffler, L., Shortridge, L.A., Brown, B., Sheppard, B.C., Deveney, K.E., Deveney, C.W., and Trunkey, D.D. (1997). Herbicide/pesticide effects on intestinal epithelial growth. *Environ. Res.* 75, 85-93.

Hamm, J.T., Wilson, B.W., and Hinton, D.E. (1998). Organophosphate-induced acetylcholinesterase inhibition and embryonic retinal cell necrosis *in vivo* in the teleost (Oryzias Latipes). *Neurotoxicology* 19, 853-870.

Harvey, M.J. and Sharma, R.P. (1980). Organophosphate cytotoxicity: The effects on protein metabolism in cultured neuroblastoma cells. *J. Environ. Pathol. Toxicol.* 3, 423-436.

Hoang, A.T., Cohen, K.J., Barrett, J.F., Bergstrom, D.A., and Dang, C.V. (1994). Participation of cyclin A in Myc-induced apoptosis. *Proc. Natl. Acad. Sci. USA* 91, 6875-6879.

Hua, S., To, W.Y., Nguyen, T.T., Wong, M.L., and Wang, C.C. (1996). Purification and characterization of proteasomes from Trypanosoma brucei. *Mol. Biochem. Parasitol.* 78, 33-46.

Kato, G.J. (1999). Human genetic diseases of proteolysis. *Hum Mutat.* 13, 87-98.

Ko, L.J. and Prives, C. (1996). p53:Puzzle and paradigm. *Genes and Devel.* 10, 1054-1072.

Kobayashi, T., Okamoto, K., Kobata, T., Hasunuma, T., Sumida, T., and Nishioka, K. (1999). Tumor necrosis factor alpha regulation of the Fas-mediated apoptosis-signaling pathway in synovial cells. *Arthritis Rheum.* 42, 519-526.

Kranenburg, O., van der Eb, A.J., and Zantema, A. (1996). Cyclin D1 is an essential mediator of apoptotic neuronal cell death. *EMBO J.* 15, 46-54.

Lakomy, M., Flieger, S., and Jastrzebski, M. (1984). Binuclear neurons in the brain of hens in experimental pesticide poisoning. *Pol. Arch. Weter.* 24, 247-252.

Lieberman, A.D., Craven, M.R., Lewis, H.A., and Nemenzo, J.H. (1998). Genotoxicity form domestic use of organophosphate pesticides. *J. Occup. Environ. Med.* 40, 954-957.

Lotti, M., Caroldi, S., Capodicasa, E., and Moretto, A. (1991). Promotion of organophosphate-induced delayed polyneuropathy by phenylmethanesulfonyl fluoride. *Toxicol. Appl. Pharmacol.* 108, 234-241.

Massicotte, C., Inzana, K.D., Ehrich, M., and Jortner, B.S. (1999). Neuropathologic effects of phenylmethylsulfonyl fluoride (PMSF)-induced promotion and protection in organophosphorus ester-induced delayed neuropathy (OPIDN) in hens. *Neurotoxicology* 20, 749-760.

Moore, R.A., Doebler, J.A., Shih, T.M., and Anthony, A. (1984). Nuclear changes in hepatocytes of soman treated rats. *Toxicol.* 31, 99-108.

Morris, E.J. and Geller, H.M. (1996). Induction of neuronal apoptosis by camptothecin, and inhibitor of DNA topoisomerase-I: Evidence for cell cycle-independent toxicity. *J. Cell Biol.* 134, 757-770.

Nuydens, R., de Jong, M., Kieboom, G.V.D., Heers, C., Dispersyn, G., Cornelissen, F., Nuyens, R., Borgers, M., and Geerts, H. (1998). Okadaic acid-induced apoptosis in neuronal cells: evidence for an abortive mitotic attempt. *J. Neurochem.* 70, 1124-1133.

Park, D.S., Morris, E.J., Greene, L.A., and Geller, H.M. (1997). G_1/S cell cycle blockers and inhibitors of cyclin-dependent kinases suppress camptothecin-induced neuronal apoptosis. *J. Neurosci.* 17, 1256-1270.

Pellegata, N.S., Antoniono, R.J., Redpath, J.L., and Stanbridge, E.J. (1996). DNA damage and p53-mediated cell cycle arrest: A reevaluation. *Proc. Nat. Acad. Sci. USA* 93, 15209-15214.

Ponce, R.A., Kavanagh, T.J., Mottet, N.K., Whittaker, S.G., and Faustman, E.M. (1994). Effects of methyl mercury on the cell cycle of primary rat CNS cells *in vitro*. *Toxicol. Appl. Pharmacol.* 127, 83-90.

Pulverer, B.J., Kyriakis, J.M., Avruch, J., Nikolakaki, E., and Woodgett, J.R. (1991). Phosphorylation of c-Jun mediated by MAP kinases. *Nature* 353, 345-349.

Robinson, J.P., Darzynkiewicz, Z., and Dean, P. (eds). 1993. DNA cell cycle analysis: Propidium iodide procedure. In *Handbook of Flow Cytometry Methods*. p97. John Wiley and Sons, Inc., New York.

Ross, M.E. (1996). Cell division and the nervous system: regulating the cycle from neural differentiation to death. *TINS* 19, 62-68.

Rupa, D.S., Reddy, P.P., and Reddi, O.S. (1989). Analysis of sister-chromatid exchanges, cell kinetics, and mitotic index in lymphocytes of smoking pesticide sprayers. *Mutat. Res.* 223, 253-258.

Titenko-Holland, N., Windham, G., Kolachana, P., Reinisch, F., Parvatham, S., Osoio, A.M., and Smith, M.T. (1997). Genotoxicity of malathion in human lymphocytes assessed using the micronucleus assay *in vitro* and *in vivo*: a study of malathion-exposed workers. *Mutat. Res.* 388, 85-95.

Tuler, S.M. and Bowen, J.M. (1989). Toxic effect of organophosphates on nerve cell growth and ultrastructure in culture. *J. Toxicol. Environ. Health* 27, 209-223.

Sarin, A., Adams, D.H., and Henkart, P.A. (1993). Protease inhibitors selectively block T cell receptor-triggered programmed cell death in a murine T cell hybridoma and activated peripheral T cells. *J. Exp. Med.* 178, 1693-1700.

Singh, S., Lehmann-Grube, B., and Goedde, H.W. (1984). Cytogenetic effects of paraoxon and methyl-parathion on cultured human lymphocytes: SCE, clastogenic activity, and cell cycle delay. *Int. Arch. Occup. Environ. Health* 54, 195-200.

Slamenova, D., Dusinska, M., Gabelova, A., Bohusova, T., and Ruppova, K. (1992). Decemitione (Imidan)-induced single-strand breaks to human DNA, mutations at the hgprt locus of V79 cells, and morphological transformations of embryo cells. *Environ. Mol. Mutagen* 20, 73-78.

Sobti, R.C., Krishan, A., and Pfaffenberger, C.D. (1982). Cytokinetic and cytogenetic effects of some agricultural chemicals on human lymphoid cells *in vitro*: Organophosphates. *Mutat. Res.* 102, 89-102.

Suffys, P., Beyaert, R., Van Roy, F., and Fiers, W. (1988). Involvement of a serine protease in tumor-necrosis-factor-mediated cytotoxicity. *Eur. J. Biochem.* 178, 257-265.

Veronesi, B., Ehrich, M., Blusztajn, J.K., Oortgiesen, M., and Durham, H. (1997). Cell culture models of interspecies selectivity to organophosphorus insecticides. *Neurotoxicology* 18, 283-298.

Viana, G.B., Davis, L.H., and Kauffman, F.C. (1988). Effects of organophosphates and nerve growth factor on muscarinic receptor binding number in rat pheochromocytoma PC12 cells. *Toxicol. Appl. Pharmacol.* 93, 257-266.

Waring, P., Khan, T., and Sjaarda, A. (1997). Apoptosis induced by gliotoxin is preceded by phosphorylation of histone H3 and enhanced sensitivity of chromatin to nuclease digestion. *J. Biol. Chem.* 272, 17929-17936.

Weinburg, R.A. (1995). The retinoblastoma protein and cell cycle control. *Cell* 81, 323-330.

Whiteside, S.T. and Israël, A. (1997). IκB proteins: Structure, function and regulation. *Sem. Cancer Biol.* 8, 75-82.

Wilson, B.W., Kawakami, T.G., Cone, N., Henderson, J.D., Rosenblatt, L.S., Goldman, M., and Dacre, J.C. (1994). Genotoxicity of the phosphoramidate agent tabun (GA). *Toxicol.* 86, 1-12.

Yin, H., Cukurcam, S., Betzendahl, I., Adler, I.D., and Eichenlaub-Ritter, U. (1998). Trichlorfon exposure, spindle aberrations, and nondisjunction in mammalian oocytes. *Chromosoma* 107, 514-522.

Zhu, W.G., Antoku, S., Kura, S., Aramaki, R., Nakamura, K., and Sasaki, H. (1995). Enhancement of hyperthermic killing in L5178Y cells by protease inhibitors. *Cancer Res.* 55, 739-742.

(*a*)

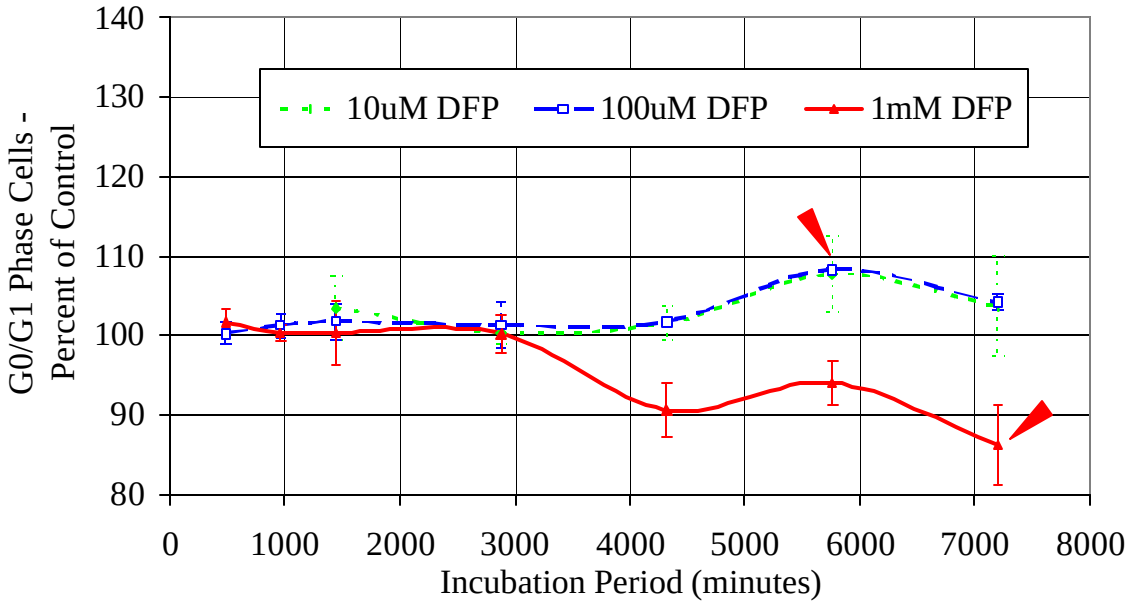

(*b*)

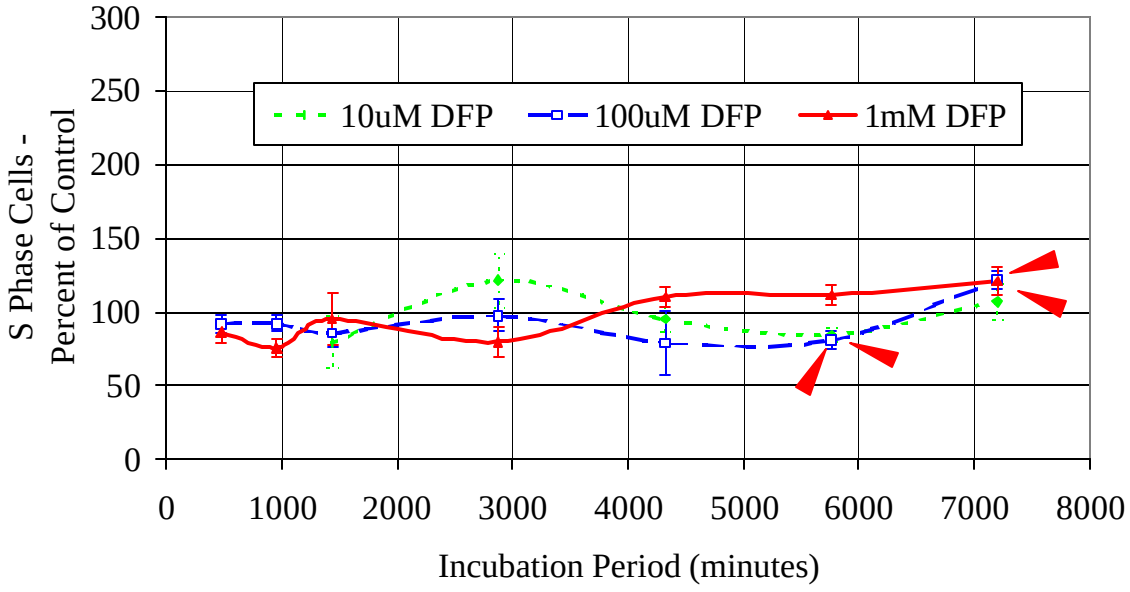

Figure 4.1. SH-SY5Y cells exposed to diisopropylphosphorofluoridate (DFP; 10µM, 100µM, and 1mM). Values are the mean of 4-13 normalized data points (percentages) ± the standard deviation. Statistical significance of exposed cells when compared to matched ethanol controls are shown ($P<0.05$, ◢). Fig. 4.1a, cells in G_0/G_1 phase; Fig. 4.1b, cells in S phase. In Fig. 4.1a, lines overlap for 10µM and 100µM DFP concentrations.

(*c*)

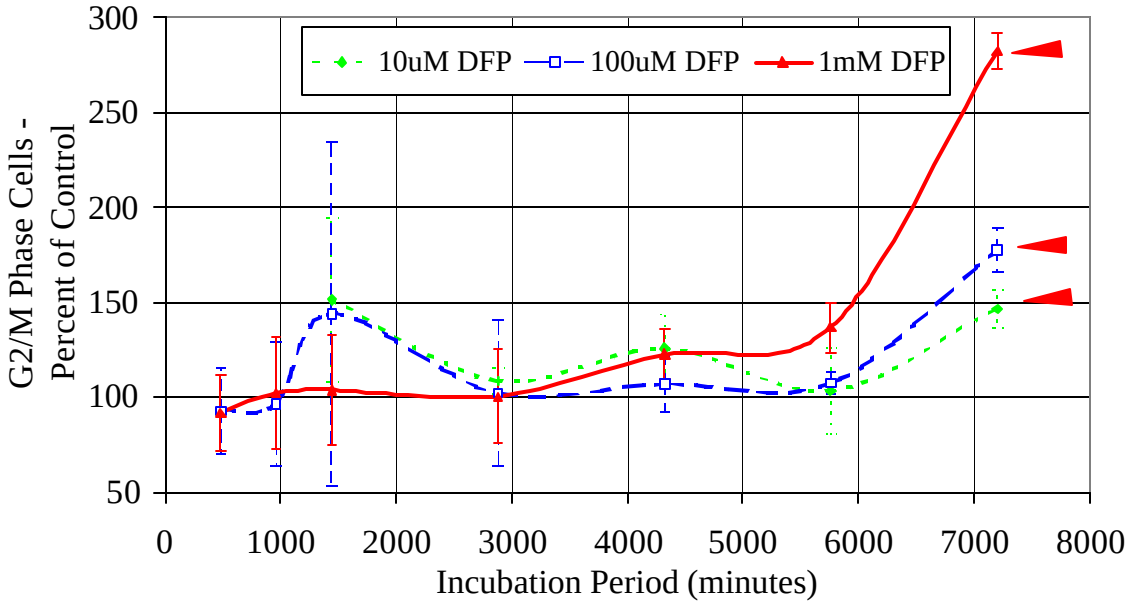

(*d*)

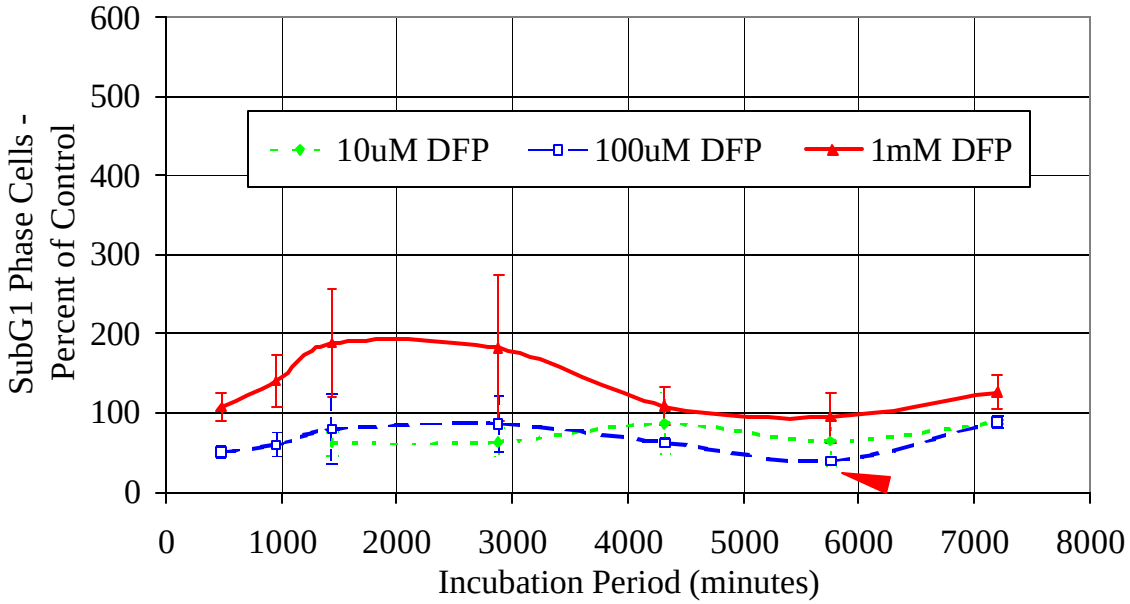

Figure 4.1. SH-SY5Y cells exposed to diisopropylphosphorofluoridate (DFP; 10µM, 100µM, and 1mM). Values are the mean of 4-13 normalized data points (percentages) ± the standard deviation. Statistical significance of exposed cells when compared to matched ethanol controls are shown ($P<0.05$, ◢). Fig. 4.1c, cells in G_2/M phase; Fig. 4.1d, cells with subG_1 (fragmented) DNA.

(*a*)

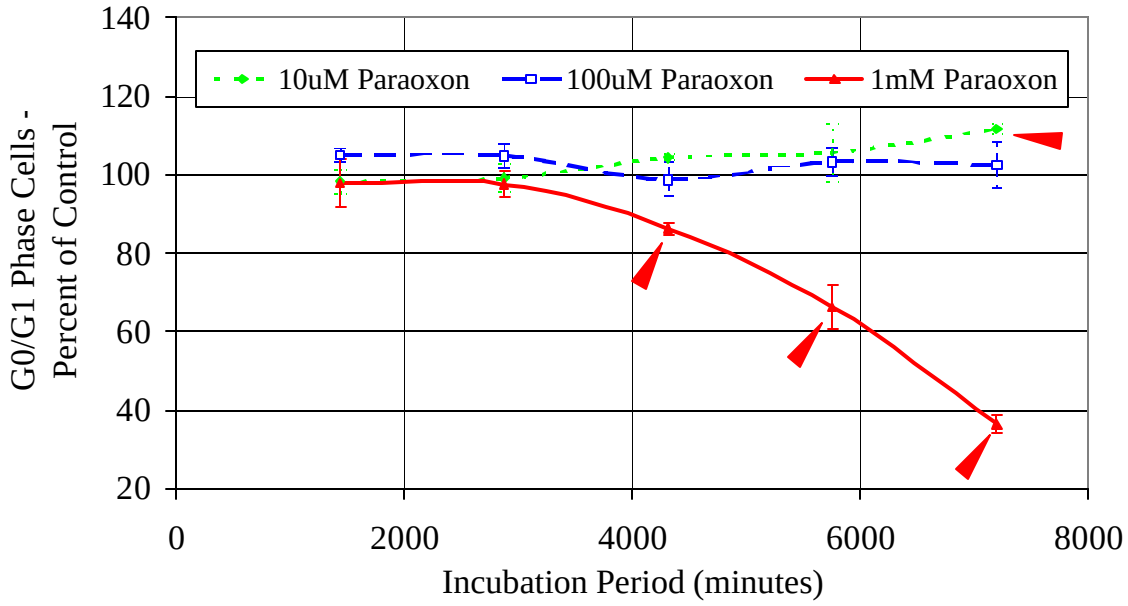

(*b*)

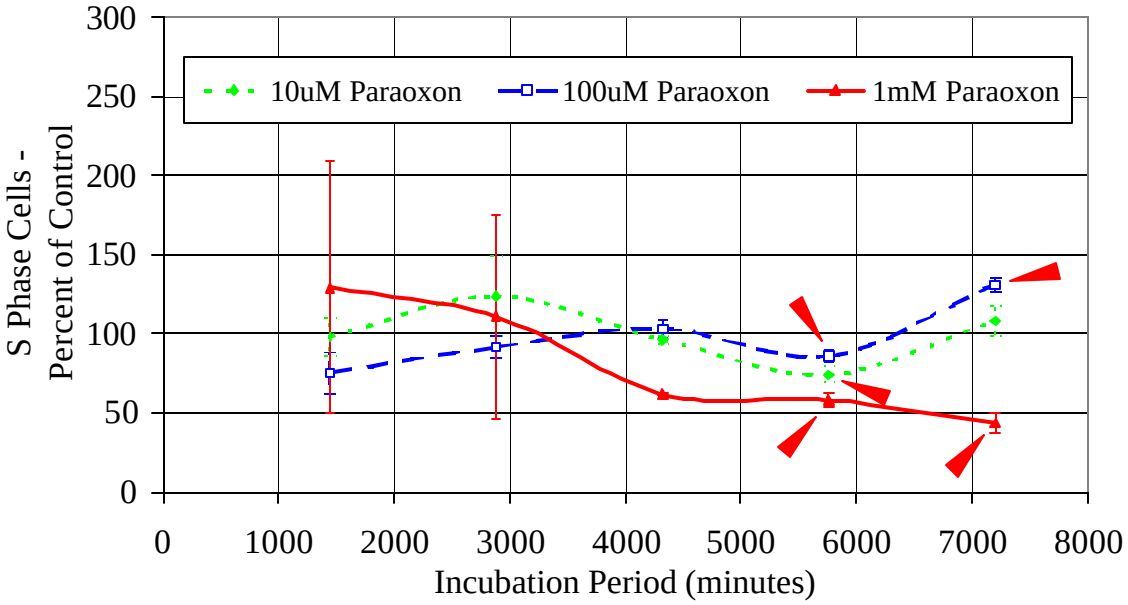

Figure 4.2. SH-SY5Y cells exposed to paraoxon (10µM, 100µM, and 1mM). Values are the mean of 4-6 normalized data points (percentages) ± the standard deviation. Statistical significance of exposed cells when compared to matched ethanol controls are shown ($P<0.05$, ◢). Fig. 4.2a, cells in G_0/G_1 phase; Fig. 4.2b, cells in S phase.

(*c*)

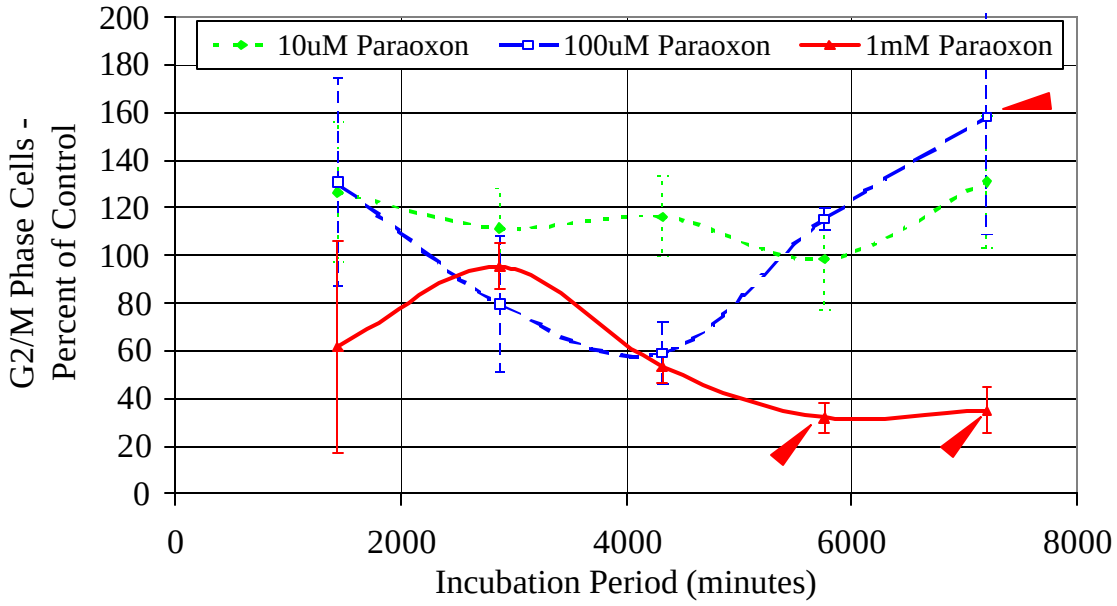

(*d*)

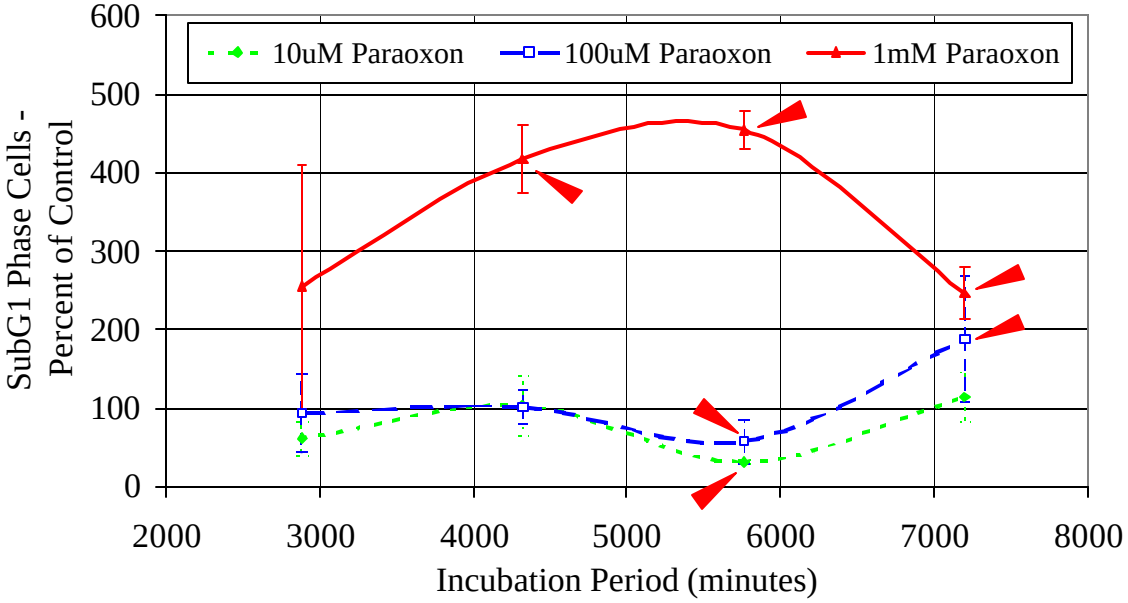

Figure 4.2. SH-SY5Y cells exposed to paraoxon (10µM, 100µM, and 1mM). Values are the mean of 4-6 normalized data points (percentages) ± the standard deviation. Statistical significance of exposed cells when compared to matched ethanol controls are shown ($P<0.05$, ◢). Fig. 4.2c, cells in G_2/M phase; Fig. 4.2d, cells with subG_1 (fragmented) DNA.

(*a*)

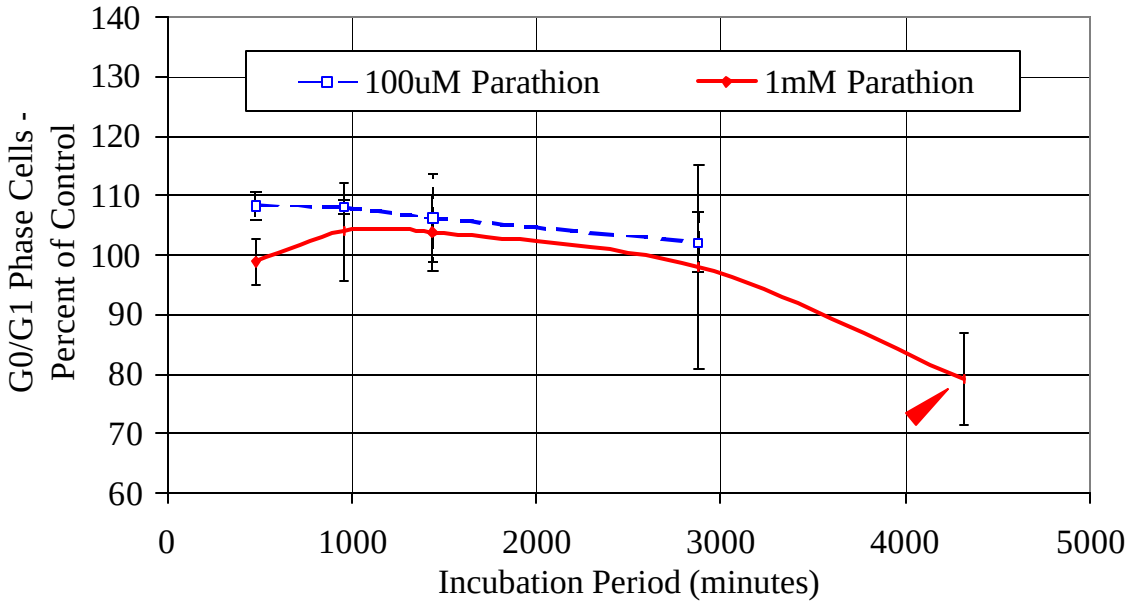

(*b*)

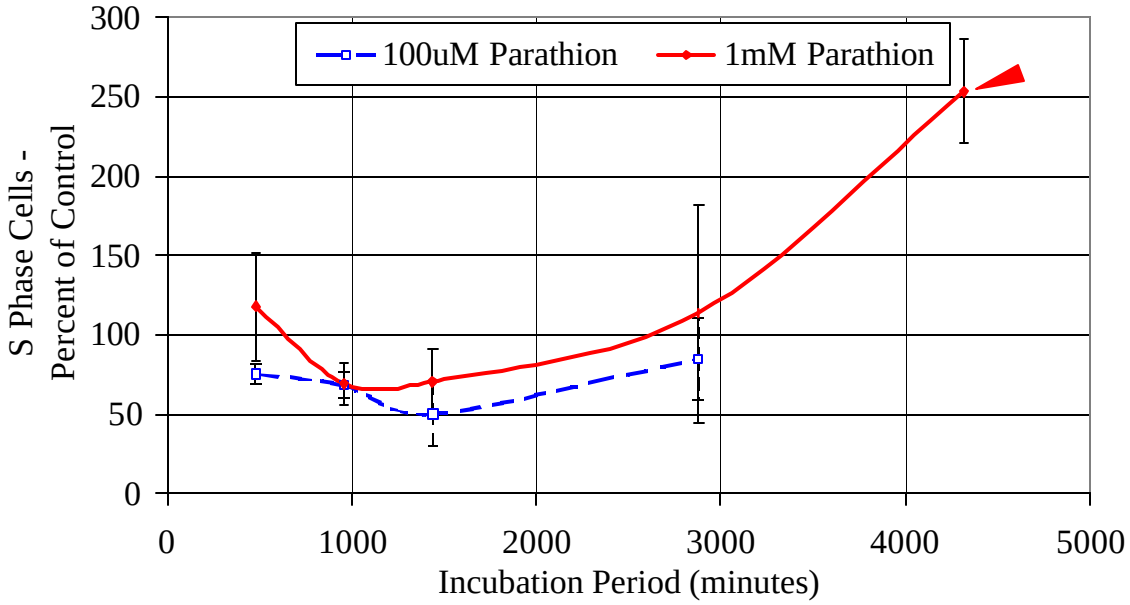

Figure 4.3. SH-SY5Y cells exposed to parathion (100µM and 1mM). Values are the mean of 9-12 normalized data points (percentages) ± the standard deviation. Statistical significance of exposed cells when compared to matched ethanol controls are shown ($P<0.05$, ◀).
Fig. 4.3a, cells in G_0/G_1 phase; Fig. 4.3b, cells in S phase.

(*c*)

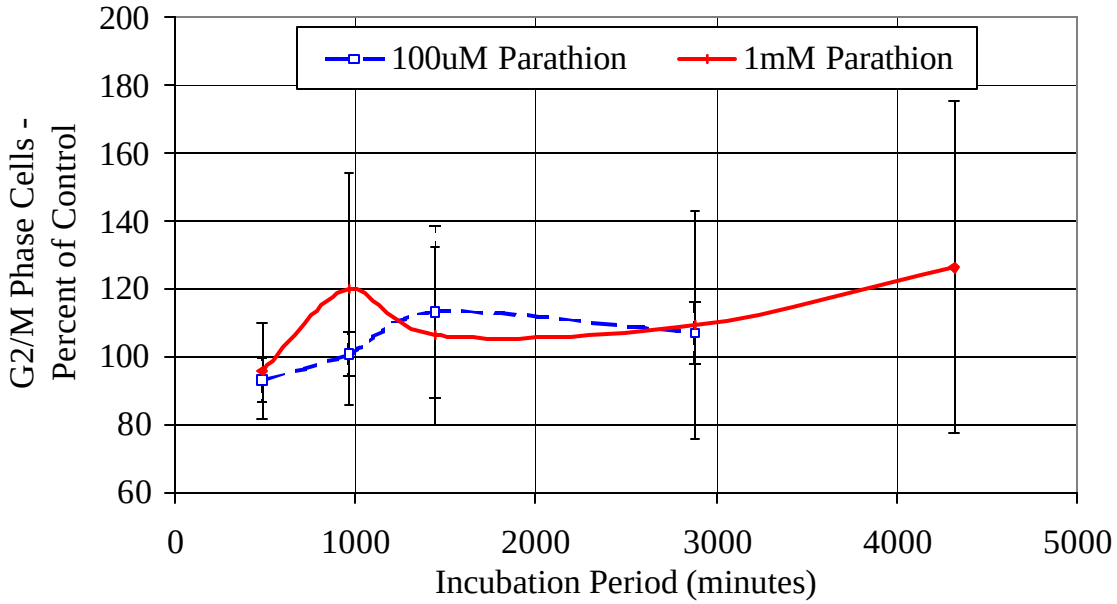

(*d*)

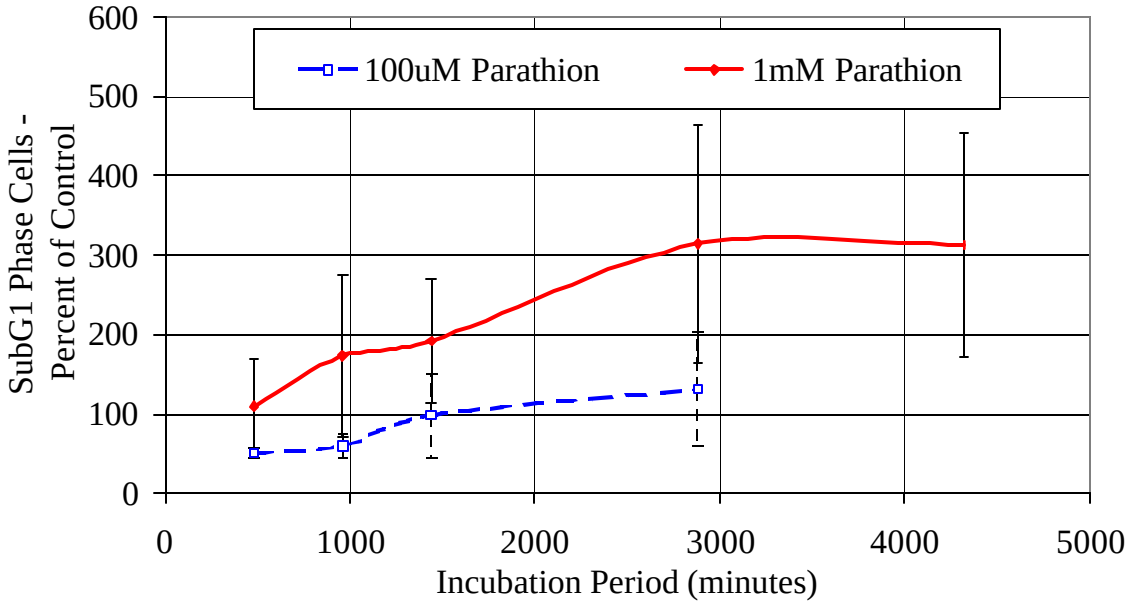

Figure 4.3. SH-SY5Y cells exposed to parathion (100µM and 1mM). Values are the mean of 9-12 normalized data points (percentages) ± the standard deviation. Statistical significance of exposed cells when compared to matched ethanol controls are shown ($P<0.05$, ◢). Fig. 4.3c, cells in G_2/M phase; Fig. 4.3d, cells with subG_1 (fragmented) DNA.

(*a*)

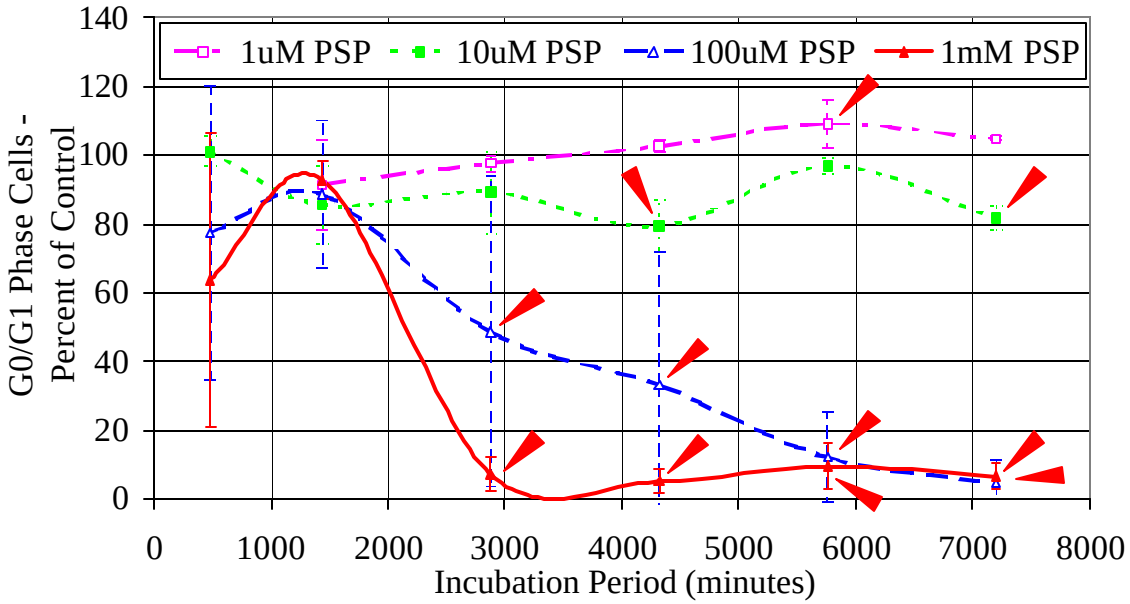

(*b*)

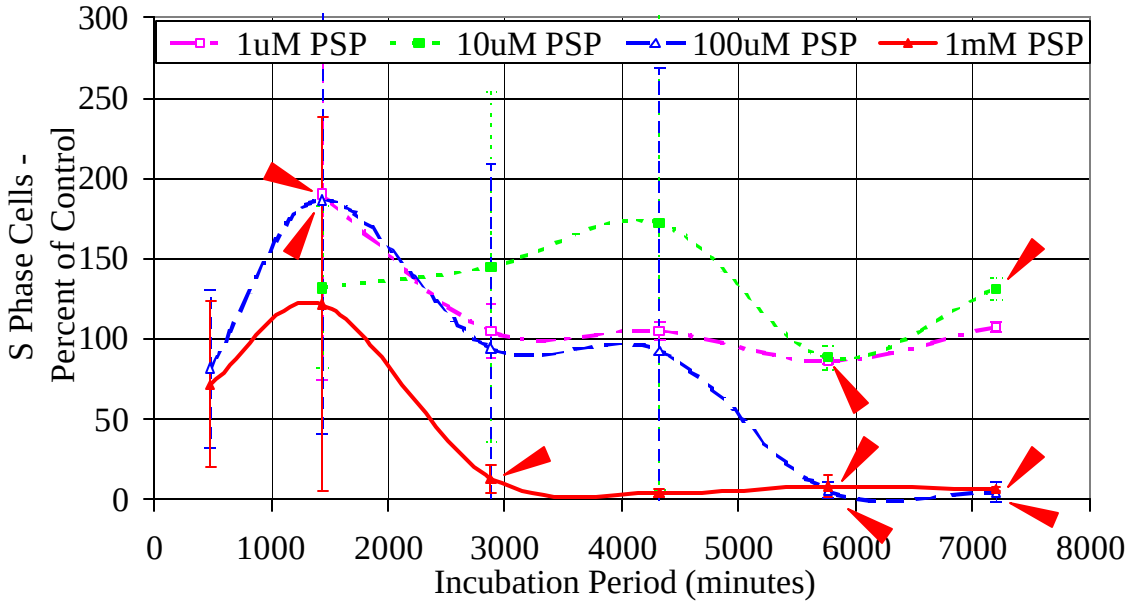

Figure 4.4. SH-SY5Y cells exposed to phenyl saligenin phosphate (PSP; 1µM, 10µM, 100µM, and 1mM). Values are the mean of 7-10 normalized data points (percentages) ± the standard deviation. Statistical significance of exposed cells when compared to matched ethanol controls are shown ($P<0.05$, ◢). Fig. 4.4a, cells in G_0/G_1 phase; Fig. 4.4b, cells in S phase.

(*c*)

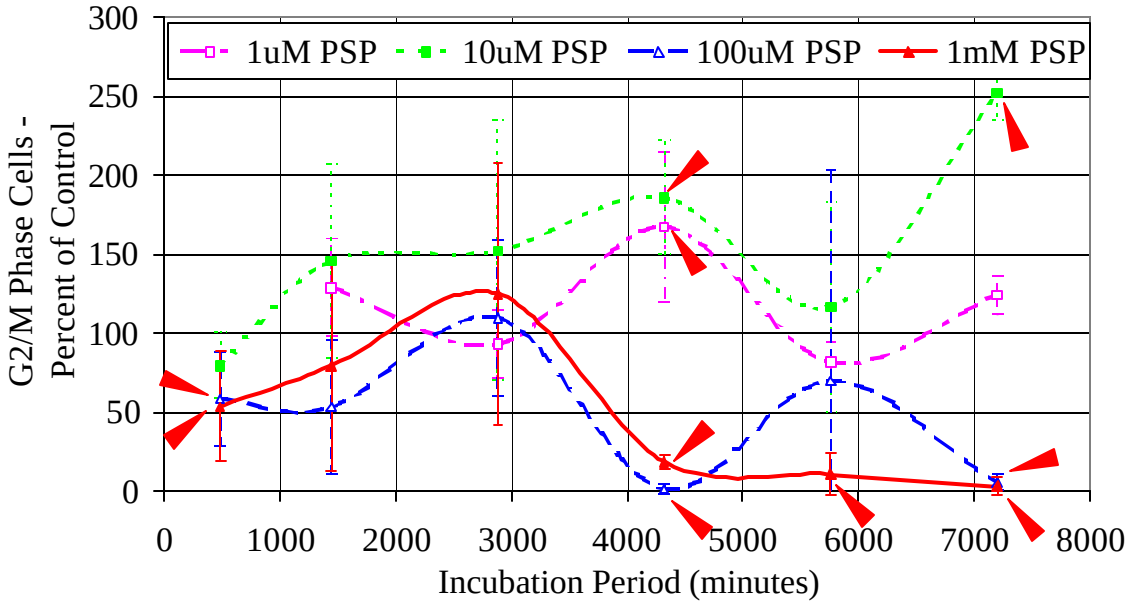

(*d*)

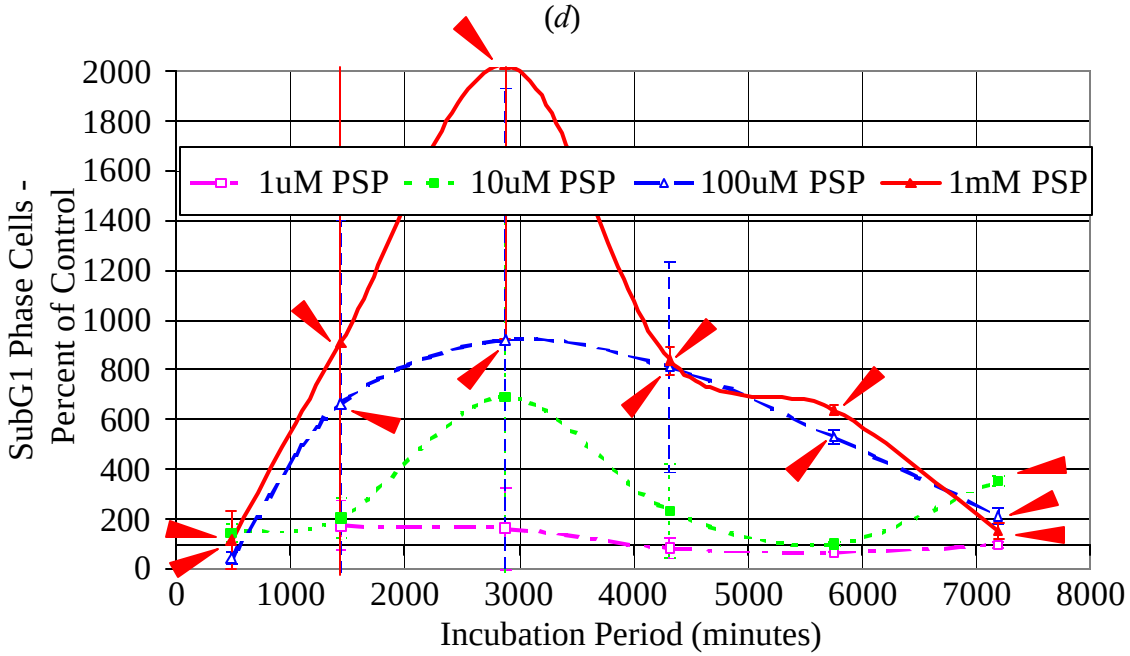

Figure 4.4. SH-SY5Y cells exposed to phenyl saligenin phosphate (PSP; 1µM, 10µM, 100µM, and 1mM). Values are the mean of 7-10 normalized data points (percentages) ± the standard deviation. Statistical significance of exposed cells when compared to matched ethanol controls are shown ($P<0.05$, ◢). Fig. 4.4c, cells in G_2/M phase; Fig. 4.4d, cells with subG_1 (fragmented) DNA.

(*a*)

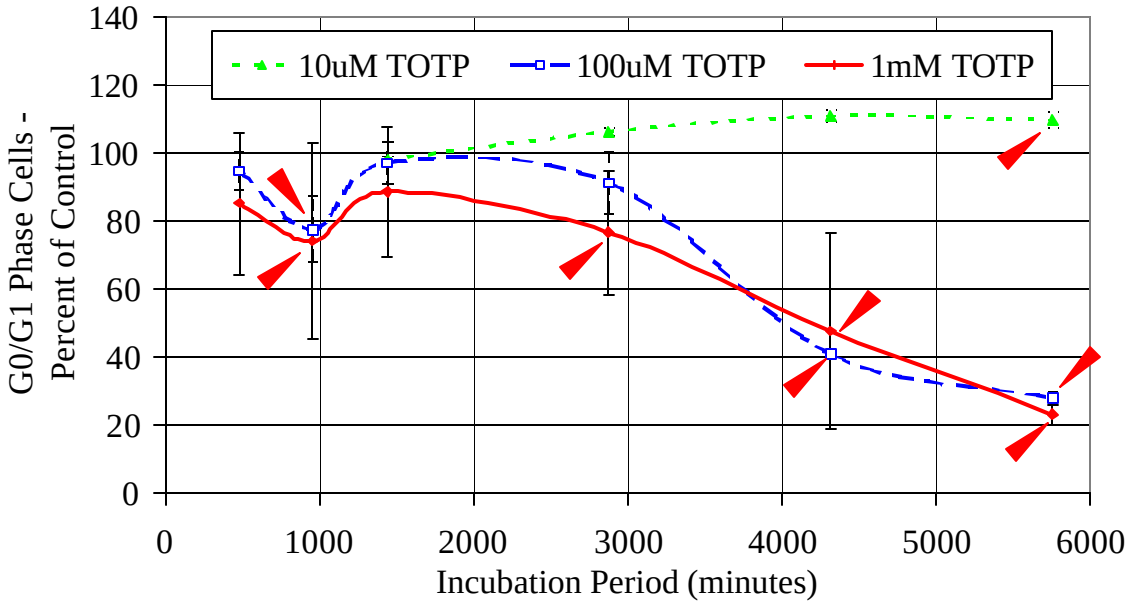

(*b*)

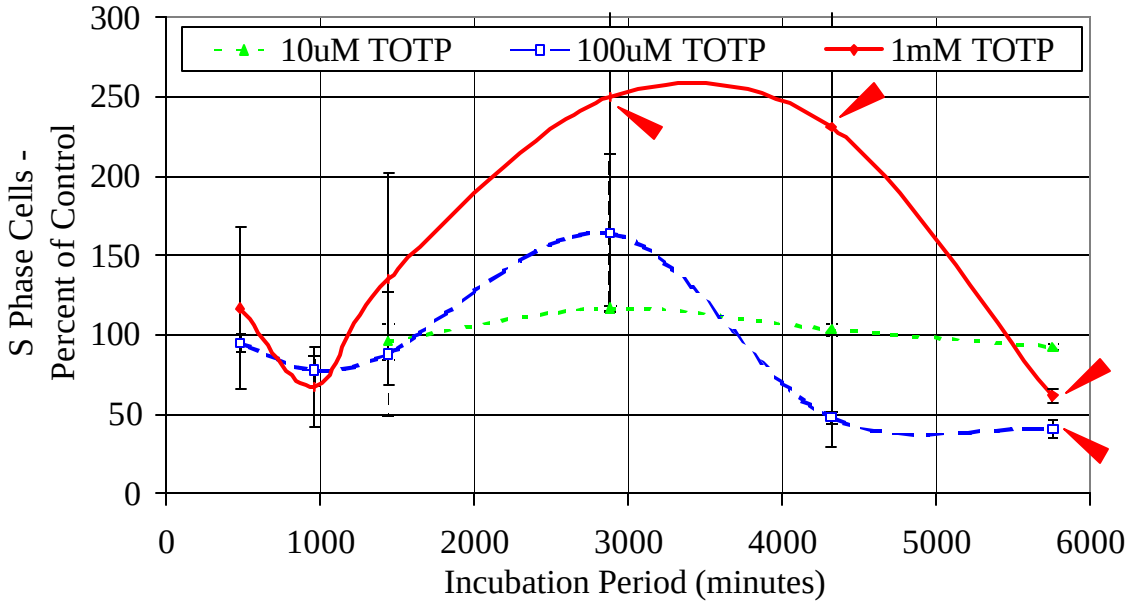

Figure 4.5. SH-SY5Y cells exposed to tri-ortho-tolyl phosphate (TOTP; 10µM, 100µM, and 1mM). Values are the mean of 3-15 normalized data points (percentages) ± the standard deviation. Statistical significance of exposed cells when compared to matched ethanol controls are shown ($P<0.05$, ◢). Fig. 4.5a, cells in G_0/G_1 phase; Fig. 4.5b, cells in S phase.

(*c*)

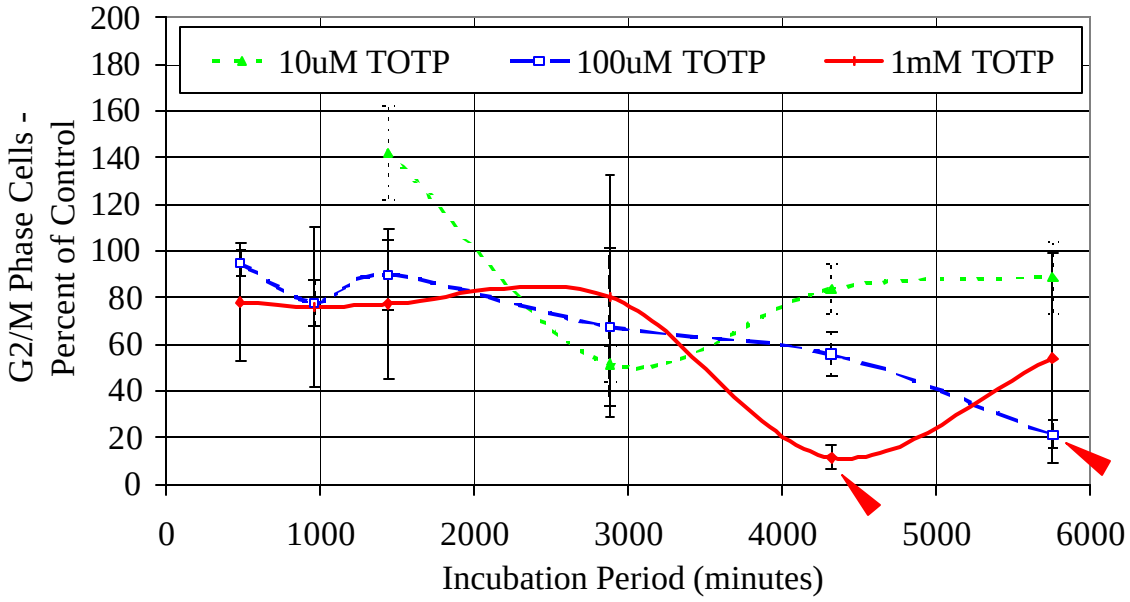

(*d*)

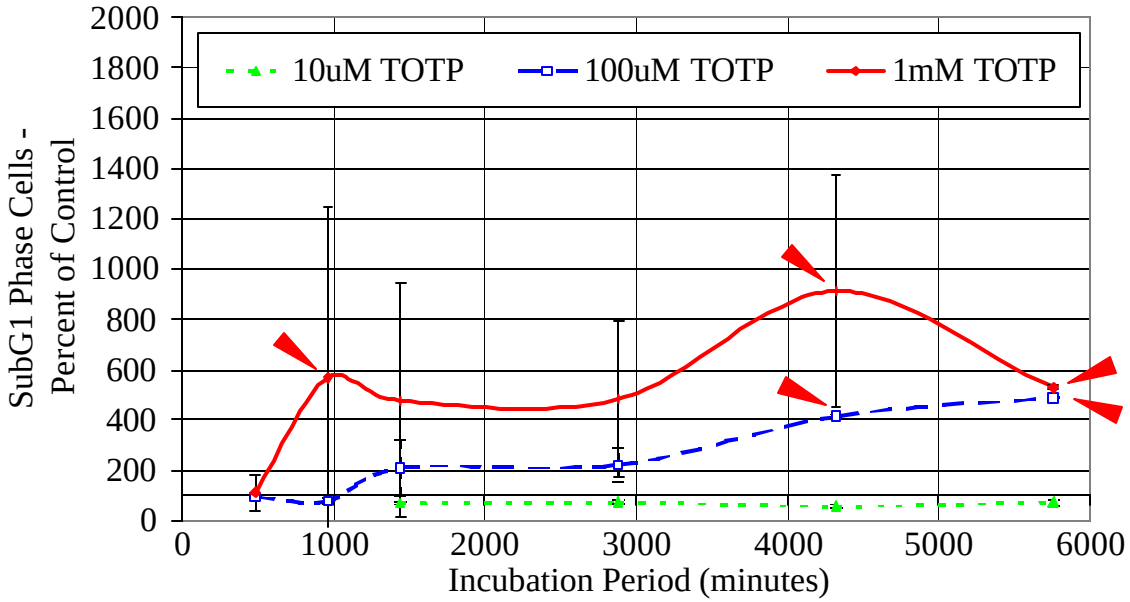

Figure 4.5. SH-SY5Y cells exposed to tri-ortho-tolyl phosphate (TOTP; 10µM, 100µM, and 1mM). Values are the mean of 3-15 normalized data points (percentages) ± the standard deviation. Statistical significance of exposed cells when compared to matched ethanol controls are shown ($P<0.05$, ◢). Fig. 4.5c, cells in G_2/M phase; Fig. 4.5d, cells with subG_1 (fragmented) DNA.

(*a*)

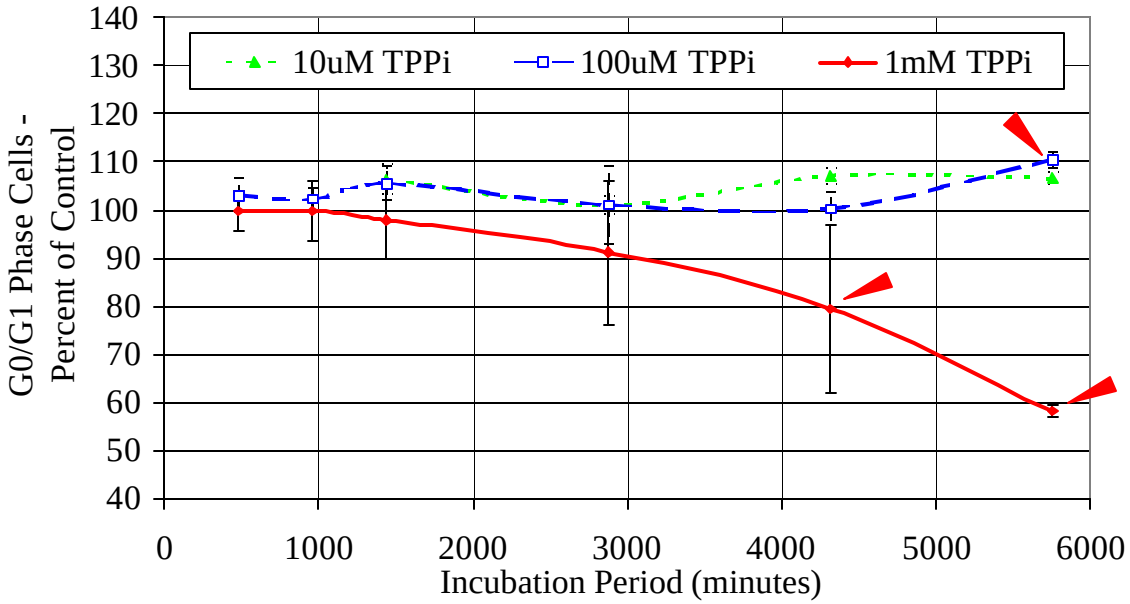

(*b*)

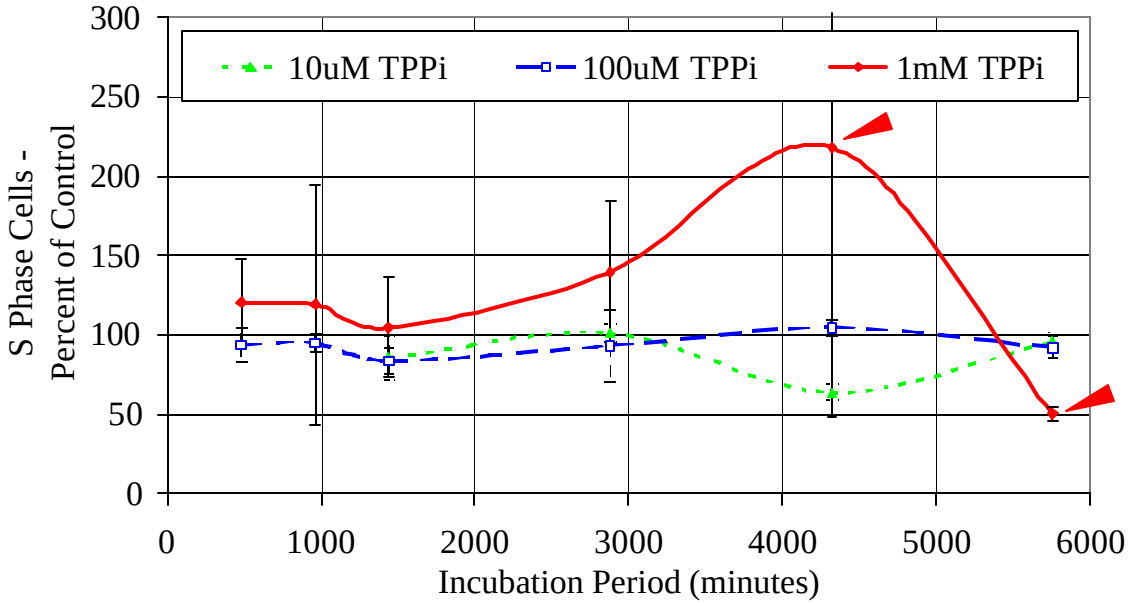

Figure 4.6. SH-SY5Y cells exposed to triphenylphosphite (TPPi; 10µM, 100µM, and 1mM). Values are the mean of 3-18 normalized data points (percentages) ± the standard deviation. Statistical significance of exposed cells when compared to matched ethanol controls are shown ($P<0.05$, ◢). Fig. 4.6a, cells in G_0/G_1 phase; Fig. 4.6b, cells in S phase.

(*c*)

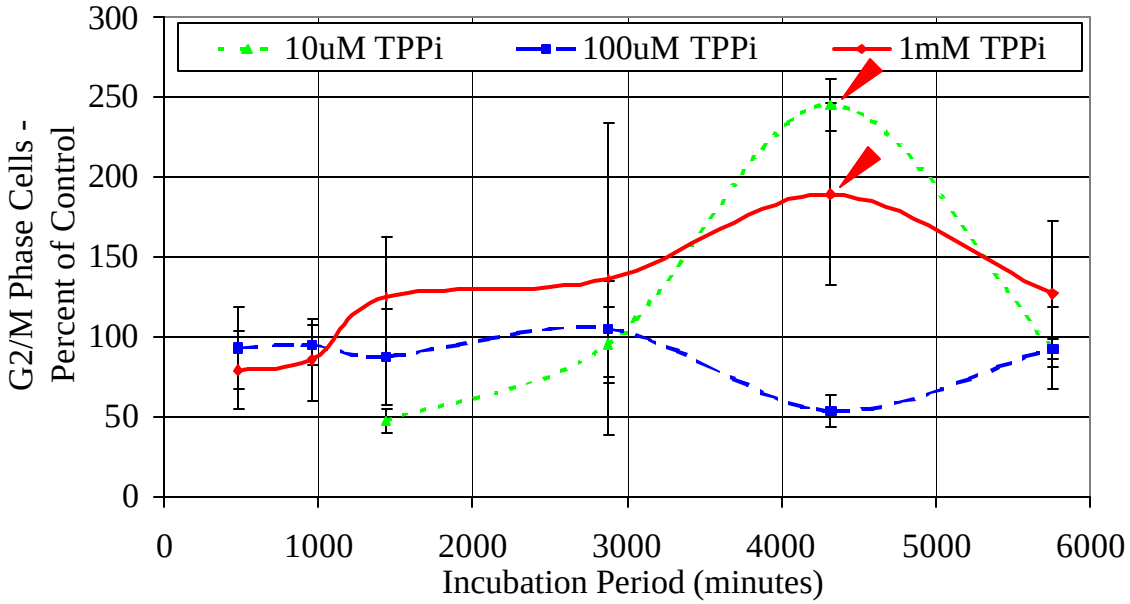

(*d*)

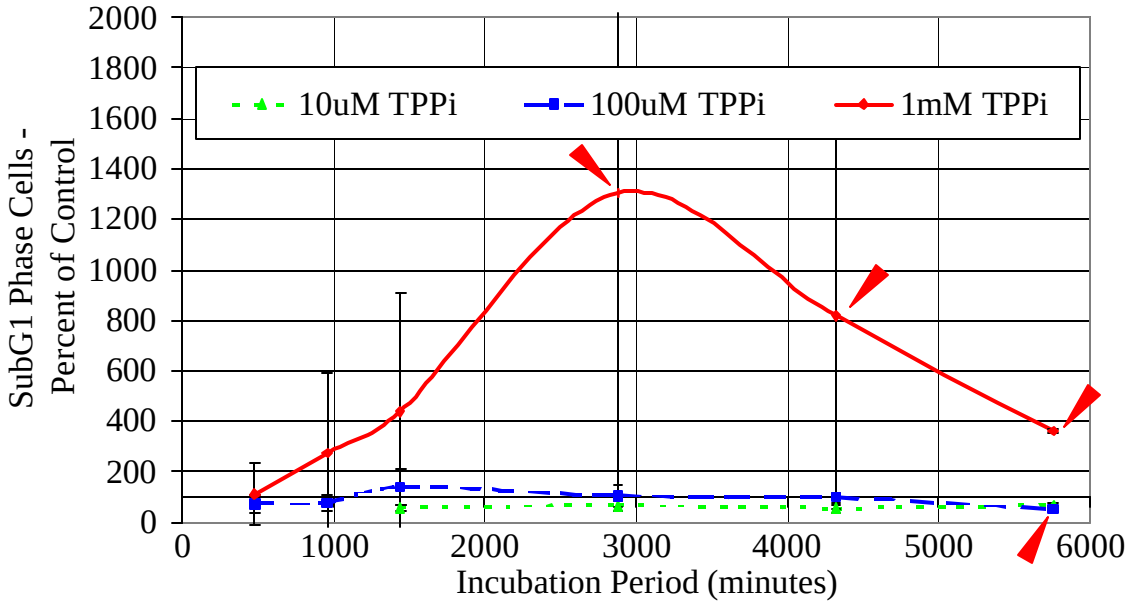

Figure 4.6. SH-SY5Y cells exposed to triphenylphosphite (TPPi; 10µM, 100µM, and 1mM). Values are the mean of 3-18 normalized data points (percentages) ± the standard deviation. Statistical significance of exposed cells when compared to matched ethanol controls are shown ($P<0.05$, ◢). Fig. 4.6c, cells in G_2/M phase; Fig. 4.6d, cells with subG_1 (fragmented) DNA.

(*a*)

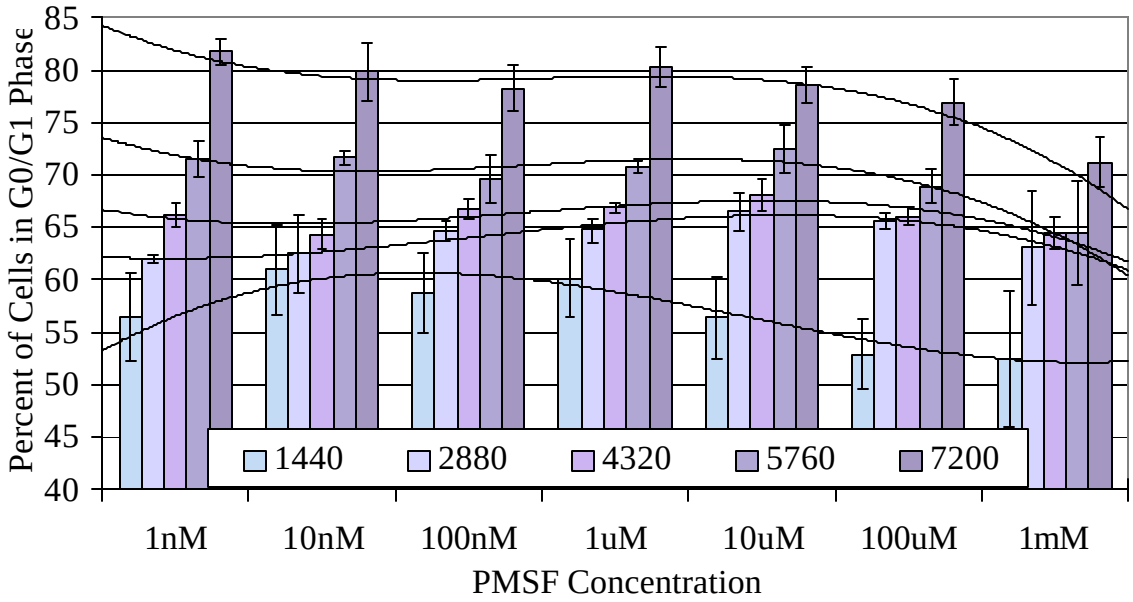

(*b*)

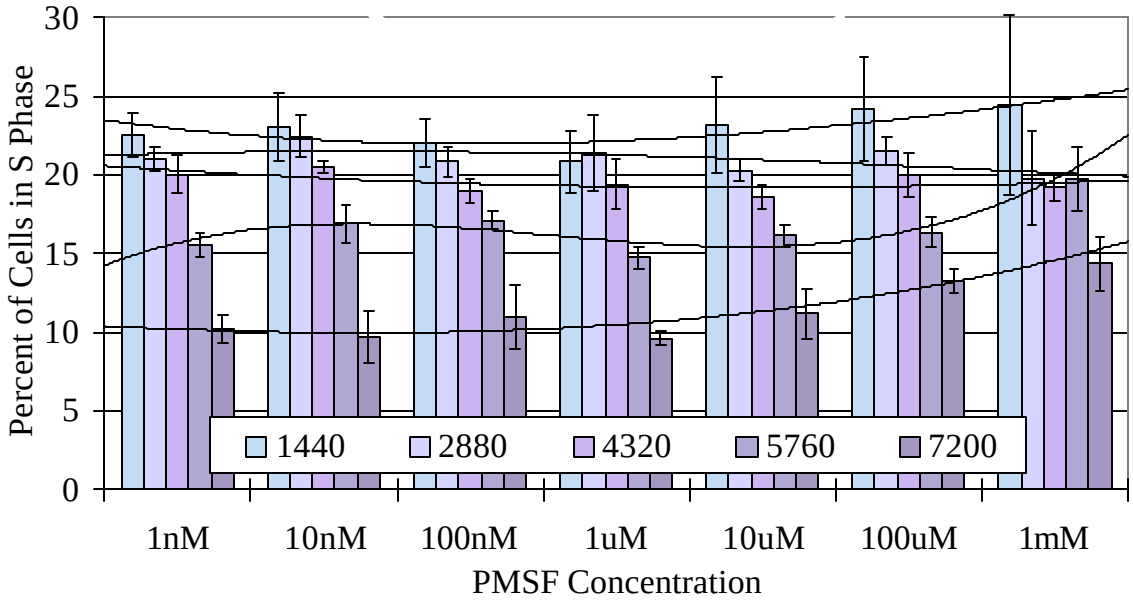

Figure 4.7. SH-SY5Y cells exposed to phenylmethylsulfonyl fluoride (PMSF; 1nM, 10nM, 100nM, 1μM, 10μM, 100μM, and 1mM). Values are the mean of 3 normalized data points (percentages) ± the standard deviation. Polynomial regression lines progress across different concentrations of PMSF at the same time point. Fig. 4.7a, cells in G_0/G_1 phase; Fig. 4.7b, cells in S phase.

(*c*)

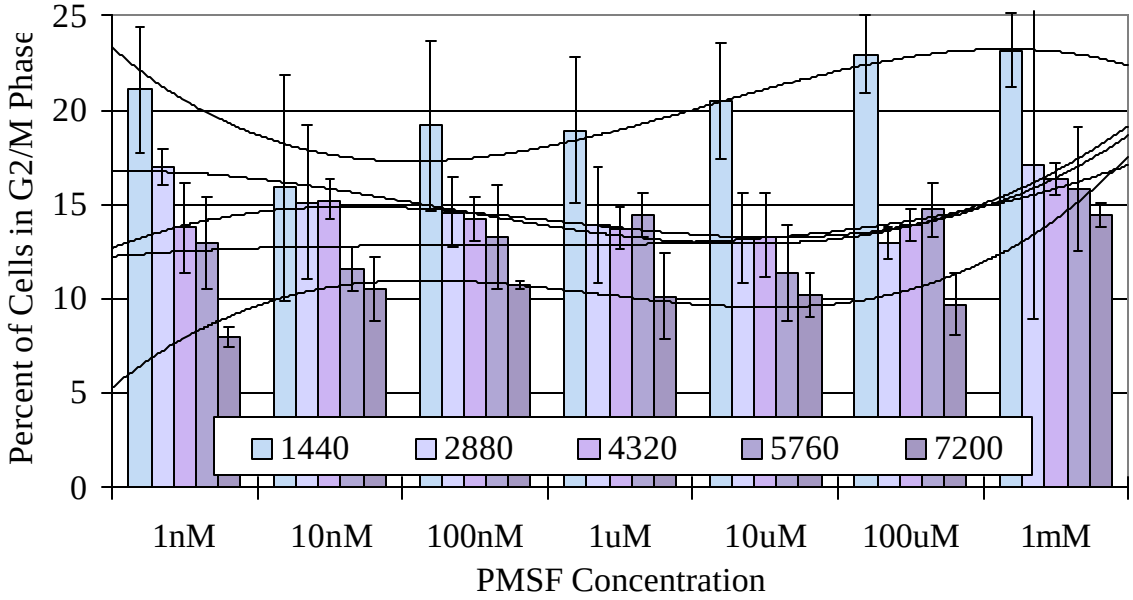

Figure 4.7. SH-SY5Y cells exposed to phenylmethylsulfonyl fluoride (PMSF; 1nM, 10nM, 100nM, 1μM, 10μM, 100μM, and 1mM). Values are the mean of 3 normalized data points (percentages) ± the standard deviation. Polynomial regression lines progress across different concentrations of PMSF at the same time point. Fig. 4.7c, cells in G_2/M phase.

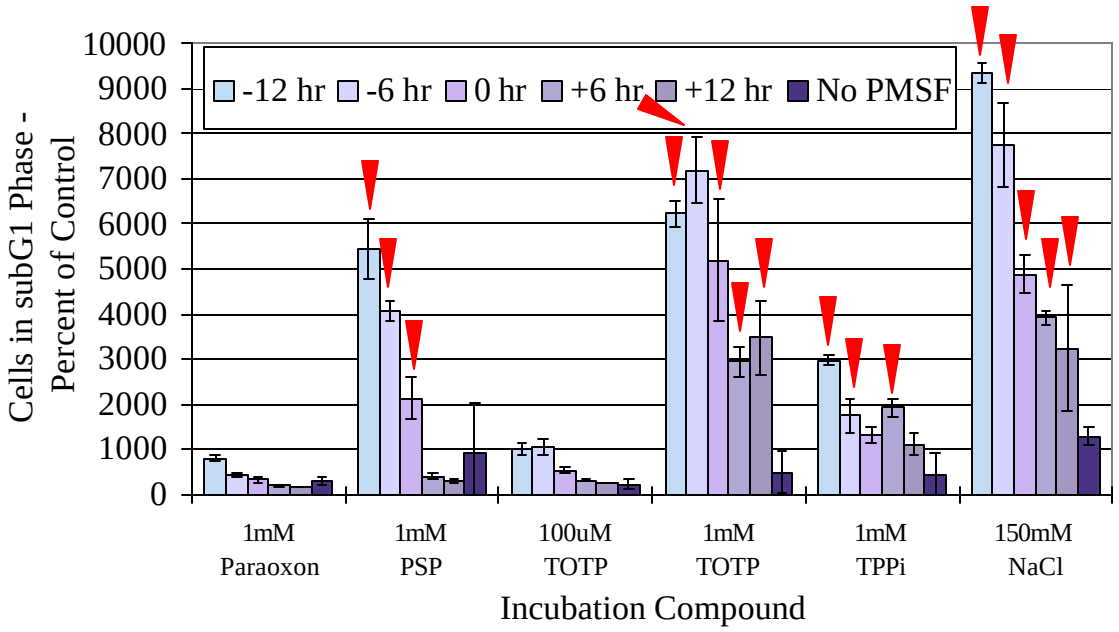

Figure 4.8. SubG$_1$ (fragmented) DNA in SH-SY5Y cells treated with OP compounds alone, or PMSF before (-12 to -6 hr), at the same time, and after (+6 to +12 hr), exposure to OP compounds (1mM paraoxon, PSP, TOTP, and TPPi; 100µM TOTP) and 150mM NaCl. Values are the mean of 3 normalized data points (percentages) ± the standard deviation. Statistical significance of exposed cells when compared to matched controls exposed to PMSF-alone are displayed ($P<0.05$,). Exposure to 150mM NaCl in media was used as a positive control for the induction of apoptosis in SH-SY5Y cells.

Chapter 5

Organophosphorus Compound-induced Modification of SH-SY5Y Human Neuroblastoma Mitochondrial Transmembrane Potential

Kent Carlson and Marion Ehrich

Published in Toxicology and Applied Pharmacology 160, 33-42, 1999

Virginia-Maryland Regional College of Veterinary Medicine,
Blacksburg, Virginia, 24061

ABSTRACT

Organophosphorus (OP) compounds inhibit mitochondrial enzymes, respiration, and ATP generation, in addition to inducing structural changes such as matrix swelling. This implicates mitochondria as primary subcellular targets for these compounds. In this study, the health and function of cellular mitochondria following OP compound exposure were assessed by evaluating the mitochondrial transmembrane potential ($\Delta\Psi_m$). This was done by measuring the changes in $\Delta\Psi_m$ in SH-SY5Y human neuroblastoma cells incubated with the cationic fluorochrome, rhodamine 123 (5µg/ml), and the OP compounds tri-ortho-tolyl phosphate (TOTP), triphenyl phosphite (TPPi), or parathion for 7.5 to 960 min. OP compounds (100µM to 1mM) induced significant concentration-dependent mitochondrial hyperpolarization with peak maxima occurring at 60 (TOTP, TPPi) or 120 (parathion) minutes. Following this, the mitochondrial membranes gradually depolarized. Pretreatment with cyclosporin A (500nM, 30 hr), a mitochondrial permeability transition pore (PTP) inhibitor, decreased the hyperpolarization. In contrast, 30 hr pretreatment with the muscarinic receptor agonist carbachol (1mM) significantly increased $\Delta\Psi_m$ and delayed subsequent depolarization. Hyperpolarization and subsequent depolarization of mitochondrial membranes occurred 16 to 24 hours prior to a loss of substrate adhesion or an increase in DNA fragmentation, indicating that mitochondria were a primary target in OP compound-initiated cytotoxicity.

INTRODUCTION

Organophosphorus (OP) compounds are utilized in a variety of domestic, agricultural, and industrial settings. Their principal use is as pesticides (Aspelin, 1997) but they also have secondary markets as plasticizers, plastic softeners, flame retardants, antioxidants, and hydraulic fluids (Mochida *et al.*, 1988; Katoh *et al.*, 1990; Mortensen and Ladefoged, 1992; Ware, 1994).

Insecticidal OP compounds are primarily recognized for their ability to induce physiological toxicity in man and animals via the inhibition of acetylcholinesterase. Toxicity on the cellular level has also been demonstrated in a diverse array of immortal cell lines *in vitro* (Mochida *et al.*, 1988; Veronesi and Ehrich, 1993a; 1993b; Ehrich *et al.*, 1997; Greenman *et al.*, 1997). Subcellular targets for the initiation of cytotoxicity have not been elucidated, however, even though nuclear (Mentzschel *et al.*, 1993; Nishio and Uyeki, 1981), enzymatic (Ehrich *et al.*, 1997), cytoskeletal (Tuler and Bowen, 1989), and plasma membrane (Antunes-Madeira *et al.*, 1994) alterations have been described.

Structural and functional alterations in mitochondria have been observed in cells exposed to OP compounds. OP compound-induced mitochondrial membrane depolarization (Holmuhamedov *et al.*, 1996), membrane disruption and matrix swelling (Knoth-Anderson *et al.*, 1992; Antunes-Madeira *et al.*, 1994), alterations in mitochondrial oxygen uptake and respiration (Spetale *et al.*, 1976; Sitkiewicz *et al.*, 1980; Skonieczna *et al.*, 1980), and inhibition of oxidative phosphorylation, the phosphorylation of exogenous ADP, and the oxidation of succinate, α-glycerophosphate, and pyruvate/malate (Holmuhamedov *et al.*, 1996) have been documented. In addition, inhibition of mitochondrial malathion carboxylesterase (Whyard *et al.*, 1994), creatinine kinase and succinate dehydrogenase (Knoth-Anderson *et al.*, 1992), cytochrome c oxidase and NADH:cytochrome c reductase (Sitkiewicz *et al.*, 1980) and 6-phosphofructokinase (Hernandez *et al.*, 1989) have been reported following exposure to OP compounds.

OP compounds have been shown to partition into cholesterol-poor mitochondrial membranes to a greater extent than into cholesterol-rich brain microsomes, myelin, or erythrocytes (Antunes-Madeira and Madeira, 1989; Antunes-Madeira *et al.*, 1994). Increased mitochondrial membrane protein and decreased cholesterol contents were thought to increase the free volume available for OP compound accumulation (Antunes-Madeira *et al.*, 1994; Lodish *et al.*, 1995). Interaction of OP compounds with mitochondrial membrane-protein boundaries may be important, because the physical and chemical characters of these protein-lipid boundary domains have to be tightly controlled for proper protein function. Changes in protein-lipid boundary microenvironments have been proposed to affect Ca^{2+} channel (Almeida *et al.*, 1984; Michaelis *et al.*, 1985; Kanwar *et al.*, 1989) and Na^{+}/K^{+} ATPase and Ca^{2+} ATPase enzyme activity (Sharma and Bhattacharya, 1995).

Mitochondrial transmembrane potential ($\Delta\Psi_m$) is a widely acknowledged measure of mitochondrial health (Waggoner, 1990; Burghardt *et al.*, 1994). Loss of $\Delta\Psi_m$ has been observed in both apoptotic (Petit *et al.*, 1997; Susin *et al.*, 1998) and necrotic (LeMasters *et al.*, 1998) forms of cell death. Decreasing $\Delta\Psi_m$ has also been postulated to participate in the development of neurodegenerative disorders (Schinder *et al.*, 1996; Schapira, 1998). The magnitude of $\Delta\Psi_m$ can be

determined by flow cytometric or microplate assays using rhodamine 123 (R123), a cationic lipophilic fluorochrome (Johnson *et al.*, 1980; Darzynkiewicz *et al.*, 1981; Davis *et al.,* 1985; Darzynkiewicz *et al.*, 1990; Darzynkiewicz *et al.*, 1992; Cossarizza *et al.*, 1994).

The temporal sequences of subcellular events following the initiation of cytotoxicity have been described for hypoxia and ischemia (LeMasters *et al.*, 1997; 1998), neurodegenerative disorders (Schinder *et al.*, 1996; Schapira, 1988), and apoptosis and necrosis (Dive *et al.*, 1992; Petit *et al.*, 1997; LeMasters *et al.*, 1998; Susin *et al.*, 1998). Many of these situations share a similar mechanistic pathway that is initiated by mitochondrial dysfunction. Severe mitochondrial dysfunction leads to the opening of a mitochondrial permeability transition pore (PTP) which allows the $\Delta\Psi_m$ to dissipate. Loss of the $\Delta\Psi_m$ uncouples oxidative phosphorylation and impairs cellular ATP generating ability. This is followed shortly by a loss of substrate adhesion, increased nuclear DNA fragmentation, and cell degradation (Nostrandt *et al.*, 1992; Rodeck *et al.*, 1997; Petit *et al.*, 1997; LeMasters *et al.*, 1998).

In this paper we evaluated the temporal changes in $\Delta\Psi_m$ that were induced by exposure to cytotoxic concentrations of the OP test compounds, tri-ortho tolyl phosphate (TOTP), triphenyl phosphite (TPPi), and parathion *in vitro*. Two of these compounds, TOTP and TPPi, have been shown to induce clinical neuropathies in sensitive animal species (Abou-Donia and Lapadulla, 1990). The third, parathion, is primarily an anticholinesterase agent, but high doses of cholinesterase-inhibiting OP compounds (paraoxon) have been reported to induce convulsions and permanent brain pathology (McDonough *et al.*, 1987). Carbachol, cyclosporin A, and high K^+ pretreatments were utilized as modulating factors of the $\Delta\Psi_m$. Carbachol, a muscarinic agonist, was used because relatively long exposures (e.g., 30 hr) increases the expression of Bcl-2, an anti-apoptotic protein (Itano *et al.*, 1996). Cyclosporin A, a PTP inhibitor (LeMasters *et al.*, 1998), was used to determine if depolarization events following OP compound incubation were modulated through a PTP. High K^+ treatments were used to discriminate plasma membrane potential ($\Delta\Psi_p$) from $\Delta\Psi_m$. Changes in $\Delta\Psi_m$ were then compared to other indicators of impending cell death such as a loss of substrate adhesion and DNA fragmentation. This allowed changes in mitochondrial health to be delineated in the temporal sequence of events following the initiation of OP compound-induced cytotoxicity.

Following exposure to OP compounds, we observed significant increase in $\Delta\Psi_m$ followed by abrupt (1mM) or gradual (100μM) mitochondrial depolarization. The amplitude and duration of these alterations were affected by carbachol or cyclosporin A pretreatment. We also demonstrated that OP compound-induced changes in $\Delta\Psi_m$ preceded a loss of substrate adhesion or DNA fragmentation.

EXPERIMENTAL METHODS

Chemicals. Triphenyl phosphite (TPPi; 98% pure), parathion (99% pure), and paraoxon (98.5% pure) were purchased from Chem Service, Inc. (West Chester, PA). Tri-ortho-tolyl phosphate (TOTP; 98% pure) and an active esterase-inhibiting congener, cyclic phenyl saligenin phosphate (PSP; 99% pure) were synthesized by Lark Enterprises (Webster, MA). Diisopropyl -phosphorofluoridate (DFP; 98% pure) was obtained from Aldrich Chemical Co. (Milwaukee, WI). Previous studies demonstrated that TPPi, DFP, PSP, and paraoxon could inhibit esterases in SH-SY5Y human neuroblastoma cells (Ehrich *et al.*, 1994; 1997), but that esterase inhibition with TOTP and parathion required preincubation with oxidizing agents or microsomal enzymes (Barber *et al.*, 1999a; 1999b). Stock solutions (100mM in ethanol) of these OP compounds were created and stored at -20ºC for no longer than 2 weeks prior to use. Carbachol and cyclosporin A were obtained from Sigma Chemical Co. (St. Louis, MO). Rhodamine 123 (R123) and propidium iodide were acquired from Molecular Probes (Eugene, OR).

Cell Culture. SH-SY5Y human neuroblastoma cells were cultured primarily as described by Ehrich *et al.* (1995). SH-SY5Y cells (passage 54-59) were grown in Hams F12 medium (Sigma) supplemented with fetal bovine serum (FBS - 15% v/v) supplied by Summit Biotech, Inc. (Fort Collins, CO). Prior to confluency, cells were harvested using 0.25% trypsin (Sigma) and seeded onto plastic 96 well microtiter plates at $4x10^5$ cells/ml. The cells were then allowed to grow at 37°C and 5% CO_2 for 3-4 days prior to treatment.

Fluorescence Microscopy and Rhodamine 123 Uptake. Mitochondrial R123 staining was qualitatively evaluated by photographing coverslipped cells 7.5 to 960 minutes following OP compound incubation. Photographs were taken on a Nikon Diaphot-TMD inverted microscope equipped with a green filter cube and Nikon Fe-2 camera (ASA800 Kodacolor film). Coverslips were washed twice in PBS (with Ca^{2+} and Mg^{2+}) prior to photography.

Transmembrane Potential. Transmembrane potential ($\Delta\Psi$) was evaluated by utilizing the mitochondrial-specific, cationic fluorescent dye, R123. R123 has been shown to directly sequester into the mitochondria without prior passage through lysosomes or other endocytic vesicles (Johnson *et al.*, 1980). Following 3-4 days of preincubation in F12 medium, cells were changed into F12 medium supplemented with 5µg/ml of R123. Cultures were incubated 8-12 hours in this medium prior to OP compound administration. No cytotoxic response was observed following incubation of control SH-SY5Y cells with 5µg/ml R123 (data not shown).

Pretreatment with carbachol (1mM in media) or cyclosporin A (500nM in 0.01% methanol) was initiated 30 hours prior to OP compound treatments. Following 7.5 to 2880 minute incubations with OP compounds, microtiter plates were assayed on a Cytofluor II multiwell fluorescence spectrometer (PerSeptive Biosystems, Bedford, MA) (excitation 530nm, emission 590nm).

Flow Cytometric Verification of Microplate Assay Transmembrane Potential and Importance of R123-OP Coincubation. Changes observed in microtiter plate $\Delta\Psi$ were verified by flow cytometry with one of the OP test compounds, TPPi. Cells were grown under similar culture conditions

as above. For exposures, cells were preloaded with R123 and then coincubated with TPPi in R123-free or R123-loaded (5μg/ml) F12 medium. Following incubation the cells were harvested with 0.25% trypsin. Cellular fluorescence was subsequently measured by a Coulter Epics XL-MCL flow cytometer (Beckman-Coulter, Opa Locka, FL) (excitation 507nm, emission 529nm). Treated cell fluorescence in the gated field (mean fluorescence intensity of the x-channel) was then compared to control fluorescence intensities to obtain percent of control. Representative flow cytometry histograms for rhodamine 123 can be seen in Appendix B. Incubation in TPPi-alone and TPPi-R123 treatment media allowed the importance of extracellular R123 movement to be evaluated.

Plasma Membrane Contribution to Transmembrane Potential. Nonspecific cytosolic accumulation of R123 was investigated by evaluating the differences in fluorescence between cultures exposed to low K^+ (normal F12 media) and high K^+ (137mM KCl, F12 media). High K^+ has been shown to depolarize the plasma membrane of certain cell types and abolish cytosolic pre-concentration of R123 (Davis *et al.*, 1985). SH-SY5Y cells possess outward K^+ currents that have voltage-dependent activation and inactivation (Forsythe *et al.*, 1992) so are sensitive to depolarization by high K^+ concentrations.

DNA Fragmentation. DNA fragmentation was estimated by using the DNA-specific fluorochrome propidium iodide (PI) and the cell culture methods described above. Following OP compound incubation, the treatment media were replaced by 75μl each of a PI buffer (PBS containing 50μg/ml PI, 1% FBS, and 0.1% sodium azide) and Vindelov's reagent (0.01M Tris, 10mM NaCl, 700U RNAse A (Sigma), 50μg/ml PI, and 0.1% of Igepal-40 (Sigma)). The microtiter plates were then incubated overnight at 4°C to allow cellular DNA to saturate with fluorochrome (Robinson *et al.*, 1993). A Coulter Epics XL-MCL flow cytometer was then utilized to analyze these samples (excitation 535nm - emission 617nm). Listmode files generated by the flow cytometer were processed through Multicycle DNA Cell Cycle Analysis Software (version 3.11 - Phoenix Flow Systems, Inc., San Diego, CA) to generate objective estimates of DNA fragmentation.

Substrate Adherence. Substrate adherence was assessed by utilizing a hemocytometer to count cells in wash media (non-adherent cells) following the termination of OP compound incubations. These counts were compared to those from matched wells on OP compound-exposed plates in which the cells had maintained attachment to the substrate. Both counts were adjusted for their relative media volumes. The percent of adherent cells was then calculated using the formula: [adherent cells/(adherent cells+non-adherent cells)]x 100.

Statistics. Each experiment had between 3 and 9 normalized data points (percentages) for each time and OP concentration. Data were converted into the percent of control and then graphed as the mean ± the standard deviation. Statistical significance ($p<0.05$) was determined by utilizing PC-SAS software (version 6.1) to perform an analysis of variance (ANOVA) followed by Duncan's Multiple Range Test.

RESULTS

Visualization of Rhodamine 123 Stained Mitochondria

Fluorescence photographs of cells were used to verify compartmentalization of the mitochondrial dye R123. Photographs taken following R123 incubation (5μg/ml) revealed staining of tubular structures approximately the same size as mitochondria (0.1-2μm). Staining of these objects was primarily perinuclear but cytoplasmic and neuritic spaces were involved as well (Fig. 5.1).

OP Compound-induced Changes in Transmembrane Potential (Rhodamine 123 Sequestration)

This study used $\Delta\Psi$ as an indicator of mitochondrial health in cells exposed to OP compounds, including TOTP, TPPi, and parathion, in concentrations from 10μM to 1mM. All compounds induced a statistically significant time and dose-dependent increase in $\Delta\Psi$ (R123 sequestration). For one test compound, TOTP, all concentrations induced significant increases in $\Delta\Psi$ within 120 minutes ($p<0.05$). With 1mM TOTP, the $\Delta\Psi$ was significantly greater at 7.5, 15, 30, and 60 minutes, but less at 240, 480, 720, and 960 minutes when compared to 100μM TOTP treatments (Fig. 5.2a). Cells pretreated for 30 hours with 1mM carbachol and then exposed to TOTP exhibited the same pattern of alterations in $\Delta\Psi$ as those with no carbachol pretreatment (Fig. 5.2b). Carbachol pretreatment significantly increased $\Delta\Psi$ at 60, 120, 240, 480, and 960 minutes when compared to cells exposed to 100μM and 1mM TOTP without carbachol pretreatments ($p<0.05$). Similar trends were observed following exposures to other OP compounds including TPPi, parathion, and paraoxon (data not shown). Increases in $\Delta\Psi$ were also noted following exposure of neuroblastoma cells to TPPi (Fig. 5.2c). For TPPi, 1mM treatments induced significantly larger increases in $\Delta\Psi$ at 240 minutes, but significantly less $\Delta\Psi$ at 960 and 1440 minutes when compared to 100μM TPPi treatments ($p<0.05$). For both TOTP and TPPi, the increase in $\Delta\Psi$ was maximal at 60 minutes but diminished at a greater rate in 1mM treatments.

Parathion also increased $\Delta\Psi$ (Fig. 5.2d). Exposure to this compound (1mM) induced a significantly larger increase in $\Delta\Psi$ at the 120 minute time point when compared to 100μM concentrations ($p<0.05$). Cyclosporin A pretreatment (500nM, 30 hours) significantly increased $\Delta\Psi$ (1.2 - 8.1x) when compared to cells not treated with this compound. However, this pretreatment decreased $\Delta\Psi$ (as a percent of control) at time points greater than 7.5 minutes when cells treated with 1mM parathion and cyclosporin A were compared to cells treated only with parathion (Fig. 5.2e). A similar trend was observed following cyclosporin A pretreatment of cells exposed to TOTP, TPPi, paraoxon, PSP, and DFP (data not shown).

Verification of Microplate Assay Transmembrane Potential and Importance of R123-OP Coincubation

Alterations in $\Delta\Psi$ demonstrated in microplate assays were verified using flow cytometry and the OP test compound TPPi (Fig. 5.3). In cultures simultaneously incubated with R123 and TPPi, significant

dose- and time-dependent increases in $\Delta\Psi$ seen when assayed by flow cytometry paralleled those observed in microplate assays (compare Fig. 5.3 and Fig. 5.2c). The increase in $\Delta\Psi$ determined by flow cytometry was significantly greater when TPPi exposures were conducted in the presence of R123 than when TPPi treatments occurred in R123-free media ($p<0.05$).

OP Compound-induced Changes in Transmembrane Potential - Contribution of the Plasma Membrane Potential and the Mitochondrial Membrane Potential

Uptake and sequestration of R123 is dependent on both the mitochondrial membrane potential ($\Delta\Psi_m$) and the plasma membrane potential ($\Delta\Psi_p$). Plasma membrane potential has been reported to preconcentrate R123 in the cytosol prior to entry in the mitochondria (Davis *et al.*, 1985). The relative contribution of $\Delta\Psi_m$ and $\Delta\Psi_p$ to overall $\Delta\Psi$ was investigated by evaluating the differences in fluorescence between cultures exposed to low K^+ and high K^+ treatment environments. High K^+ has been shown to depolarize the plasma membrane and abolish cytosolic pre-concentration of R123 (Davis *et al.*, 1985).

Results demonstrated that the $\Delta\Psi_m$ comprised the majority of $\Delta\Psi$. For the test compounds TOTP, TPPi, and parathion, $\Delta\Psi_p$ contributed only 2 to 28% of the total $\Delta\Psi$ (Table 5.1.).

The Temporal Sequence of Events When Observing OP Compound-induced Changes in Transmembrane Potential, DNA Fragmentation, and Substrate Adhesion

Three separate experimental protocols were combined graphically to assess the temporal sequence of mitochondrial, cytoskeletal (substrate adhesion), or nuclear modifications following cellular exposure to OP compounds.

TOTP exposure induced dose- and time-dependent changes in $\Delta\Psi$ and DNA fragmentation (Fig. 5.4a). TOTP-induced alterations in $\Delta\Psi$ appeared as early as 7.5 minutes after exposure. Significant changes in DNA fragmentation were not observed until after incubation times > 480 minutes. TOTP did not induce any significant changes in substrate adhesion.

Changes in $\Delta\Psi$ elicited by PSP were similar to TOTP-induced changes in $\Delta\Psi$ (Fig. 5.4b), with significant change occurring by 7.5 minutes. As with TOTP, PSP induced significant DNA fragmentation later (> 360 minutes) than changes in the $\Delta\Psi$. PSP also elicited changes in substrate adhesion at 100µm and 1mM concentrations after 240 and 120 minutes, respectively.

TPPi treatments induced dose- and time-dependent changes in $\Delta\Psi$, substrate adhesion, and DNA fragmentation (Fig. 5.4c). Alterations in $\Delta\Psi$ occurred at incubation times > 15 minutes. Significant DNA fragmentation did not occur until time points >1440 minutes. TPPi also induced a significant loss in substrate adhesion, but this did not occur until 2880 minutes.

Parathion also induced dose- and time-dependent changes in $\Delta\Psi$ and DNA fragmentation (Fig. 5.4d). Alterations in the $\Delta\Psi$ occurred as early as 15 minutes after exposure. Treatments did not induce

a loss of substrate adhesion at any incubation times. Significant increases in DNA fragmentation did not occur until exposures were >1440 minutes.

DISCUSSION

The objective of this study was to use $\Delta\Psi$ to evaluate mitochondria as intracellular targets for OP compound-induced cytotoxicity. Alterations in $\Delta\Psi_m$ were found to occur prior to changes in substrate adhesion and DNA fragmentation and illustrated a potential sequence of events for OP compound-mediated cell death.

OP compound-induced changes in $\Delta\Psi$ appeared to be unrelated to the capability of the test compounds to inhibit SH-SY5Y esterases (acetylcholinesterase, neuropathy target esterase) generally recognized as targets for OP toxicoses *in vivo* (Abou-Donia and Lapadula, 1990; Ecobichon, 1994).TPPi is an active esterase inhibitor; TOTP and parathion are not unless metabolized (Ehrich *et al.*, 1994; 1997; Barber *et al.*, 1999a; 1999b). Other compounds tested in these studies could inhibit acetylcholinesterase (PSP, DFP, paraoxon) or neuropathy target esterase (PSP, DFP) in these cells. In addition, hyperpolarization and depolarization rates in the first 480 minutes following 1mM exposures (PSP > TOTP > parathion > TPPi > paraoxon > DFP) could not be correlated to the ability of the OP compound to cause neurological deficits.

In this study we observed that R123 discretely partitioned into intracellular organelles and only diffusely stained the cytosol. Stained organelles were approximately 0.1 to 2μm in size and had a perinuclear and neuritic distribution. Similar characteristics were described by others when using R123 (5μg/ml) for staining mitochondria in sperm, erythrocytes, lymphocytes, and fibroma, fibroblast, and cardiac cells (Johnson *et al.*, 1980; Burghardt *et al.*, 1994). In addition, one study demonstrated that R123 did not incorporate into the nucleus, endoplasmic reticulum, golgi, or plasma membrane, or pass through endocytic vesicles or lysosomes (Johnson *et al.*, 1980). Diffuse R123 staining of the cytosol was expected in this study because $\Delta\Psi_p$ has been shown to preconcentrate R123 in the cytosol (Davis *et al.*, 1985). R123 fluorescence intensity was shown to be directly proportional to dye concentrations from 0.1μg/ml to 100μg/ml (38.1nM to 38.1μM, data not shown), even though others suggested that R123 concentration-independent fluorescence was possible (Burghardt *et al.*, 1994).

TOTP, TPPi, and parathion induced dose- and time-dependent alterations in $\Delta\Psi$. Increases in $\Delta\Psi$ 1.2 to 2.3x over matched vehicle controls were observed at 60 minutes following exposure. The $\Delta\Psi$ subsequently decreased over time in a dose-dependent manner. Increased $\Delta\Psi$, termed hyperpolarization, occurs because cationic R123 accumulates in electronegative environments. Decreased $\Delta\Psi$, called depolarization, occurs following the loss of electronegativity (Davis *et al.*, 1985).

Hyperpolarization has been attributed to a variety of mechanisms such as increased mitochondrial mass and number per cell (Darzynkiewicz *et al.*, 1981). This was unlikely to have occurred in the present study because of the short incubation times (60-120 minutes) before maximal increases in $\Delta\Psi$.

Unregulated mitochondrial matrix volume is another mechanism by which increased hyperpolarization or R123 sequestration can occur (Davis *et al.*, 1985; Cossarizza *et al.*, 1994). Increases in matrix volume can also lead to swelling and rupture of the mitochondrial outer membrane

(Reed *et al.*, 1998), which would be followed by a depolarization in $\Delta\Psi_m$. Mitochondrial swelling and disruption have previously been described in cultured cells following exposure to OP compounds (Knoth-Anderson *et al.*, 1992) and mitochondrial membrane depolarization has been observed following exposure to OP test compounds in this study.

Mitochondrial or cellular receptor activation has been reported to induce mitochondrial hyperpolarization (Bachar *et al.*, 1992; Simpson and Russell, 1998). In the latter study, changes in $\Delta\Psi$ were correlated to fluctuations in cytosolic Ca^{2+} as modulated by plasma membrane and endoplasmic reticulum Ca^{2+} pumps. We, however, did not observe any changes in hyperpolarization following extracellular Ca^{2+} complexation with EGTA (data not shown).

Respiratory increases can also induce mitochondrial hyperpolarization (Selivanov *et al.*, 1998). However, most data on OP compound-mediated mitochondrial effects have documented inhibition of oxygen consumption, respiration, oxidative metabolism, and mitochondrial enzymes (Spetale *et al.*, 1976; Sitkiewicz *et al.*, 1980; Skonieczna *et al.*, 1980; Hernandez *et al.*, 1989; Knoth-Anderson *et al.*, 1992; Whyard *et al.*, 1994; Holmuhamedov *et al.*, 1996), suggesting that OP compounds do not elevate $\Delta\Psi$ through increased mitochondrial respiration.

Other investigators have demonstrated that increased $\Delta\Psi_p$ can hyperpolarize cells (Davis *et al.*, 1985). Our study demonstrated, however, that the relative contribution of $\Delta\Psi_p$ to OP compound-induced changes in $\Delta\Psi$ was low (2% to 28%). In addition, significant increases in $\Delta\Psi_p$ were not observed during hyperpolarization peaks. This indicated that hyperpolarization was not dependent on the $\Delta\Psi_p$ and that the majority of depolarization in $\Delta\psi$ was due to changes in $\Delta\Psi_m$ and not $\Delta\Psi_p$.

Carbachol (1mM) administration during TOTP exposure increased the amplitude of hyperpolarization and significantly delayed depolarization. Carbachol is a muscarinic receptor agonist that has been reported to stimulate phosphoinositide hydrolysis (Katz and Marquis, 1992), elicit transient increases in Ca^{2+} from intracellular sources (Forsythe *et al.*, 1992; Itano *et al.*, 1996), cause Ca^{2+}-dependent release of noradrenaline (Murphy *et al.*, 1991), and induce protein kinase C to phosphorylate MAP kinase (Offermanns *et al.*, 1993). High concentration (1mM) and relatively long (e.g., 30 hr) carbachol treatments have also been reported to induce SH-SY5Y cells to increase the expression of Bcl-2, an anti-apoptotic protein (Itano *et al.*, 1996). Bcl-2 has been demonstrated to stabilize the mitochondrial outer membranes and prevent mitochondrial PTPs from opening (Cai *et al.*, 1998). Prevention of PTP opening can diminish oxidative uncoupling, ATP depletion, and a dissipation of the $\Delta\Psi_m$ (Reed *et al.*, 1998), which may have contributed to the increased amplitude and duration of $\Delta\Psi$ seen following OP compound exposure in this study.

Cyclosporin A has been described as a high affinity inhibitor of mitochondrial PTPs (Bernardi, 1996). Overall increase in $\Delta\Psi$ following cyclosporin A pretreatment was observed in this and other studies with SH-SY5Y cells (Cassarino *et al.*, 1998). Cyclosporin A treatments decreased overall $\Delta\Psi$ in this study, however, when compared as the percent of control to other treatments without this compound. Cyclosporin A pretreatments implicated the mitochondrial PTP as a potential modulator for

both events. The mechanistic pathway, however, must be different than that induced by carbachol, because diametrically opposite responses in $\Delta\Psi$ were evinced by these compounds.

In this study, transmembrane hyperpolarization induced by 100μM and 1mM TPPi was verified with flow cytometry. Flow cytometric measures of R123 sequestration followed the same time course as in microplate assays. The flow cytometric technique, however, was more sensitive and provided larger differences in $\Delta\Psi$ than did the microplate assays. This study also demonstrated that increased R123 sequestration was not entirely due to influx of extracellular R123. Cells exposed to TPPi without concurrent R123 incubation had similar $\Delta\Psi$ patterns but lower amplitudes as those OP compound treatments with concurrent R123 incubation. Therefore, redistribution of existing intracellular R123 concentrations in addition to extracellular influx contributed to OP compound-induced increases in fluorescence.

Our last experiments documented that in all cases OP compound-induced changes in $\Delta\Psi_m$ occurred at much earlier time points than DNA fragmentation or a loss of substrate adhesion. This data matched cytotoxic temporal sequences observed in part by others (Nostrandt *et al.*, 1992; Rowles *et al.*, 1995; Honglin *et al.*, 1997) and illustrated that mitochondria could be important in the initiation of OP compound-induced cytotoxicity. OP compound-related differences in temporal onset for losses in substrate adhesion and DNA fragmentation suggested, however, that cells respond somewhat differently to each OP compound. The amplitude of hyperpolarization correlated well to losses in substrate adhesion and increases in DNA fragmentation, however, even though these were temporally distinct events. In treatments that induced large hyperpolarizations, DNA fragmentation and a loss of substrate adhesion occurred at earlier incubation timepoints than those treatments that induced less hyperpolarization. These observations implied that $\Delta\Psi_m$ was a good indicator of early OP compound-induced cytotoxicity in SH-SY5Y human neuroblastoma cells.

The role of mitochondrial hyperpolarization and depolarization in OP compound-induced cytotoxicity needs to be further defined. Whether these changes in membrane potential are unavoidable responses to a cytotoxic insult or cytoprotective in nature is not known. Both ideas merit more investigation.

ACKNOWLEDGMENTS

We wish to thank Joan Kalnitsky for flow cytometric assistance and Dr. Lorraine Landis for critical reading of the manuscript. This work was supported in part by funds from the Virginia-Maryland Regional College of Veterinary Medicine and a Society of Toxicology - Novartis predoctoral fellowship.

REFERENCES

Abou-Donia, M.B. and Lapadulla, D.M. (1990). Mechanisms of organophosphorus ester-induced delayed neurotoxicity: Type I and Type II. *Annu. Rev. Pharmacol. Toxicol.* 30, 405-440.

Almeida, L.M., Vaz, W.L.Z., Zachariasse, K.A., and Madeira, V.M.C. (1984). Modulation of sarcoplasmic reticulum Ca^{2+} pump activity by membrane fluidity. *Biochemistry* 23, 4714-4720.

Antunes-Madeira, M.C. and Madeira, V.M.C. (1989). Membrane partitioning of organophosphorus and organochlorine insecticides and its implications for mechanisms of toxicity. *Pestic. Sci.* 26, 167-179.

Antunes-Madeira, M.C., Videira, R.A., and Madeira, V.M.C. (1994). Effects of parathion on membrane organization and its implications for the mechanisms of toxicity. *Biochim. Biophys. Acta.* 1190, 149-154.

Aspelin, A.L. (1997). Pesticides industry sales and usage: 1994 and 1995 market estimates. *Biological and Economic Analysis Division, Office of Pesticide Programs, Office of Prevention, Pesticides and Toxic Substances.* U.S. Environmental Protection Agency. Washington D.C.

Bachar, H., Haver, E., Ilani, A., and Lichtstein, D. (1992). Modulation of rat olfactory bulb mitochondrial function by atrial natriuretic peptide. *Pflügers Arch.* 422, 204-206.

Barber, D.S., Correll, L., and Ehrich, M. (1999a). Comparison of two *in vitro* activation systems for protoxicant organophosphorus esterase inhibitors. *Toxicol. Sci.* 47, 16-23.

Barber, D.S., Correll, L., and Ehrich, M. (1999b). Comparative effectiveness of organophosphorus protoxicant activating systems in neuroblastoma cells and brain homogenates. *J. Toxicol. Environ. Health* 57, 63-74.

Bernardi, P. (1996). The permeability transition pore. Control points of a cyclosporin A-sensitive mitochondrial channel involved in cell death. *Biochim. Biophys. Acta* 1275, 5-9.

Burghardt, R.C., Barhoumi, R., Doolittle, D.J., and Phillips, T.D. (1994). Application of cellular fluorescence imaging for in vitro toxicology testing. In *Principles and Methods of Toxicology* (W. Hayes, Ed.), pp.1231-1258. Raven Press, Ltd., New York.

Cai, J., Yang, J., and Jones, D.P. (1998). Mitochondrial control of apoptosis: The role of cytochrome c. *Biochim. Biophys. Acta* 1366, 139-149.

Cassarino, D.S., Swerdlow, R.H., Parks, J.K., Parker, W.D. Jr., and Bennett, J.P. Jr. (1998). Cyclosporin A increases resting mitochondrial membrane potential in SY5Y cells and reverses the

depressed mitochondrial membrane potential of Alzheimer's disease cybrids. *Biochem. Biophys. Res. Commun.* 248, 168-173.

Cossarizza, A., Kalashnikova, G., Grassilli, E., Chiappelli, F., Salvioli, S., Capri, M., Barbieri, D., Troiano, L., Monti, D., and Franceschi, C. (1994). Mitochondrial modifications during rat thymocyte apoptosis: A study at the single cell level. *Exp. Cell Res.* 214, 323-330.

Darzynkiewicz, Z., Staiano-Coico, L., and Melamed, M. (1981). Increased mitochondrial uptake of rhodamine 123 during lymphocyte stimulation. *Proc. Nat. Acad. Sci. (USA)* 78, 2383-2387.

Darzynkiewicz, Z. and Traganos, F. (1990). Multiparameter flow cytometry in studies of the cell cycle. In *Flow Cytometry and Sorting, Second Edition*, pp. 469-501. Wiley-Liss, Inc., New York.

Darzynkiewicz, Z., Bruno, S., Del Bino, G., Gorczyca, W., Hotz, M.A., Lassota, P., and Traganos, F. (1992). Features of apoptotic cells measured by flow cytometry. *Cytometry* 13, 795-808.

Davis, S., Weiss, M.J., Wong, J.R., Lampidis, T.J., and Chen, L.B. (1985). Mitochondrial and plasma membrane potentials cause unusual accumulation and retention of rhodamine 123 by human breast adenocarcinoma-derived MCF-7 cells. *J. Biol. Chem.* 260, 13844-13850.

Dive, C., Gregory, C.D., Phipps, D.J., Evans, D.L., Milner, A.E., and Wyllie, A.H. (1992). Analysis and discrimination of necrosis and apoptosis (programmed cell death) by multiparameter flow cytometry. *Biochim. Biophys. Acta* 1133, 275-285.

Ecobichon, D.J. (1994). Organophosphorus ester insecticides. In *Pesticides and Neurological Disease* (D.J. Ecobichon and R.M. Joy, Eds.), pp. 171-249. CRC Press, Boca Raton, Florida.

Ehrich, M., Correll, L., and Veronesi, B. (1994). Neuropathy target esterase inhibition by organophosphorus esters in human neuroblastoma cells. *Neurotoxicology* 15, 309-314.

Ehrich, M., Correll, L., Carlson, K., Wilcke, J., and Veronesi, B. (1995). Examination of culture conditions on esterase activities in human and mouse neuroblastoma cells. *In Vitro Toxicol.* 8, 199-207.

Ehrich, M., Correll, L., and Veronesi, B. (1997). Acetylcholinesterase and neuropathy target esterase inhibitions in neuroblastoma cells to distinguish organophosphorus compounds causing acute and delayed neurotoxicity. *Fundam. Appl. Toxicol.* 38, 1-9.

Forsythe, I.D., Lambert, D.G., Nahorski, S.R., and Linsdell, P. (1992). Elevation of cytosolic calcium by cholinoceptor agaonists in SH-SY5Y human neuroblastoma cells: Estimation of the contribution of voltage-dependent currents. *Br. J. Pharmacol.* 107, 207-214.

Greenman, S.B., Rutten, M.J., Fowler, W.M., Scheffler, L., Shortridge, L.A., Brown, B., Sheppard, B.C., Deveney, K.E., Deveney, C.W., and Trunkey, D.D. (1997). Herbicide/pesticide effects on intestinal epithelial growth. *Environ. Res.* 75, 85-93.

Hernandez, A.F., Pla, A., and Villanueva, E. (1989). Decreased phosphofructokinase activity during the development of triorthocresyl-phosphate-induced delayed neuropathy. *Toxicol. Lett.* 49, 35-40.

Holmuhamedov, E.L., Kholmoukhamedova, G.L., and Baimuradov, T.B. (1996). Non-cholinergic toxicity of organophosphates in mammals: Interaction of ethaphos with mitochondrial functions. *J. Appl. Toxicol.* 16, 475-481.

Honglin, L., Bergeron, L., Cryns, V., Pasternak, M.S., Zhu, H., Shi, L., Greenberg, A., and Yuan, J. (1997). Activation of caspase-2 in apoptosis. *J. Biol. Chem.* 272, 21010-21017.

Itano, Y., Ito, A., Uehara, T., and Nomura, Y. (1996). Regulation of Bcl-2 protein expression in human neuroblastoma SH-SY5Y cells: Positive and negative effects of protein kinases C and A, respectively. *J. Neurochem.* 67, 131-137.

Johnson, L.V., Walsh, M.L., and Chen, L.B. (1980). Localization of mitochondria in living cells with rhodamine 123. *Proc. Nat. Acad. Sci. (USA)* 77, 990-994.

Jortner, B.S., Carlson, K., Mullins, J., Perkins, S., and Ehrich, M. (1998). Early neurotoxic effect of chlorpyrifos-oxon in chicken embryo brain reaggregate cultures. *Toxicol. Sci.* 42S, 125-126.

Kanwar, U., Batla, A., Sanyal, S., Minocha, R., Majumdar, S., and Ranga, A. (1989). Gossypol inhibition of Ca^{2+} uptake and Ca^{2+}-ATPase in human ejaculated spermatozoal plasma membrane vesicles. *Contraception* 39, 431-445.

Katoh, K., Konno, N., Yamauchi, T., and Fukushima, M. (1990). Effects of age on susceptibility of chickens to delayed neurotoxicity due to triphenyl phosphite. *Pharmacol. Toxicol.* 66, 387-392.

Katz, L.S. and Marquis, J.K. (1992). Organophosphate-induced alterations in muscarinic receptor binding and phosphoinositide hydrolysis in the human SK-N-SH cell line. *Neurotoxicology* 13, 365-378.

Knoth-Anderson, J., Veronesi, B., Jones, K., Lapadula, D.M., and Abou-Donia, M.B. (1992). Triphenyl phosphite-induced ultrastructural changes in bovine adrenomedullary chromaffin cells. *Toxicol. Appl. Pharmacol.* 112, 110-119.

LeMasters, J.J., Nieminen, A.-L., Qian, T., and Lawrence, C. (1997). The mitochondrial permeability transition in toxic hypoxic and reperfusion injury. *Mol. Cell. Biochem.* 174, 159-165.

LeMasters, J.J., Nieminen, A.-L., Qian, T., Trost, L.C., Elmore, S.P., Nishimura, Y., Crowe, R.A., Cascio, W.E., Bradham, C.A., Brenner, D.A., and Herman, B. (1998). The mitochondrial permeability transition in cell death: A common mechanism in necrosis, apoptosis and autophagy. *Biochim. Biophys. Acta* 1366, 177-196.

Lodish, H., Baltimore, D., Berk, A., Zipursky, S.L., Matsudaira, P., and Darnell, J. (1995). *Molecular Cell Biology, Third Edition*. W.H. Freeman and Co., New York.

McDonough, J.H. Jr., McLeod, C.G. Jr., and Nipwoda, M.T. (1987). Direct microinjection of soman or VX into the amygdala produces repetitive limbic convulsions and neuropathology. *Brain Res.* 435, 123-137.

Mentzschel, A., Schmuck, G., DeKant, W., and Henschler, D. (1993). Genotoxicity of neurotoxic triaryl phosphates: Identification of DNA adducts of the ultimate metabolites, saligenin phosphates. *Chem. Res. Toxicol.* 6, 294-301.

Michaelis, M.L., Kitos, T.E., and Tehan, O. (1985). Differential effects of ethanol on two synaptic membrane Ca^{2+} transport systems. *Alcohol* 2, 129-132.

Mochida, K., Gomyoda, M., Fujita, T., and Yamagata, K. (1988). Tricresyl phosphate and triphenyl phosphate are toxic to cultured human, monkey and dog cells. *Zbl. Bakt. Hyg. B.* 185, 427-429.

Mortensen, A. and Ladefoged, O. (1992). Delayed neurotoxicity of trixylenyl phosphate and a trialkyl/aryl phosphate mixture, and the modulating effect of atropine on tri-o-tolyl phosphate-induced neurotoxicity. *Neurotoxicology* 13, 347-354.

Murphy, N.P., Ball, S.G., and Vaughan, P.F.T. (1991). Potassium- and carbachol-evoked release of [^{3}H]noradrenaline from human neuroblastoma cells, SH-SY5Y. *J. Neurochem.* 56, 1810-1815.

Nishio, A. and Uyeki, E.M. (1981). Induction of sister chromatid exchanges in Chinese hamster ovary cells by organophosphate insecticides and their oxygen analogs. *J. Toxicol. Environ. Health* 8, 939-946.

Nostrandt, A.C., Rowles, T.K., and Ehrich, M. (1992). Cytotoxic effects of organophosphorus esters and other neurotoxic chemicals on cultured cells. *In Vitro Toxicol.* 5, 127-136.

Offermanns, S., Bombien, E., and Schultz, G. (1993). Stimulation of tyrosine phosphorylation and mitogen-activated-protein (MAP) kinase activity in human SH-SY5Y neuroblastoma cells by carbachol. *Biochem. J.* 294, 545-550.

Petit, P.X., Zamzami, N., Vayssiere, J.-L., Mignotte, B., Kroemer, G., and Castedo, M. (1997). Implication of mitochondria in apoptosis. *Mol. Cell. Biochem.* 174, 185-188.

Reed, J.C., Jurgensmeier, J.M., and Matsuyama, S. (1998). Bcl-2 family proteins and mitochondria. *Biochim. Biophys. Acta.* 1366, 127-137.

Robinson, J.P., Darzynkiewicz, Z., and Dean, P. (1993). DNA cell cycle analysis: Propidium iodide procedure. In *Handbook of Flow Cytometry Methods*, p. 97. John Wiley and Sons, Inc., New York.

Rodeck, U., Jost, M., DuHadaway, J., Kari, C., Jensen, P.J., Risse, B., and Ewert, D.L. (1997). Regulation of Bcl-x_L expression in human keratinocytes by cell-substratum adhesion and the epidermal growth factor receptor. *Proc. Nat. Acad. Sci. (USA)* 94, 5067-5072.

Rowles, T.K., Song, X., and Ehrich, M. (1995). Identification of endpoints affected by exposure of human neuroblastoma cells to neurotoxicants at concentrations below those that affect cell viability. *In Vitro Toxicol.* 8, 3-13.

Schapira, A.H.V. (1998). Mitochondrial dysfunction in neurodegenerative disorders. *Biochim. Biophys. Acta* 1366, 225-233.

Schinder, A.F., Olson, E.C., Spitzer, N.C., and Montal, M. (1996). Mitochondrial dysfunction is a primary event in glutamate neurotoxicity. *J. Neurosci.* 16, 6125-6133.

Selivanov, V.A., Ichas, F., Holmuhamedov, E.L., Jouaville, L.S., Evtodienko, Y.V., and Mazat, J.-P. (1998). A model of mitochondrial Ca^{2+}-induced Ca^{2+} release simulating the Ca^{2+} oscillations and spikes generated by mitochondria. *Biophys. Chem.* 72, 111-121.

Sharma, S.K. and Bhattacharya, B.K. (1995). Altered glycine transport by cerebral tissue and decreased Na^+ and Ca^{2+} pump activities during organophosphorus-ester-induced delayed neurotoxicity development period. *J. Biochem. Toxicol.* 10, 233-238.

Simpson, P.B., and Russell, J.T. (1998). Mitochondrial Ca^{2+} uptake and release influence metabotropic and ionotropic cytosolic Ca^{2+} responses in rat oligodendrocyte progenitors. *J. Physiol.* 508, 413-426.

Sitkiewicz, D., Skonieczna, M., Krzywicka, K., Dziedzic, E., Staniszewska, K., and Bicz, W. (1980). Effect of organophosphorus insecticides on the oxidative processes in rat brain synaptosomes. *J. Neurochem.* 34, 619-626.

Skonieczna, M., Sitkiewicz, D., and Bicz, W. (1980). Modification of oxidative phosphorylation in brain mitochondria during development and aging by the oxygen analog of Ronnel. *Pest. Biochem. Physiol.* 14, 314-318.

Spetale, M.R., Morisoli, L.S., and Garay, E.A.R. (1976). The effect of organophosphorus compounds on respiration by rat liver mitochondria. *Il Farmaco Ed. Sc.* 32, 116-122.

Susin, S.A., Zamzami, N., and Kroemer, G. (1998). Mitochondria as regulators of apoptosis: Doubt no more. *Biochim. Biophys. Acta* 1366, 151-165.

Tuler, S.M. and Bowen, J.M. (1989). Toxic effect of organophosphates on nerve cell growth and ultrastructure in culture. *J. Toxicol. Environ. Health* 27, 209-223.

Veronesi, B. and Ehrich, M. (1993a). Using neuroblastoma cell lines to examine organophosphate neurotoxicity. *In Vitro Toxicol*. 6, 57-65.

Veronesi, B. and Ehrich, M. (1993b). Differential cytotoxic sensitivity in mouse and human cell lines exposed to organophosphate insecticides. *Toxicol. Appl. Pharmacol.* 120, 240-246.

Waggoner, A.S. (1990). Fluorescent probes for cytometry. In *Flow Cytometry and Sorting, Second Edition*. pp. 209-225. Wiley-Liss, Inc. New York.

Ware, G.W. (1994). Chapter 4: Insecticides. In *The Pesticide Book, Fourth Edition* (G.W. Ware, Ed.), pp. 41-74. Thomson Publications, Fresno California.

Whyard, S., Russell, R.J., and Walker, V.K. (1994). Insecticide resistance and malathion carboxylesterase in the sheep blowfly, *Lucilia cuprina*. *Biochem. Genet.* 32, 9-24.

Table 5.1. Contribution of the mitochondrial membrane potential to the total change in transmembrane potential induced by OP compounds.[a]

Minutes Incubation	30	60	120	240
0% ETOH	82 ± 4.2	83 ± 3.9	88 ± 2.5	92 ± 5.8
0.1% ETOH	94 ± 2.1	90 ± 2.1	89 ± 3.2	87 ± 4.7
1% ETOH	87 ± 4.1	86 ± 7.5	87 ± 3.2	90 ± 9.2
100mM TOTP	98 ± 1.9	80 ± 3.5	72 ± 2.7	77 ± 4.0
1mM TOTP	81 ± 4.2	81 ± 3.6	79 ± 3.4	85 ± 9.4
100mM TPPi	93 ± 6.8	95 ± 3.3	91 ± 1.1	95 ± 3.8
1mM TPPi	93 ± 3.2	88 ± 2.8	93 ± 1.9	90 ± 1.1
100mM Parathion	87 ± 7.4	83 ± 3.0	83 ± 2.5	74 ± 6.0
1mM Parathion	87 ± 5.6	87 ± 6.5	93 ± 5.3	90 ± 1.9

[a] Results are expressed as percent of the total transmembrane potential (mitochondrial transmembrane potential + plasma membrane potential = 100%, the total,transmembrane potential), mean ± SD, n=3.

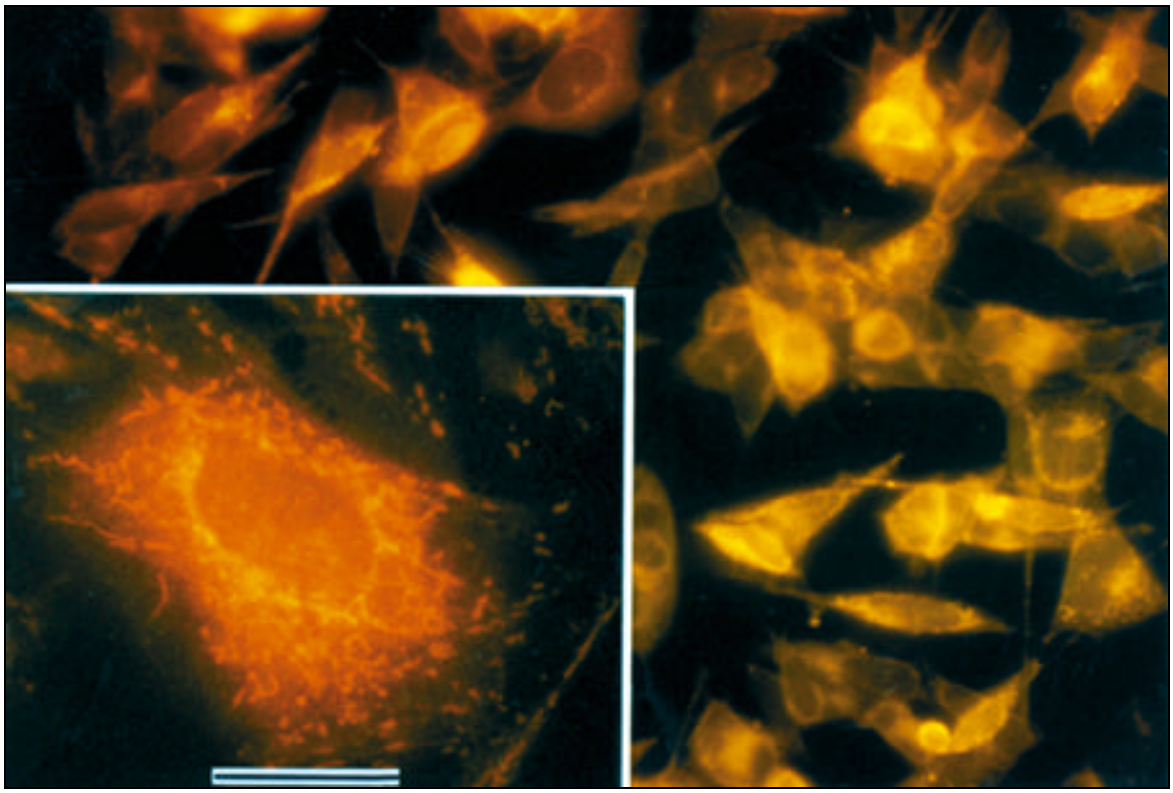

Figure 5.1. Mitochondrial fluorescence in SH-SY5Y cells. Cells were incubated for 8 hours at 37°C in a 5µg/ml rhodamine 123 solution. The large photograph is at 400x; inset photograph at the bottom left is 1000x. Scale bar on inset = 10µm.

(*a*)

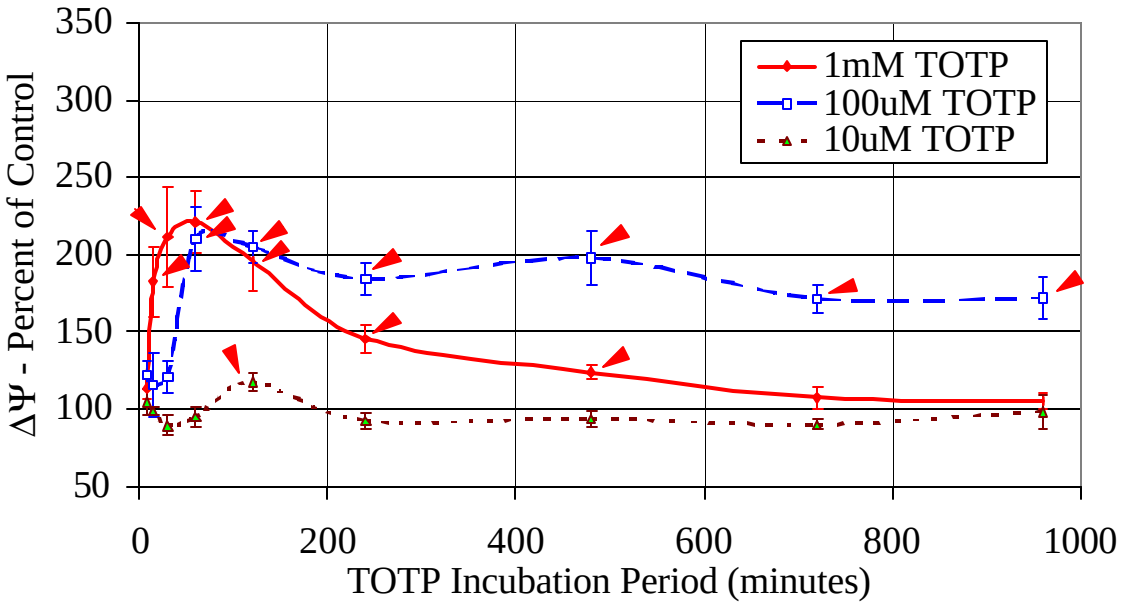

(*b*)

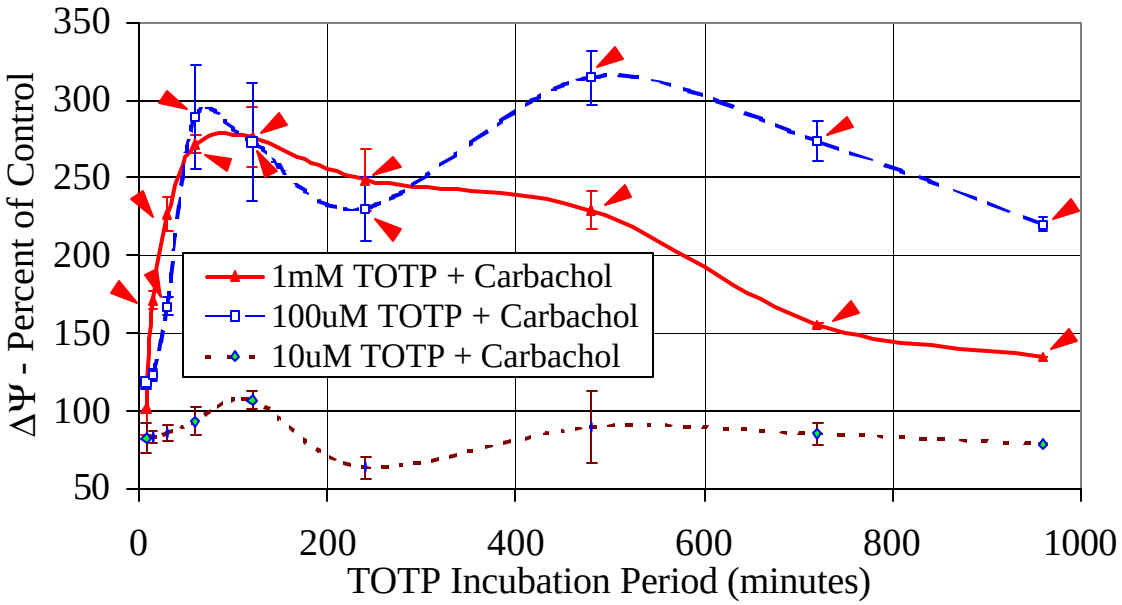

Figure 5.2. OP compound-induced changes in cellular transmembrane potential. Values are the mean of 3-12 normalized data points (percentages) ± the standard deviation and are graphed as the percent of control. Statistical significance of total transmembrane potentials when compared to vehicle controls are also displayed ($p \leq 0.05$, ▲). Figure 5.2a, TOTP alone (n=6); Figure 5.2b, TOTP effects after carbachol pretreatment (1mM, 30 hr, n=6).

(*c*)

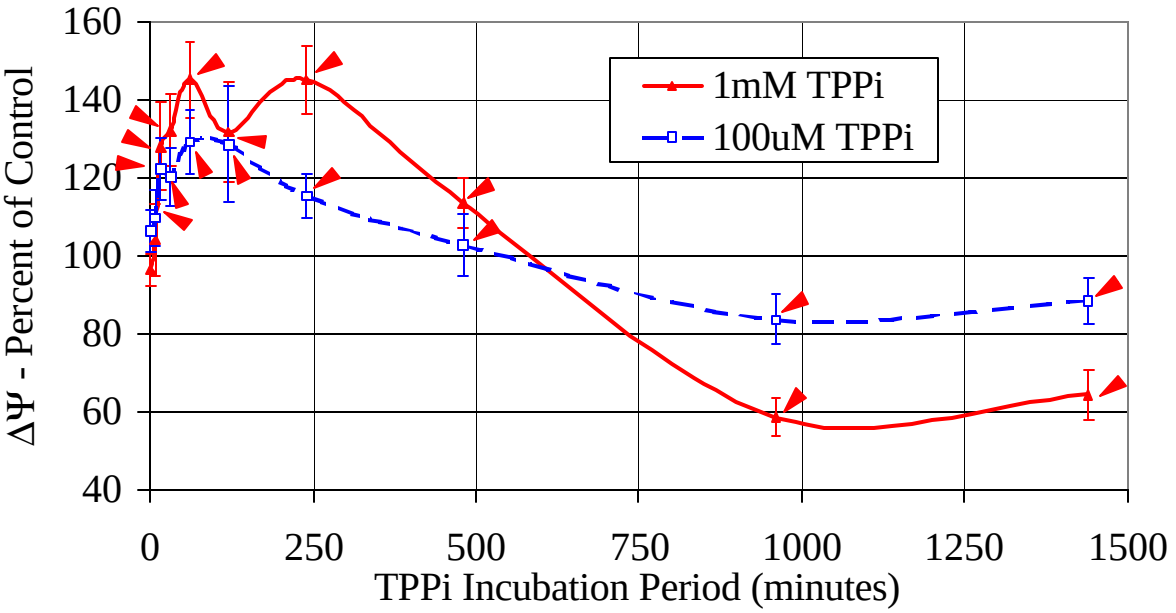

(*d*)

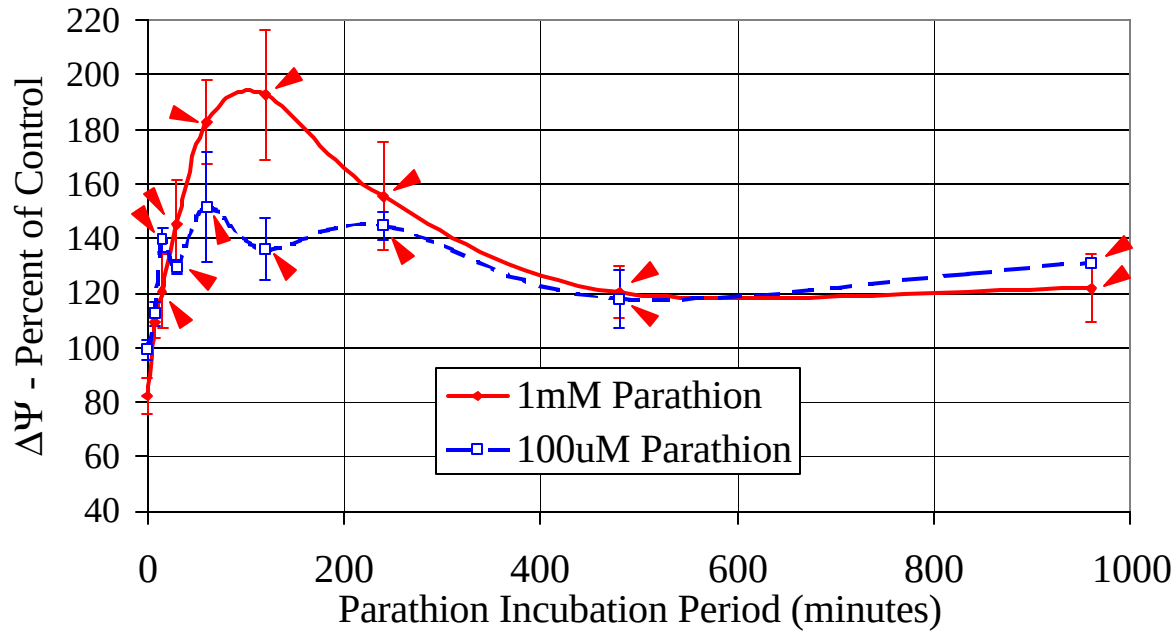

Figure 5.2. OP compound-induced changes in cellular transmembrane potential. Values are the mean of 3-12 normalized data points (percentages) ± the standard deviation and are graphed as the percent of control. Statistical significance of total transmembrane potentials when compared to vehicle controls are also displayed ($p \leq 0.05$, ▲). Figure 5.2c, TPPi alone (n=9); Figure 5.2d, parathion alone (n=3).

(*e*)

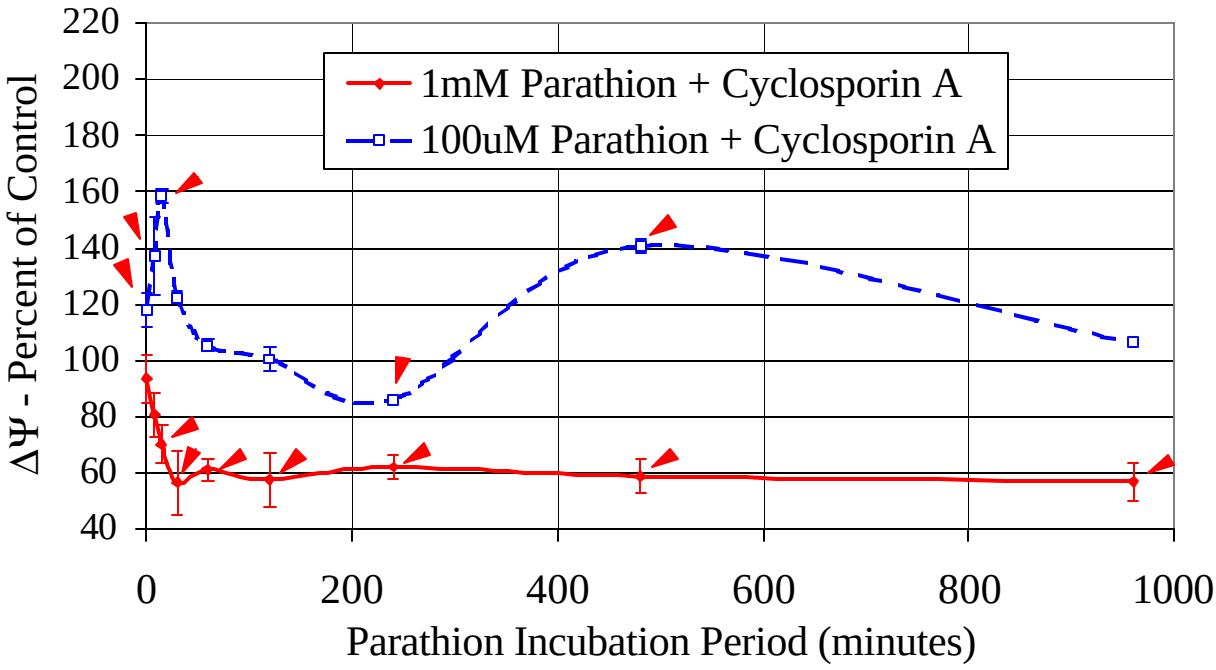

Figure 5.2. OP compound-induced changes in cellular transmembrane potential. Values are the mean of 3-12 normalized data points (percentages) ± the standard deviation and are graphed as the percent of control. Statistical significance of total transmembrane potentials when compared to vehicle controls are also displayed ($p \leq 0.05$, ◢). Figure 5.2e, parathion effects after cyclosporin A pretreatment (500nM, 30 hr, n=3).

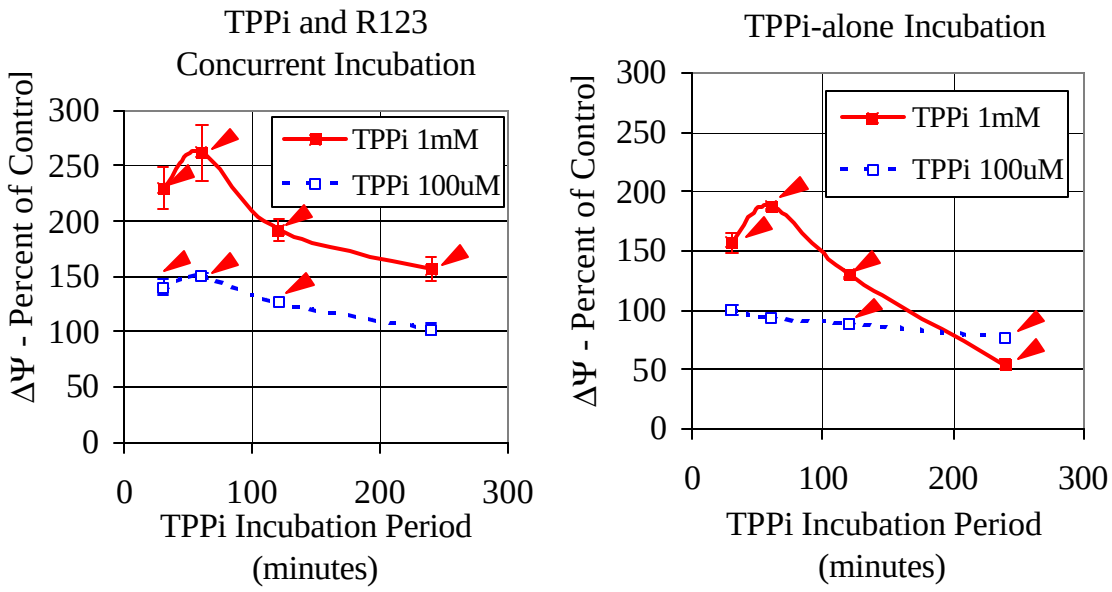

Figure 5.3. TPPi-induced changes in transmembrane potential as assessed by flow cytometry. In the left panel cells were incubated concurrently with TPPi and R123; in the right panel TPPi incubation took place after preincubation with R123. Values are the mean of 3 normalized data points (percentages) and are graphed as the percent of control ± the standard deviation. Statistical significance of total transmembrane potentials compared to vehicle controls are also displayed ($p \leq 0.05$, ◄).

(*a*)

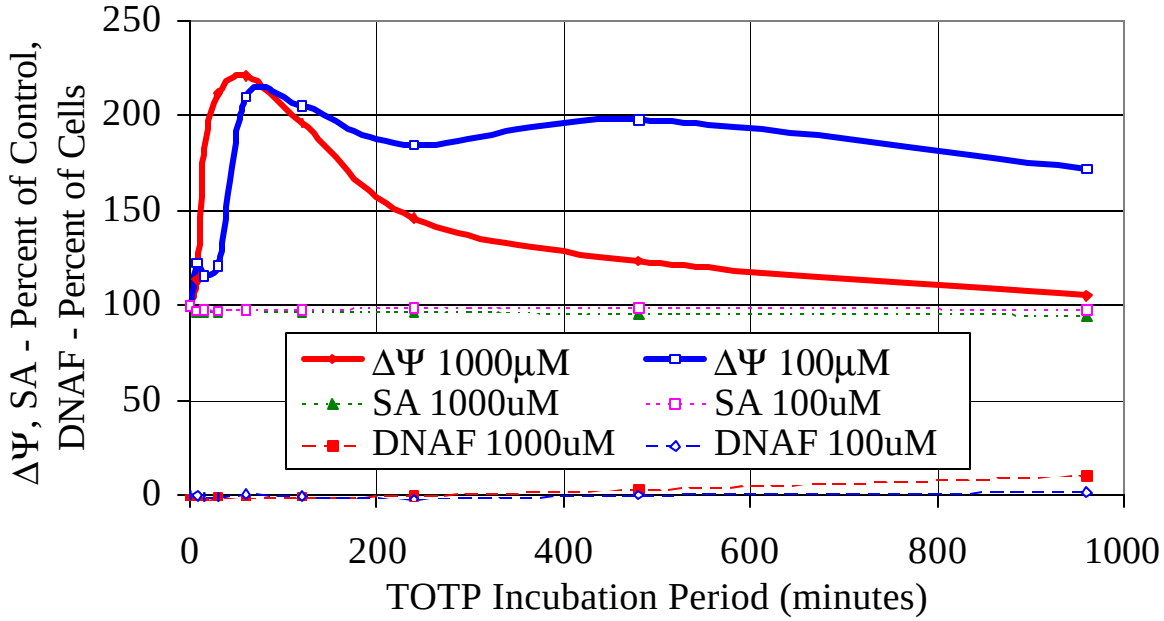

(*b*)

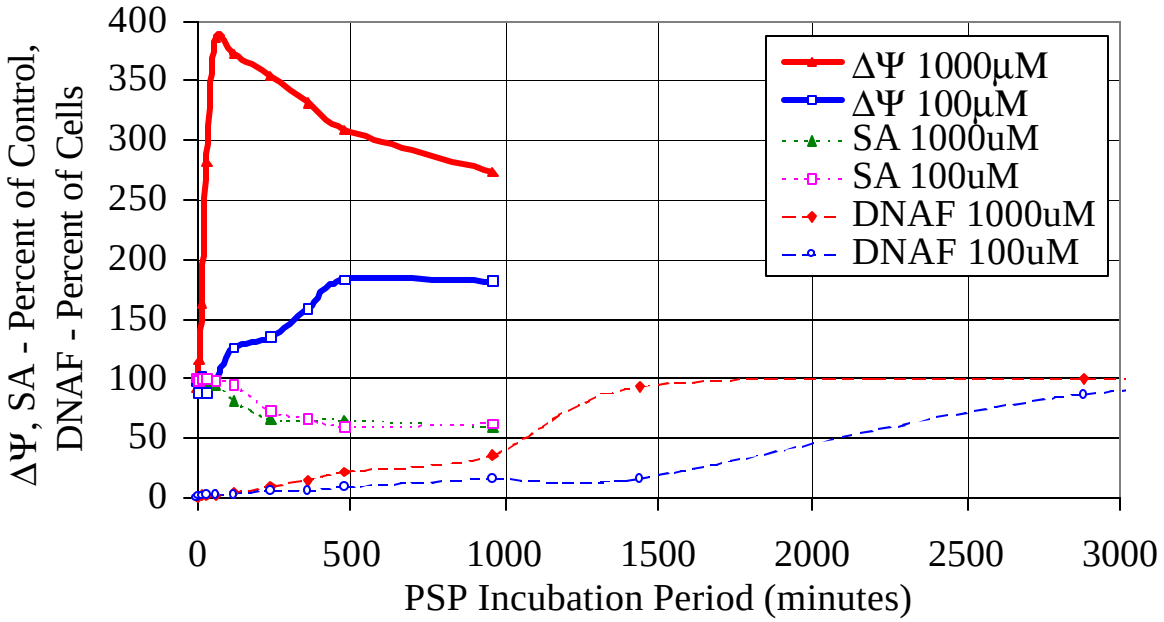

Figure 5.4. OP compound-induced changes in transmembrane potential (ΔΨ), substrate adhesion (SA), and DNA fragmentation (DNAF). Values are the mean of 3-9 normalized data points (percentages) and are graphed as the percent of control (ΔΨ, SA) or percent of cells (DNAF). Figure 5.4a, TOTP; Figure 5.4b, PSP. Significant decreases in SA occurred at 120 and 240 minutes (1mM and 100μM PSP, respectively). Significant increases in DNAF occurred at 960 min (1mM TOTP) and 360 min (1mM PSP).

(*c*)

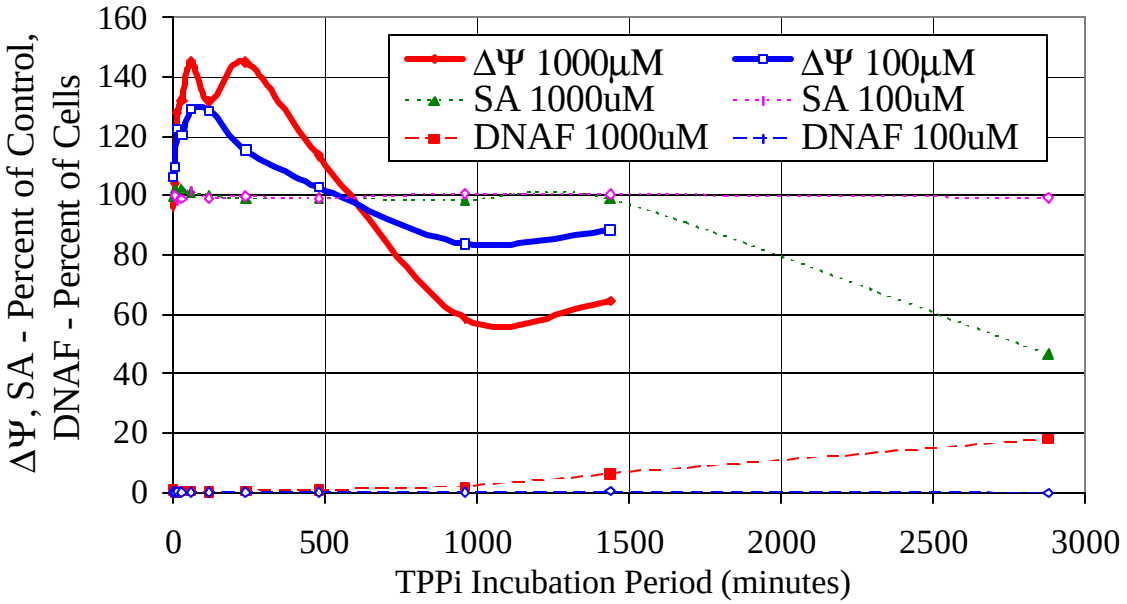

(*d*)

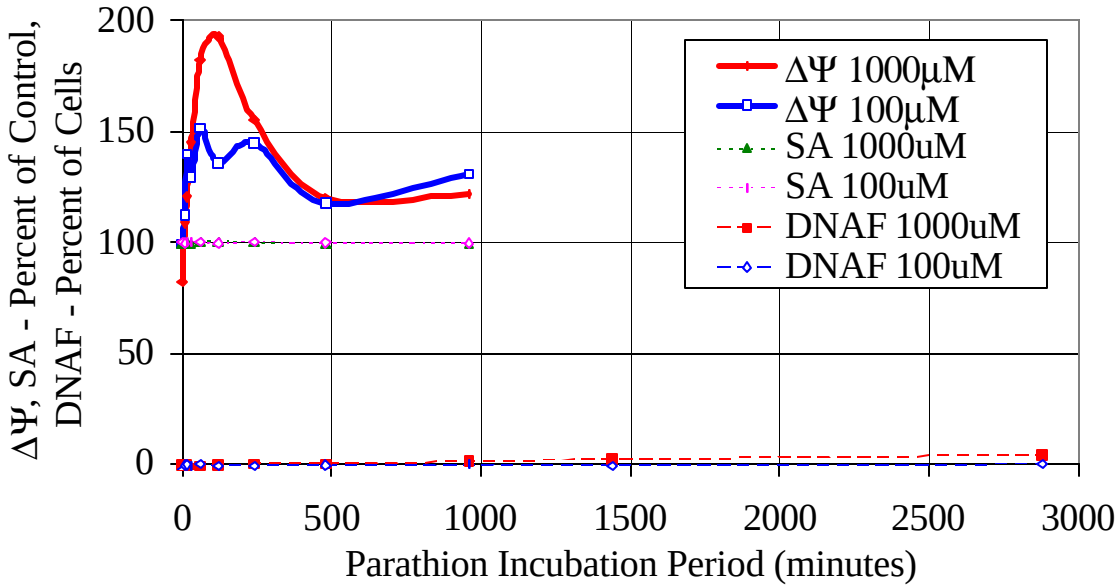

Figure 5.4. OP compound-induced changes in transmembrane potential (ΔΨ), substrate adhesion (SA), and DNA fragmentation (DNAF). Values are the mean of 3-9 normalized data points (percentages) and are graphed as the percent of control (ΔΨ, SA) or percent of cells (DNAF). Figure 5.4c, TPPi; Figure 5.4d, parathion. Significant decreases in SA occurred at 2880 minutes for 1mM TPPi exposures ($p<0.05$). Significant increases in DNAF occurred at 2880 min (1mM TPPi) and 2880 min (1mM parathion).

Chapter 6

Organophosphorus Compounds Alter Intracellular F-actin in SH-SY5Y Human Neuroblastoma Cells

Kent Carlson and Marion Ehrich

Virginia-Maryland Regional College of Veterinary Medicine,
Blacksburg, Virginia, 24061

ABSTRACT

Exposure to organophosphorus (OP) compounds induces SH-SY5Y cells to undergo a predominately apoptotic form of death. The mechanisms involved have not been fully described, but may include changes in cytoskeletal filamentous actin (f-actin) concentrations. We investigated OP compound-induced alterations in f-actin and total protein by utilizing flow cytometric and spectrophotometric techniques. SH-SY5Y human neuroblastoma cell lines were exposed to diisopropylphosphorofluoridate (DFP), paraoxon, parathion, tri-ortho-tolyl phosphate (TOTP), and triphenyl phosphite (TPPi) at 100μM to 1mM concentrations for 0 to 2880 minutes. Following exposure to OP compounds the cells were disrupted for the assessment of total protein or fixed and labeled with Alexa™ 488 phalloidin for the determination of f-actin concentration. One millimolar OP compound exposures statistically decreased the relative brightness (amount) of f-actin staining after 15 min (PSP, TOTP), 240 min (TPPi), and 1440 min (parathion) ($p<0.05$). One hundred micromolar exposures significantly decreased the amount of f-actin after 30 min (PSP) and 960 min (TOTP) and increased it following incubation for 240 min (TPPi) or 2880 min (parathion) ($p<0.05$). Incubations with 100μM parathion significantly increased the amount of total protein by 60 min following exposure ($p<0.05$). In contrast, 100μM and 1mM) PSP exposures decreased the concentration of total proteins after 480 min ($p<0.05$). Results suggest that the loss of f-actin is an early event preceding OP compound-induced cell death. The loss of f-actin is also is independent of OP compound-induced effects on total protein levels.

INTRODUCTION

Cytotoxic concentrations of some organophosphorus (OP) compounds induce SH-SY5Y cells to undergo a predominately apoptotic form of death (Carlson *et al.*, 2000). The molecular mechanisms involved in this process have not been precisely identified, even though alterations in mitochondrial (Carlson and Ehrich, 1999), enzymatic (Ehrich *et al.*, 1997), cytoskeletal (Tuler and Bowen, 1989), nuclear and genetic (Chen *et al.*, 1981; Chen *et al.*, 1982; Yin *et al.*, 1998), proteolytic (Carlson *et al.*, 2000), and plasma membrane (Antunes-Madeira *et al.*, 1994) structures and systems have been described.

Recent investigations have determined that *in vitro* exposure to OP compounds affects cell cycling (Carlson and Ehrich, 2000b) and substrate adherence (Carlson and Ehrich, 1999). Other OP compound-induced alterations includes protein metabolism (Harvey and Sharma, 1980; Reddy *et al.*, 1990), neurite (filopodia) length (Knoth-Anderson *et al.*, 1992; Nostrandt *et al.*, 1992; Flaskos *et al.*, 1994) and neurosecretion (Knoth-Anderson *et al.*, 1992; Knoth-Anderson and Abou-Donia, 1993; Liu *et al.*, 1994). These changes are consistent with alterations in actin polymerization.

Actin is the most abundant protein in eukaryotic cells and comprises from 5 to 20% of the total cellular protein (Alberts *et al.*, 1994). Changes in substrate adhesion, filopodial mobility (Zigmond, 1996; Hall, 1998), and the cell cycle (Meijerman *et al.*, 1999) are dependent on the state of actin polymerization. Actin polymerization is also required for neurosecretion (Viviani *et al.*, 1996). Because all of these endpoints are affected in OP compound-exposed cells, this investigation was conducted to evaluate if the concentration of filamentous actin (f-actin) changed following OP compound exposure. In addition, because actin constitutes such a large proportion of the protein in cells, we investigated the relationship of changes in f-actin to changes in total protein following exposure to OP compounds.

MATERIALS AND METHODS

Chemicals. Diisopropylphosphorofluoridate (DFP; 98% pure), paraoxon (98.5% pure), parathion (99% pure), tri-ortho-tolyl phosphate (TOTP; 98% pure), and triphenyl phosphite (TPPi; 98% pure) were purchased from Chem Service, Inc. (West Chester, PA). Phenyl saligenin phosphate (PSP; 99% pure) was synthesized by Lark Enterprises (Webster, MA). Stock solutions (100mM in ethanol) of these OP compounds were made and stored in the dark at -20ºC for no longer than 2 weeks prior to use. Alexa™ 488 phalloidin was acquired from Molecular Probes (Eugene, OR).

Cell Culture. SH-SY5Y human neuroblastoma cells were cultured primarily as described by Carlson and Ehrich (2000a). SH-SY5Y cells (passage 57-60) were grown in Hams F12 medium (Sigma) supplemented with fetal bovine serum (FBS - 15% v/v) supplied by Summit Biotech, Inc. (Fort Collins, CO). Prior to confluency, cells were harvested using 0.25% trypsin (Sigma) and seeded onto plastic 96 well microtiter plates or 8 well Lab-Tek™ multichamber glass slides (Nunc; Rochester, NY) at $4x10^5$ cells/ml. The cells were then allowed to grow at 37°C and 5% CO_2 for 3-4 days prior to exposure to 100µM to 1mM concentrations of OP compounds for 0 to 2880 min.

Fluorescence Microscopy of F-actin. Cells grown in 8 well multichamber slides were exposed to 1% ethanol, 1mM parathion, and 1mM TPPi for 0, 720, and 1440 min. Following treatment, the cells were washed with PBS and fixed, permeabilized, and washed again using a Cytofix/Cytoperm™ Kit (Pharmingen). Alexa™ 488 phalloidin (0.2U) was then added to each well and allowed to incubate overnight in the dark at 4°C. Following incubation, cells were washed with PBS and evaluated microscopically for f-actin staining using a Nikon Diaphot-TMD inverted microscope equipped with a 40X fluorescence objective and "B" filter cube. Photographic documentation of representative nuclear morphologies were made with a Nikon Fe-2 camera (ASA800 Kodacolor film).

Flow Cytometric Evaluation of DNA Content and F-actin Concentration. DNA was first prepared for cell cycle analysis as in Carlson and Ehrich (2000b). After pipetting the PI/cell solution into flow cytometry tubes, 0.2U of Alexa™ 488 phalloidin was added to each sample for the staining of f-actin. These samples incubated in the dark at 4°C for 16-24 hours. Five thousand cell events were then analyzed on a Coulter Epics XL-MCL flow cytometer (excitation 495nm - emission 518nm). Listmode files generated by the flow cytometer were processed through Epics XL Flow Cytometry Workstation software (version 1.5, Beckman-Coulter Corp., Opa Locka, FL) to generate objective estimates of f-actin brightness. Treated cell fluorescence in the gated field (mean fluorescence intensity of the x-channel) was then compared to control fluorescence intensities to obtain percent of control. Representative flow cytometry histograms for Alexa™ 488 phalloidin/FITC can be seen in Appendix C.

Total Protein Concentration. Total protein was evaluated by utilizing a dye with an affinity for protein binding (Bio-Rad; Richmond, CA) and spectrophotometry at 595nm. OP-exposed and control samples were normalized to mg/ml of protein by using bovine serum albumin standards (Sigma) and SOFTmax PRO software (Bio-Rad).

Statistics. Each quantitative experiment for f-actin had between 3 and 8 normalized data points (percentages) for each time and OP concentration. Experiments determining total protein had 16 normalized data points (percentages) for each time and OP concentration. Data were converted into the percent of control and then graphed as the mean ± the standard deviation. Statistical significance ($p<0.05$) was determined by utilizing PC-SAS software (version 6.1) to perform an analysis of variance (ANOVA) followed by Duncan's Multiple Range Test.

RESULTS

Fluorescence Microscopy of F-actin.

Fluorescent photographs of cells were used to verify discrete f-actin staining by Alexa™ 488 phalloidin. Control (ethanol) photographs revealed staining of organized filamentous structures similar in nature to f-actin contractile bundles and filopodia (Fig. 6.1a). Exposure to 1mM parathion decreased the filamentous nature of these structures over time (Fig. 6.1b, 6.1c). TPPi exposure (1mM) also decreased the staining of strand-like filaments over time and increased staining of pin-point structures in the cytosol (Fig. 6.1d). Pin-point staining was not visualized in any control photographs.

Flow Cytometric Evaluation of DNA Content and F-actin Concentration.

The relative brightness (amount) of f-actin was determined in order to assess cytoskeletal effects induced by OP compounds. Control and OP-exposed samples varied in relative brightness between experiments. Brightness baselines for ethanol controls ranged from 1.19-4.44 relative units (RU) to 19.5-27.2 RU.

One millimolar OP compound exposures statistically decreased the amount of f-actin after 15 min (PSP, TOTP), 240 min (TPPi), and 1440 min (parathion) (Fig. 6.2b, 6.2c, and 6.2a, respectively; $p<0.05$). Lower concentrations (100μM) significantly decreased the amount of f-actin after 30 min (PSP) and 960 min (TOTP) (Fig. 6.2b; $p<0.05$). One hundred micromolar OP compound exposure also statistically increased the amount of f-actin after 240 min and 2880 min after exposure to TPPi and parathion, respectively ($p<0.05$). No significant differences in the amount of f-actin were observed following incubation with 100μM or 1mM DFP (data not shown).

Total Protein Concentration.

Protein concentration was estimated in OP compound-exposed cells in order to determine if changes in f-actin were dependent or independent of changes in total protein levels. Estimates of total protein for ethanol control samples ranged from 0.323 to 0.594 mg protein per ml solution.

Staurosporine (50nM), the positive control for the induction of apoptosis, increased the total amount of protein at 7.5, 30, 60, 120, 180, 240, 480, 960, and 1400 min following exposure (data not shown; $p<0.05$). Exposure to 1mM parathion also significantly increased total protein at most time points after 60 min (e.g. at 60, 180, 240, 480, 960, and 2880 min). In addition, exposure to lower concentrations of parathion (100μM) increased the concentration of total protein at 60, 120, 480, 1400 min (Fig. 6.3b; $p<0.05$). In contrast, the amount of total protein decreased significantly after incubation with 1mM (480, 960, and 2880 min) and 100μM (480, 960, 1440, and 2880 min) exposures with PSP (Fig. 6.3c; $p<0.05$).

There were few other consistent significant changes in total protein following exposure to OP compounds. DFP only significantly increased the amount of total protein at the 120 (100μM), 240

(1mM), and 1440 (100μM) min time point (Fig. 6.3a; $p<0.05$). Exposure to 100μM paraoxon significantly increased the total protein only during the 120 and 1440 min incubations (Fig. 6.3b; $p<0.05$). The amount of total protein following exposure to 1mM TOTP increased at 120 min (100μM, 1mM) and 180 min (100μM) timepoints (Fig. 6.3c; $p<0.05$). Exposure to TPPi also significantly increased the total protein concentration at 30 min (100μM), 60 min (1mM), 120 min (100μM), and 1440 min (100μM). One millimolar concentrations of TPPi, however, significantly decreased total protein at the 2880 min incubation period (Fig. 6.3a; $p<0.05$).

DISCUSSION

One millimolar test concentrations of all OP compounds except DFP (parathion, PSP, TOTP, and TPPi) significantly decreased the brightness (amount) of f-actin over time. At this test concentration, the timing of significant decreases in the amount of f-actin was dependent on exposure to particular OP compounds (DFP - none; parathion > 1440 min; PSP > 15 min; TOTP > 15 min; TPPi > 240 min). The loss in f-actin occurred prior to losses in substrate adhesion (DFP - none; parathion - none; PSP > 120; TOTP - none; TPPi > 1440 min) (Carlson and Ehrich, 1999) and may have been due to depolymerization or degradation. In addition, compounds with the highest cytotoxicity (e.g. PSP) had less intervening time between f-actin loss and the loss of substrate adhesion. Similar patterns were followed by lower concentration (100μM) exposures to OP compounds.

The loss in f-actin staining may be due to depolymerization into globular actin (g-actin). Depolymerization of f-actin into g-actin can occur following ATP depletion, ATP hydrolysis, or a loss of ATP binding ability (Alberts *et al.*, 1994). ATP-dependent caspase activation has been demonstrated following exposure to similar concentrations of OP compounds used in this study (Carlson *et al.*, 2000) and argue that ATP depletion probably does not account for changes in f-actin.

Depletion of f-actin in the presence of OP compounds may also occur through degradation. Polyubiquitin complex-induced degradation of f-actin has been demonstrated following exposure to OP compounds (Calore *et al.*, 1999). General proteases such as calpains which have elevated activity following exposure to certain OP compounds (El-Fawal *et al.*, 1990) have also been reported to degrade actin (Inomata *et al.*, 1989). Even though OP compounds induce apoptosis at the concentrations used in this study, it is unlikely that caspase proteases were involved in changes in f-actin. Actin has proven to be resistant to caspase-induced degradation in intact apoptotic cells (Song *et al.*, 1997). Similarly, activation of the apoptotic protease, caspase-3 (DFP - none; parathion > 2880 min; PSP > 1440 min; TOTP > 480 min; TPPi > 2880 min) has been shown to occur after f-actin degradation (Carlson *et al.*, 2000).

OP compound-induced alterations in f-actin were independent of OP compound-induced changes in the total cellular protein. The concentration of total protein was highly variable in most circumstances and dependent on the OP compound. One millimolar exposures to PSP significantly decreased the concentration of f-actin hours before decreasing the concentration of total proteins. Similarly, exposure to 1mM parathion elicited increases in the concentration of total proteins that occurred hours before changes in f-actin. Both lines of evidence supported the conclusion that f-actin concentration was independent of the total protein concentration.

The difference in protein levels between OP compounds (PSP and parathion) may be related to differing patterns of cytotoxic events following exposure. Cytotoxic concentrations of PSP (100μM and 1mM) act rapidly and induce a form of cell death intermediate between apoptosis and oncotic necrosis (Carlson *et al.*, 2000). Cytotoxic concentrations of parathion (1mM), in contrast, act gradually and induce traditional apoptosis in exposed cells. PSP may shut down most cellular apparatus, while parathion increases the production of death related proteins. Increased protein synthesis in cells

undergoing apoptosis has been observed in this study with staurosporine and in other circumstances (Zhao *et al.*, 1995; Preston *et al.*, 1996; Donato and Perez, 1998).

This study reports that OP compounds change the status of f-actin early preceding *in vitro* cell death. This may be important for explaining the mechanisms involved in previous reports observing losses in substrate adhesion or neurite length, and changes in cell cycle status or neurotransmitter release following exposure to OP compounds (Carlson and Ehrich, 1999; Carlson and Ehrich, 2000b; Knoth-Anderson *et al.*, 1992; Nostrandt *et al.*, 1992; Flaskos *et al.*, 1994; Knoth-Anderson and Abou-Donia, 1993; Liu *et al.*, 1994).

ACKNOWLEDGMENTS

We wish to thank Joan Kalnitsky for flow cytometric assistance. This work was supported by the EPA grant R825356, a Society of Toxicology-Novartis predoctoral fellowship, and funds from the Virginia-Maryland Regional College of Veterinary Medicine.

REFERENCES

Alberts, B., Bray, D., Lewis, J., Raff, M., Roberts, K., and Watson, J.D. (1994). Chapter 16: The cytoskeleton. In *Molecular Biology of the Cell*, pp. 821-861. Garland Publishing, Inc., New York.

Antunes-Madeira, M.C., Videira, R.A., and Madeira, V.M.C. (1994). Effects of parathion on membrane organization and its implications for the mechanism of toxicity. *Biochim. Biophys. Acta* 1190, 149-154.

Calore, E.E., Sesso, A., Puga, F.R., Cavaliere, M.J., Calore, N.M., and Weg, R. (1999). Early expression of ubiquitin in myofibers of rats in organophosphate intoxication. *Ecotoxicol. Environ. Saf.* 43, 187-194.

Carlson, K. and Ehrich, M. (1999). Organophosphorus compound-induced modification of SH-SY5Y human neuroblastoma mitochondrial transmembrane potential. *Toxicol. Appl. Pharmacol.* 160, 33-42.

Carlson, K. and Ehrich, M. (2000a). Human neuroblastoma cell viability and growth are affected by altered culture conditions. *In Vitro Toxicol.* submitted.

Carlson, K. and Ehrich, M. (2000b). Organophosphorus Compounds Alter the Cell Cycle Phase of SH-SY5Y Human Neuroblastoma Cells. *In Prep.*

Carlson, K., Jortner, B., and Ehrich, M. (2000). Organophosphorus compound-induced apoptosis in SH-SY5Y human neuroblastoma cells. *Toxicol. Appl. Pharmacol.* submitted.

Chen, H.H., Hsueh, J.L., Sirianni, S.R., and Huang, C.C. (1981). Induction of sister-chromatid exchanges and cell cycle delay in cultured mammalian cells treated with eight organophosphorous pesticides. *Mutat. Res.* 88, 307-316.

Chen, H.H., Sirianni, S.R., and Huang, C.C. (1982). Sister chromatid exchanges in Chinese hamster cells treated with seventeen organophosphorus compounds in the presence of a metabolic activation system. *Environ. Mut.* 4, 621-624.

Donato, N.J. and Perez, M. (1998). Tumor necrosis factor-induced apoptosis stimulates p53 accumulation and $p21^{WAF1}$ proteolysis in ME-180 cells. *J. Biol. Chem.* 273, 5067-5072.

Ehrich, M., Correll, L., and Veronesi, B. (1997). Acetylcholinesterase and neuropathy target esterase inhibitions in neuroblastoma cells to distinguish organophosphorus compounds causing acute and delayed neurotoxicity. *Fundam. Appl. Toxicol.* 38, 1-9.

El-Fawal, H.A.N., Correll, L., Gay, L., and Ehrich, M. (1990). Protease activity in brain, nerve, and muscle of hens given neuropathy-inducing organophosphates and a calcium channel blocker. *Toxicol. Appl. Pharmacol.* 103, 133-142.

Flaskos, J., McLean, W.G., and Hargreaves, A.J. (1994). The toxicity of organophosphate compounds towards cultured PC12 cells. *Toxicol. Lett.* 70, 71-76.

Hall, A. (1998). Rho GTPases and the actin cytoskeleton. *Science* 279, 509-514.

Harvey, M.J. and Sharma, R.P. (1980). Organophosphate cytotoxicity: the effects on protein metabolism in cultured neuroblastoma cells. *J. Environ. Path. Toxicol.* 3, 423-436.

Inomata, M., Hayashi, M., Nakamura, M., Saito, Y., and Kawashima, S. (1989). Properties of erythrocyte membrane binding and autolytic activation of calcium-activated neutral protease. *J. Biol. Chem.* 264, 18838-18843.

Knoth-Anderson, J., Veronesi, B., Jones, K., Lapadula, D.M., and Abou-Donia, M.B. (1992). Triphenyl phosphite-induced ultrastructural changes in bovine adrenomedullary chromaffin cells. *Toxicol. Appl. Pharmacol.* 112, 110-119.

Knoth-Anderson, J. and Abou-Donia, M.B. (1993). Differential effects of triphenylphosphite and diisopropylphosphorofluoridate on catecholamine secretion from bovine adrenomedullary chromaffin cells. *J. Toxicol. Env. Health* 38, 103-114.

Liu, P.-S., Kao, L.-S., and Lin, M.-K. (1994). Organophosphates inhibit catecholamine secretion and calcium influx in bovine adrenal chromaffin cells. *Toxicology* 90, 81-91.

Meijerman, I., Blom, W.M., de Bont, H.J.G.M., Mulder, G.J., and Nagelkerke, J.F. (1999). Changes of g-actin localization in the mitotic spindle region or nucleus during mitosis and after heat shock: a histochemical study of g-actin in various cell lines with fluorescent labeled vitamin D-binding protein. *Biochim. Biophys. Acta* 1452, 12-24.

Nostrandt, A.C., Rowles, T.K., and Ehrich, M. (1992). Cytotoxic effects of organophosphorus esters and other neurotoxic chemicals on cultured cells. *In Vitro Toxicol.* 5, 127-136.

Preston, G.A., Lyon, T.T., Yin, Y., Lang, J.E., Solomon, G., Annab, L., Srinivasan, D.G., Alcorta, D.A., and Barrett, J.C. (1996). Induction of apoptosis by c-fos protein. *Mol. Cell. Biol.* 16, 211-218.

Reddy, M.S., Kodavanti, P.R., and Rao, K.V. (1990). Toxic impact of phosphamidon on protein degradation in phasic and tonic muscles of the marine prawn, Penaeus indicus (H. Milne Edwards). *Arch. Int. Physiol. Biochim.* 98, 347-351.

Song, Q., Wei, T., Lees-Miller, S., Alnemri, E., Watters, D., and Lavin, M.F. (1997). Resistance of actin to cleavage during apoptosis. *Proc. Natl. Acad. Sci. USA* 94, 157-162.

Tuler, S.M. and Bowen, J.M. (1989). Toxic effect of organophosphates on nerve cell growth and ultrastructure in culture. *J. Toxicol. Env. Health* 27, 209-223.

Viviani, B., Galli, C.L., and Marinovich, M. (1996). Is actin polymerization relevant to neurosecretion? A study on neuroblastoma cells. *Biochem. Biophys. Res. Com.* 223, 712-717.

Yin, H., Cukurcam, S., Betzendahl, I., Adler, I.D., and Eichenlaub-Ritter, U. (1998). Trichlorfon exposure, spindle aberrations, and nondisjunction in mammalian oocytes. *Chromosoma* 107, 514-522.

Zhao, X., Gschwend, J.E., Powell, C.T., Foster, R.G., Day, K.C., and Day, M.L. (1997). Retinoblastoma protein-dependent growth signal conflict and caspase activity are required for protein kinase C-signaled apoptosis of prostate epithelial cells. *J. Biol. Chem.* 272, 22751-22757.

Zigmond, S.H. (1996). Signal transduction and actin filament organization. *Curr. Op. Cell Biol.* 8, 66-73.

(*a*)

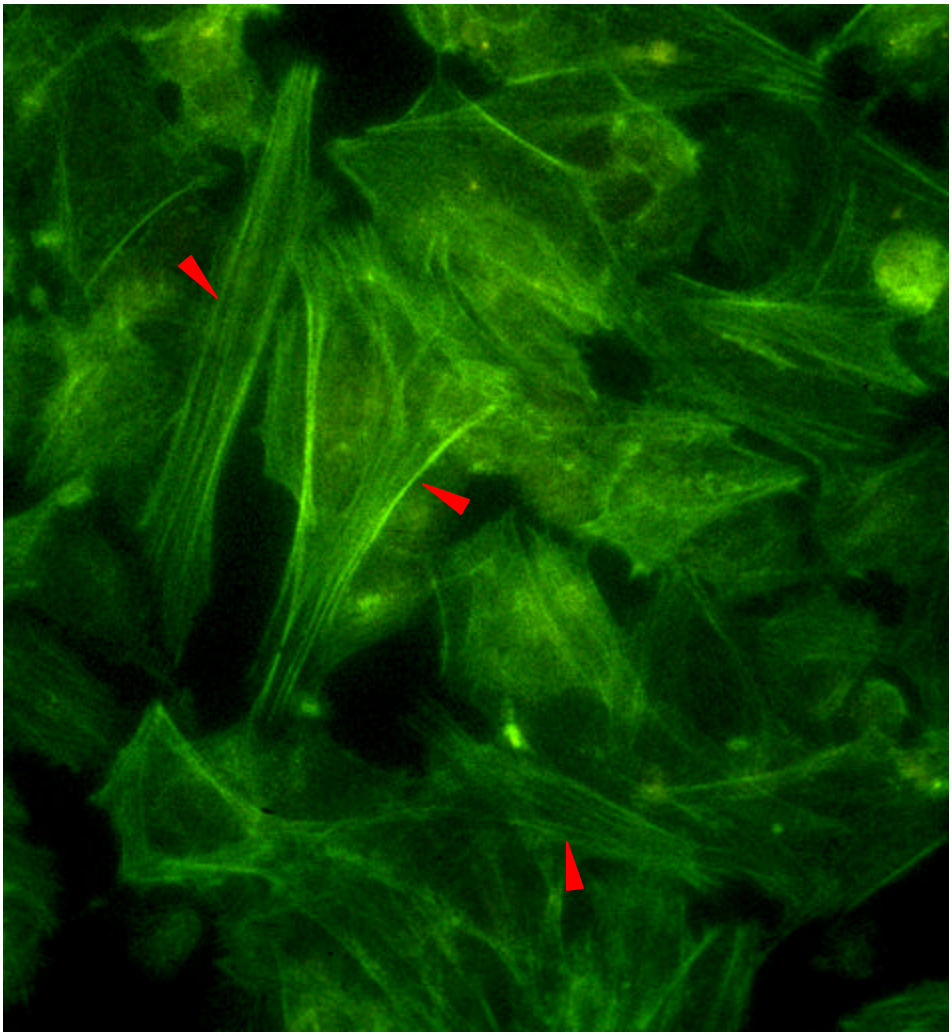

Figure 6.1. F-actin fluorescence in SH-SY5Y cells. Cells were incubated with 0.2U of Alexa™ 488 phalloidin, washed in PBS, and visualized on a fluorescence microscope. Fig. 6.1a, 1% ethanol (1440 min). Arrowheads (➤) indicate filamentous structures analogous to f-actin contractile bundles. Full arrows (←) show punctate staining in parathion or TPPi exposed cells. The photos are at 400x.

(*b*)

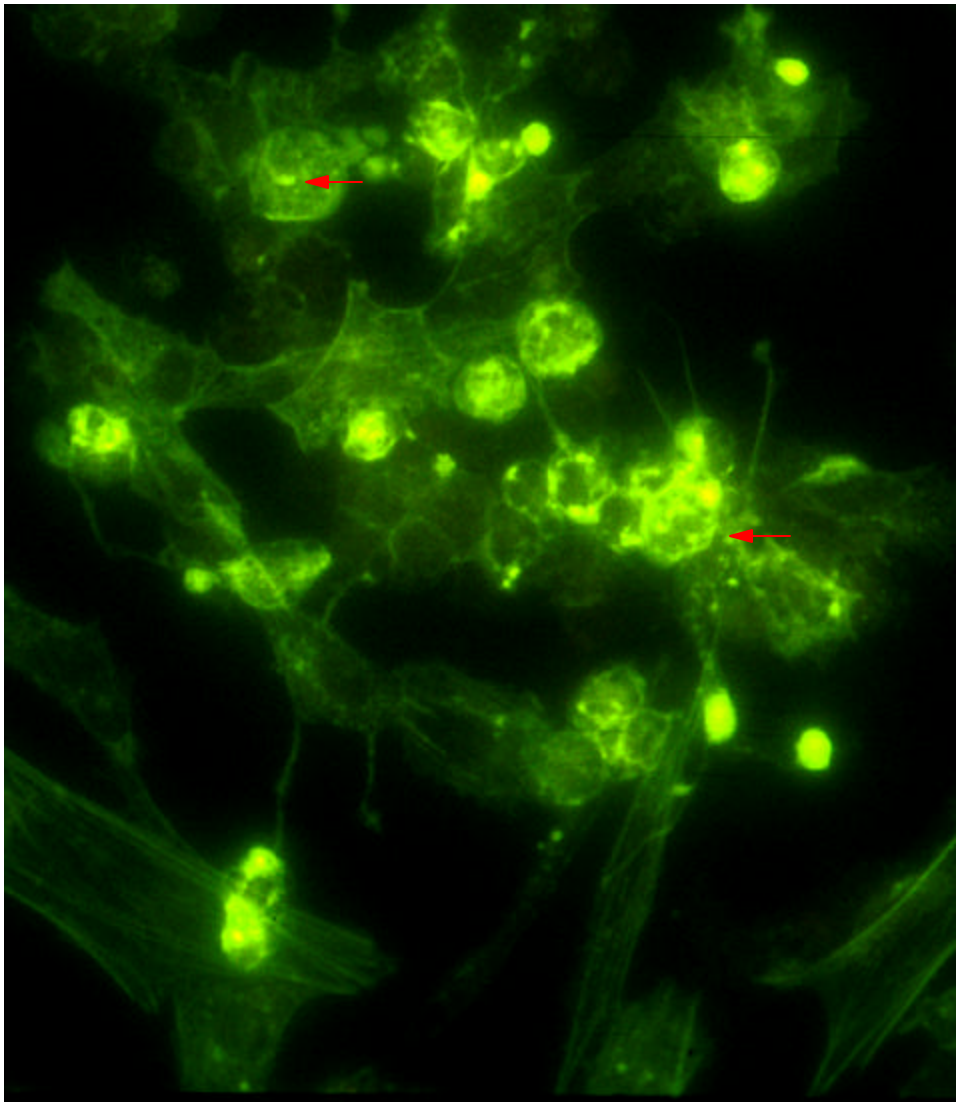

Figure 6.1. F-actin fluorescence in SH-SY5Y cells. Cells were incubated with 0.2U of Alexa™ 488 phalloidin, washed in PBS, and visualized on a fluorescence microscope. Fig. 6.1b, 1mM parathion (720 min). Arrowheads ( ) indicate filamentous structures analogous to f-actin contractile bundles. Full arrows (←) show punctate staining in parathion or TPPi exposed cells. The photos are at 400x.

(*c*)

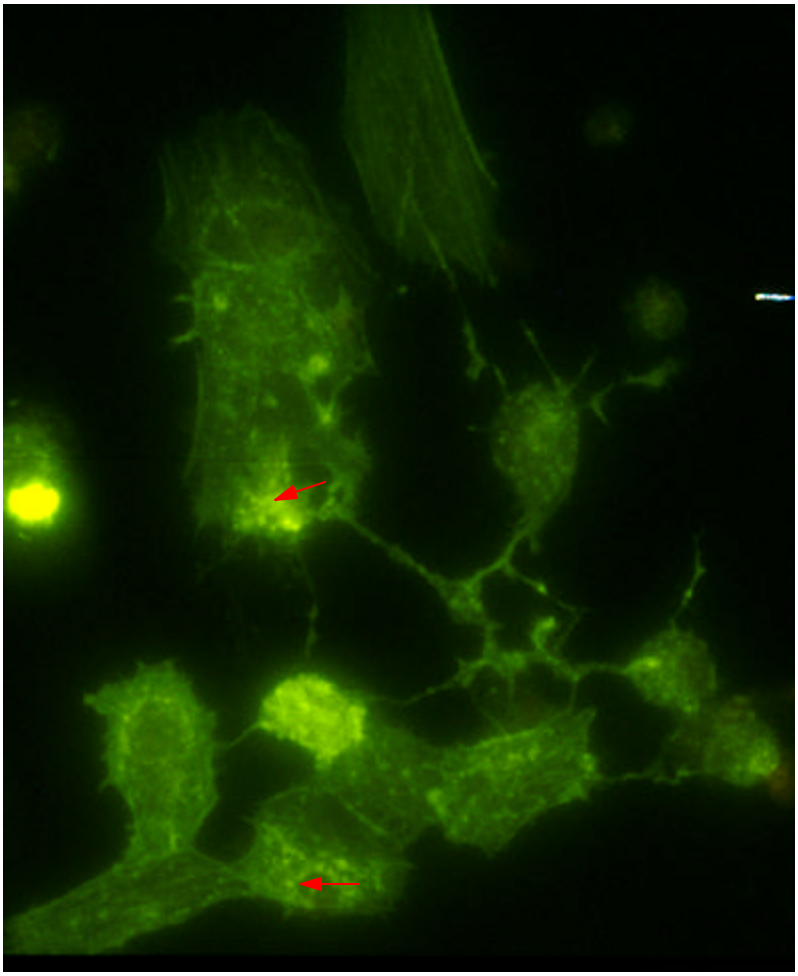

Figure 6.1. F-actin fluorescence in SH-SY5Y cells. Cells were incubated with 0.2U of Alexa™ 488 phalloidin, washed in PBS, and visualized on a fluorescence microscope. Fig. 6.1c, 1mM parathion (1440 min). Arrowheads ( ) indicate filamentous structures analogous to f-actin contractile bundles. Full arrows ( ) show punctate staining in parathion or TPPi exposed cells. The photos are at 400x.

(*d*)

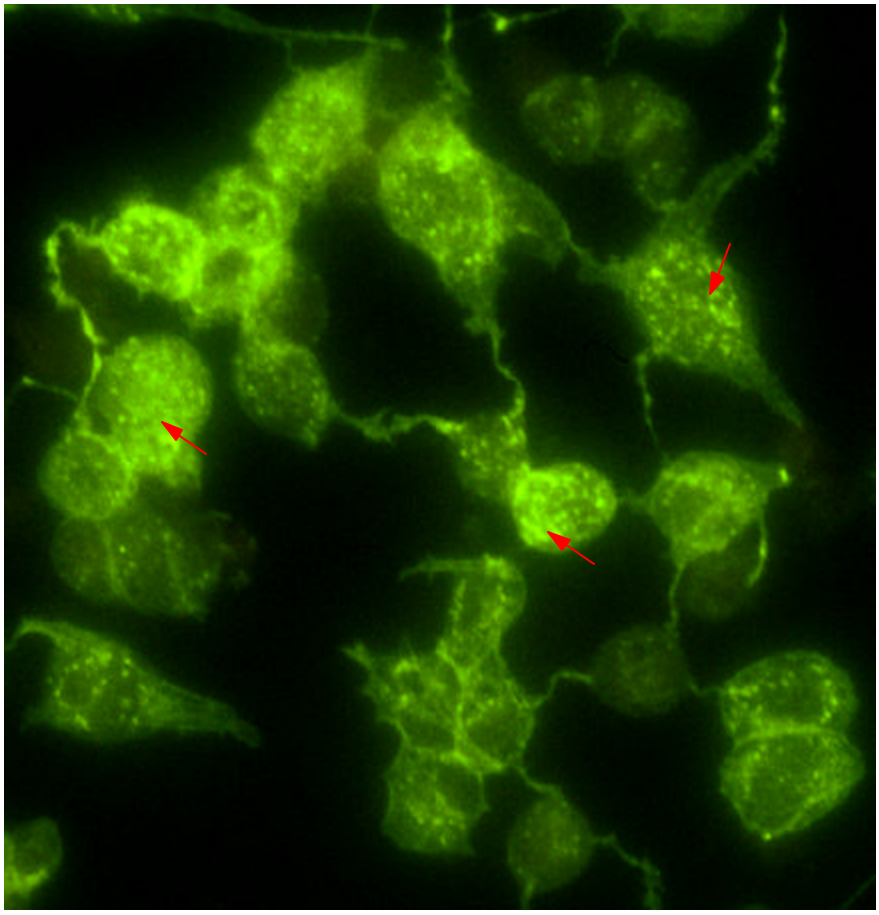

Figure 6.1. F-actin fluorescence in SH-SY5Y cells. Cells were incubated with 0.2U of Alexa™ 488 phalloidin, washed in PBS, and visualized on a fluorescence microscope. Fig. 6.1d, 1mM TPPi (1440 min). Arrowheads (➤) indicate filamentous structures analogous to f-actin contractile bundles. Full arrows (←) show punctate staining in parathion or TPPi exposed cells. The photos are at 400x.

(*a*)

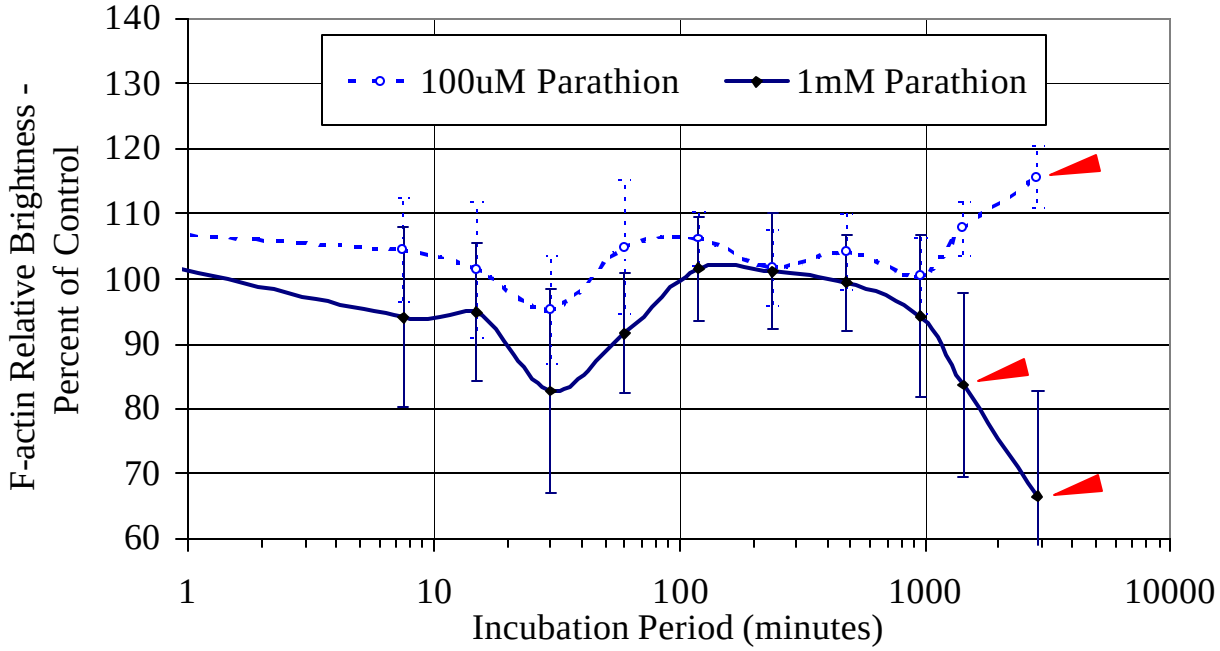

(*b*)

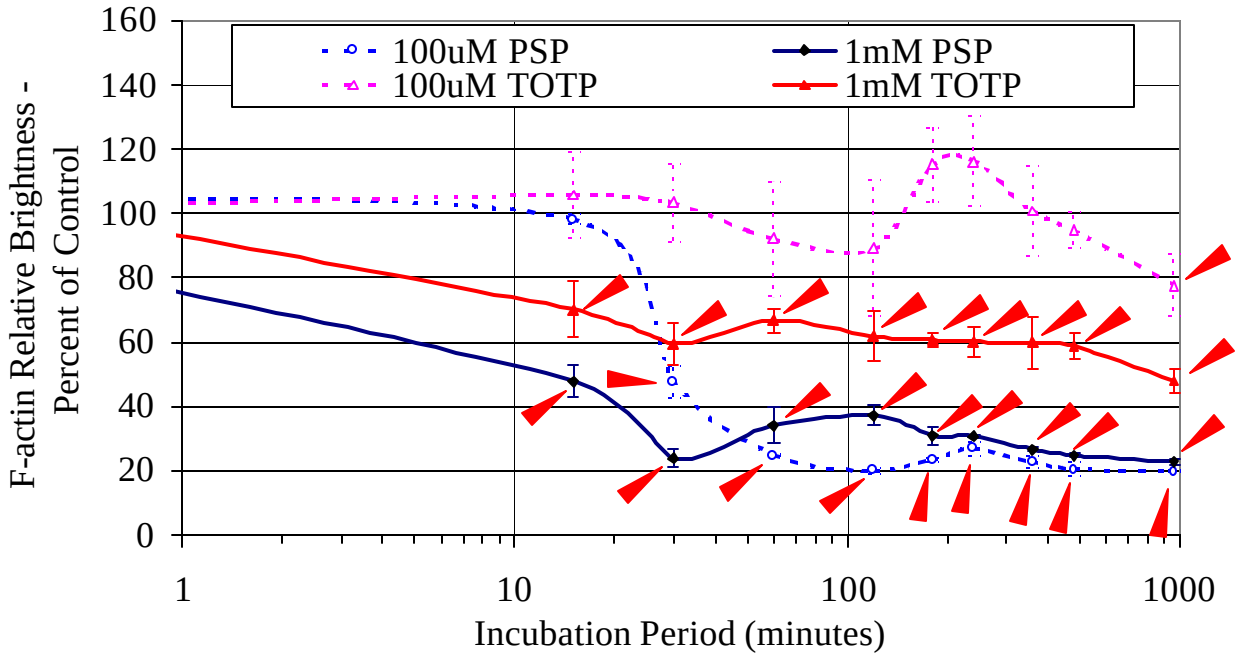

Figure 6.2. The relative brightness (amount) of f-actin in SH-SY5Y cells. Cells were exposed to OP compounds, fixed, and then stained with 0.2U of Alexa™ 488 phalloidin for 16-24 hours. Values are the mean of 3-8 normalized data points (percentages) ± the standard deviation. Statistical significance of exposed cells when compared to matched ethanol controls are shown ($P<0.05$, ◀). Fig. 6.2a, Parathion (100µM and 1mM); Fig. 6.2b, PSP and TOTP (100µM and 1mM).

(*c*)

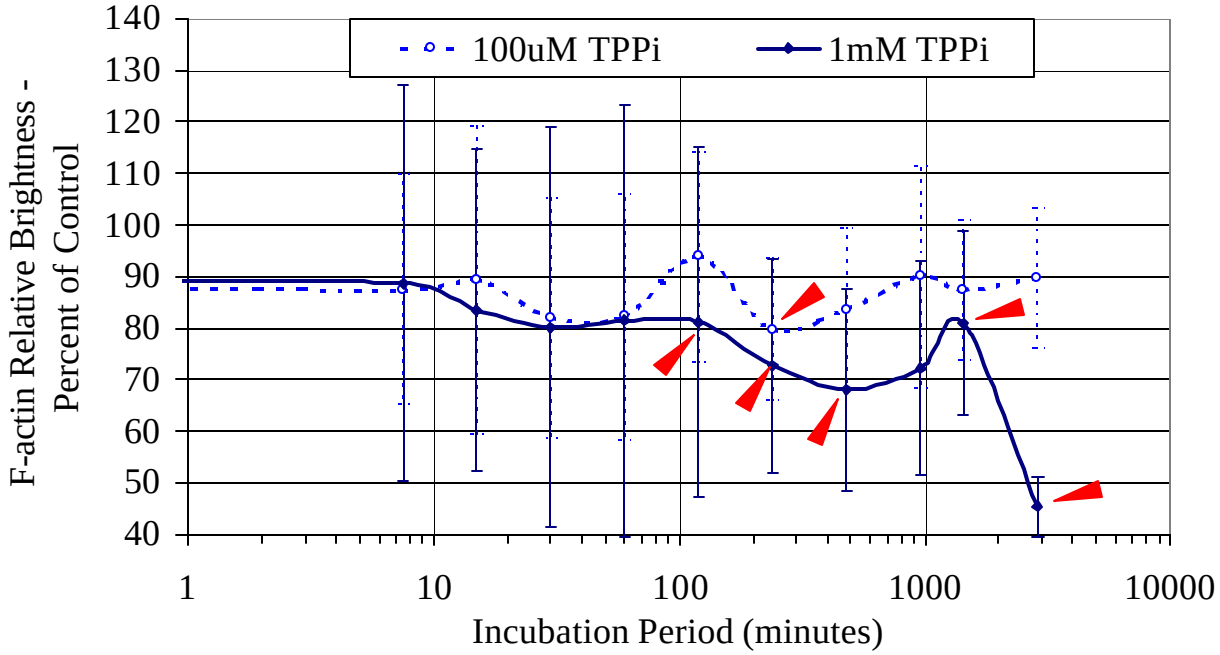

Figure 6.2. The relative brightness (amount) of f-actin in SH-SY5Y cells. Cells were exposed to OP compounds, fixed, and then stained with 0.2U of Alexa™ 488 phalloidin for 16-24 hours. Values are the mean of 3-8 normalized data points (percentages) ± the standard deviation. Statistical significance of exposed cells when compared to matched ethanol controls are shown ($P<0.05$, ◀).
Fig. 6.2c, TPPi (100µM and 1mM).

(*a*)

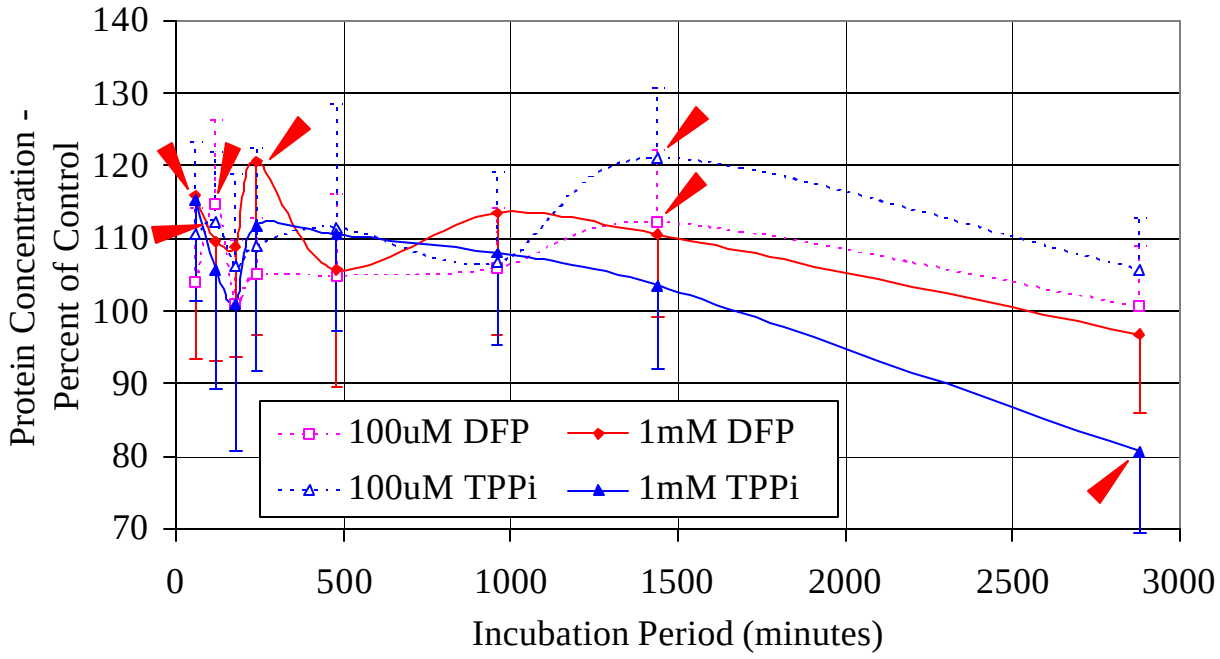

(*b*)

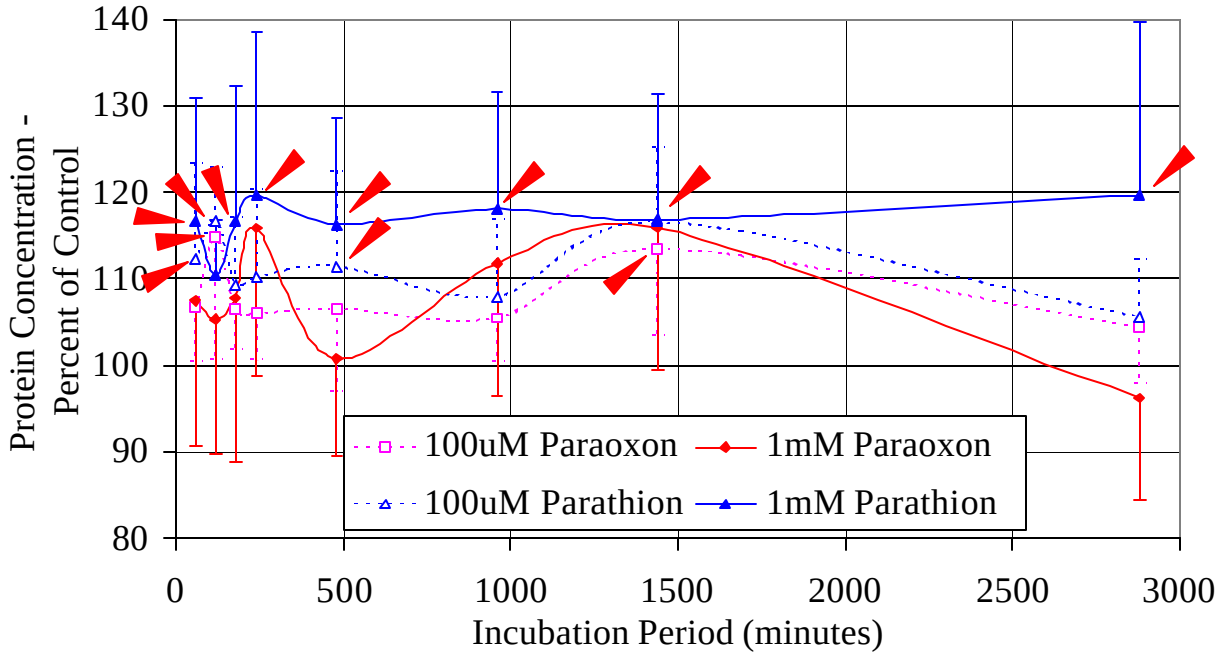

Figure 6.3. The total concentration of protein (as a percent of control) in SH-SY5Y cells. Cells were exposed to OP compounds, the media removed, and cells disrupted through freezing. Protein concentrations were then determined by using a protein binding dye. Values are the mean of 16 normalized data points (percentages) ± the standard deviation. Statistical significance of exposed cells when compared to matched ethanol controls are shown ($P<0.05$, ◢). Fig. 6.3a, DFP and TPPi (100µM and 1mM); Fig. 6.3b, Paraoxon and Parathion (100µM and 1mM).

(*c*)

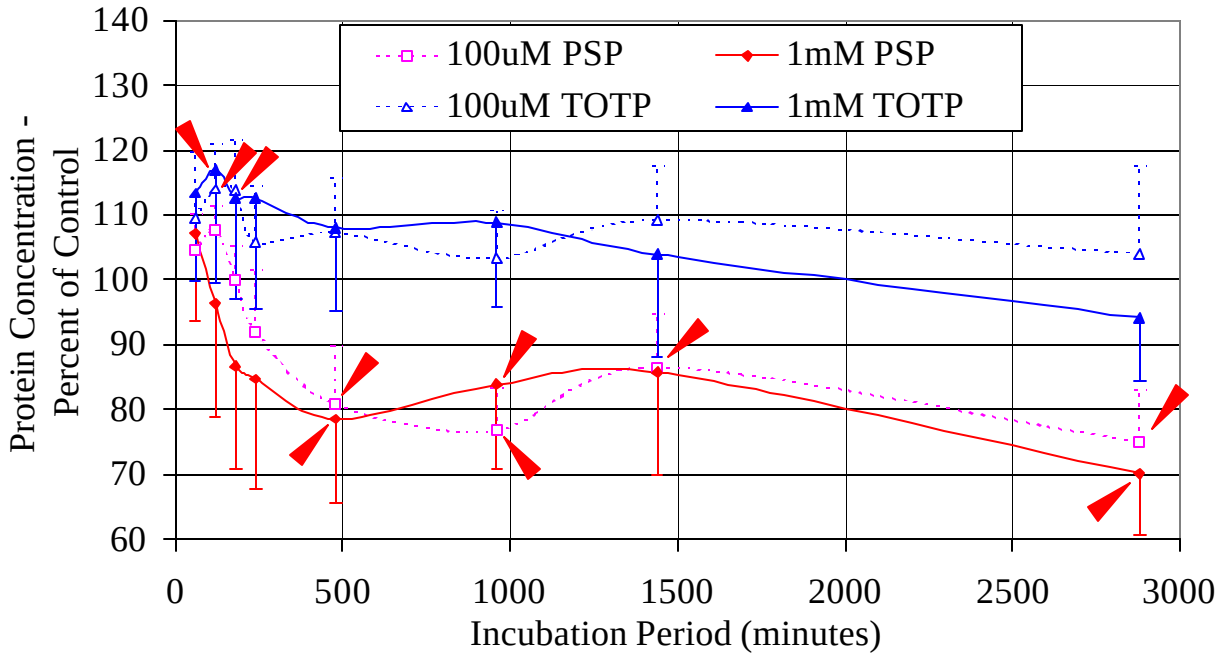

Figure 6.3. The total concentration of protein (as a percent of control) in SH-SY5Y cells. Cells were exposed to OP compounds, the media removed, and cells disrupted through freezing. Protein concentrations were then determined by using a protein binding dye. Values are the mean of 16 normalized data points (percentages) ± the standard deviation. Statistical significance of exposed cells when compared to matched ethanol controls are shown ($P<0.05$, ◢). Fig. 6.3c, PSP and TOTP (100µM and 1mM).

Chapter 7

Organophosphorus Compound-induced Apoptosis in SH-SY5Y Human Neuroblastoma Cells

Accepted for Publication by Toxicology and Applied Pharmacology

Kent Carlson, Bernard S. Jortner, and Marion Ehrich

Virginia-Maryland Regional College of Veterinary Medicine,
Blacksburg, Virginia, 24061

ABSTRACT

Organophosphorus (OP) compounds have been shown to be cytotoxic to SH-SY5Y human neuroblastoma cell cultures. The mechanisms involved in OP compound-induced cell death (apoptosis versus necrosis) were assessed morphologically by looking at nuclear fragmentation and budding using the fluorescent stain Hoechst 33342 (10μg/ml). Hoechst staining revealed significant paraoxon (1mM), parathion (1mM), phenyl saligenin phosphate (PSP, 10μM and 100μM), tri-ortho-tolyl phosphate (TOTP, 100μM and 1mM), and triphenyl phosphite (TPPi, 1mM) induced time-dependent increases in traditional apoptosis ($p<0.05$). In many cells, PSP and TOTP (1mM) also induced nuclear condensation with little fragmentation or budding which was suggestive of another mode of cell death. Pretreatment with cyclosporin A (500nM, 30 hr) decreased apoptosis following 1mM parathion and TOTP exposures. Apoptotic nuclear changes were verified by DNA gel electrophoresis. Activation of caspase-3, a cysteine aspartate protease, was also monitored using flow cytometry. OP compounds induced significant time-dependent increases in caspase-3 activation following paraoxon (1mM), parathion (100μM, 1mM), PSP (10μM, 100μM, 1mM), TOTP (100μM, 1mM), and TPPi (1mM) exposure ($p<0.05$). Pretreatment with cyclosporin A (500nM, 30 hr) significantly decreased caspase-3 activation during extended incubations with paraoxon, parathion, and TPPi ($p<0.05$). In addition, pretreatment with the caspase-3 inhibitor Ac-DEVD-CHO and the caspase-8 inhibitor Ac-IETD-CHO (25uM, 8h) significantly decreased caspase-3 activation following exposure to 1mM PSP and parathion ($p<0.05$). Pretreatment with the serine protease inhibitor phenylmethylsulfonyl fluoride (PMSF; 1mM, 8h) also significantly decreased caspase activation following 1mM PSP and TOTP exposures ($p<0.05$). Alteration of OP compound-induced nuclear fragmentation or caspase-3 activation by pretreatment with cyclosporin A, Ac-IETD-CHO, or PMSF suggested that OP compound-induced cytotoxicity may be modulated through multiple sites including mitochondrial permeability pores, receptor mediated caspase pathways, or serine proteases.

INTRODUCTION

Organophosphorus (OP) compounds are utilized primarily as insecticides (Aspelin, 1997). Secondary markets including plasticizers, plastic softeners, flame retardents, antioxidants, and hydraulic fluids are also economically important (Mochida *et al.*, 1988; Katoh *et al.*, 1990; Mortensen and Ladefoged, 1992; Ware, 1994; Weiner and Jortner, 1999).

OP compounds induce a variety of detrimental effects in man and animals. Acute physiological toxicity is initiated via the inhibition of acetylcholinesterase (AChE; Abou-Donia, 1995). Pathological developments may also occur following OP compound exposure (Baron 1981; Abou-Donia and Lapadula, 1990; Abou-Donia, 1995, Weiner and Jortner, 1999). Of these later effects, neuropathic (Carrington *et al.*, 1988; Veronesi and Pope, 1990, Funk *et al.*, 1994), myopathic (Cavanagh, 1964; Dettbarn, 1984), and cardiomyopathic (McLeod, 1985; Singer *et al.*, 1987; Baze, 1993) sequelae are attributed to necrotic processes. Even though almost all OP compounds can cause *in vivo* toxicity by AChE inhibition, they may also induce other activities within exposed cells (Pope, 1999).

OP compound-induced i*n vitro* cytotoxicity has been demonstrated using a variety of techniques, including the fragmentation of DNA (Carlson and Ehrich, 1999), a loss of capability to retain neutral red (Veronesi and Ehrich 1993a; 1993b; Veronesi *et al.*, 1997), inhibition of protein synthesis (Harvey and Sharma, 1980; Marinovich *et al.*, 1996), leakage of lactate dehydrogenase (Bagchi *et al.*, 1995), inclusion of trypan blue (Nostrandt *et al.*, 1992; Flaskos *et al.*, 1994), inhibition of culture growth (Mochida *et al.*, 1988), inhibition of glucose metabolism (Harvey and Sharma, 1980), inhibition of the incorporation of ^{3}[H]adenosine into ATP (Knoth-Anderson *et al.*, 1992) and morphologic changes (Harvey and Sharma, 1980; Tuler and Bowen, 1989; Knoth-Anderson *et al.*, 1992).

Specific mechanisms involved in OP compound-induced *in vitro* cell death have not been extensively described. Two *in vivo* studies (Akbarsha and Sivasamy, 1998; Hamm *et al.*, 1998) reported that apoptotic processes were involved in phosphamidon and diazinon-induced cytotoxicity, respectively. Hamm *et al.* (1998) additionally concluded that necrosis contributed to diisopropylphosphorofluoridate- (DFP) and diazinon-induced toxicity.

Cell death has two basic forms, apoptosis and necrosis. Discrimination between these two mechanisms is based on morphology, enzymatic activity, ATP concentration, and adjacent cellular effects (Fawthrop *et al.*, 1991; Majno and Joris, 1995; Levin, 1998). The induction of necrosis, or accidental cell death, is a violent lytic process of little benefit to the host organism. Unlike necrosis, apoptotic cell death has evolved in multicellular organisms as a means to control morphologic, immunologic, and pathologic development (Thompson, 1995; Duke *et al.*, 1996).

The utilization of both morphologic and biochemical (e.g. caspase protease) methods are important for the determination of cell death. Toxicant-induced cell death can present a mixture of characters ascribed to either apoptosis or necrosis. For example, nontraditional apoptotic characters such as nuclear condensation without fragmentation and the loss of oligonucleotide ladders following

electrophoresis have been described. These are termed Type II apoptosis (Boix *et al.*, 1997) or apoptotic necrosis (Majno and Joris, 1995) respectively, depending on whether they are an intermediate form of apoptosis or result from a stalled apoptotic program that has undergone secondary necrosis. In these circumstances, utilization of one method for mechanistic determinations would result in an inaccurate description of the mode of cell death .

Investigators of cell death rely primarily on gross nuclear changes and DNA fragmentation patterns to differentiate between traditional apoptosis and necrosis (Eastman, 1995; Fraker *et al.*, 1995; McGahon *et al.*, 1995). Apoptotic cell death induces the nucleus to condense and partition into buds that can be seen as discrete clusters of nuclear material following fluorescence staining. Necrotic processes, in contrast, result in nuclear pyknosis, karyolysis, or karyorrhexis. In addition, Martin *et al.* (1994) notes that apoptotic fragmentation of DNA ultimately occurs at internucleosomal linker regions and generates 180-200 base pair oligonucleotide multiples that can be resolved as DNA "ladders" following electrophoresis. Necrotic processes, however, cleave DNA randomly and present as electrophoretic smears.

Cohen (1998) and McConkey (1998) report that differentiation of apoptosis from necrosis can also be done on a biochemical basis by monitoring the activation of caspase proteases. Caspase-3 (YAMA, CPP32/apopain), an effector caspase, is activated in cascade fashion following a wide variety of apoptotic stimulants including staurosporine (Postmantur *et al.*, 1997), withdrawal of nerve growth factor (Mukasa *et al.*, 1997), tumor necrosis factor (Wissing *et al.*, 1997), anti-Fas ligand (Wang *et al.*, 1998b), and ceramide and serum free conditions (Keane *et al.*, 1997). Activated caspase-3 degrades cytoskeletal substrates (Nath *et al.*, 1996; Song *et al.*, 1997; Wang *et al.*, 1998a), signaling proteins (Widmann *et al.*, 1998), and other intracellular molecules (Cryns *et al.*, 1996; Tann *et al.*, 1997; Wang *et al.*, 1998b) and so is important in cellular degradation and subsequent remodeling into apoptotic particles.

In this paper we evaluate the mechanisms involved in DFP, parathion, paraoxon, phenyl saligenin phosphate (PSP), tri-ortho-tolyl phosphate (TOTP), and triphenyl phosphite (TPPi) induced *in vitro* cytotoxicity. Four of these compounds, DFP, PSP, TOTP, and TPPi initiate a central and peripheral neuropathy in sensitive species, termed OP-induced delayed neuropathy (OPIDN). The remaining compounds, paraoxon and parathion, have potent anticholinesterase activity, but typically do not induce neuropathic sequelae (Abou-Donia and Lapadulla, 1990; Abou-Donia, 1995).

Compounds which alter mitochondrial activity were used in conjunction with OP compounds to modulate cytotoxicity. These compounds included carbachol, which increases the mitochondrial transmembrane potential ($\Delta\Psi_m$) and Bcl-2 levels (Carlson and Ehrich, 1999; Itano *et al.*, 1996), and cyclosporin A, which decreases $\Delta\Psi_m$ and inhibits mitochondrial permeability transition pores (PTP) (Carlson and Ehrich, 1999; LeMasters *et al.*, 1998). Other compounds which modulate cytotoxicity were also used and included Ac-DEVD-CHO, an inhibitor of caspase-3 (Li *et al.*, 1997; Garcia-Calvo *et al.*, 1998), Ac-IETD-CHO, which inhibits caspase-8 (Garcia-Calvo *et al.*, 1998), or phenylmethylsulfonyl fluoride (PMSF), an inhibitor of serine proteases (Sarin *et al.*, 1993).

EXPERIMENTAL METHODS

Chemicals. Diisopropylphosphorofluoridate (DFP; 98% pure), paraoxon (98.5% pure), parathion (99% pure), tri-ortho-tolyl phosphate (TOTP; 98% pure), and triphenyl phosphite (TPPi; 98% pure) were purchased from Chem Service, Inc. (West Chester, PA). Phenyl saligenin phosphate (PSP; 99% pure) was purchased from Lark Enterprises (Webster, MA). Stock solutions (100mM in ethanol) of these OP compounds were made and stored at -20ºC for no longer than 2 weeks prior to use. Staurosporine, phenylmethylsulfonyl fluoride (PMSF), carbachol, and cyclosporin A were obtained from Sigma Chemical Co. (St. Louis, MO). Ac-DEVD-CHO and Ac-IETD-CHO were procured from Pharmingen (San Diego, CA).

Cell Culture. SH-SY5Y human neuroblastoma cells were cultured as described by Ehrich *et al.* (1995). These clonal cells are roughly diploid, genetically stable (Perez-Polo *et al.*, 1979), and have been utilized in other toxicant systems to investigate cell death (Nakagawa-Yagi, 1994; Cece *et al.*, 1995; Tredici *et al.*, 1995; Li *et al.*, 1996; Boix *et al.*, 1997; Prince and Oreland, 1997).

SH-SY5Y cells (passage 57-60) were grown in Hams F12 medium (Sigma) supplemented with fetal bovine serum (FBS - 15% v/v) supplied by Gibco (Grand Island, NY) in order to maintain predominately neuroblast morphologies. Prior to confluency, cells were harvested using 0.25% trypsin (Sigma) and seeded onto plastic 24 well microtiter plates (Corning; Corning, NY), 100mm culture dishes (Corning), 4 well, or 8 well Lab-Tek™ multichamber glass slides (Nunc; Rochester, NY) at $4x10^5$ cells/ml. The cells were then allowed to grow at 37°C and 5% CO_2 for 2-4 days prior to treatment.

Fluorescence Microscopy of Nuclear Morphology (Apoptosis). Traditional apoptosis is most easily determined via the visualization of late stage DNA fragmentation into DNA particles (Martin *et al.*, 1994; Majno and Joris, 1995, Duke *et al.*, 1996). This is achieved by fluorescently labeling DNA with DNA-specific dyes such as Hoechst 33342 (Dive *et al.*, 1992; Cobb *et al.*, 1996).

Cells grown in 4 and 8 well multichamber slides were either pretreated with carbachol (1mM in media) or cyclosporin A (500nM in 0.01% methanol) for 30 hr or exposed directly to OP compounds (10µM - 1mM) for 7.5 to 5760 min. Staurosporine (50-500nM in 0.05-0.5% methanol) was used as a positive control. Following treatment, the cells were centrifuged on a Hettich cytospin (Tuttlingen, Germany) for 5 min at 600 to 1000rpm and then fixed in acetone/ethanol (1:1 v/v). Subsequently, the slides were air dried and stained with the DNA specific fluorochrome Hoechst 33342 (10µg/ml) for 15 min.

Stained cells were evaluated visually for apoptotic nuclear fragmentation (not condensation). Observations of 6 random cell groups per slide well were made using a Nikon Diaphot-TMD inverted microscope equipped with a 40X fluorescence objective and UV filter cube. Photographic documentation of representative nuclear morphologies were made with a Nikon Fe-2 camera (ASA800 Kodacolor film). Nuclei displaying apoptotic characters were counted and compared numerically to morphologically normal nuclei in the same respective field. Percent of apoptotic nuclei were calculated

by the equation: [apoptotic nuclei / (apoptotic nuclei + normal nuclei)] X 100. Similar methods have been used to identify apoptosis in SH-SY5Y (Boix *et al.*, 1997; Prince and Oreland, 1997), HL-60 (Verhaegen, 1998), and other cell lines (McGahon *et al.*, 1995).

Agarose Gel Evaluation of DNA Fragmentation. Many apoptotic stimulants induce the discrete fragmentation of DNA into oligonucleotide multiples of 180-200 base pairs (Majno and Joris, 1995; McGahon *et al.*, 1995). These fragments can be visualized as a "ladder" pattern following DNA gel electrophoresis for verification of apoptosis (McGahon *et al.*, 1995; Li *et al.*, 1996).

DNA was isolated from SH-SY5Y cells following 4, 8, 12, 24, 48, and 72 hour OP compound treatments. Cells floating in the media and attached to the plate were harvested separately in 0.25% trypsin/EDTA (Sigma), washed in cold PBS (pH 7.2-7.4, Ca^{2+} and Mg^{2+} free), and incubated in lysis buffer (10mM Tris-HCl, pH 7.6, 20mM EDTA, pH 8.0, 0.5% v/v Triton X-100) for 30 min at room temperature.

Lysed cell components were transferred to microfuge tubes and centrifuged at 4°C for 30 min at 10,000g. Following centrifugation, soluble oligonucleotide fragments (supernatant) were transferred into new microfuge tubes. Lysis buffer was then added back to the pellet (cellular debris and bound nuclear remnants). Protein in the pellet and supernatant fractions was digested by the addition of Proteinase K (Sigma; 20mg/ml) and RNAse A (Sigma; 1mg/ml) followed by a 2 hour incubation at 50°C. Both fractions were then extracted (1:1 v/v) with Tris-equilibrated (pH 8.0) phenol and then phenol / chloroform / isoamyl alcohol (25/24/1 v/v). One-half volume of cold ammonium acetate (7.5M) and two volumes of cold ethanol (100%) were added to the aqueous phase and the mix incubated at -20°C overnight.

On the following day the tubes were centrifuged in the cold at 16,000g for 60 min, the supernatant discarded, and the DNA pellets partially dried. Pellets were then redissolved in TE buffer (10mM Tris, 10mM EDTA, pH 7.8) and stored overnight at 4°C.

Gel loading dye (Sigma, 6x) was added to the samples prior to gel loading and electrophoresis. Isolated DNA and control standards (Sigma; 123bp and 1-10kbp ladders) were electrophoresed on 1.8 percent agarose gels (Gibco) in TBE buffer (45mM Tris, 45mM boric acid, 10mM EDTA, pH 7.8) for 6 hours at 50 volts. Banding patterns were visualized with a Foto/Eclipse UV transilluminator - video CCD camera, and recorded with the Foto/Archiver - Mitsubishi P90 thermal printer.

Flow Cytometric Evaluation of Caspase-3 Activation. Caspase activation is a hallmark of apoptotic processes (Chinnaiyan and Dixit, 1996; Cohen, 1998) and is reported to occur following staurosporine exposure in SH-SY5Y cells (Postmantur *et al.*, 1997).

Caspase-3 activation was measured by using phycoerythrin-conjugated anti-active caspase-3 antibodies (Pharmingen) and the cell culture methods described previously. In some experiments, cultures were pretreated with cyclosporin A (500nM in 0.01% methanol; 30 hr), Ac-DEVD-CHO (25µM in media; 8 hr), Ac-IETD-CHO (25µM in media; 8 hr), or PMSF (1mM in 1% ethanol; 8 hr)

prior to OP compound exposures. Following OP compound incubation, cells were harvested using 0.25% trypsin/EDTA (Sigma), and fixed, permeabilized, and washed using a Cytofix/Cytoperm™ Kit (Pharmingen). Anti-active caspase-3 antibodies (1:1000) were then added and allowed to incubate overnight at 4°C. A Coulter Epics XL-MCL flow cytometer was then utilized to examine 5,000 to 8,000 gated cell samples (excitation 488nm - emission 575nm). Treated cell fluorescence in the gated field (mean fluorescence intensity of the x-channel) was then compared to control fluorescence intensities to obtain percent of control. Representative flow cytometry histograms for phycoerythrin can be seen in Appendix D.

Transmission Electron Microscopy of Subcellular Structures. Observation of ultrastructural details has been utilized as a classic method for the determination of cytotoxic mechanisms (Kerr *et al.*, 1995). Ultrastructural changes induced by OP compound or solvent control treatments were observed via electron microscope as in Cece *et al.* (1995), Kerr *et al.* (1995), Tredici *et al.* (1995), Li *et al.* (1996), and Boix *et al.* (1997).

Cultures were treated with ethanol (solvent control; 0.1%, 1% v/v), PSP, or TOTP (100µM or 1mM) for 85, 255, 585, and 1290 minutes. Following incubation, cells were harvested using 0.25% trypsin/EDTA (Sigma) and fixed (4% paraformaldehyde, 2% glutaraldehyde, 0.1M sodium phosphate buffer, pH 7.3) at 4°C. Fixed cell pellets were then postfixed in 1% osmium tetroxide (Stevens Metallurgical, NY, NY) for 1 hour, suspended in 2% agar, and embedded in a Poly/Bed 812 resin (Polysciences, Warrington, PA). Thin sections (60-80µm) were then cut using a diamond knife and Reichert-Jung Ultracut E microtome, stained with lead citrate as in Reynolds (1963), and photographed using a JEOL JEM 100CX II transmission electron microscope. Micrograph magnifications ranged from 12,480 to 51,300x.

Statistics. Each quantitative experiment had between 3 and 16 normalized data points (percentages) for each time and OP concentration. Data were converted into the percent of control and then graphed as the mean ± the standard deviation. Statistical significance ($p<0.05$) was determined by utilizing PC-SAS software (version 6.1) to perform an analysis of variance (ANOVA) followed by Duncan's Multiple Range Test.

RESULTS

Fluorescence Microscopy of Nuclear Morphology (Apoptosis).

Fluorescence microscopy of nuclear morphology was used to visualize and count fragmentation patterns consistent with traditional apoptosis. Untreated and solvent (ethanol) treated control nuclei stained heterogeneously with Hoechst 33342. Few apoptotic nuclei were observed in solvent control (0 to 3.9%) or media-only (0.1 to 1.2%) treatments. Cytoplasmic staining was diffuse or non-existent in the majority of these cells (Fig. 7.1a). Staining of apoptotic nuclear buds and fragments were observed following most OP compound exposures (e.g. parathion, Fig. 7.1b) and were morphologically similar to positive control staurosporine treatments (500nM; 1440 min; Fig. 7.1d). PSP and TOTP (1mM) exposure also induced substantial nuclear condensation or shrinkage and a loss of internal nuclear structure with little subsequent fragmentation in many cells (Fig. 7.1c).

Nuclear apoptosis was statistically increased following parathion (1mM; > 960 min), TOTP (1mM; 1440, 2880 min), TPPi (1mM; 1440, 4320 min), staurosporine (500nM; >1440 min), and paraoxon (1mM; 4320 min) exposure ($p<0.05$, Fig. 7.2a, 7.2b). Significant time-dependent increases in nuclear apoptosis were also observed for parathion (100µM), TOTP (100µM), PSP (10µM and 100µM), paraoxon (100µM), and staurosporine (50nM) treatments ($p<0.05$, data not shown). No significant differences from solvent controls were observed following DFP treatments (data not shown).

Carbachol pretreatment (1mM; 30h) did not have a notable effect on apoptosis induced by 1mM parathion, TOTP, or paraoxon (Fig. 7.3a, 7.3b). Pretreatment with carbachol increased nuclear apoptosis following exposure to 1mM TPPi, however (Fig. 7.3b). Cyclosporin A pretreatment (500nM; 30h) decreased nuclear apoptosis following 1mM parathion or TOTP exposure (Fig. 7.3a) and increased it following exposure to paraoxon and TPPi (Fig. 7.3b). No significant differences were observed when ethanol, DFP, or PSP exposed cells were pretreated with carbachol or cyclosporin A (data not shown). Media-only and solvent control cells preincubated with carbachol or cyclosporin A induced between 0.3 and 4.7 percent apoptosis.

Agarose Gel Evaluation of DNA Fragmentation.

DNA gel electrophoresis was used to corroborate conclusions generated from Hoechst staining on the mode of cell death induced by exposure to OP compounds. DNA gel electrophoresis allowed any patterns in endonucleolytic activity to be visualized fluorescently.

Electrophoretic banding consistent with apoptosis was observed in OP compound treated cells still attached to the plate as well as those floating free in the media (Fig. 7.4). Banding was consistently more intense in unattached cell fractions, especially in paraoxon and parathion exposed cells. One millimolar paraoxon, parathion, TOTP, TPPi, and 500nM staurosporine exposures induced visible banding as early as 1440 minutes. Higher concentration PSP treatments (100µM or 1mM) induced the formation of random size oligonucleotides, however, which were visualized as electrophoretic lane

smears (data not shown). This pattern of DNA fragmentation conforms with those induced by necrotic processes.

Flow Cytometric Evaluation of Caspase-3 Activation.

Caspase-3 activation was assessed in order to complement the results of nuclear morphology studies. Statistically significant increases in caspase-3 activation (fluorescence brightness) were induced by paraoxon (1mM), parathion (100µM, 1mM), PSP (10µM, 100µM, 1mM), TOTP (100µM, 1mM), and TPPi (1mM) in a time-dependent manner (Fig. 7.5a, 7.5b).

Cyclosporin A pretreatment (500nM; 8 hr) significantly increased caspase-3 activation following early paraoxon (1mM; 1440 min) and parathion (1mM; 480, 1440 min) exposure when compared to cells treated with OP-alone (Fig. 7.6a). In contrast, pretreatment with cyclosporin A significantly decreased caspase-3 activation following 2880 minute exposure to 1mM paraoxon, parathion, and TPPi when compared to OP-alone treatments ($p<0.05$, Fig. 7.6a, 7.6b).

Pretreatment with caspase inhibitors (Ac-DEVD-CHO and Ac-IETD-CHO; 25µM; 8 hr) significantly decreased caspase-3 activation following 1mM parathion and PSP exposures when compared to inhibitor free exposures ($p<0.05$, Fig. 7.7a, 7.7b; 1440, 2880 min). Pretreatment with Ac-IETD-CHO significantly inhibited caspase-3 activation following 480 minute PSP (1mM) exposures as well, when compared to PSP-alone exposures ($p<0.05$). Pretreatment with Ac-DEVD-CHO or Ac-IETD-CHO resulted in no significant differences when compared to 1mM TOTP- or TPPi-alone exposures, however (Fig. 7.7c, 7.7d).

The caspase-8 inhibitor Ac-IETD-CHO significantly inhibited caspase-3 activity to a greater extent than the caspase-3 inhibitor Ac-DEVD-CHO when administered before PSP (1mM; 300, 1320, 1800 min) or parathion (1mM; 1440 min) ($p<0.05$). Caspase-3 inhibition via Ac-DEVD-CHO was not significantly different from Ac-IETD-CHO when administered before 1mM TOTP or TPPi, however, even though Ac-IETD-CHO pretreatment resulted in comparatively lower caspase-3 activation in 66% of the time.

Pretreatment with PMSF (1mM; 8 hr), a serine protease inhibitor, significantly reduced the amount of caspase-3 activation following incubations with parathion (1mM; 480 min), PSP (1mM; 1320, 1800 min), and TOTP (1mM; 2880 min) when compared to OP-alone treatments ($p<0.05$, Fig. 7.7a, 7.7b, 7.7c). PMSF also had significantly greater inhibitory effect than Ac-DEVD-CHO following parathion (1mM; 480 min), PSP (1mM; 300, 1320, 1800 min), or TOTP (1mM; 480, 2880 min) or Ac-IETD-CHO following parathion (1mM; 2880 min), PSP (1mM; 1320, 1800 min), or TOTP (1mM; 2880 min) exposures ($p<0.05$).

Transmission Electron Microscopy of Subcellular Structures.

Transmission electron microscopy (TEM) of ultrastructural components was used to evaluate changes that occur in SH-SY5Y cells exposed to cytotoxic concentrations of OP compounds. Control (1% ETOH v/v; 1290 min) TEMs displayed cells with well defined nuclei, nucleoli, mitochondria, and multiple neurites (Fig. 7.8a). Control cells also had compact nuclear membranes, glycogen granules, and little evidence of cytoplasmic vacoulation or lipid droplet formation.

Treated cells (1mM TOTP or PSP; 1290 min) displayed degenerative morphologies (Fig. 7.8b, 7.8c). Degenerative morphologies were typified by swollen or ruptured mitochondria, a reduction in neurite size and length, membrane-bound vesicle or lipid droplet formation, and plasma membrane degradation. In most cases, inner and outer leaflet separation in intact nuclear membranes also appeared to be greater than controls in these cultures. Membrane-bound vesicle formation appeared early (<85 min) following exposure to OP compounds. Formation was also prior to the onset of mitochondrial degeneration (PSP and TOTP) or neurite reduction (TOTP), and developed in a dose- and time-dependent fashion.

DISCUSSION

This study evaluated the mechanisms involved in OP compound-induced cytotoxic reactions. Five OP compounds; paraoxon (1mM), parathion (1mM), PSP (10μM and 100μM), TOTP (100μM and 1mM), and TPPi (1mM) were shown to induce similar forms of time-dependent cell death in SH-SY5Y human neuroblastoma cell lines. Cytotoxicity following exposure to these compounds was characterized by nuclear condensation, budding and fragmentation, caspase-3 activation, and electrophoretic ladder-like oligonucleotide patterns. These observations in combination with caspase-3 inhibition via Ac-DEVD-CHO and Ac-IETD-CHO suggested that this form of cell death was traditional apoptosis as described by Kerr *et al.* (1972).

Higher concentrations (1mM) of two compounds, PSP and TOTP, also induced an early form of death in many cells that was not traditionally apoptotic. The effects of these concentrations differed from others in that they induced random DNA fragmentation and nuclear shrinkage without subsequent apoptotic budding.

Electrophoretic data and ultrastructural observations such as profound subcellular degeneration suggested that exposure to 1mM concentrations of PSP and TOTP modulated a necrotic reaction. Similar patterns of high concentration evoked necrosis and lower concentration induced apoptosis have been described for many toxicants including N-methyl-D-aspartate or peroxynitrite (Bonfoco *et al.*, 1995), antimycin A (Itano and Nomura, 1995), tributlytin and triphenyltin (Stridh *et al.*, 1999), and sulfur mustard (Dabrowska *et al.*, 1996).

High concentration PSP and TOTP-induced caspase-3 activation and inhibition data suggested that apoptosis also contributed to the cytotoxic reaction. Caspase-3 (Yama / CPP32 / apopain) activation from a 32-kDa precursor protein into mature 17k-Da and 12-kDa subunits (Han *et al.*, 1997) has been demonstrated to occur following many apoptotic stimuli (Keane *et al.*, 1997; McGinnis *et al.*, 1998; Kobayashi *et al.*, 1999) in an ATP dependent manner (Eguchi *et al.*, 1997). Activation leads to the degradation of numerous substrates including; spectrin (Nath *et al.*, 1996; Wang *et al.*, 1998a), actin (Song *et al.*, 1997), α-fodrin and poly(ADP-ribose) polymerase (Cryns *et al.*, 1996), calpastatin (Wang *et al.*, 1998b), calcium/calmodulin-dependent protein kinases (McGinnis *et al.*, 1998), and other signaling proteins (Widmann *et al.*, 1998).

The possibility existed that caspase-3 proteases were nonspecifically activated following exposure to 1mM PSP or TOTP. This was unlikely, however, because caspase-3 activation occurred in a coordinated fashion prior to increases in flow cytometrically measured DNA fragmentation, in some circumstances by as much as 480 min (Carlson and Ehrich, 1999). Similar patterns of caspase-3 activation occurring prior to DNA fragmentation have been described (Chinnaiyan and Dixit, 1996; Keane *et al.*, 1997).

Because 1mM PSP and TOTP exposures induced caspase-3 activation, random DNA fragmentation, and necrotic morphological changes, two possibilities for the mode of cell death could be suggested: a stalled primary apoptosis followed by secondary necrosis, or an intermediate form of

apoptosis. The former has been described (Papassotiropoulos *et al.*, 1996) and termed apoptotic necrosis (Majno and Joris, 1995) while the latter has been labeled as Type-II apoptosis (Boix *et al.*, 1997).

The ability to induce these forms of cell death may be related to cellular ATP content. Leist *et al.* (1997) and Eguchi *et al.* (1997) reported that apoptotic cell death could be switched to necrosis following ATP depletion. OP compound-induced decreases in ATP content, ADP phosphorylation, or phosphofructokinase activity have been described in *in vitro* (Knoth-Anderson *et al.*, 1992; Holmuhamedov *et al.*, 1996) and *in vivo* studies (Hernandez *et al.*, 1989). Depletion of ATP by excessive stimulation of muscle fibers has also been hypothesized to result in OP compound-induced muscle necrosis (Dettbarn, 1984).

Interestingly, *in vitro* studies have suggested that mitochondrial transmembrane potential ($\Delta\Psi_m$) remains relatively intact initially following OP compound exposure (Carlson and Ehrich, 1999). A direct correlation between $\Delta\Psi_m$ and ATP production has been drawn by many authors (Petit *et al.*, 1997; Lemasters *et al.*, 1998) and infers that OP compound-exposed mitochondria are still capable of generating ATP. This fact, in combination with evidence of ATP-dependent caspase-3 activation after nuclear shrinkage (Fig. 7.2, 7.5-7.7; Eguchi *et al.*, 1997), argued against ATP depletion as an influence in high concentration PSP- or TOTP-induced intermediate forms of cell death.

In this study, carbachol pretreatment (1mM, 30h) did not decrease nuclear apoptosis as expected. Carbachol, a muscarinic receptor agonist, has been reported to increase $\Delta\Psi_m$ (Carlson and Ehrich, 1999), plasma membrane potential (Ueda and Okada, 1989), c-fos and c-myc (Yagel and Costa, 1999), and Bcl-2 levels (Itano *et al.*, 1996), all which can be construed as potentially protective mechanisms. Numerous studies have documented carbachol-induced protective effects against excitotoxic stimuli (Koh *et al.*, 1991), co-culture induced apoptosis (Rinner *et al.*, 1994), nondepolarizing conditions and M3 muscarinic receptor activation (Yan *et al.*, 1995), or low K^+ induced cytotoxicity (Castoldi *et al.*, 1998). In this study, however, carbachol did not protect cells exposed to OP compounds. Our studies are more related to others that observed carbachol-induced apoptosis in Jurkat T cells (Izquierdo *et al.*, 1996) and rat thymocytes (Yamada *et al.*, 1997). Cytoprotective and cytodestructive effects have both been correlated to muscarinic receptor activation. Overall, it is not clear why carbachol did not protect SH-SY5Y cells from apoptosis following exposure to OP compounds. Differences in species or cell type may have determined the nature of carbachol-induced effects. This postulate deserves more investigation.

Prophylactic administration of cyclosporin A (500nM, 30h) decreased nuclear apoptosis and caspase-3 activation following exposure to some, but not all, OP compounds. Administration of cyclosporin A to cell cultures has been shown to increase cytoprotective effects (Huang *et al.*, 1997; Seaton *et al.*, 1998; Sugano *et al.*, 1999). These effects are modulated through the inhibition of mitochondrial permeability transition pores (MPT; Petronilli *et al.*, 1993; Bernardi, 1996), the opening of which can lead to mitochondrial depolarization and dysfunction. Cytoprotective effects of cyclosporin A have been shown to occur prior to the activation of caspase-3 (Bradham *et al.*, 1998; Hortelano *et al.*, 1999; Okamoto *et al.*, 1999) and hence nuclear fragmentation. Therefore, inhibition of detrimental

MPT opening by cyclosporin A may account for the reductions in apoptosis and caspase-3 activation observed in this study.

The synthetic tetrapeptide caspase inhibitors Ac-DEVD-CHO and Ac-IETD-CHO decreased caspase activation following PSP and parathion exposures. Enzymatic assays have shown that these compounds greatly inhibit caspase-3 and caspase-8, respectively (Garcia-Calvo *et al.*, 1998). Caspase-8 (FLICE/MACH) activation occurs primarily following TNF- or Fas-ligand (APO-1, CD95) receptor stimulation (Morishima, 1999). Following activation, caspase-8 proteolytically activates effector capases 3, 6, or 7 through mitochondrially independent or dependent (damage) pathways (Morishima, 1999).

Inhibition of caspase-3 activation by Ac-DEVD-CHO implied that caspase-3 was a proteolytic effector in OP compound-induced apoptosis. Significantly greater inhibition of caspase-3 activation by Ac-IETD-CHO when compared to Ac-DEVD-CHO suggested that TNF or Fas receptor stimulation may have also been involved in OP compound-induced apoptosis. OP compound-induced activation of apoptosis through TNF or Fas-receptors may also explain why DFP exposures are not cytotoxic. Sarin *et al.* (1993) and Higuchi *et al.* (1995) observed that DFP blocked apoptotic nuclear morphologies and DNA fragmentation induced by T cell receptor complexes (TNF / Fas-ligand). Fas receptors have been documented in neuroblastoma cell lines similar to the SH-SY5Y cells used for the present experiments, but their role in cell death for these cultures is questionable (Barthlen *et al.*, 1999).

Pretreatment with PMSF significantly decreased OP compound-induced caspase-3 activation to a greater extent than Ac-DEVD-CHO or Ac-IETD-CHO following parathion, PSP, or TOTP exposures. PMSF, a serine protease inhibitor, has been shown to inhibit apoptosis following T cell receptor activation (Sarin *et al.*, 1993). Prophylactic administration of PMSF has also been reported to decrease spinal cord and peripheral nerve lesions following TOTP or DFP exposure (Carrington and Abou-Donia, 1983; Carrington *et al.*, 1988). It has not been determined whether the present *in vitro* observations correlate with *in vivo* effects reported in the literature. Nevertheless, at the very least, serine proteases play an important role in OP compound-induced apoptosis.

In the current study, the relative capability of an OP compound to induce apoptosis was inversely related to its capacity for AChE or NTE inhibition. Parathion induced apoptosis to the greatest extent and was followed by TOTP > TPPi > paraoxon > PSP > DFP (Fig. 7.2a, 7.2b, 7.5a, 7.5b). Parathion, TOTP, and PSP have been shown to have a limited capacity to inhibit SH-SY5Y AChE when compared to paraoxon and DFP (Veronesi *et al.*, 1997; Ehrich and Correll, 1998; Ehrich *et al.*, 1994, 1997). Similarly, parathion, TOTP, and paraoxon have been reported to have little ability to inhibit SH-SY5Y neurotoxic esterase (neuropathy target esterase, NTE) when compared to DFP, PSP, and TPPi (Ehrich *et al.*, 1994). This inverse relationship to esterases is not unexpected. Similar findings have been documented with AChE inhibition and cell death (Soreq *et al.*, 1994) or $\Delta\Psi_m$ (Carlson and Ehrich, 1999).

It was unlikely that conversion of protoxicants such as parathion and TOTP into active AChE or NTE inhibitors (paraoxon and tri-cresyl phosphate, respectively) were responsible for cytotoxicity

observed in this study. SH-SY5Y cells have been shown to have a limited metabolic capability for converting OP compounds (Ehrich *et al.*, 1994, Barber *et al.*, 1999). In addition, the concentrations used to induce cytotoxicity in this study were much higher than those found to inhibit SH-SY5Y AChE or NTE (Veronesi *et al.*, 1997; Ehrich and Correll, 1998; Ehrich *et al.*, 1994, 1997).

In this study, we observed significant OP compound-induced increases in caspase-3 activation followed by increased nuclear fragmentation characteristic of traditional apoptosis. High concentrations of PSP and TOTP (1mM) also induced caspase-3 activation and nuclear condensation with little nuclear fragmentation in many cells, however, which was more indicative of apoptotic necrosis or Type-II apoptosis. In addition, pretreatment with carbachol, cyclosporin A, protease inhibitors (Ac-DEVD-CHO, Ac-IETD-CHO), and PMSF altered OP compound-induced caspase-3 activation and nuclear fragmentation. This suggested that multifunctional pathways such as muscarinic receptor activation or an increase in Bcl-2, mitochondrial permeability transition pore closure, receptor-mediated caspase activation, or serine protease activation were involved in OP compound-induced cytotoxicity.

ACKNOWLEDGMENTS

We wish to thank Joan Kalnitsky for flow cytometric assistance. This work was supported in part by US EPA grant R825356, the Virginia-Maryland Regional College of Veterinary Medicine, and a Society of Toxicology - Novartis predoctoral fellowship.

REFERENCES

Abou-Donia, M.B. (1995). Organophosphorus pesticides. In *Handbook of Toxicology* (L.W. Chang and R.S. Dyer, Ed.), pp. 419-473. Marcel Dekker, Inc., New York, NY.

Abou-Donia, M.B. and Lapadulla, D.M. (1990). Mechanisms of organophosphorus ester-induced delayed neurotoxicity: Type I and Type II. *Annu. Rev. Pharmacol. Toxicol.* 30, 405-440.

Akbarsha, M.A. and Sivasamy, P. (1998). Male reproductive toxicity of phosphamidon: Histopathological changes in epididymis. *Ind. J. Exp. Biol.* 36, 34-38.

Aspelin, A.L. (1997). Pesticides industry sales and usage: 1994 and 1995 market estimates. *Biological and Economic Analysis Division, Office of Pesticide Programs, Office of Prevention, Pesticides and Toxic Substances.* U.S. Environmental Protection Agency. Washington D.C.

Bagchi, D., Bagchi, M., Hassoun, E.A., and Stohs, S.J. (1995). *In vitro* and *in vivo* generation of reactive oxygen species, DNA damage, and lactate dehydrogenase leakage by select pesticides. *Toxicology* 104, 129-140.

Barber, D.S., Correll, L., and Ehrich, M. (1999). Comparison of two *in vitro* activation systems for protoxicant organophosphorus esterase inhibitors. *Toxicol. Sci.* 47, 16-23.

Baron, R.L. (1981). Delayed neurotoxicity and other consequences of organophosphate esters. *Ann. Rev. Entomol.* 26, 29-48.

Barthlen, W., Schafer, J., Girgert, R., Schuster, M., and Schweizer, P. (1999). Apoptosis of cultured neuroblastoma cells is induced by ceramide and not by ligation of the Fas/Apo-1/CD95 receptor. *Chemotherapy* 45, 258-267.

Baze, W.B. 1993. Soman-induced morphological changes: An overview in the non-human primate. *J. Appl. Toxicol.* 13, 173-177.

Bernardi, P. (1996). The permeability transition pore. Control points of a cyclosporin A-sensitive mitochondrial channel involved in cell death. *Biochim. Biophys. Acta* 1275, 5-9.

Boix, J., Llecha, N., Yuste, V.-J., and Comella, J.X. (1997). Characterization of the cell death process induced by staurosporine in human neuroblastoma cell lines. *Neuropharmacology* 36, 811-821.

Bonfoco, E., Krainc, D., Ankarcrona, M., Nicotera, P., and Lipton, S.A. (1995). Apoptosis and necrosis: Two distinct events induced, respectively, by mild and intense insults with N-methyl-D-aspartate or nitric oxide/superoxide in cortical cell cultures. *Proc. Natl. Acad. Sci. USA* 92, 7162-7166.

Bradham, C.A., Qian, T., Streetz, K., Trautwein, C., Brenner, D.A., and LeMasters, J.J. (1998). The mitochondrial permeability transition is required for tumor necrosis factor alpha-mediated apoptosis and cytochrome c release. *Mol. Cell Biol.* 18, 6353-6364.

Carlson, K. and Ehrich, M. (1999). Organophosphorus compound-induced modification of SH-SY5Y human neuroblastoma mitochondrial transmembrane potential. *Toxicol. Appl. Pharmacol.* 160, 33-42.

Carrington, C.D. and Abou-Donia, M.B. (1983). The time course of protection from delayed neurotoxicity induced by tri-o-cresyl phosphate and O, O-diisopropyl phosphorofluoridate by phenylmethylsulfonyl fluoride in chickens. *Toxicol. Lett.* 18, 251-256.

Carrington, C.D., Brown, H.R., and Abou-Donia, M.B. (1988). Histopathological assessment of triphenyl phosphite neurotoxicity in the hen. *Neurotoxicology* 2, 223-234.

Cavanagh, J.B. (1964). Peripheral nerve changes in ortho-cresyl phosphate poisoning in the cat. *J. Pathol. Bacteriol.* 87, 365-383.

Cece, R., Barajon, I., and Tredici, G. (1995). Cisplatin induces apoptosis in SH-SY5Y human neuroblastoma cell line. *Anticancer Res.* 15, 777-782.

Chinnaiyan, A.M. and Dixit, V.M. (1996). The cell-death machine. *Curr. Biol.* 6, 555-562.

Cobb, J.P., Hotchkiss, R.S., Karl, I.E., and Buchman, T.G. (1996). Mechanisms of cell injury and death. *Br. J. Anaesth.* 77, 3-10.

Cohen, G.M. (1998). Activation of caspases in apoptosis. I*n Cellular and Molecular Pathways in Apoptosis and Necrosis: Continuing Education Course PM* (8). pp. 4-19. Society of Toxicology 37th Annual Meeting, Seattle, WA.

Cryns, V.L., Bergeron, L., Zhu, H., Li, H., and Yuan, J. (1996). Specific cleavage of α-fodrin during fas- and tumor necrosis factor-induced apoptosis is mediated by an interleukin-1β-converting enzyme/ced-3 protease distinct from poly(ADP-ribose) polymerase protease. *J. Biol. Chem.* 271, 31277-31282.

Dabrowska, M.I., Becks, L.L., Lelli Jr., J.L., Levee, M.G., and Hinshaw, D.B. (1996). Sulfur mustard induces apoptosis and necrosis in endothelial cells. *Toxicol. Appl. Pharmacol.* 141, 568-583.

Dettbarn, W.-D. (1984). Pesticide induced muscle necrosis: Mechanisms and prevention. *Fundam. Appl. Toxicol.* 4, S18-S26.

Dive, C., Gregory, C.D., Phipps, D.J., Evans, D.L., Milner, A.E., and Wyllie, A.H. (1992). Analysis and discrimination of necrosis and apoptosis (programmed cell death) by multiparameter flow cytometry. *Biochim. Biophys. Acta* 1133, 275-285.

Duke, R.C., Ojcius, D.M., and Young, J.D.-E. (1996). Cell suicide in health and disease. *Sci. Am.* Dec., 80-87.

Eastman, A. (1995). Assays for DNA fragmentation, endonucleases, and intracellular pH and Ca^{2+} associated with apoptosis. In *Methods in Cell Biology* (46). pp. 41-55. Academic Press, Inc., San Diego, CA.

Eguchi, Y., Shimizu, S., and Tsujimoto, Y. (1997). Intracellular ATP levels determine dell death fate by apoptosis or necrosis. *Cancer Res.* 57, 1835-1840.

Ehrich, M., Correll, L., and Veronesi, B. (1994). Neuropathy target esterase inhibition by organophosphorus esters in human neuroblastoma cells. *Neurotoxicology* 15, 309-314.

Ehrich, M., Correll, L., Carlson, K., Wilcke, J., and Veronesi, B. (1995). Examination of culture conditions on esterase activities in human and mouse neuroblastoma cells. *In Vitro Toxicol.* 8, 199-207.

Ehrich, M., Correll, L., and Veronesi, B. (1997). Acetylcholinesterase and neuropathy target esterase inhibitions in neuroblastoma cells to distinguish organophosphorus compounds causing acute and delayed neurotoxicity. *Fundam. Appl. Toxicol.* 38, 1-9.

Ehrich, M. and Correll, L. (1998). Inhibition of carboxylesterases in SH-SY5Y human and NB41A3 mouse neuroblastoma cells by organophosphorus esters. *J. Toxicol. Environ. Health*, Part A 53, 101-115.

Fawthrop, D.J., Boobis, A.R., and Davies, D.S. (1991). Mechanisms of cell death. *Arch. Toxicol.* 65, 437-444.

Flaskos, J., McLean, W.G., and Hargreaves, A.J. (1994). The toxicity of organophosphate compounds towards cultured PC12 cells. *Toxicol. Lett.* 70, 71-76.

Fraker, P.J., King, L.E., Lill-Elghanian, D., and Telford, W.G. (1995). Quantification of apoptotic events in pure and heterogeneous populations of cells using the flow cytometer. In *Methods in Cell Biology* (46). pp. 57-76. Academic Press, Inc., San Diego, CA.

Funk, K.A., Henderson, J.D., Liu, C.-H., Higgins, R.J., and Wilson, B.W. (1994). Neuropathology of organophosphate-induced delayed neuropathy (OPIDN) in young chicks. *Arch. Toxicol.* 68, 308-316.

Garcia-Calvo, M., Peterson, E.P., Leiting, B., Ruel, R., Nicholson, D.W., and Thornberry, N.A. (1998). Inhibition of human caspases by peptide-based and macromolecular inhibitors. *J. Biol. Chem.* 273, 32608-32613.

Hamm, J.T., Wilson, B.W., and Hinton, D.E. (1998). Organophosphate-induced acetylcholinesterase inhibition and embryonic retinal cell necrosis *in vivo* in the teleost (Oryzias Latipes). *Neurotoxicology* 19, 853-870.

Han, Z., Hendrickson, E.A., Bremner, T.A., and Wyche, J.H. (1997). A sequential two-step mechanism for the production of the mature p17:p12 form of caspase-3 in vitro. *J. Biol. Chem.* 272, 13432-13436.

Harvey, M.J. and Sharma, R.P. (1980). Organophosphate cytotoxicity: The effects on protein metabolism in cultured neuroblastoma cells. *J. Environ. Pathol. Toxicol.* 3, 423-436.

Hernandez, A.F., Pla, A., and Villanueva, E. (1989). Decreased phosphofructokinase activity during the development of triorthocresyl-phosphate-induced delayed neuropathy. *Toxicol. Lett.* 49, 35-40.

Higuchi, M., Singh, S., Chan, H., and Aggarwal, B.B. (1995). Protease inhibitors differentially regulate tumor necrosis factor-induced apoptosis, nuclear factor-κB activation, cytotoxicity, and differentiation. *Blood* 86, 2248-2256.

Holmuhamedov, E.L., Kholmoukhamedova, G.L., and Baimuradov, T.B. (1996). Non-cholinergic toxicity of organophosphates in mammals: Interaction of ethaphos with mitochondrial functions. *J. Appl. Toxicol.* 16, 475-481.

Hortelano, S., Lopez-Collazo, E., and Bosca, L. (1999). Protective effect of cyclosporin A and FK506 from nitric oxide-dependent apoptosis in activated macrophages. *Br. J. Pharmacol.* 126, 1139-1146.

Huang, Q.Q., Fang, M., Zhang, H.Q., and Xue, S.B. (1997). Cyclosporine inhibited calcium-mediated apoptosis of HL-60 cells. *Chung Kuo Yao Li Hsueh Pao* 18, 262-266.

Itano, Y. and Nomura, Y. (1995). 1-Methyl-4-phenyl-pyridinium ion (MPP^+) causes DNA fragmentation and increases BCL-2 expression in human neuroblastoma, SH-SY5Y cells, through different mechanisms. *Brain Res.* 704, 240-245.

Itano, Y., Ito, A., Uehara, T., and Nomura, Y. (1996). Regulation of Bcl-2 protein expression in human neuroblastoma SH-SY5Y cells: Positive and negative effects of protein kinases C and A, respectively. *J. Neurochem.* 67, 131-137.

Izquierdo, M., Ruiz-Ruiz, M.C., and Lopez-Rivas, A. (1996). Stimulation of phosphatidylinositol turnover is a key event for Fas-dependent, activation-induced apoptosis in human T lymphocytes. *J. Immunol.* 157, 21-28.

Katoh, K., Konno, N., Yamauchi, T., and Fukushima, M. (1990). Effects of age on susceptibility of chickens to delayed neurotoxicity due to triphenyl phosphite. *Pharmacol. Toxicol.* 66, 387-392.

Keane, R.W., Srinivasan, A., Foster, L.M., Testa, M.-P., Örd, T., Nonner, D., Wang, H.-G., Reed, J.C., Bredesen, D.E., and Kayalar, C. (1997). Activation of CPP32 during apoptosis of neurons and astrocytes. *J. Neurosci. Res.* 48, 168-180.

Kerr, J.F.R., Wyllie, A.H., and Currie, A.R. (1972). Apoptosis: A basic biological phenomenon with wide-ranging implications in tissue kinetics. *Br. J. Cancer* 26, 239-257.

Kerr, J.F.R., Gobé, G.C., Winterford, C.M., and Harmon, B.V. (1995). Anatomical methods in cell death. In *Methods in Cell Biology* (46). pp. 1-27. Academic Press, Inc., San Diego, CA.

Knoth-Anderson, J., Veronesi, B., Jones, K., Lapadula, D.M., and Abou-Donia, M.B. (1992). Triphenyl phosphite-induced ultrastructural changes in bovine adrenomedullary chromaffin cells. *Toxicol. Appl. Pharmacol.* 112, 110-119.

Kobayashi, T., Okamoto, K., Kobata, T., Hasunuma, T., Sumida, T., and Nishioka, K. (1999). Tumor necrosis factor alpha regulation of the Fas-mediated apoptosis-signaling pathway in synovial cells. *Arthritis Rheum.* 42, 519-526.

Koh, J.Y., Palmer, E., and Cotman, C.W. (1991). Activation of the metabotropic glutamate receptor attenuates N-methyl-D-aspartate neurotoxicity in cortical cultures. *Proc. Natl. Acad. Sci. USA* 88, 9431-9435.

Leist, M., Single, B., Castoldi, A.F., Kühnle, S., and Nicotera, P. (1997). Intracellular adenosine triphosphate (ATP) concentration: A switch in the decision between apoptosis and necrosis. *J. Exp. Med.* 185, 1481-1486.

LeMasters, J.J., Nieminen, A.-L., Qian, T., Trost, L.C., Elmore, S.P., Nishimura, Y., Crowe, R.A., Cascio, W.E., Bradham, C.A., Brenner, D.A., and Herman, B. (1998). The mitochondrial permeability transition in cell death: A common mechanism in necrosis, apoptosis and autophagy. *Biochim. Biophys. Acta* 1366, 177-196.

Levin, S. (1998). Apoptosis, necrosis, or oncosis: What is your diagnosis? A report from the cell death nomenclature committee of the Society of Toxicologic Pathologists. *Toxicol. Sci.* 41, 155-156.

Li, H., Bergeron, L., Cryns, V., Pasternack, M.S., Zhu, H., Shi, L., Greenberg, A., and Yuan, J. (1997). Activation of caspase-2 in apoptosis. *J. Biol. Chem.* 272, 21010-21017.

Li, Y.-P., Bushnell, A.F., Lee, C.-M., Perlmutter, L.S., and Wong, S.K.-F. (1996). β-amyloid induces apoptosis in human-derived neurotypic SH-SY5Y cells. *Brain Res.* 738, 196-204.

Majno, G. and Joris, I. (1995). Apoptosis, oncosis, and necrosis. *Am. J. Pathol.* 146, 3-15.

Marinovich, M., Ghilardi, F., and Galli, C.L. (1996). Effect of pesticide mixtures on in vitro nervous cells: Comparison with single pesticides. *Toxicology* 108, 201-206.

Martin, S.J., Green, D.R., and Cotter, T.G. (1994). Dicing with death: dissecting the components of the apoptosis machinery. *TIBS* 19, 26-30.

McConkey, D.J. (1998). Intracellular ATP: A switch between apoptosis and necrosis. I*n Cellular and Molecular Pathways in Apoptosis and Necrosis: Continuing Education Course PM* (8). pp. 42-56. Society of Toxicology 37th Annual Meeting, Seattle, WA.

McGahon, A.J., Martin, S.J., Bissonnette, R.P., Mahboubi, A., Shi, Y., Mogil, R.J., Nishioka, W.K., and Green, D.R. (1995). The end of the (cell) line: Methods for the study of apoptosis *in vitro*. In *Methods in Cell Biology* (46). pp. 153-185. Academic Press, Inc., San Diego, CA.

McGinnis, K.M., Whitton, M.M., Gnegy, M.E., and Wang, K.K.W. (1998). Calcium/calmodulin-dependent protein kinase IV is cleaved by caspase-3 and calpain in SH-SY5Y human neuroblastoma cells undergoing apoptosis. *J. Biol. Chem.* 273, 19993-20000.

McLeod Jr., C.G. (1985). Pathology of nerve agents: Perspectives on medical management. *Fundam. Appl. Toxicol.* 5, S10-S16.

Mochida, K., Gomyoda, M., Fujita, T., and Yamagata, K. (1988). Tricresyl phosphate and triphenyl phosphate are toxic to cultured human, monkey and dog cells. *Zbl. Bakt. Hyg. B.* 185, 427-429.

Morishima, N. (1999). Changes in nuclear morphology during apoptosis correlate with vimentin cleavage by different caspases located either upstream or downstream of Bcl-2 action. *Genes Cells* 4, 401-414.

Mortensen, A. and Ladefoged, O. (1992). Delayed neurotoxicity of trixylenyl phosphate and a trialkyl/aryl phosphate mixture, and the modulating effect of atropine on tri-o-tolyl phosphate-induced neurotoxicity. *Neurotoxicology* 13, 347-354.

Mukasa, T., Urase, K., Momoi, M.Y., Kimura, I., and Momoi, T. (1997). Specific expression of CPP32 in sensory neurons of mouse embryos and activation of CPP32 in the apoptosis induced by a withdrawal of NGF. *Biochem. Biophys. Res. Commun.* 231, 770-774.

Nakagawa-Yagi, Y. (1994). Induction of apoptotic cell death in differentiating neuroblastoma SH-SY5Y cells by colchicine. *Biochem. Biophys. Res. Commun.* 199, 807-817.

Nath, R., Raser, K.J., Stafford, D., Hajimohammadreza, I., Posner, A., Allen, H., Talanian, R.V., Yuen, P., Gilbertson, R.B., and Wang, K.K.W. (1996). Non-erythroid α-spectrin breakdown by calpain and interleukin 1β-converting-enzyme-like protease(s) in apoptotic cells: contributory roles of both protease families in neuronal apoptosis. *Biochem. J.* 319, 683-690.

Nostrandt, A.C., Rowles, T.K., and Ehrich, M. (1992). Cytotoxic effects of organophosphorus esters and other neurotoxic chemicals on cultured cells. *In Vitro Toxicol.* 5, 127-136.

Okamoto, T., Hitomi, Y., and Hara, A. (1999). The protective effect of cyclosporine A on anti-Fas antibody-induced hepatitis in mice. *Jpn. J. Pharmacol.* 79, 485-488.

Papassotiropoulos, A., Ludwig, M., Naib-Majani, W., and Rao, G.S. (1996). Induction of apoptosis and secondary necrosis in rat dorsal root ganglion cell cultures by oxidized low density lipoprotein. *Neurosci. Lett.* 209, 33-36.

Perez-Polo, J.R., Werrbach-Perez, K., and Tiffany-Castiglioni, E. (1979). A human clonal cell line model of differentiating neurons. *Dev. Biol.* 71, 341-355.

Petit, P.X., Zamzami, N., Vayssiere, J.-L., Mignotte, B., Kroemer, G., and Castedo, M. (1997). Implication of mitochondria in apoptosis. *Mol. Cell Biochem.* 174, 185-188.

Petronilli, V., Cola, C., Massari, S., Colonna, R., and Bernardi, P. (1993). Physiological effectors modify voltage sensing by the cyclosporin A-sensitive permeability transition pore of mitochondria. *J. Biol. Chem.* 268, 21939-21945.

Pope, C.N. (1999). Organophosphorus pesticides: Do they all have the same mechanism of toxicity? *J. Toxicol. Environ. Health*, Part B, 2, 161-181.

Postmantur, R., McGinnis, K., Nadimpalli, R., Gilbertsen, R.B., and Wang, K.K.W. (1997). Characterization of CPP32-like protease activity following apoptotic challenge in SH-SY5Y neuroblastoma cells. *J. Neurochem.* 68, 2328-2337.

Prince, J.A. and Oreland, L. (1997). Staurosporine differentiated human SH-SY5Y neuroblastoma cultures exhibit transient apoptosis and trophic factor independence. *Brain Res. Bull.* 43, 515-523.

Reynolds, E.S. (1963). The use of lead citrate at high pH as an electron opaque stain in electron microscopy. *J. Cell Biol.* 17, 208-212.

Rinner, I., Kukulansky, T., Felsner, P., Skreiner, E., Globerson, A., Kasai, M., Hirokawa, K., Korsatko, W., and Schauenstein, K. (1994). *Biochem. Biophys. Res. Commun.* 203, 1057-1062.

Sarin, A., Adams, D.H., and Henkart, P.A. (1993). Protease inhibitors selectively block T cell receptor-triggered programmed cell death in a murine T cell hybridoma and activated peripheral T cells. *J. Exp. Med.* 178, 1693-1700.

Seaton, T.A., Cooper, J.M., and Schapira, A.H.V. (1998). Cyclosporin inhibition of apoptosis induced by mitochondrial complex I toxins. *Brain Res.* 809, 12-17.

Singer, A.W., Jaax, N.K., Graham, J.S., and McLeod, C.G. (1987). Cardiomyopathy in soman and sarin intoxicated rats. *Toxicol. Lett.* 36, 243-249.

Song, Q., Wei, T., Lees-Miller, S., Alnemri, E., Watters, D., and Lavin, M.F. (1997). Resistance of actin to cleavage during apoptosis. *Proc. Natl. Acad. Sci. USA* 94, 157-162.

Soreq, H., Patinkin, D., Lev-Lehman, E., Grifman, M., Ginzberg, D., Eckstein, F., and Zakut, H. (1994). Antisense oligonucleotide inhibition of acetylcholinesterase gene expression induces progenitor cell expansion and suppresses hematopoietic apoptosis ex vivo. *Proc. Natl. Acad. Sci. USA* 91, 7907-7911.

Stridh, H., Orrenius, S., and Hampton, M.B. (1999). Caspase involvement in the induction of apoptosis by the environmental toxicants tributyltin and triphenyltin. *Toxicol. Appl. Pharmacol*. 156, 141-146.

Sugano, N., Ito, K., and Murai, S. (1999). Cyclosporin A inhibits H_2O_2-induced apoptosis of human fibroblasts. *FEBS Lett.* 447, 274-276.

Tann, X., Martin, S.J., Green, D.R., and Wang, J.Y.J. (1997). Degradation of retinoblastoma protein in tumor necrosis factor- and CD95-induced cell death. *J. Biol. Chem.* 272, 9613-9616.

Thompson, C.B. (1995). Apoptosis in the pathogenesis and treatment of disease. *Science* 267, 1456-1462.

Tredici, G., Petruccioli, M.G., Tarelli, L.T., Cece, R., and Pizzini, G. (1995). Ultrastructural and confocal laser scanning microscopical aspects in cultured human neuroblastoma SH-SY5Y cells. *It. J. Anat. Embryol.* 100, 47-53.

Tuler, S.M. and Bowen, J.M. (1989). Toxic effect of organophosphates on nerve cell growth and ultrastructure in culture. *J. Toxicol. Environ. Health* 27, 209-223.

Ueda, S. and Okada, Y. (1989). Acid secretagogues induce Ca^{2+} mobilization coupled to K^+ conductance activation in rat parietal cells in tissue culture. *Biochim. Biophys. Acta* 1012, 254-260.

Verhaegen, S. (1998). Microscopical study of cell death via apoptosis. *Amer. Mic. Anal.* Jan., 19-21.

Veronesi, B. and Pope, C. (1990). The neurotoxicity of parathion-induced acetylcholinesterase inhibition in neonatal rats. *Neurotoxicology* 11, 609-626.

Veronesi, B. and Ehrich, M. (1993a). Using neuroblastoma cell lines to examine organophosphate neurotoxicity. *In Vitro Toxicol*. 6, 57-65.

Veronesi, B. and Ehrich, M. (1993b). Differential cytotoxic sensitivity in mouse and human cell lines exposed to organophosphate insecticides. *Toxicol. Appl. Pharmacol.* 120, 240-246.

Veronesi, B., Ehrich, M., Blusztajn, J.K., Oortgiesen, M., and Durham, H. (1997). Cell culture models of interspecies selectivity to organophosphorus insecticides. *Neurotoxicology* 18, 283-298.

Wang, K.K.W., Postmantur, R., Nath, R., McGinnis, K., Whitton, M., Talanian, R.V., Glantz, S.B., and Morrow, J.S. (1998a). Simultaneous degradation of αII- and βII-spectrin by caspase 3 (CPP32) in apoptotic cells. *J. Biol. Chem.* 273, 22490-22497.

Wang, K.A., Postmantur, R., Nadimpalli, R., Nath, R., Mohan, P., Nixon, R.A., Talanian, R.V., Keegan, M., Herzog, L., and Allen, H. (1998b). Caspase-mediated fragmentation of calpain inhibitor protein calpastatin during apoptosis. *Arch. Biochem. Biophys.* 356, 187-196.

Ware, G.W. (1994). Chapter 4: Insecticides. In *The Pesticide Book, Fourth Edition* (G.W. Ware, Ed.), pp. 41-74. Thomson Publications, Fresno California.

Weiner, M.L. and Jortner, B.S. (1999). Organophosphate-induced delayed neurotoxicity of triarylphosphates. *Neurotoxicology* 20, 653-674.

Widmann, C., Gibson, S., and Johnson, G.L. (1998). Caspase-dependent cleavage of signaling proteins during apoptosis. *J. Biol. Chem.* 273, 7141-7147.

Wissing, D., Mouritzen, H., Egeblad, M., Poirier, G.G., and Jäättelä, M. (1997). Involvement of caspase-dependent activation of cytosolic phospholipase A_2 in tumor necrosis factor-induced apoptosis. *Proc. Natl. Acad. Sci. USA* 94, 5073-5077.

Yagle, K. and Costa, L.G. (1999). Effects of alcohol on immediate-early gene expression in primary cultures of rat cortical astrocytes. *Alcohol Clin. Exp. Res.* 23, 446-455.

Yamada, T., Murayama, T., and Nomura, Y. (1997). Muscarinic acetylcholine receptors on rat thymocytes: their possible involvement in DNA fragmentation. *Jpn. J. Pharmacol.* 73, 311-316.

Yan, G.M., Lin, S.Z., Irwin, R.P., and Paul, S.M. (1995). Activation of muscarinic cholinergic receptors blocks apoptosis of cultured cerebellar granule neurons. *Mol. Pharmacol.* 47, 248-257.

(*a*)

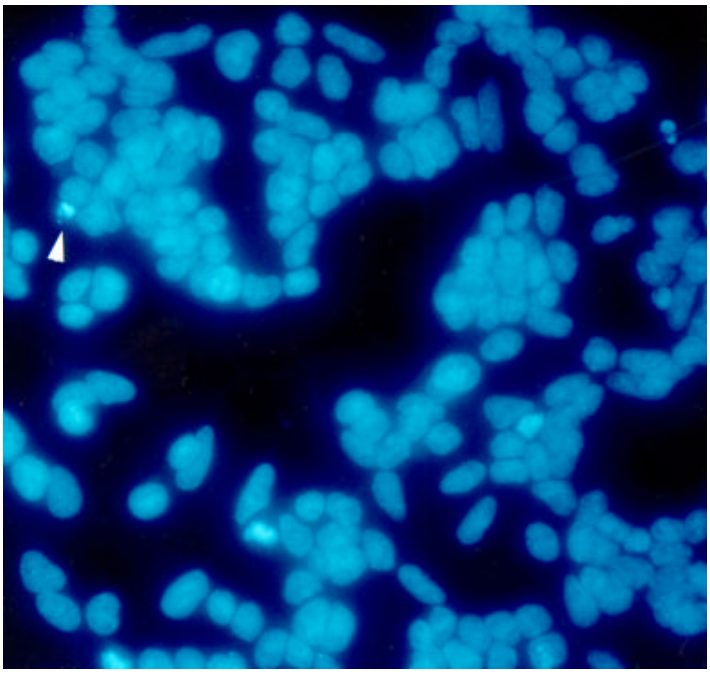

(*b*)

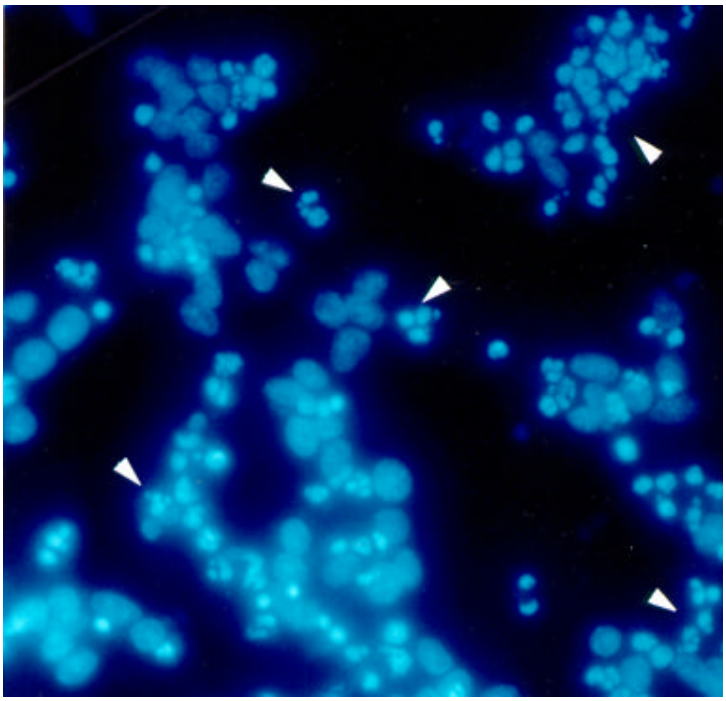

Figure 7.1. Nuclear fluorescence in SH-SY5Y cells. Cells were incubated in a 10µg/ml Hoechst 33342 solution following acetone/ethanol fixation. Fig. 7.1a is 1% ethanol (v/v) incubation for 1440 min; Fig. 7.1b is cells incubated with 1mM parathion for 1440 min. Arrowheads indicate late stage apoptotic nuclei. The photos are at 400x.

(*c*)

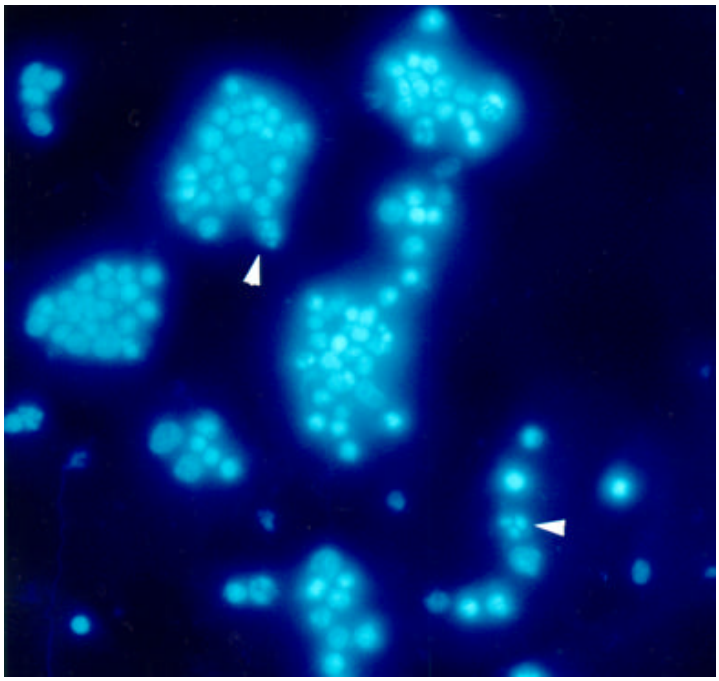

(*d*)

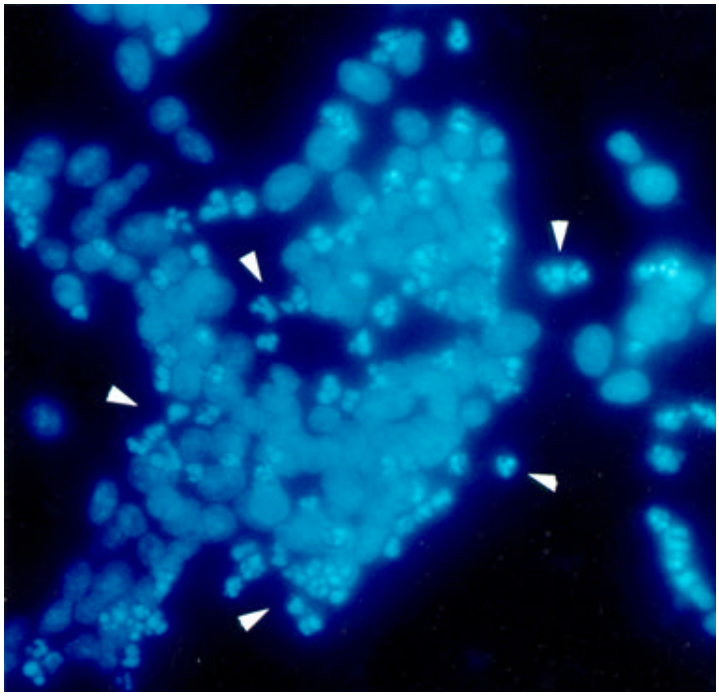

Figure 7.1. Nuclear fluorescence in SH-SY5Y cells. Cells were incubated in a 10µg/ml Hoechst 33342 solution following acetone/ethanol fixation. Fig. 7.1c is cells incubated with 1mM TOTP for 1440 min; Fig. 7.1d is a 500nM staurosporine treatment for 1440 min (positive control). Arrowheads indicate late stage apoptotic nuclei. The photos are at 400x.

(*a*)

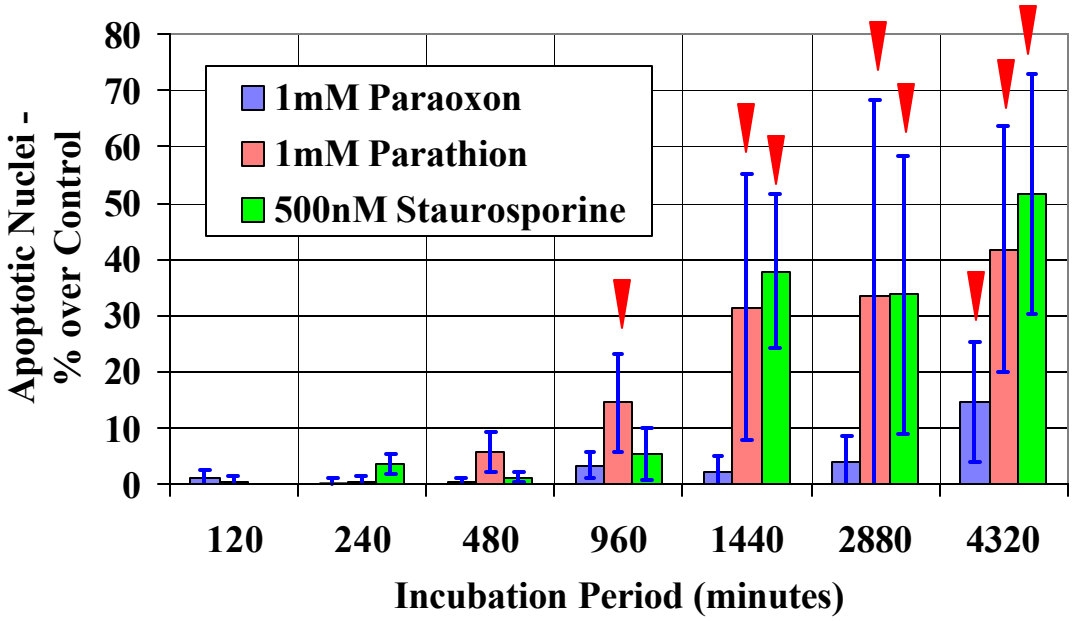

(*b*)

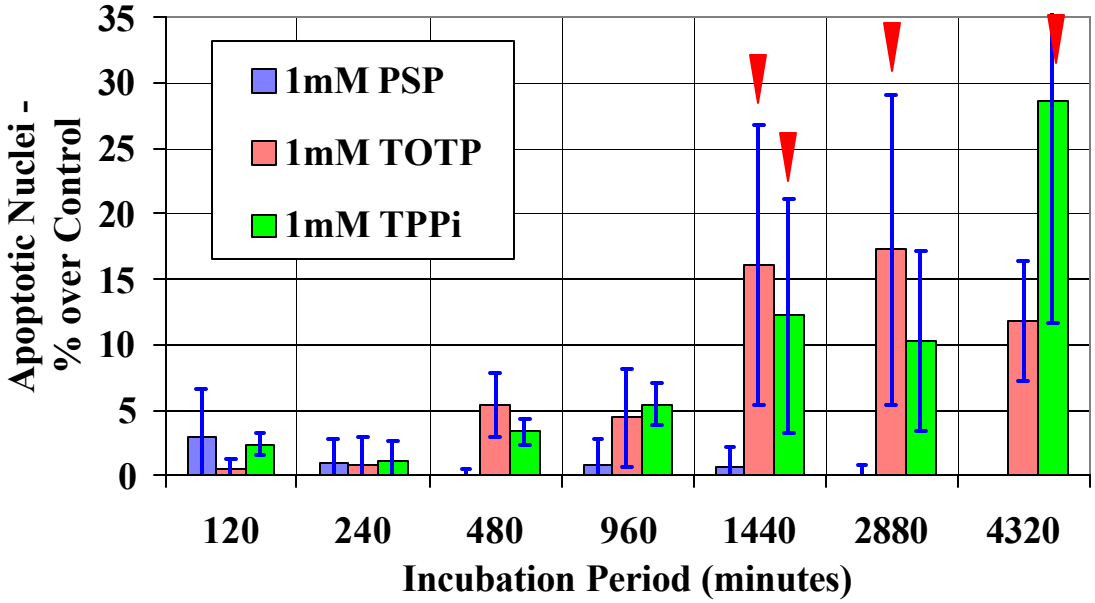

Figure 7.2. OP compound-induced changes in nuclear fragmentation. Values are the mean of 6-16 normalized data points (percentages) and are graphed as percent over control ± the standard deviation. Statistical significance of apoptotic nuclear fragmentation when compared to solvent controls are displayed ($p<0.05$, ◢). Fig. 7.2a, 1mM paraoxon, 1mM parathion, and 500nM staurosporine; Fig. 7.2b, 1mM PSP, 1mM TOTP, and 1mM TPPi.

(*a*)

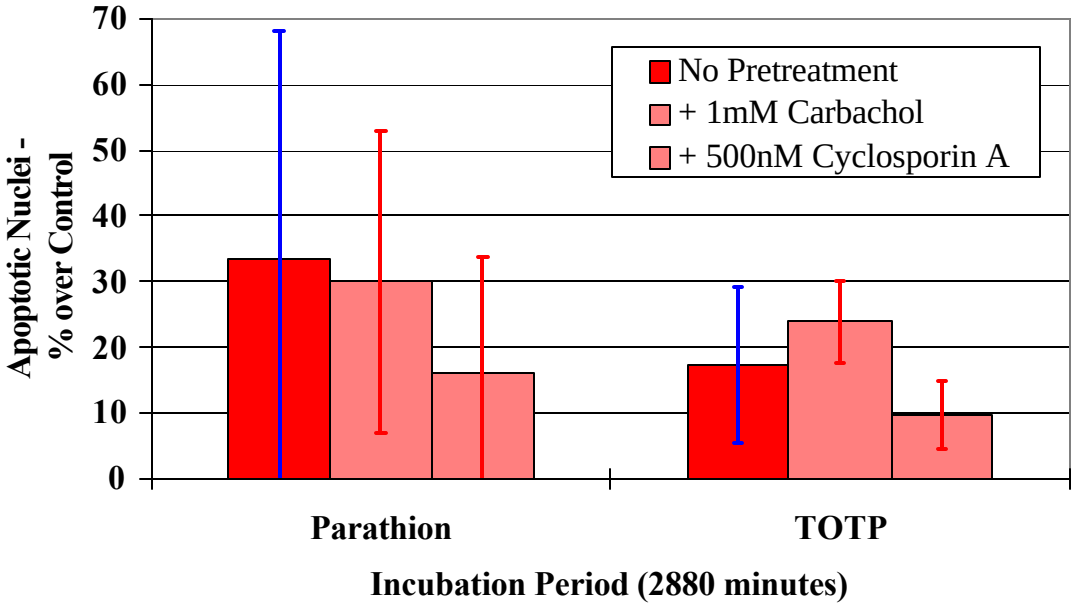

(*b*)

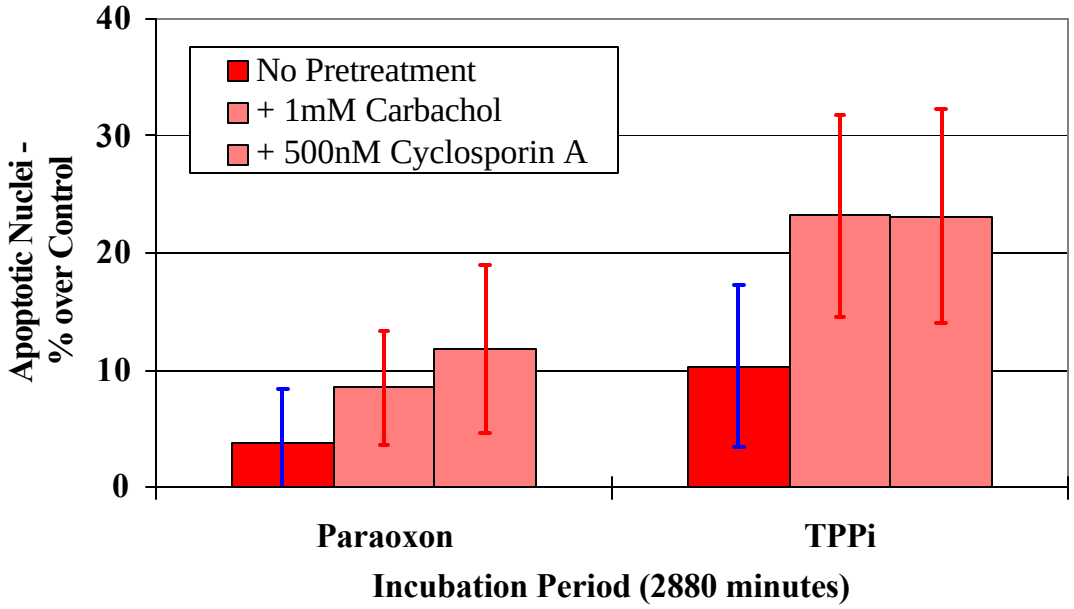

Figure 7.3. OP compound-induced changes in nuclear fragmentation following 30 hr pretreatment with 1mM carbachol or 500nM cyclosporin A. Values are the mean of 6 -14 normalized data points (percentages) and are graphed as percent over control ± the standard deviation. Fig. 7.3a, 1mM parathion and 1mM TOTP; Fig. 7.3b, 1mM paraoxon and 1mM TPPi.

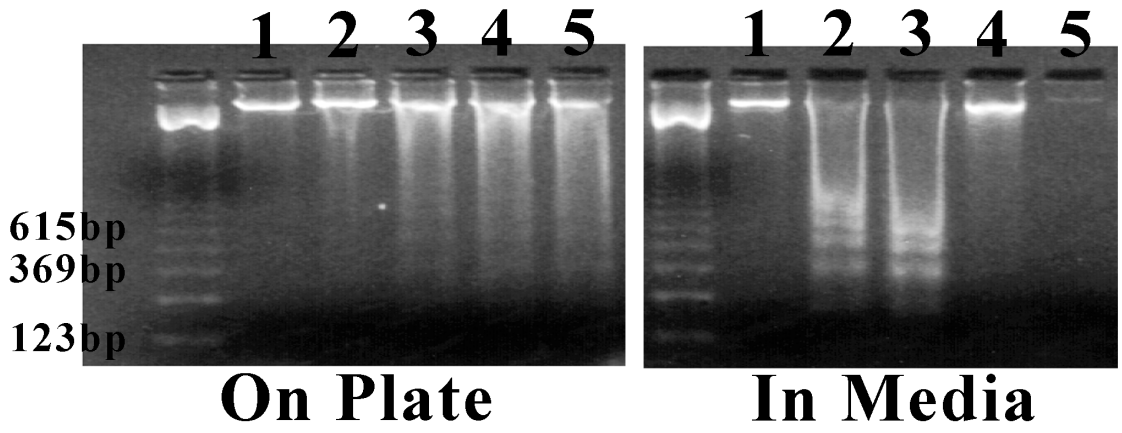

Figure 7.4. OP compound-induced DNA fragmentation as viewed by gel electrophoresis. The unnumbered lane is a 123 base pair DNA standard. Lane 1 = 1% ETOH (v/v); Lane 2 = 1mM paraoxon; Lane 3 = 1mM parathion; Lane 4 = 1mM TOTP; Lane 5 = 1mM TPPi. The left panel depicts cells attached to the plate; the right panel is from cells floating in the media, both following OP compound incubation (4320 min). Results were duplicated in one other experiment.

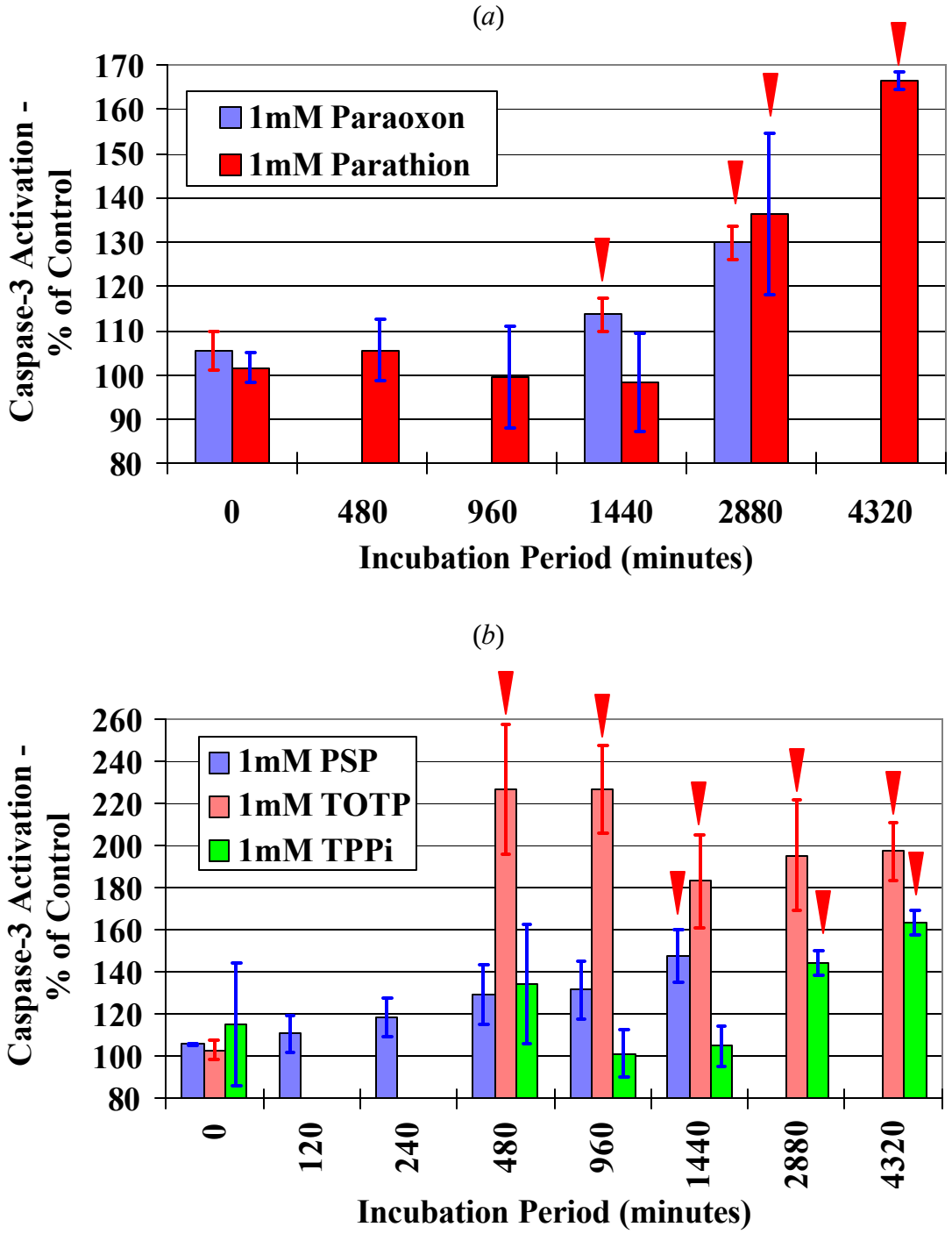

Figure 7.5. OP compound-induced changes in caspase-3 activation. Values are the mean of 3-7 normalized data points (percentages) and are graphed as percent of control ± the standard deviation. Statistical significance of caspase-3 activation when compared to solvent controls are displayed ($p<0.05$,). Fig. 7.5a, 1mM paraoxon and 1mM parathion; Fig. 7.5b, 1mM PSP, 1mM TOTP, and 1mM TPPi. Absence of a bar identifying an OP compound at a particular time point indicates no data.

(*a*)

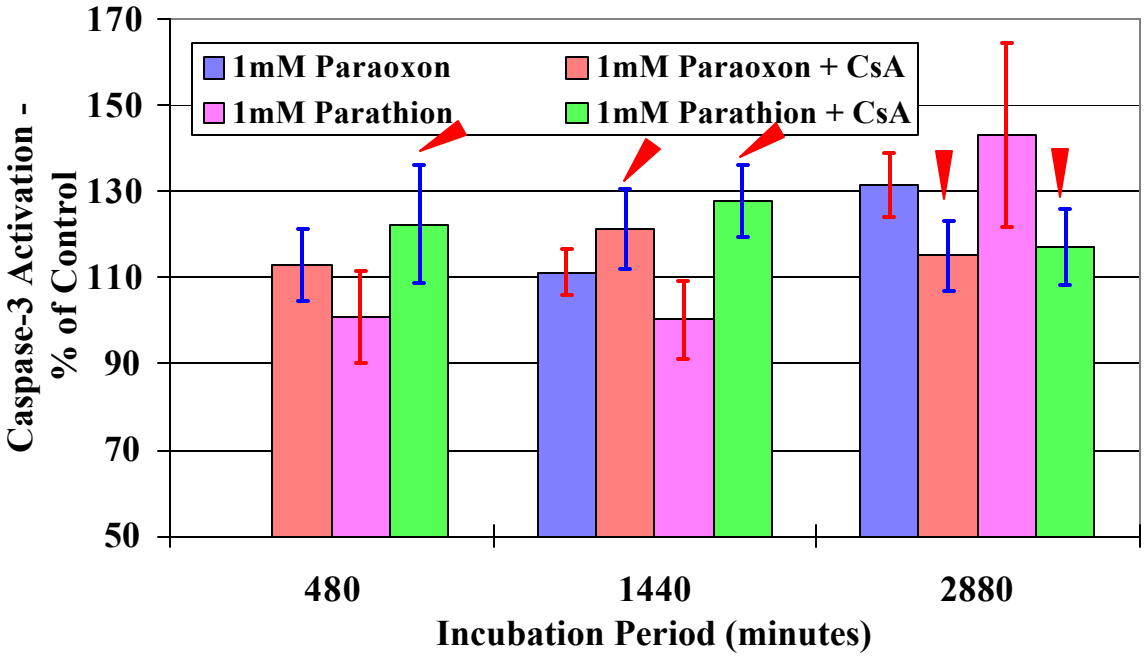

(*b*)

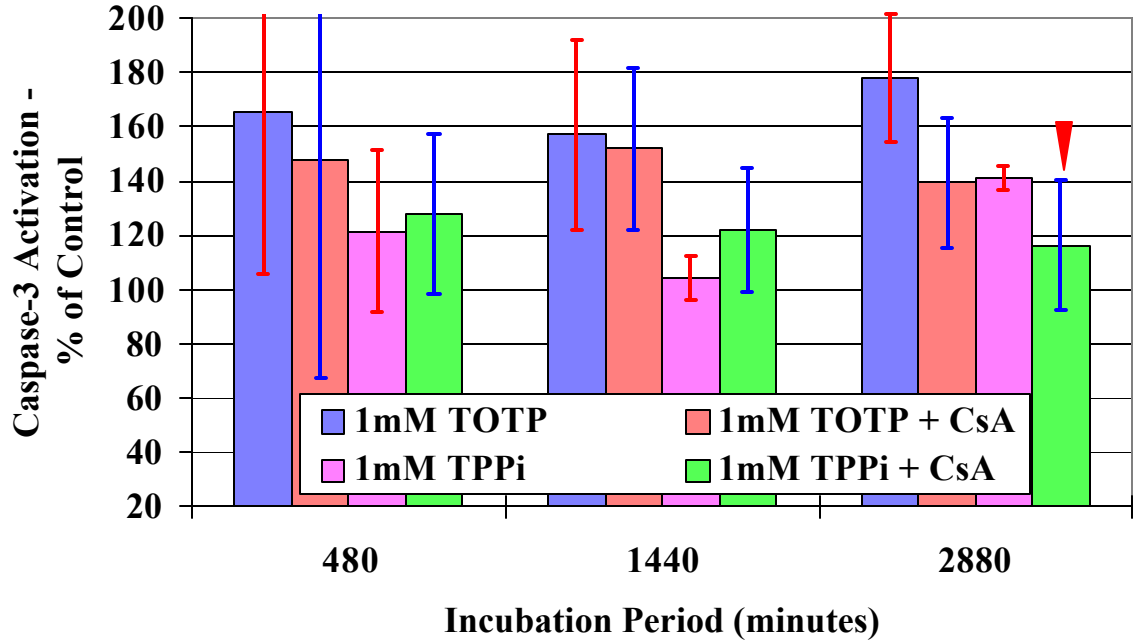

Figure 7.6. OP compound-induced changes in caspase-3 activation following pretreatment with 500nM cyclosporin A (CsA, 30h). Values are the mean of 3 normalized data points (percentages) and are graphed as percent of control ± the standard deviation. Statistical significance of caspase-3 activation in cells without pretreatment when compared to cells with pretreatment are displayed ($p<0.05$, ◢). Fig. 7.6a, 1mM paraoxon and 1mM parathion; Fig. 7.6b, 1mM TOTP and 1mM TPPi. Absence of a bar identifying an OP compound at a particular time point indicates no data.

(*a*)

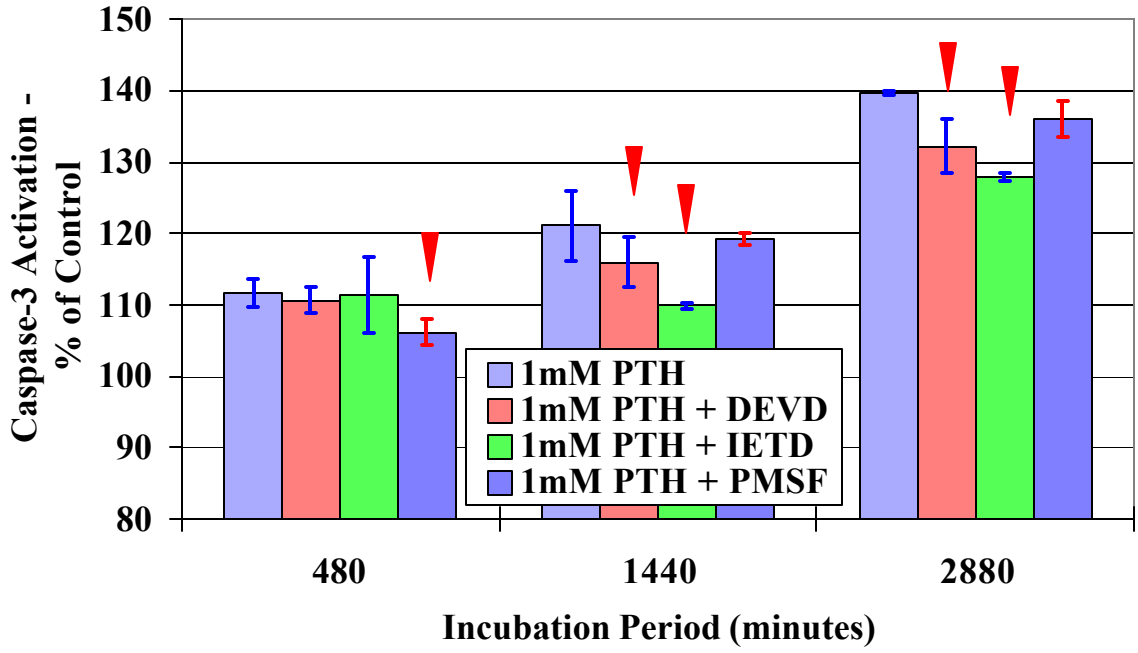

(*b*)

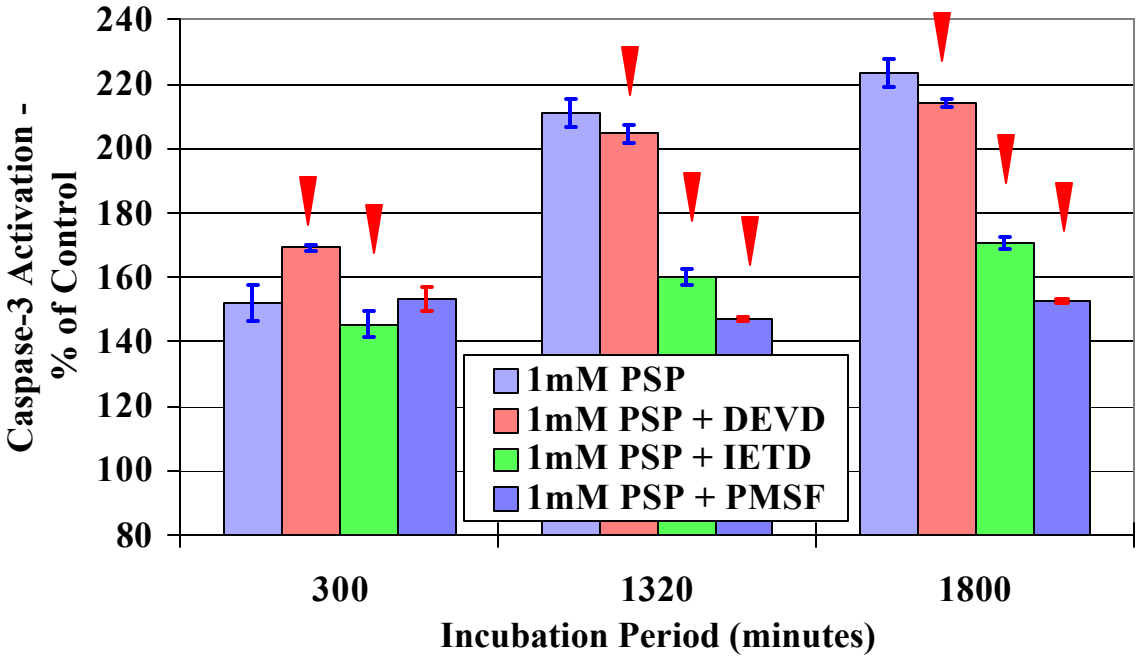

Figure 7.7. OP compound-induced changes in caspase-3 activation following 8 hr pretreatment with 25µM Ac-DEVD-CHO (DEVD), 25µM Ac-IETD-CHO (IETD), or 1mM phenylmethylsulfonyl fluoride (PMSF). Values are the mean of 3 normalized data points (percentages) and are graphed as percent of control ± the standard deviation. Statistical significance of caspase-3 activation in cells without pretreatment when compared to cells with pretreatments are displayed ($p<0.05$, ◢). Fig. 7.7a, 1mM parathion (PTH); Fig. 7.7b, 1mM PSP.

(*c*)

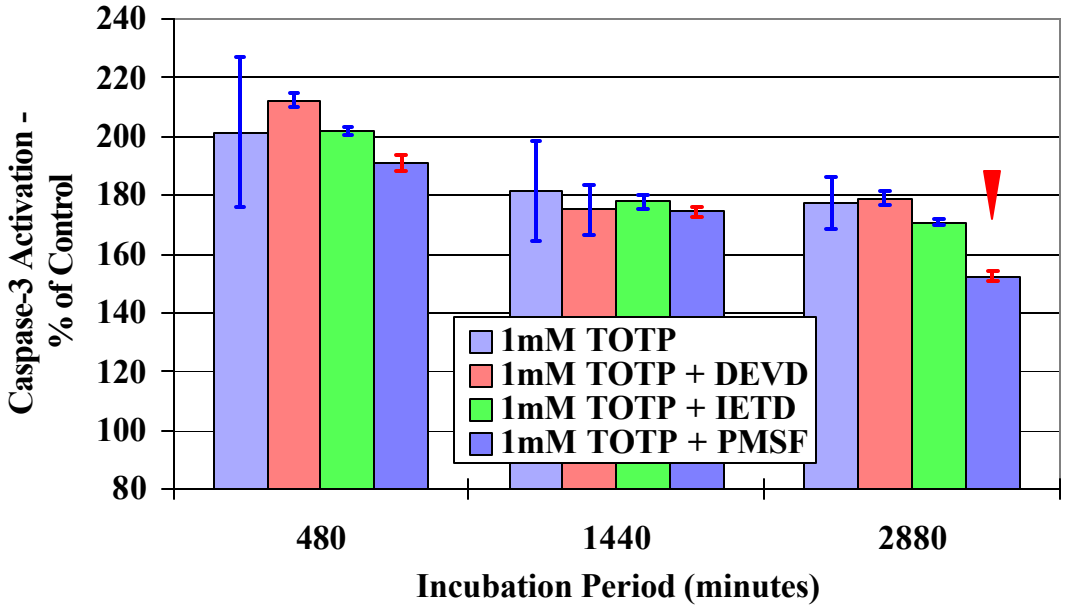

(*d*)

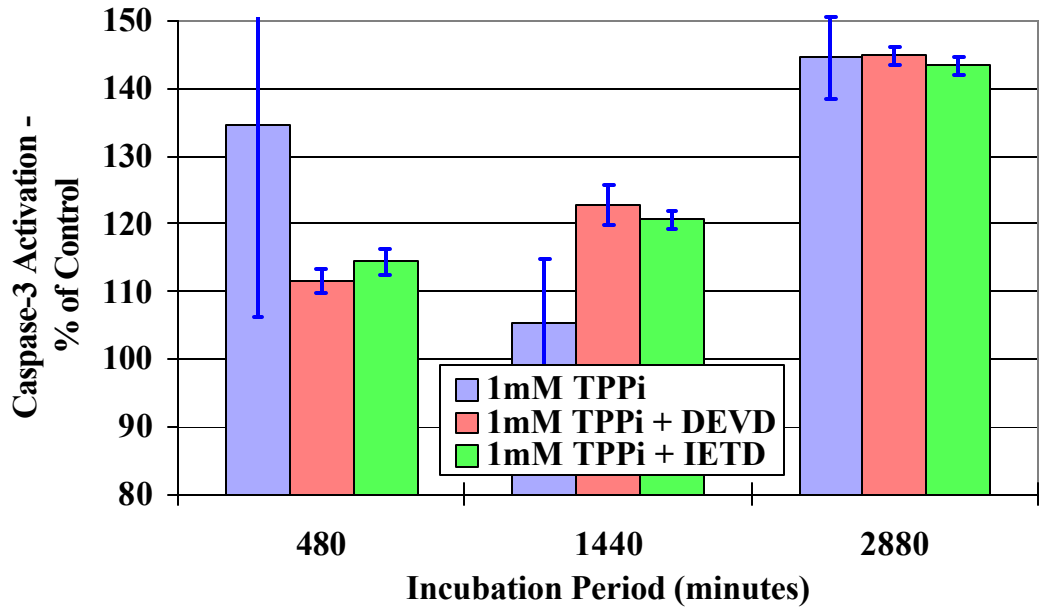

Figure 7.7. OP compound-induced changes in caspase-3 activation following 8 hr pretreatment with 25µM Ac-DEVD-CHO (DEVD), 25µM Ac-IETD-CHO (IETD), or 1mM phenylmethylsulfonyl fluoride (PMSF). Values are the mean of 3 normalized data points (percentages) and are graphed as percent of control ± the standard deviation. Statistical significance of caspase-3 activation in cells without pretreatment when compared to cells with pretreatments are displayed ($p<0.05$, ◢). Fig. 7.7c, 1mM TOTP; Fig. 7.7d, 1mM TPPi.

(*a*)

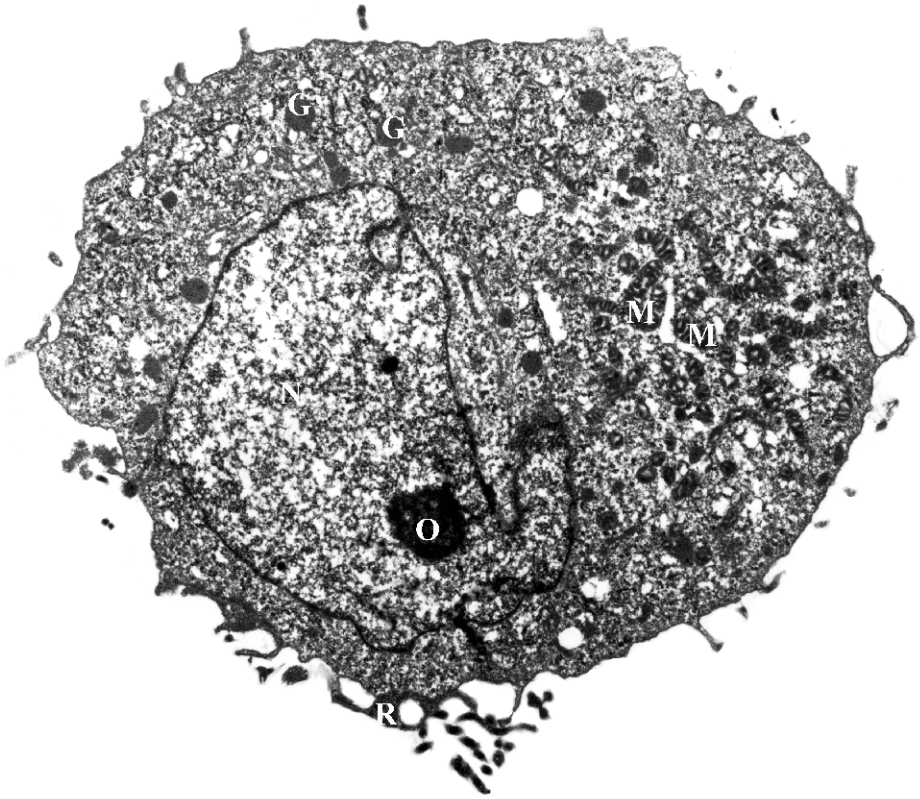

Figure 7.8. Electron micrograph of SH-SY5Y cell ultrastructure. Fig. 7.8a shows 1% ethanol (v/v) treated cells (1290 min). The photo is at 15,080x. Nuclei (N), nucleoli (O), mitochondria (M), glycogen granules (G), and neurites (R) are shown.

(*b*)

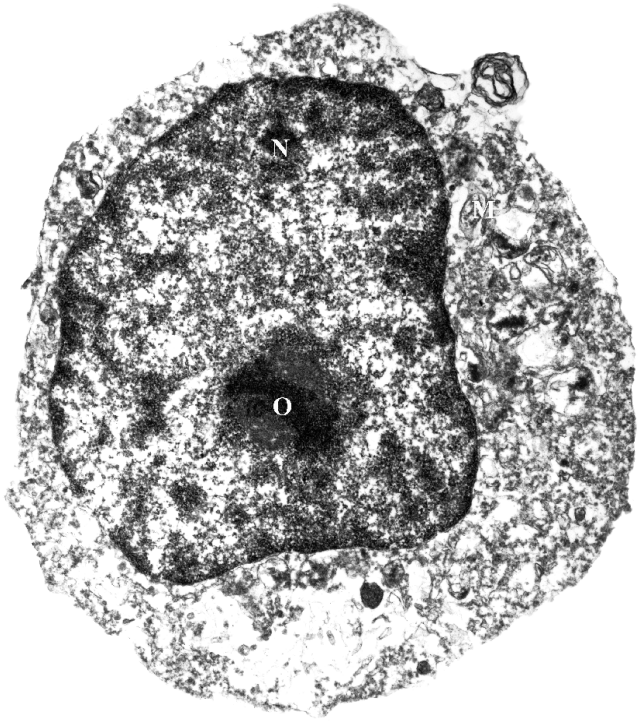

(*c*)

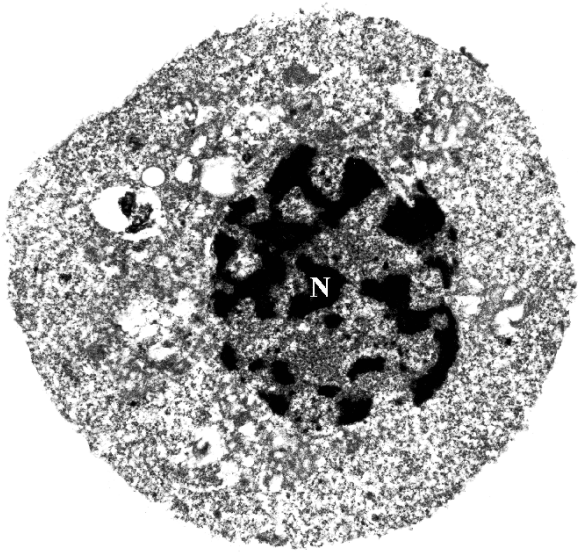

Figure 7.8. Electron micrographs of SH-SY5Y cell ultrastructure. Fig. 7.8b and 7.8c show degenerate morphology of cells exposed to 1mM PSP or TOTP, respectively (1290 min). The photos are at 18,720, and 12,480x, respectively. Nuclei (N), nucleoli (O), mitochondria (M), glycogen granules (G), and neurites (R) are shown.

Chapter 8

The Distribution of Degenerating Neurons in Organophosphorus Compound-induced Delayed Neurotoxicity (OPIDN) in White Leghorn Hens as Assessed by Fluoro-Jade

Kent Carlson, Bernard S. Jortner, and Marion Ehrich

Virginia-Maryland Regional College of Veterinary Medicine,
Blacksburg, Virginia, 24061

ABSTRACT

Certain organophosphorus (OP) compounds induce a delayed neuropathy (OPIDN) that involves central and peripheral nervous system tissue. This study evaluated the distribution and extent of OPIDN in brain and lumbar spinal cord tissue of white Leghorn hens using Fluoro-Jade, a novel fluorescent stain for identifying degenerating neural axons, terminals, and perikarya. Hens were injected with phenyl saligenin phosphate (PSP, 2.5mg/kg intramuscular - IM), triphenyl phosphite (TPPi, 500mg/kg subcutaneous - SC), or dimethyl sulfoxide (DMSO, 0.5ml/kg IM or SC) and evaluated daily for signs of neural dysfunction. Three birds from each treatment were sacrificed after one, two, and three weeks. Their brains and spinal cords were then removed, fixed in formalin, and embedded in paraffin. Microtome-cut sections (7μm) were then stained with Fluoro-Jade (0.001%, w/v). PSP- or TPPi-injected hens displayed increasing neurological dysfunction over the three week period that progressed gradually from leg weakness to ataxia and paralysis. Staining with Fluoro-Jade revealed time-dependent PSP- and TPPi-induced degeneration of nerve fibers, terminals, and cell bodies in lamina VII, spinocerebellar, and medial pontine-spinal tracts in the lumbar spinal cord. Staining of parasaggital brain sections from PSP- and TPPi-injected hens revealed time-dependent heavy degeneration in cerebellar white matter and mossy fibers of foliae I-V and IX. Scattered degeneration was also observed in medullary, pontine, and midbrain nuclei and paleostriatal fibers surrounding the optic tract. TPPi-induced degeneration also affected additional cerebellar folia, and medullary, pontine, midbrain, and forebrain nuclei and fiber tracts. These results demonstrate that Fluoro-Jade is a sensitive method for staining degenerating neuronal tissue.

INTRODUCTION

Silver impregnation staining is a traditional method used for the detection of neurodegeneration via light microscopy. This protocol selectively stains degenerating neuronal soma, axons (fibers), dendrites, and terminals through a largely unknown mechanism (Switzer III, 2000). Silver staining is highly sensitive but can be variable. Therefore, other less labor intensive, more consistent methods should be considered when assessing neurodegeneration.

Fluoro-Jade is a novel fluorescence stain that has been promoted for the detection of neuronal degeneration. It is described as more reliable, simpler in technique, and comparatively as sensitive as silver staining procedures (Schmued *et al.*, 1997). Fluoro-Jade has been used to determine cell death following sleep deprivation (Cirelli *et al.*, 1999) and intrastriatal nigral grafts (Emgard *et al.*, 1999). It has also been used to observe neural degeneration associated with cytosolic phospholipase A2 upregulation (Hornfelt *et al.*, 1999), and exposure to fenfluramine (Schmued *et al.*, 1999), riluzole (Kanthasamy *et al.*, 1999), trimethyl tin and kainic acid (Noraberg *et al.*, 1999), 2-amino-3-hydroxy-5-methyl-4-isoxazole propionate (AMPA) (Kristensen *et al.*, 1999), methamphetamine (Schmued and Bowyer, 1997; Eisch *et al.*, 1998; Eisch and Marshall, 1998), and D-amphetamine (Bowyer *et al.*, 1998). The sensitivity of Fluoro-Jade has been validated by *in vivo* testing using kainic acid, 3-nitropropionic acid, isoniazid, ibogaine, domoic acid, and dizocilpine maleate (MK-801) (Schmued and Hopkins, 2000). Interestingly, validation with other compounds (1-methyl-4-phenyl-1,2,3,6-tetrahydropyridine (MPTP), methamphetamine, and d-fenfluramine) revealed additional neurodegeneration not seen with other methods (Freyaldenhoven *et al.*, 1997; Schmued and Hopkins, 2000). The sensitivity, specificity, and ease of use promotes Fluoro-Jade for use as a staining candidate in the study of neuropathic conditions associated with exposure to organophosphorus (OP) compounds.

Exposure to certain OP compounds can induce a progressive neuropathy termed organophosphate-induced delayed neuropathy (OPIDN). The distribution of lesion development is dependent on the oxidation state of the phosphorus atom in the OP compound and the species model used (Abou-Donia, 1995). Silver staining methods have been used in many model species such as quail (Varghese *et al.*, 1995a, 1995b), hens (Janzik and Glees, 1966; Tanaka and Bursian, 1989; Tanaka *et al.*, 1992), ferrets (Stumpf *et al.*, 1989; Tanaka *et al.*, 1990, 1994), slow lorises (Ahmed and Glees, 1971), cats (Prineas, 1969; Bouldin and Cavanagh, 1979), and rats (Veronesi and Dvergsten, 1987) to assess the distribution and extent of OP compound-induced neuronal degeneration. Silver staining has revealed that pentavalent OP compounds that induce OPIDN (Type I compounds) such as phenyl saligenin phosphate (PSP), induce bilateral degeneration in peripheral nerve, spinal cord, cerebellum, and medullary-pontine nuclei (Prineas, 1969; Bouldin and Cavanagh, 1979; Stumpf *et al.*, 1989; Tanaka and Bursian, 1989). This method has also shown that trivalent OP compounds such as triphenyl phosphite (TPPi) (Type II compounds), induce neuropathic conditions in midbrain and forebrain nuclei and tracts in addition to those areas affected by Type I degeneration (Veronesi and Dvergsten, 1987; Tanaka *et al.*, 1990, 1992, 1994; Varghese *et al.*, 1995a, 1995b).

This study evaluated the temporal and spatial distribution of delayed neuropathy, as discerned by Fluoro-Jade, in white Leghorn hen brains and spinal cord following exposure to the OP compounds

PSP and TPPi. Histopathological findings were correlated to clinical observations of neurological dysfunction.

EXPERIMENTAL METHODS

Chemicals. Triphenyl phosphite (TPPi, 98% pure) was purchased from Chem Services (West Chester, PA). Phenyl saligenin phosphate (PSP, 99% pure) was synthesized by Lark Enterprises (Webster, MA). Dimethyl sulfoxide was obtained from Sigma (St. Louis, MO). Sodium pentobarbital was purchased from Veterinary Laboratories, Inc. (Lenexa, Kansas). Organophosphorus (OP) compounds were diluted in DMSO the same day (TPPi, 1000mg/ml) or diluted and stored at 23°C for three days (PSP, 5mg/ml) prior to dosing hens.

Animal Maintenance, Dosing, and Sacrifice. White Leghorn hens (>10 months old, 1.5 - 1.9kg) obtained from the Department of Animal and Poultry Science (Virginia Polytechnic Institute and State University) were housed in groups of four in wire cages (57 x 84 x 61cm) and fed and watered *ad libitum*.

Nine hens were randomly assigned to each treatment group (PSP, 2.5mg/kg; TPPi, 500mg/kg; and DMSO, 0.5ml/kg), dosed subcutaneously (DMSO, TPPi) or intramuscularly (DMSO, PSP) as in Tanaka *et al.* (1992) and Massicotte *et al.* (1999), respectively, and then returned to cages with similarly dosed birds. Hens within treatment groups were then assigned sacrifice dates randomly (7, 14, or 21 days). Hens disabled by paralysis at later timepoints were fed and watered manually on a daily basis.

On the sacrifice date, hens were euthanatized with sodium pentobarbital (65mg/ml) via a brachial wing vein. Immediately following, the brain with attached cervical spinal cord and the lumbar spinal cord were carefully dissected free, sagittally sectioned, and one-half dropped into either ice-cold 10% neutral buffered formalin or methanol/phosphate buffered saline (PBS, pH 7.4) (6:1, v/v) fixatives.

Tissue Processing. Brain and lumbar spinal cord tissue were stored in formalin and methanol/PBS (at 4°C or -20°C, respectively) for 4 days. Methanol/PBS and formalin fixed samples were trimmed (parasagittal sections of brain, coronal sections of lumbar spinal cord) and sealed in tissue cassettes. Methanol/PBS fixed samples were further processed by dehydration in absolute methanol (x 2, 1 hr each) while formalin fixed samples were dehydrated by a graded series of alcohols. Both sets of tissues were then cleared with xylene and infiltrated with warm paraffin (56-63°C) under pressure in a Sakura-VIP "Tissue Tek" tissue processor (Torrance, CA). Tissues were then transferred to embedding molds and embedded in a Shandon Histo-Center 2 (Pittsburg, PA) machine. Sections (7μm) were cut from chilled paraffin blocks using a Leica 2030 rotary microtome (Deerfield, IL), attached to positively charged slides, incubated at 37-40°C for 4 hours, and then baked for 20-30 min at 60°C.

Clinical Evaluation. Hens were observed daily for evidence of neurological dysfunction. Clinical evaluations were performed unblinded by one person and averaged for all three birds in the treatment/time set. Observations were based on criteria modified from Stumpf *et al.* (1989). Numerical scores were designated; 0 - no deficits, 1 - slight leg weakness, 2 - leg weakness and reluctance to walk, 3 - mild ataxia, 4 - severe ataxia, 5 - mild paresis, and 6 - severe paresis.

Fluoro-Jade Staining. Sections were stained primarily as in Schmued and Hopkins (2000). Briefly, methanol/PBS and formalin fixed sections were prepared for staining by deparaffinizing in xylene (15 min X 2), rehydrating in a graded series of ethanol, and rinsing in distilled water. Slides were then immersed for 15 min in freshly prepared 0.06% (w/v) potassium permanganate, rinsed in distilled water, and immersed in the dark for 30 min in a 0.001% (w/v) Fluoro-Jade staining solution (Histo-Chem Inc.; Jefferson, AR). Stained slides were then rinsed in distilled water, dried by air convection in a chemical hood, dehydrated in xylene, and coverslipped with DPX (Aldrich Chemical Co; Milwaukee, WI). Observations of degenerating neurons were made with a Nikon Diaphot-TMD inverted microscope equipped with 10 and 20X fluorescence objectives and a "B" filter cube. Photographic documentation of representative degenerative areas were made with a Nikon Fe-2 camera (ASA200 Kodacolor film). The location of brain and spinal cord tracts were identified using an atlas of the chick brain (Kuenzel and Masson, 1988) and publications (Tanaka and Bursian, 1989; Tanaka *et al.*, 1992).

Statistics. Clinical observations had 3 -9 data points for each time and OP concentration. These data were graphed as the median ± the range. Qualitative histochemical studies had 3 samples for each time point. The findings from all samples within each treatment (n=9) were combined into composite drawings to illustrate the entire amount of neuronal degeneration elicited by OP compounds.

RESULTS

Clinical Evaluation.

Clinical evaluation was utilized to appraise the rate of neurodegeneration and potential survivability issues. No clinical deficits were observed in hens following DMSO injections. A progression from leg weakness to ataxia and then to paralysis was observed in hens injected with PSP (2.5mg/kg) or TPPi (500mg/kg). This was reflected by increases in clinical scores of neurological dysfunction. Scores for OP compound-treated hens were increased over DMSO controls from day 6 onward (Fig. 8.1). Increased agitation and activity following OP compound injections were the only acute symptoms.

Fluoro-Jade Staining.

Fluoro-Jade staining was utilized to identify degenerating neuronal soma, tracts (fibers), and terminals in transverse lumbar spinal cord sections and parasaggital brain sections of hens exposed to neuropathic OP compounds. Neural degeneration was identified by an increased level of fluorescent (yellow) brightness in the affected areas. Degenerating soma, tracts, and terminals were discriminated from artefactual staining of red blood cells, capillaries, and blood vessels by comparing size (nuclei) and continuity (tracts versus vessels). Formalin fixed sections were superior to methanol/PBS fixed sections for the localization of these degenerating areas (data not shown). Control sections had minimal artefactual staining around the tissue periphery (Fig. 8.2a, 8.2c, 8.2e).

Spinal Cord. Fluoro-Jade staining intensity was increased over control in the ventral spinocerebellar, dorsal spinocerebellar, and lateral vestibulospinal (medial-pontine) tracts (Fig. 8.2b, 8.2d, and 8.2f) in transverse sections of the lumbar spinal cord of hens exposed to PSP and TPPi. Sparse staining was evident in these tracts on day 7. A mild (PSP) or moderate (TPPi) increase in staining brightness (terminal, axonal, and cell soma degeneration) was present by day 14. Fluorescence brightness was greatest for both compounds on day 21, with TPPi having the greatest amount of degeneration in these tracts overall (Fig. 8.3c, 8.3f). Scattered individual degenerating tracts were present in deeper sections of the lateral and ventral column and in layer VII of the gray matter on days 14 and 21. DMSO-injected hens displayed little or no increase in fluorescence intensity over background (Fig. 8.2a, 8.2c, 8.2e). Overall, there was little staining variability within treatment groups of the spinal cord.

Brain. Fluoro-Jade staining of brain tissue resulted in sections with a dull yellow fluorescence. Degenerating tracts, soma, and terminals stained much brighter than the surrounding dull matrix and were easily able to be discerned, even when the fibers were quite small. Even so, the variation in stained regions between same treatment samples was more prevalent in brain when compared to spinal cord sections.

Exposure to PSP increased the staining brightness (degeneration) of cerebellar white matter and mossy fibers of foliae I-V in parasaggital brain sections. Cerebellar white matter degeneration qualitatively increased as the length of postexposure time increased.

Exposure to PSP also magnified the intensity of staining in degenerating fibers and terminals in regions approximating the solitary, medial pontine, gracile-cuneate, medial and lateral vestibular, ventromedial and anterior hypothalamic, and magnocellular nuclei. Fibers in the paleostriatum and dorsal supraoptic decussation additionally stained to a greater extent than controls (Fig. 8.3a, 8.3b). Increased cell soma brightness (degeneration) was also observed in subcerebellar regions corresponding to the locations of vestibular nuclei. Staining on day 7 was light for most affected areas. Increased staining was noted on day 14 in most of the tracts, soma, and terminals in these regions. Interestingly, fibers, soma, and terminals located in the area of the vestibular and magnocellular nuclei decreased in staining brightness as the length of postexposure time increased past day 14.

TPPi induced an increase in staining brightness in cerebellar areas affected by PSP in addition to folia VI, VIII, and X (Fig. 8.3d). As with PSP, the Fluoro-Jade staining brightness in the affected tracts and terminals was minimum at day 7 and increased over time in all cerebellar folia and mossy fibers.

TPPi also increased the brightness of staining in neuronal fibers and terminals located in approximately the same position as basal optic and ectomamillary, red, ovoid, medial and lateral habenular, subrotund, anterior ansa lenticular, medial pontine, dorsal reticular gigantocellular, dorsomedial anterior thalamic, medial and lateral septal, supraspinal, and dorsal facial motor nerve nuclei. Increases in staining brightness were light by day 7 and increased in density up until day 14. Subsequent to day 14, many affected tracts and fibers decreased in staining brightness.

Fiber tracts in approximately the same location as the lateral forebrain bundle, medial longitudinal fasciculus, ansa lenticularis, parolfactory lobe, prepiriform cortex, intermediate neostriatum, periventricular stratum griseum, paleostriatum, medullary stria, ventral hyperstriatum, occipitomesencephalicus tract, olfactory bulb, and the optic tract were also affected by TPPi (Fig. 8.3d, 8.3e). These structures followed similar time-dependent changes in staining density as did other regions located in approximation to brain nuclei.

DISCUSSION

This study evaluated the onset and distribution of OPIDN in white Leghorn hens by utilizing Fluoro-Jade, a novel fluorochrome specific for localizing neuronal degeneration in axons, terminals and cell soma. Degenerative changes (increases in staining brightness) induced by PSP and TPPi were observed in brain and spinal cord tissue. Neural dysfunction was also assessed by using a simplified method for scoring clinical observations.

Clinical Evaluation.

The onset and rate of progression of PSP- and TPPi-induced clinical dysfunction paralleled each other and were higher than DMSO control hens from day 6 onward. All dosed hens eventually progressed to paralysis by day 21.

The manifestation of clinical dysfunction following PSP (2.5mg/kg) exposure in this study was similar to that of Jortner and Ehrich (1987) and El-Fawal *et al.* (1990). In this study, both onset and progression for TPPi-induced symptoms were similar to that of Tanaka *et al.* (1992) in which a 1000mg/kg dosing strategy was used in hens. TPPi-induced clinical dysfunction in our hen model occurred much later and was less variable, however, than when administering similar doses (500mg/kg) to other avian models such as the quail (Varghese *et al.*, 1995b). This suggested that a dose threshold may exist, beyond which TPPi may not induce any additional neurodegeneration in the hen.

Fluoro-Jade Staining.

Extensive PSP- and TPPi-induced neuronal degeneration was fluorescently labeled by Fluoro-Jade in brain and spinal cord sections. Degeneration *in toto* seemed to increase for both compounds up until day 14. Following this, most areas (except cerebellum and spinal cord) displayed reduced amount of degeneration (decreased staining of fibers, terminals, soma). Similar decreases in degeneration over time have been observed in hen medullary nuclei (vestibular, raphae magnus) exposed to TOTP (Tanaka and Bursian, 1989), quail auditory nuclei and tracts exposed to TPPi (Varghese *et al.*, 1995a), and hen tibial nerves exposed to PSP or TOTP (Jortner and Ehrich, 1987). Apparent decreases in degeneration may result from the clearance of neuronal debris, dilution of staining signal by gliosis, an intrinsic deficiency in the staining protocol, or neural regeneration (in the peripheral nervous system).

The distribution and density of PSP- and TPPi-induced spinal cord degeneration in spinocerebellar and medial-pontine tracts as assessed by Fluoro-Jade was similar to that previously reported by Jortner and Ehrich (1987) and Tanaka *et al.* (1992), respectively. Degeneration patterns elicited by PSP and TPPi also matched that induced by TOTP (Tanaka and Bursian, 1989). The extent of staining was less in Lamina VII of the gray matter in our study, however, when compared to the silver staining done by Tanaka *et al.* (1992). The extent of PSP-induced spinal cord degeneration was more consistent in this study than reported in Jortner and Ehrich (1987), however. In the current study the clinical scores paralleled neuropathological developments for all birds.

Detailed descriptions of PSP-induced brain neuropathy have not been published, although mapping has been done for a related protoxicant, TOTP. Exposure to TOTP induced the degeneration of lateral vestibular, lateral and medial deep cerebellar, gracile-cuneate, external cuneate and lateral cervical, solitary, inferior olivary, lateral paragigantocellular reticular, gigantocellular, lateral reticular, and raphae magnus nuclei when assessed with Fink-Heimer silver staining. Nerve fiber and terminal degeneration was also observed in cerebellar deep nuclei, granular layer mossy fibers, and white matter of the cerebellar anterior lobe folia (Tanaka and Bursian, 1989). Degenerative fibers and terminals were also found in these regions when assessed by Fluoro-Jade. Additional occurrences in approximately the same location as the magnocellular; medial pontine; medial vestibular; and ventromedial and anterior hypothalamic nuclei; and the paleostriatum and dorsal supraoptic decussation also had degenerative fibers and terminals when stained with Fluoro-Jade.

TPPi-induced neuronal degeneration has been described in detail for hens (Tanaka *et al.*, 1992), rats (Veronesi and Dvergsten, 1987), ferrets (Tanaka *et al.*, 1990, 1994), and quail (Varghese *et al.*, 1995a, 1995b). In hens, silver stained degenerating areas were observed in the lateral reticular, lateral cervical, gracile-cuneate, external cuneate, lateral paragigantocellular reticular, parvocellular, gigantocellular reticular, lateral vestibular, cerebellar deep, spiriform, and the lateral mesenphalic nucleus pars dorsalis following exposure to TPPi (Tanaka *et al.*, 1992). In Tanaka's investigation, degenerating fibers and terminals were observed in the granule cell layers and mossy fibers of cerebellar foliae I-VI. TPPi also elicited degeneration in the medial longitudinal fasciculus, bands of fibers running from the paleostriatum primitivum into the lateral forebrain bundle and ansa lenticularis, fibers from the ansa lenticularis to the dorso-intermediate posterior thalamic nucleus, fibers coursing caudally to the lateral spiriform and pedunculopontine tegmental nucleus, and fibers passing from the spiriform nucleus to the deeper layers of the optic tectum (Tanaka *et al.*, 1992).

Fluoro-Jade staining of brain sections from TPPi-treated hens revealed substantial degeneration in excess of that reported for silver impregnation staining. Staining of degenerating terminals and fibers was observed in regions encompassing the solitary, medial pontine, medial vestibular, magnocellular, red, ovoid, medial and lateral habenular, subrotund, dorsomedial anterior thalamic, medial and lateral septal, supraspinal, and dorsal facial motor nerve nuclei of hens exposed to TPPi. An increase in somal degeneration was also noted in subcerebellar locations occupied by vestibular nuclei. Fiber and terminal degeneration was also observed regions that included the periventricular stratum griseum; the medullary stria; the occipito-mesencephalicus tract; the basal optic and ectomamillary nuclei; the ventromedial and anterior hypothalamic nuclei; the dorsal supraoptic decussation; and the optic tract.

Degenerative changes in regions with optical importance contrast results reported by Tanaka *et al.* (1992) and Varghese *et al.* (1995a) in which little or no degeneration, respectively, was found in structures associated with hen or quail optic tracts following exposure to TPPi. Degenerative involvement of regions near the basal ganglia (paleostriatum), ventral hyperstriatum, parolfactory lobe, prepiriform cortex, olfactory bulb, and the intermediate neostriatum in the current study was also more intense than described in Tanaka's investigation. Staining of these locations resembled that in quail, however, in which the area L of Rose located in the neostriatum caudalis underwent significant TPPi-induced degeneration (Varghese *et al.*, 1995a).

The distribution of PSP- and TPPi-induced neuropathic changes for both compounds as assessed by Fluoro-Jade was more extensive than previously described for the hen. Conflicting reports of the distribution of OP compound-induced neurodegeneration could be based in interpretative or methodological differences. In this study, coronal sections were not taken of brain tissue. The designation of nuclei and tracts, therefore, had to be approximate because of the inability to know their three-dimensional location. Another confounding factor was that serial sections from each parasaggital tissue slice were not stained. This obviated plotting of the progression of degeneration along fiber tracts and their termini, which could have led to a greater clarity of the structures affected.

Thickness of stained specimen may also have accounted for differences in staining distribution. Tanaka and Bursian (1989) and Tanaka *et al.* (1992) utilized 40µM thick sections for Fink-Heimer silver staining, in comparison to 7µm thick sections used in this study. Observation of thicker sections would allow for higher confidence when designating structures, and also theoretically reveal more information on neurodegenerative trends.

Differences in the distribution of Fluoro-Jade staining when compared to other methods such as silver impregnation may also have been representative of actual changes. Increased resolution of neurodegeneration in axons, terminals, and soma in Fluoro-Jade stained sections have been reported following 1-methyl-4-phenyl-1,2,3,6-tetrahydropyridine (MPTP), methamphetamine, and d-fenfluramine administration (Freyaldenhoven *et al.*, 1997; Schmued and Hopkins, 2000).

In any case, discrete staining, ease of use, and relatively low cost make Fluoro-Jade an excellent candidate for the assessment of neuropathic degeneration associated with exposure to OP compounds.

ACKNOWLEDGMENTS

We wish to thank Linda Correll, Jason Hunt, Sandy Perkins, and Jill Songer for assistance with supplies, tissue processing, embedding, and sectioning. This work was supported by an EPA grant R825356 and funds from the Virginia-Maryland Regional College of Veterinary Medicine.

REFERENCES

Abou-Donia, M.B. (1995). Chapter 13: Organophosphorus Pesticides. In *Handbook of Toxicology*. (Chang, L.W. and Dyer, R.S., eds). Marcel Dekker, Inc., New York. pp419-473.

Ahmed, M.M. and Glees, P. (1971). Neurotoxicity of tricresylphosphate (TCP) in slow loris (*Nycticebus coucang coucang*). *Acta Neuropath.* 19, 94-98.

Bouldin, T.W. and Cavanagh, J.B. (1979). Organophosphorus neuropathy: I. A teased-fiber study of the spatio-temporal spread of axonal degeneration. *Am. J. Pathol.* 94, 240-251.

Bowyer, J.F., Peterson, S.L., Rountree, R.L., Tor-Agbidye, J., and Wang, G.J. (1998). Neuronal degeneration in rat forebrain resulting from D-amphetamine-induced convulsions is dependent on seizure severity and age. *Brain Res.* 809, 77-90.

Cirelli, C., Shaw, P.J., Rechtschaffen, A., and Tononi, G. (1999). No evidence of brain cell degeneration after long-term sleep deprivation in rats. *Brain Res.* 840, 184-193.

Eisch, A.J. and Marshall, J.F. (1998). Methamphetamine neurotoxicity: dissociation of striatal dopamine terminal damage from parietal cortical cell body injury. *Synapse* 30, 433-445.

Eisch, A.J., Schmued, L.C., and Marshall, J.F. (1998). Characterizing cortical neuron injury with Fluoro-Jade labeling after a neurotoxic regimen of methamphetamine. *Synapse* 30, 329-333.

El-Fawal, H.A.N., Jortner, B.S., Ehrich, M. (1990). Modification of phenyl saligenin phosphate-induced delayed effects by calcium channel blockers: In vivo and in vitro electrophysiological assessment. *Neurotoxicol.* 11, 573-592.

Emgard, M., Karlsson, J., Hansson, O., and Brundin, P. (1999). Patterns of cell death and dopaminergic neuron survival in intrastriatal nigral grafts. *Exp. Neurol.* 160, 279-288.

Freyaldenhoven, T.E., Ali, S.F., and Schmued, L.C. (1997). Systemic administration of MPTP induces thalamic neuronal degeneration in mice. *Brain Res.* 759, 9-17.

Hornfelt, M., Edstrom, A., and Ekstrom, P.A. (1999). Upregulation of cytosolic phospholipase A2 correlates with apoptosis in mouse superior cervical and dorsal root ganglia neurons. *Neurosci. Lett.* 265, 87-90.

Janzik, H.H. and Glees, P. (1966). Chromatolysing spinal neurons in the chick following tricresylphosphate (TCP) intoxication. *Acta Neuropathol.* 6, 303-306.

Jortner, B.S. and Ehrich, M. (1987). Neuropathological effects of phenyl saligenin phosphate in chickens. *Neurotoxicol.* 8, 303-314.

Kanthasamy, A.G., Yun, R.J., Nguyen, B., and Truong, D.D. (1999). Effect of riluzole on the neurological and neuropathological changes in an animal model of cardiac arrest-induced movement disorder. *J. Pharmacol. Exp. Ther.* 288, 1340-1348.

Kristensen, B.W., Noraberg, J., Jakobsen, B., Gramsbergen, J.B., Ebert, B., and Zimmer, J. (1999). Excitotoxic effects of non-NMDA receptor agonists in organotypic corticostriatal slice cultures. *Brain Res.* 841, 143-159.

Kuenzel, W.J., and Masson, M. (1988). *A stereotaxic atlas of the brain of the chick (Gallus domesticus).* The Johns Hopkins University Press, Baltimore, MD. pp. 1-166.

Massicotte, C., Inzana, K.D., Ehrich, M., and Jortner, B.S. (1999). Neuropathologic effects of phenylmethylsulfonyl fluoride (PMSF)-induced promotion and protection in organophosphorus ester-induced delayed neuropathy (OPIDN) in hens. *Neurotoxicology* 20, 749-760.

Noraberg, J., Kristensen, B.W., and Zimmer, J. (1999). Markers for neuronal degeneration in organotypic slice cultures. *Brain Res. Brain Res. Protoc.* 3, 278-290.

Prineas, J. (1969). The pathogenesis of dying-back polyneuropathies: Part I. An ultrastructural study of experimental tri-ortho-cresyl phosphate intoxication in the cat. *J. Neuropath. Expt. Neurol.* 28, 571-597.

Schmued, L.C. and Bowyer, J.F. (1997). Methamphetamine exposure can produce neuronal degeneration in mouse hippocampal remnants. *Brain Res.* 759, 135-140.

Schmued, L.C., Albertson, C., and Slikker Jr., W. (1997). Fluoro-Jade: a novel fluorochrome for the sensitive and reliable histochemical localization of neuronal degeneration. *Brain Res.* 751, 37-46.

Schmued, L.C., Slikker Jr., W., Clausing, P., and Bowyer, J. (1999). D-fenfluramine produces neuronal degeneration in localized regions of the cortex, thalamus, and cerebellum of the rat. *Toxicol. Sci.* 48, 100-106.

Schmued, L.C. and Hopkins, K.J. (2000). Fluoro-Jade: Novel fluorochrome for detecting toxicant-induced neuronal degeneration. *Toxicol. Pathol.* 28, 91-99.

Stumpf, A.M., Tanaka Jr., D., Aulerich, R.J., and Bursian, S.J. (1989). Delayed neurotoxic effects of tri-o-tolyl phosphate in the European ferret. *J. Toxicol. Env. Health* 26, 61-73.

Tanaka Jr., D. and Bursian, S.J. (1989). Degeneration patterns in the chicken central nervous system induced by ingestion of the organophosphorus delayed neurotoxin tri-ortho-tolyl phosphate. A silver impregnation study. *Brain Res.* 484, 240-256.

Tanaka Jr., D., Bursian, S.J., Lehning, E.J., and Aulerich, R.J. (1990). Exposure to triphenyl phosphite results in widespread degeneration in the mammalian central nervous system. *Brain Res.* 531, 294-298.

Tanaka Jr., D., Bursian, S.J., and Lehning, E.J. (1992). Neuropathological effects of triphenyl phosphite on the central nervous system of the hen (*Gallus domesticus*). *Fundam. Appl. Toxicol.* 18, 72-78.

Tanaka Jr., D., Bursian, S.J., and Aulerich, R.M. (1994). Age-related effects of triphenyl phosphite-induced delayed neuropathy on central visual pathways in the European ferret (*Mustela putorius furo*). *Fundam. Appl. Toxicol.* 22, 577-587.

Varghese, R.G., Bursian, S.J., Tobias, C., and Tanaka Jr., D. (1995a). Triphenyl phosphite-induced neuropathy in the avian forebrain: A silver impregnation study of the visual and auditory systems of the Japanese quail. *Neurotoxicol.* 16, 105-114.

Varghese, R.G., Bursian, S.J., Tobias, C., and D. Tanaka Jr., D. (1995b). Organophosphorus-induced delayed neurotoxicity: A comparative study of the effects of tri-ortho-tolyl phosphate and triphenyl phosphite on the central nervous system of the Japanese quail. *Neurotoxicol.* 16, 45-54.

Veronesi, B. and Dvergsten, C. (1987). Triphenyl phosphite neuropathy differs from organophosphorus-induced delayed neuropathy in rats. *Neuropathol. Appl. Neurobiol.* 13, 193-208.

Switzer III, R.C. (2000). Application of silver degeneration stains for neurotoxicity testing. *Toxicol. Pathol.* 28, 70-83.

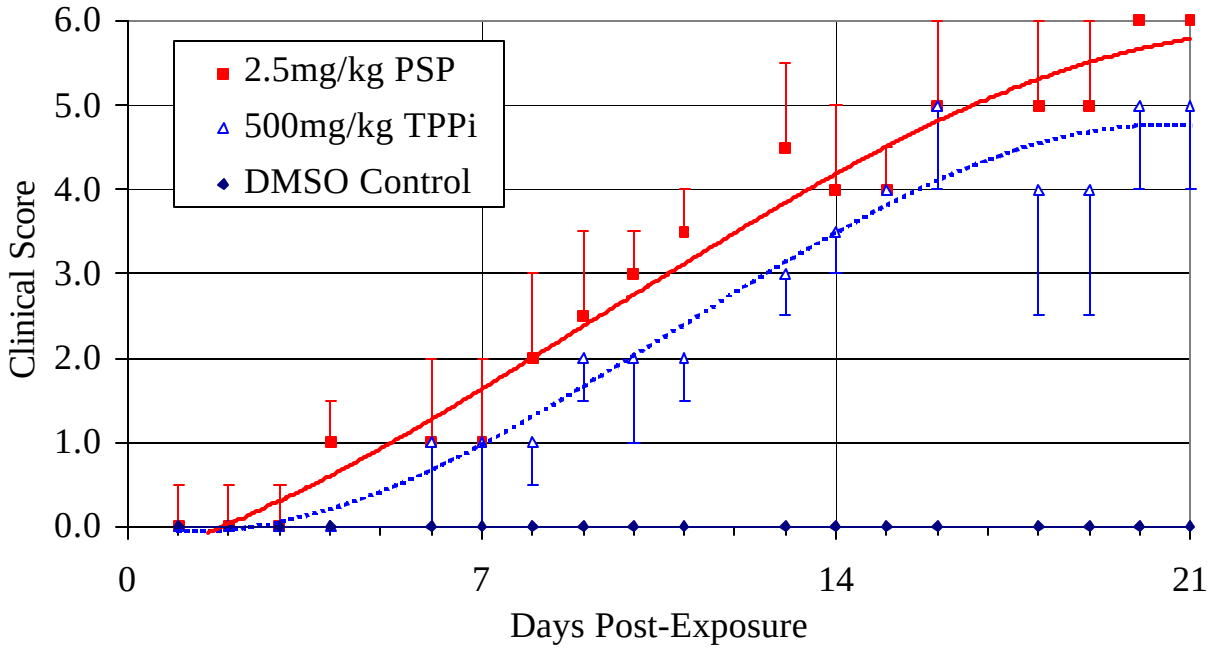

Figure 8.1. Clinical neurologic dysfunction assessed on a scale from 0 (no effect) to 6 (severe paralysis). Values are the median of 3 to 9 data points and are expressed as the median ± range. Increasing clinical scores reflect a progression to severe paralysis and are detailed in the Materials and Methods.

(*a*)

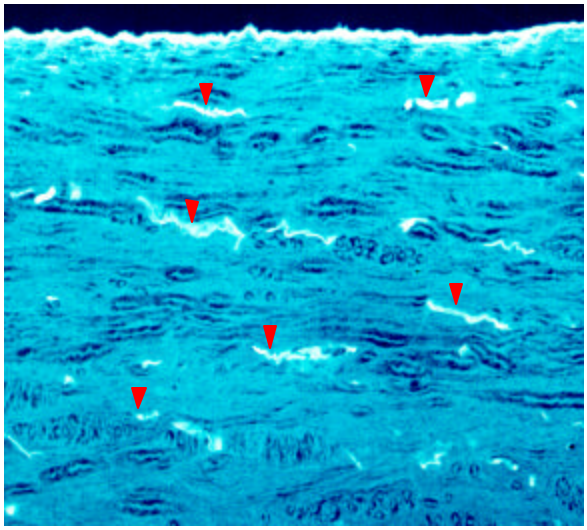

(*b*)

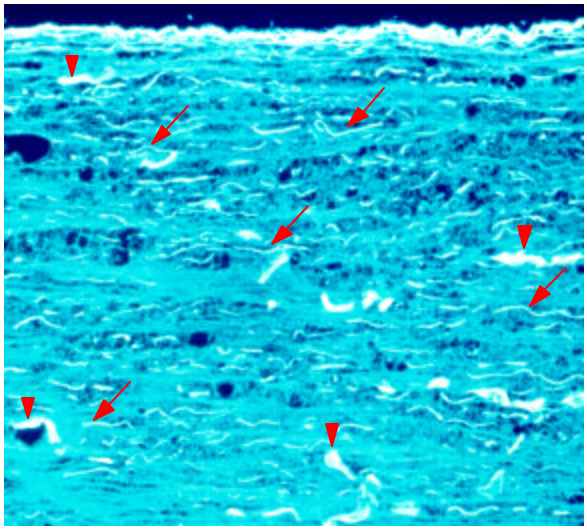

Figure 8.2. Fluoro-Jade fluorescence in control and TPPi-exposed spinal cord (SC) sections from postexposure day 21. Sections were deparaffinized, immersed in 0.06% (w/v) potassium permanganate, and then immersed for 30 min in the dark in a 0.001% (w/v) Fluoro-Jade staining solution. TPPi-induced spinal cord degeneration was similar in distribution but more extensive than PSP-induced degeneration (not shown). Fig. 8.2a, DMSO-exposed longitudinal section of cervical SC (approximate location dorsal C2-C3) (200X); Fig. 8.2b, TPPi-exposed longitudinal section of cervical SC (approximate location dorsal C2-C3) (200X). Arrowheads (◄) mark staining artifacts (capillaries, blood cells). Full arrows (◄——) indicate degenerating axons.

(*c*)

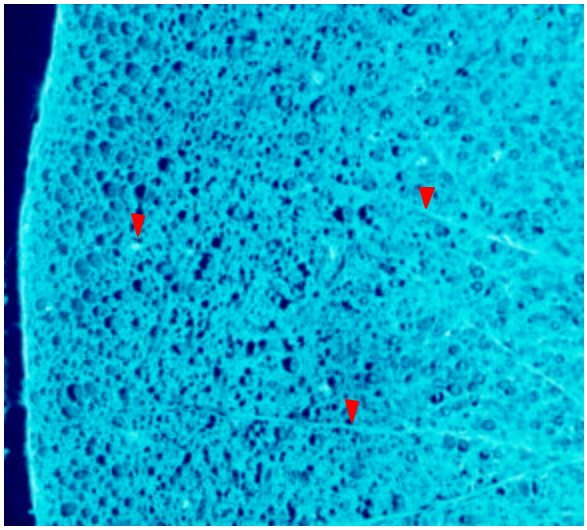

(*d*)

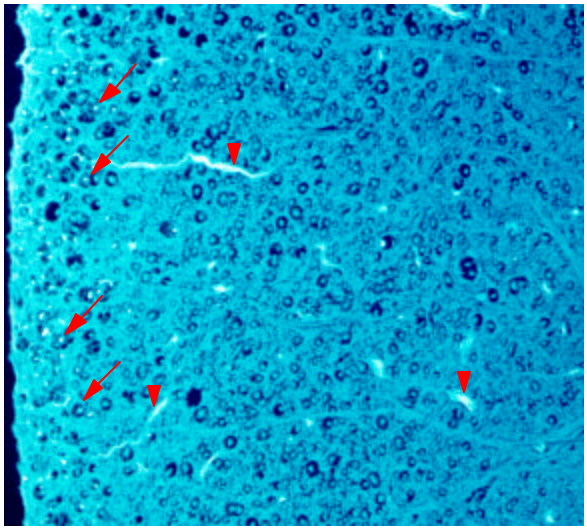

Figure 8.2. Fluoro-Jade fluorescence in control and TPPi-exposed spinal cord (SC) sections from postexposure day 21. Sections were deparaffinized, immersed in 0.06% (w/v) potassium permanganate, and then immersed for 30 min in the dark in a 0.001% (w/v) Fluoro-Jade staining solution. TPPi-induced spinal cord degeneration was similar in distribution but more extensive than PSP-induced degeneration (not shown). Fig. 8.2c, DMSO-exposed transverse section of lumbar spinocerebellar tracts (100X); Fig. 8.2d, TPPi-exposed transverse section of lumbar spinocerebellar tracts (100X). Arrowheads (◀) mark staining artifacts (capillaries, blood cells). Full arrows (←) indicate degenerating axons.

(*e*)

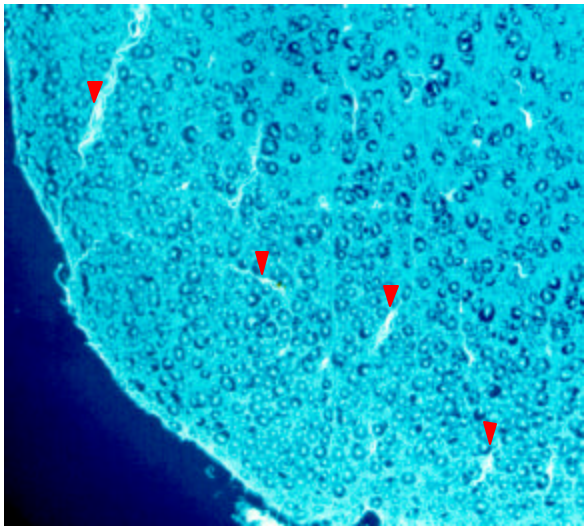

(*f*)

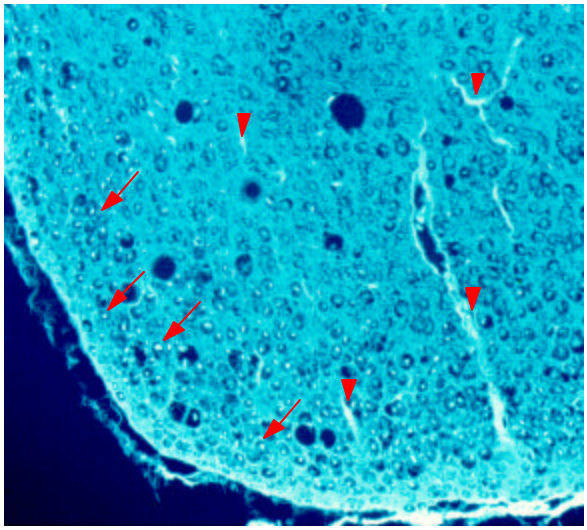

Figure 8.2. Fluoro-Jade fluorescence in control and TPPi-exposed spinal cord (SC) sections from postexposure day 21. Sections were deparaffinized, immersed in 0.06% (w/v) potassium permanganate, and then immersed for 30 min in the dark in a 0.001% (w/v) Fluoro-Jade staining solution. TPPi-induced spinal cord degeneration was similar in distribution but more extensive than PSP-induced degeneration (not shown). Fig. 8.2e, DMSO-exposed transverse section of lumbar medial-pontine tracts (100X); Fig. 8.2f, TPPi-exposed transverse section of lumbar medial-pontine tracts (100X). Arrowheads (◀) mark staining artifacts (capillaries, blood cells). Full arrows (←) indicate degenerating axons.

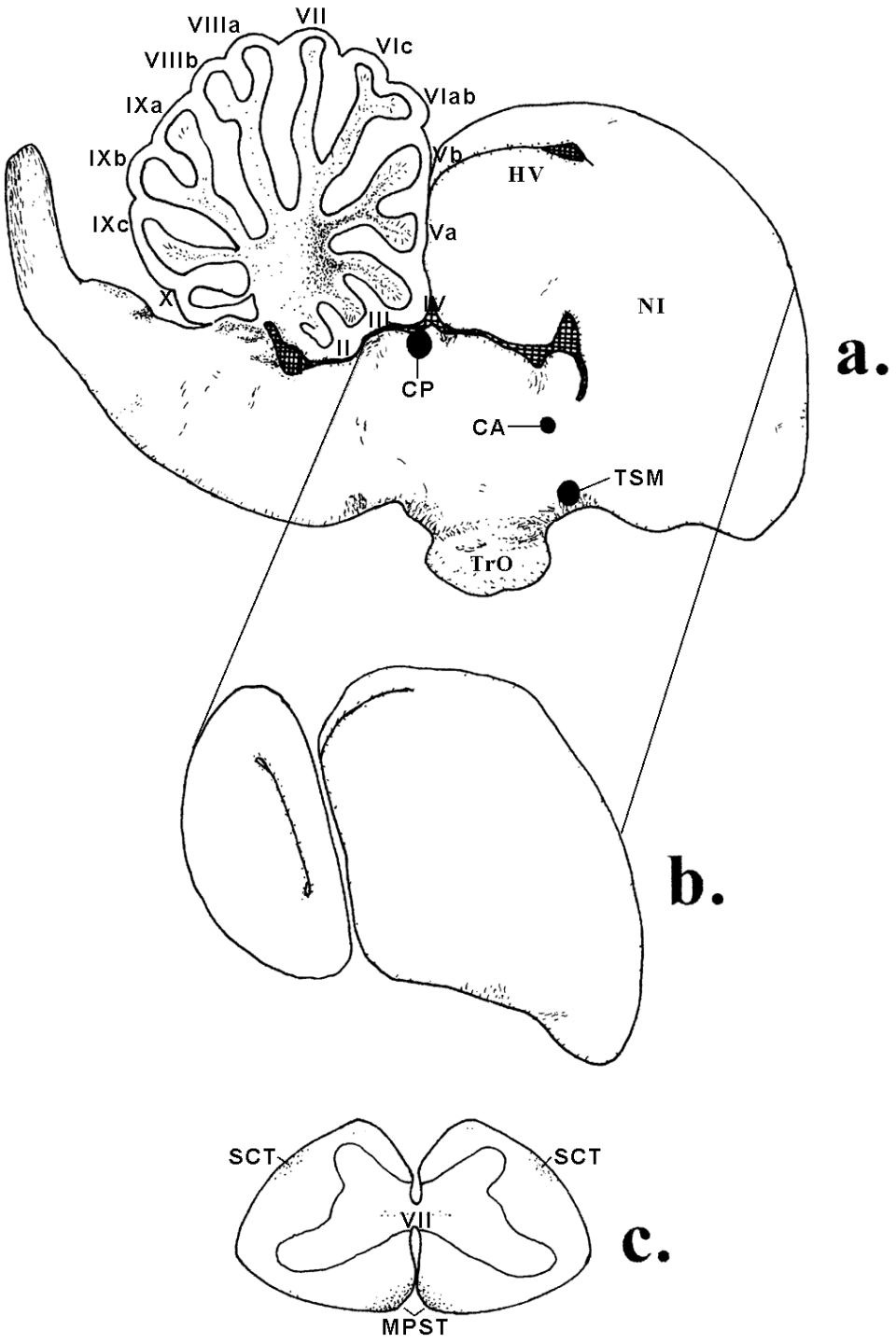

Figure 8.3. Composite drawings of OP compound-induced neuron terminal (stipples), cell body (heavy dots), and tract (dashes) degeneration in parasaggital views of the brain and coronal sections of the lumbar spinal cord of a hen. Drawings were made from original notes on all sections from postexposure days 7, 14 and 21. Fig. 8.3a, PSP, parasagittal section of the brain; Fig. 8.3b, PSP, parasagittal section of the forebrain and optic tectum; Fig. 8.3c, PSP, transverse section of the lumbar spinal cord.

Abbreviations: CA - Commisura anterior, CP - Commisura posterior, HV - Hyperstriatum ventrale, MPST - Medial-pontine spinal tract, NI - Neostriatum intermedium, SCT - Spinocerebellar tract, TrO - Tractus opticus, TSM - Tractus septomesencephalicus

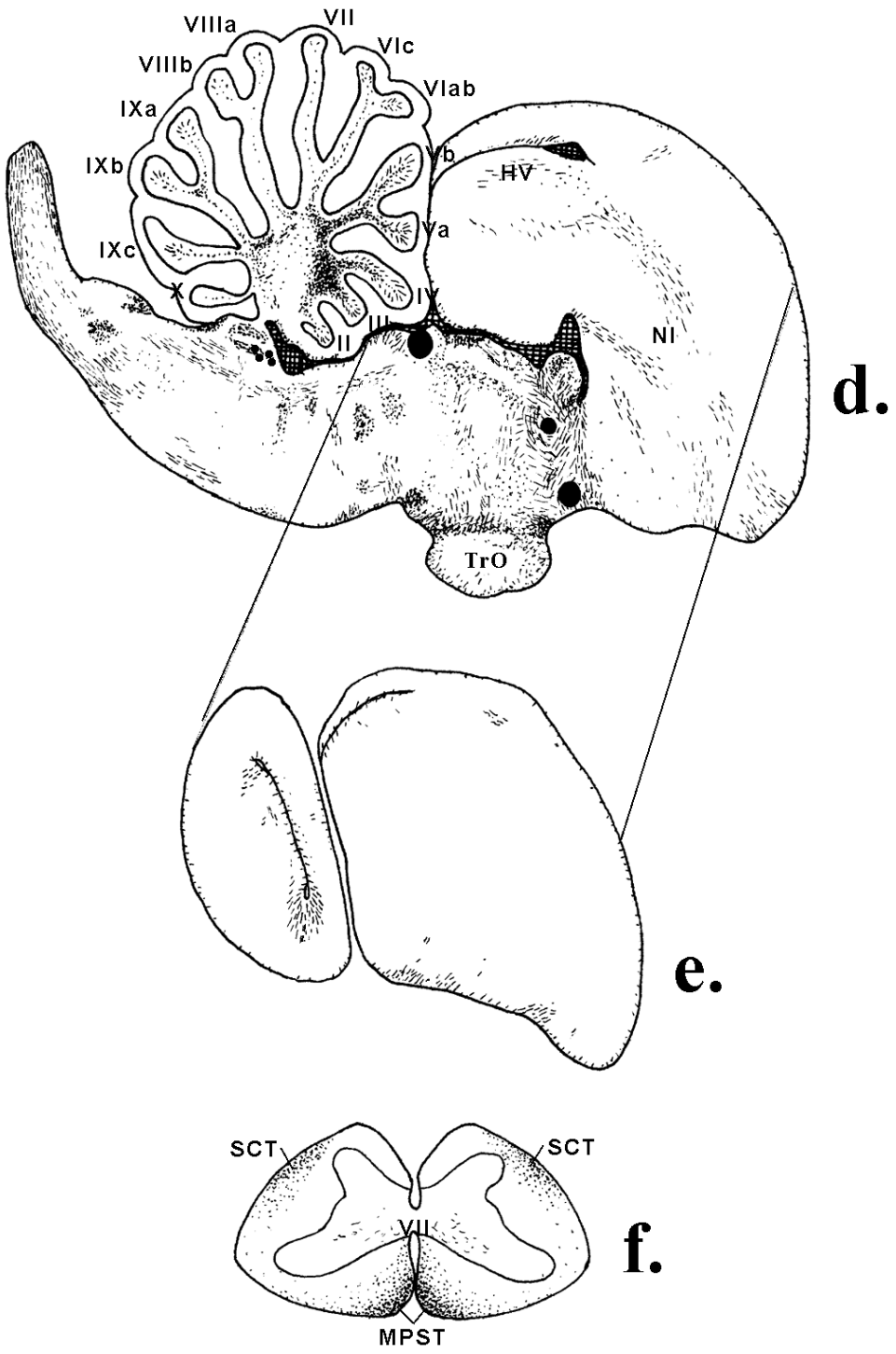

Figure 8.3. Composite drawings of OP compound-induced neuron terminal (stipples), cell body (heavy dots), and tract (dashes) degeneration in parasaggital views of the brain and coronal sections of the lumbar spinal cord of a hen. Drawings were made from original notes on all sections from postexposure days 7, 14 and 21. Fig. 8.3d, TPPi, parasagittal section of the brain; Fig. 8.3e, TPPi, parasagittal section of the forebrain and optic tectum; Fig. 8.3f, TPPi, transverse section of the lumbar spinal cord.

Abbreviations: CA - Commisura anterior, CP - Commisura posterior, HV - Hyperstriatum ventrale, MPST - Medial-pontine spinal tract, NI - Neostriatum intermedium, SCT - Spinocerebellar tract, TrO - Tractus opticus, TSM - Tractus septomesencephalicus

Chapter 9

The Mode of Cell Death (Apoptosis versus Oncotic Necrosis) in Organophosphorus Compound-induced Delayed Neurotoxicity (OPIDN) in White Leghorn Hens

Kent Carlson, Bernard S. Jortner, and Marion Ehrich

Virginia-Maryland Regional College of Veterinary Medicine,
Blacksburg, Virginia, 24061

ABSTRACT

Certain organophosphorus (OP) compounds induce a delayed neuropathy (OPIDN) that involves the death of central nervous system tissue. This study evaluated the mode of cell death in parasagittal brain and cervical spinal cord and transverse lumbar spinal cord tissue sections of white Leghorn hens undergoing OPIDN. Three methods; a TdT-FragEL™ DNA fragmentation kit, a monoclonal antibody to single-stranded DNA (F7-26), and Hoechst 33342 dye staining (10µg/ml) were used to determine apoptosis and necrosis, apoptosis, and apoptosis, respectively, in histopathological sections prepared previously (Chapter 8). All hens exposed to OP compounds demonstrated clinical signs of OPIDN and had time-dependent degeneration in axons, terminals, and perikarya in central nervous system tissue as assessed by Fluoro-Jade (Chapter 8). In the present study, obvious patterns of perikaryal nuclear degradation were not observed following analysis of sections from each staining technique, even though positive controls were successfully generated. This suggested that 1) there may have been little or no cell death occurring in OPIDN at the designated sample times and places or 2) that methodological problems need to be resolved before accurate descriptions of OPIDN-induced *in vivo* cell death can occur.

INTRODUCTION

Organophosphorus (OP) compounds are used as insecticides, plasticizers, plastic softeners, flame retardents, antioxidants, and hydraulic fluids (Mochida *et al.*, 1988; Katoh *et al.*, 1990; Mortensen and Ladefoged, 1992; Ware, 1994; Aspelin, 1997; Weiner and Jortner, 1999).

Certain OP compounds can induce an acute toxic response via the inhibition of acetylcholinesterase (AChE; Abou-Donia, 1995). Pathological developments can also occur following exposure to some OP compounds (Baron 1981; Abou-Donia and Lapadula, 1990; Abou-Donia, 1995, Weiner and Jortner, 1999). Of these later effects, neuropathic (Carrington *et al.*, 1988; Veronesi and Pope, 1990, Funk *et al.*, 1994), myopathic (Cavanagh, 1964; Dettbarn, 1984), and cardiomyopathic (McLeod, 1985; Singer *et al.*, 1987; Baze, 1993) sequelae are attributed to necrotic processes.

Neuropathic changes occur in the central and peripheral nervous system and are termed organophosphate-induced delayed neuropathy (OPIDN). The distribution of neuropathy is dependent on chemical characteristics of the OP compound and has led to the distinction of two forms (Type-I and Type-II) which are typified by exposures to phenyl saligenin phosphate (PSP) and triphenyl phosphite (TPPi), respectively (Abou-Donia, 1995).

Although neuropathic sequela involved in OPIDN are described as necrotic, specific modes of cell death (apoptosis versus necrosis) have not been investigated. Other investigators (Akbarsha and Sivasamy, 1998; Hamm *et al.*, 1998) suggest that OP compounds may induce apoptotic processes following *in vivo* exposures.

This study evaluated the mode of cell death in white Leghorn hen brains and spinal cord following exposure to the OP compounds PSP and TPPi. Regions of degeneration identified by Fluoro-Jade (Chapter 8) were stained on new sections with; a TdT-FragEL™ DNA fragmentation kit, a monoclonal antibody to single-stranded DNA (F7-26), and Hoechst 33342 dye (10µg/ml) to determine cells dying of apoptosis and necrosis, apoptosis, and apoptosis, respectively.

EXPERIMENTAL METHODS

Chemicals. Triphenyl phosphite (TPPi, 98% pure) was purchased from Chem Services (West Chester, PA). Phenyl saligenin phosphate (PSP; 99% pure) was synthesized by Lark Enterprises (Webster, MA). Dimethyl sulfoxide was obtained from Sigma (St. Louis, MO). Sodium pentobarbital was purchased from Veterinary Laboratories, Inc. (Lenexa, Kansas). Organophosphorus (OP) compounds were diluted in DMSO the same day (TPPi, 1000mg/ml) or diluted and stored at 23°C for three days (PSP, 5mg/ml) prior to dosing hens.

Animal Maintenance, Dosing, and Sacrifice. White Leghorn hens (>10 months old, 1.5 - 1.9kg) obtained from the Department of Animal and Poultry Science (Virginia Polytechnic Institute and State University) were housed in groups of four in wire cages (57 x 84 x 61cm) and fed and watered *ad libitum*.

Nine hens were randomly assigned to each treatment group (PSP, 2.5mg/kg; TPPi, 500mg/kg; and DMSO, 0.5ml/kg), dosed subcutaneously (DMSO, TPPi) or intramuscularly (DMSO, PSP), and then returned to cages with similarly dosed birds. Hens within treatment groups were then assigned sacrifice dates randomly (7, 14, or 21 days). Hens disabled by paralysis at later timepoints were fed and watered manually on a daily basis.

On the sacrifice date, hens were euthanatized with sodium pentobarbital (65mg/ml) via a brachial wing vein. Immediately following, the brain with attached cervical spinal cord and the lumbar spinal cord were carefully dissected free, sagittally sectioned, and one-half dropped into either ice-cold 10% neutral buffered formalin or methanol/PBS (6:1, v/v) fixatives.

Tissue Processing. Brain and lumbar spinal cord tissue were stored in formalin and methanol/PBS (at 4°C or -20°C, respectively) for 4 days. Methanol/PBS and formalin fixed samples were trimmed (parasagittal sections of brain, coronal sections of lumbar spinal cord) and sealed in tissue cassettes. Methanol/PBS fixed samples were further processed by dehydration in absolute methanol (x 2, 1 hr each) while formalin fixed samples were dehydrated by a graded series of alcohols. Both sets of tissues were then cleared with xylene and infiltrated with warm paraffin (56-63°C) under pressure in a Sakura-VIP "Tissue Tek" tissue processor (Torrance, CA). Tissues were then transferred to embedding molds and embedded in a Shandon Histo-Center 2 (Pittsburg, PA) machine. Sections (7µm) were cut from chilled paraffin blocks using a Leica 2030 rotary microtome (Deerfield, IL), attached to positively charged slides, incubated at 37-40°C for 4 hours, and then baked for 20-30 min at 60°C.

TdT-FragEL™ DNA Fragmentation Staining. Staining for DNA fragmentation using this method has been validated in studies using tissue from glioblastoma, colon and breast cancer, prostate tumors (Oncogene), rat decidual tissue (Gu *et al.*, 1994) and rat brain (Xiao and Bullock, 1996). Investigations using similar methods have demonstrated that this protocol detects both apoptotic and necrotic cells (Didenko *et al.*, 1996; Frankfurt *et al.*, 1996).

Formalin fixed sections were stained as recommended by the manufacturer (Oncogene™ Research Products, Cambridge, MA). Slides were deparaffinized by immersion in xylene for 15 minutes at room temperature (X3). These were rehydrated for 5 minutes each in a series of graded alcohols (100%, 100%, 90%, 80%, 70%) before rinsing with a Tris-Buffered Saline solution (TBS; 20mM Tris, pH 7.6, 140mM NaCl). The tissue on each slide was encircled with a hydrophilic slide marker and incubated in a 20µg/ml proteinase K - Tris solution at room temperature for 35 min. Slides were then rinsed in TBS, incubated for 5 minutes with 3% H_2O_2 at room temperature, washed in TBS, and equilibrated for 20 minutes in 1X TdT (terminal deoxynucleotidyl transferase) equilibration buffer (1M sodium cacodylate, 0.15M Tris, 1.5mg/ml BSA, 3.75mM $CoCl_2$, pH 6.6) at room temperature. A 1X TdT labeling reaction mix was subsequently added to slides and incubated at 37°C for 2.5 hours. After incubation, slides were rinsed in TBS and incubated with stop solution for 5 minutes (0.5M EDTA, pH 8) at room temperature. Slides were then incubated in a blocking buffer (4% BSA in PBS) for 10 minutes, and a 1X conjugate (peroxidase streptavidin) for 30 minutes at room temperature. Following a rinse in TBS, slides were incubated at room temperature for 15 minutes in a color development solution (0.7mg/ml 3, 3′Diaminobenzidine, 0.6mg/ml H_2O_2/urea, 1mM $NiCl_2$ in tap water), rinsed with distilled water, counterstained with 0.3% (w/v) methyl green, and coverslipped with DPX. Dark-brown to black stained areas (positive for apoptotic or necrotic DNA fragmentation) were identified using the Nikon Diaphot-TMD inverted microscope equipped with 10, 20, or 40X objectives.

A positive control slide included by the manufacturer (HL-60 leukemia cells exposed to 0.5µg/ml actinomycin D) was processed in parallel with sections from this study.

F7-26 Monoclonal Antibody to Single-Stranded DNA Staining. This method indirectly detects apoptosis-induced decreases in DNA thermal stability by staining for single-stranded DNA following immersion in a hot water bath. Staining with F7-26 is specific for the early stages of apoptosis prior to DNA fragmentation or nuclear condensation (Desjardins *et al.*, 1995; Frankfurt *et al.*, 1996).

Methanol/PBS fixed sections were stained for single-stranded DNA primarily as in Frankfurt *et al.* (1996). Sections were deparaffinized as above and then immersed in three changes of methanol/PBS (6:1 v/v) for 20 minutes each. Slides were then rinsed in a PBS-detergent solution (PBS without calcium or magnesium, 0.2% Triton X-100, 5mM $MgCl_2$), transferred to tubes containing PBS/5mM $MgCl_2$, and immersed in a 99°C water bath for 5 minutes. After immersion, the slides were quickly transferred into ice-cold PBS for 10 min, immersed in 3% H_2O_2, and then immersed in 0.1% (w/v) bovine serum albumin (Sigma) for 30 minutes. Slides were then incubated with the monoclonal antibody F7-26 (Alexis Corp; San Diego, CA), a biotin-conjugated rat anti-mouse antibody (Pharmingen; San Diego, CA), ExtraAvidin-peroxidase (Sigma), and DAB (Sigma) for 15 minutes each. Sections were counterstained with hematoxylin, air-dried, and then coverslipped using DPX. Darkly-brown stained areas (positive for apoptosis) were identified using the Nikon Diaphot-TMD inverted microscope equipped with 10, 20, or 40X objectives.

Positive control sections were generated as recommended by the manufacturer by incubating sections in a tube of distilled water during the 99°C water bath treatments. All other steps were the same.

Hoechst 33342 Nuclear Staining. Staining with Hoechst 33342 has been used to specifically detect apoptotic nuclei in previous *in vitro* investigations into OP compound-induced cell death (Carlson *et al.*, 2000). Others (Dive *et al.*, 1992; Cobb *et al.*, 1996) have also utilized this method to detect condensed apoptotic nuclei or apoptotic nuclear particles.

Methanol/PBS and formalin fixed slides were rehydrated as above and then stained for 15 min in the dark with 10µg/ml of the DNA specific fluorochrome, Hoechst 33342 (Molecular Probes; Eugene, OR). Slides were then rinsed in distilled water for 1 min (X 3), air-dried, dehydrated in xylene (X 3), and coverslipped with DPX. Degenerating regions identified by Fluoro-Jade staining (Chapter 8) were evaluated visually for apoptotic nuclear fragmentation or condensation using the Nikon Diaphot-TMD inverted microscope, a 20X fluorescence objective, and a "UV" filter cube. Documentation of representative nuclear morphologies in these degenerating areas were made with a Nikon Fe-2 camera (ASA200 Kodacolor film).

Analysis. Qualitative histochemical studies had 3 samples for each time point. The findings from all samples within each treatment were combined to illustrate the entire amount of cell death elicited by OP compounds.

RESULTS

These three staining methods were utilized to identify the mode of cell death (apoptosis versus oncotic necrosis) in parasaggital brain and transverse lumbar spinal cord sections of hens exposed to OP compounds that induce OPIDN.

TdT-FragEL™ DNA Fragmentation Staining. TdT staining was utilized in order to evaluate total cell death (apoptosis and oncotic necrosis) in histopathology sections.

The positive control slide had greater than 50% of the cells stain dark-brown or black. In contrast, cells unaffected by the treatment stained green with the methyl green counterstain. Darkly-stained and methyl-green stained cells were randomly arranged on this cell suspension slide preparation.

Tissue sections from hens with and without OPIDN stained light brown/green in an indiscriminate manner. No obvious pattern nor localization of cellular death could be demonstrated from these slides. In some cases, entire sections stained a uniform light brown/green color. In other cases, sections stained primarily green. In no circumstances were there nuclei or cells as darkly colored as in the positive control.

F7-26 Monoclonal Antibody to Single-Stranded DNA Staining. F7-26 staining was used in order to evaluate the amount of apoptotic cell death in histopathological sections.

Positive control sections qualitatively stained a darker shade of light brown than matched sections processed in parallel. Staining was random and ranged from uniform coverage of some areas to increased staining of tissue margins. In no circumstances were the nuclei exclusively stained.

Tissue sections from hens with and without OPIDN stained a light brownish red in random locations within each section. As with the positive control, some tissue areas were stained uniformly and others decreased in intensity from tissue margins inward.

Hoechst 33342 Nuclear Staining. Hoechst 33342 staining was used to identify apoptotic nuclear fragmentation or condensation.

When visualized with a fluorescent microscope, stained nuclei appeared bright white on a dark blue or black (cytosolic) background in both DMSO solvent control tissues and tissues from hens undergoing OPIDN. Neuronal nuclei were discriminated from erythrocyte nuclei by their larger sizes.

Inspection of tissue sections from hens with and without OPIDN revealed 3 nuclei in dorsal spinocerebellar regions of TPPi-treated hens that could have been construed as undergoing apoptosis (apoptotic nuclear condensation or nuclear particles). In addition, there was no evidence of localization or patterns associated with these occurrences.

DISCUSSION

This study evaluated the mode of cell death (apoptosis versus oncotic necrosis) in OPIDN in white Leghorn hens by utilizing three techniques that assess nuclear fragmentation and condensation. Areas in which perikaryal degeneration (death) was present had previously been identified using Fluoro-Jade, a novel stain for degenerating neural cells.

Results from all three staining methods were inconclusive as to the type of cell death (apoptosis or necrosis) involved in OPIDN. Both colorimetric stains (TdT and F7-26) revealed no instances of cell death even though positive controls for TdT staining worked well. Fluorescent staining for cell death worked adequately and neuronal nuclei were easily discriminated from background tissue and erythrocyte nuclei. Following a rapid survey of all sections, there were only three instances, all in the dorsal spinocerebellar region, in which increased fluorescence in nuclear structures may have been construed as an apoptotic form of cell death.

The apparent lack of cell death may be authentic. Authors have reported perikaryal degeneration and neuronal necrosis (Carrington *et al.*, 1988, Funk *et al.*, 1994, Varghese *et al.*, 1995a, 1995b) but have not definitively described whether the neurons are dead. Dead neurons may also have been phagocytosed or degraded to the extent that they were no longer recognized by detection assays. Crowe *et al.* (1997) reported that detection of neuronal apoptosis was difficult in *in vivo* rat and monkey models because few cells typically died and those that did were cleared in hours. This suggested that if apoptosis had occurred in OPIDN, a critical period for the detection of neuronal apoptosis may have been missed.

The inability to discern any cell death may also relate to the methods used. Positive control sections processed with F7-26 antibodies were darker than matched sections processed normally. The staining in both circumstances was diffuse and encompassed cytosolic and nuclear sites. Staining of single stranded DNA should have occurred primarily in the nucleus and indicated that there was little specificity for this stain. On F7-26 stained slides, the random distribution of staining from outer tissue margins to inner ones probably did not involve technical aspects of processing the slides (e.g. evaporation), because parafilm slide covers were used during the entire process to limit evaporation. Individual slide variations associated with staining probably were not associated with lab technique either, because all slides were processed in batches.

Inconclusive results in this series of investigations does not refute or support the hypothesis that cell death involved in OPIDN is apoptotic or necrotic. Critical re-evaluation of these parameters will undoubtedly reveal how much cell death occurs and which mode of death predominates in OPIDN.

ACKNOWLEDGMENTS

We wish to thank Linda Correll, Jason Hunt, Sandy Perkins, and Jill Songer for assistance with supplies, tissue processing, embedding, and sectioning. This work was supported by an EPA grant R825356 and funds from the Virginia-Maryland Regional College of Veterinary Medicine.

REFERENCES

Abou-Donia, M.B. and Lapadulla, D.M. (1990). Mechanisms of organophosphorus ester-induced delayed neurotoxicity: Type I and Type II. *Annu. Rev. Pharmacol. Toxicol.* 30, 405-440.

Abou-Donia, M.B. (1995). Chapter 13: Organophosphorus Pesticides. In *Handbook of Toxicology*. (Chang, L.W. and Dyer, R.S., eds). Marcel Dekker, Inc., New York. pp419-473.

Akbarsha, M.A. and Sivasamy, P. (1998). Male reproductive toxicity of phosphamidon: Histopathological changes in epididymis. *Ind. J. Exp. Biol.* 36, 34-38.

Aspelin, A.L. (1997). Pesticides industry sales and usage: 1994 and 1995 market estimates. *Biological and Economic Analysis Division, Office of Pesticide Programs, Office of Prevention, Pesticides and Toxic Substances.* U.S. Environmental Protection Agency. Washington D.C.

Baron, R.L. (1981). Delayed neurotoxicity and other consequences of organophosphate esters. *Ann. Rev. Entomol.* 26, 29-48.

Baze, W.B. 1993. Soman-induced morphological changes: An overview in the non-human primate. *J. Appl. Toxicol.* 13, 173-177.

Carlson, K., Jortner, B., and Ehrich, M. (2000). Organophosphorus compound-induced apoptosis in SH-SY5Y human neuroblastoma cells. *Toxicol. Appl. Pharmacol.* Accepted for publication.

Carrington, C.D., Brown, H.R., and Abou-Donia, M.B. (1988). Histopathological assessment of triphenyl phosphite neurotoxicity in the hen. *Neurotoxicology* 2, 223-234.

Cavanagh, J.B. (1964). Peripheral nerve changes in ortho-cresyl phosphate poisoning in the cat. *J. Pathol. Bacteriol.* 87, 365-383.

Cobb, J.P., Hotchkiss, R.S., Karl, I.E., and Buchman, T.G. (1996). Mechanisms of cell injury and death. *Br. J. Anaesth.* 77, 3-10.

Crowe, M.J., Bresnahan, C., Shuman, S.L., Masters, J.N., and Beattie, M.S. (1997). Apoptosis and delayed degeneration after spinal cord injury in rats and monkeys. *Nat. Med.* 3, 73-76.

Desjardins, L.M. and MacManu, J.P. (1995). An adherent cell model to study different stages of apoptosis. *Exp. Cell Res.* 216, 380-387.

Dettbarn, W.-D. (1984). Pesticide induced muscle necrosis: Mechanisms and prevention. *Fundam. Appl. Toxicol.* 4, S18-S26.

Didenko, V.V. and Hornsby, P.J. (1996). Presence of double-strand breaks with single-base 3′ overhangs in cells undergoing apoptosis but not necrosis. *J. Cell Biol.* 135, 1369-1376.

Dive, C., Gregory, C.D., Phipps, D.J., Evans, D.L., Milner, A.E., and Wyllie, A.H. (1992). Analysis and discrimination of necrosis and apoptosis (programmed cell death) by multiparameter flow cytometry. *Biochim. Biophys. Acta* 1133, 275-285.

Frankfurt, O.S., Robb, J.A., Sugarbaker, E.V., and Villa, L. (1996). Monoclonal antibody to single-stranded DNA is a specific and sensitive cellular marker of apoptosis. *Exp. Cell Res.* 226, 387-397.

Funk, K.A., Henderson, J.D., Liu, C.-H., Higgins, R.J., and Wilson, B.W. (1994). Neuropathology of organophosphate-induced delayed neuropathy (OPIDN) in young chicks. *Arch. Toxicol.* 68, 308-316.

Gu, Y., Jow, G.M., Moulton, B.C., Lee, C., Sensibar, J.A., Park-Sarge, O.K., Chen, J.T., and Gibori, G. (1994). Apoptosis in decidual tissue regression and reorganization. *Endocrinology* 135, 1272-1279.

Hamm, J.T., Wilson, B.W., and Hinton, D.E. (1998). Organophosphate-induced acetylcholinesterase inhibition and embryonic retinal cell necrosis *in vivo* in the teleost (Oryzias Latipes). *Neurotoxicology* 19, 853-870.

Katoh, K., Konno, N., Yamauchi, T., and Fukushima, M. (1990). Effects of age on susceptibility of chickens to delayed neurotoxicity due to triphenyl phosphite. *Pharmacol. Toxicol.* 66, 387-392.

McLeod Jr., C.G. (1985). Pathology of nerve agents: Perspectives on medical management. *Fundam. Appl. Toxicol.* 5, S10-S16.

Mochida, K., Gomyoda, M., Fujita, T., and Yamagata, K. (1988). Tricresyl phosphate and triphenyl phosphate are toxic to cultured human, monkey and dog cells. *Zbl. Bakt. Hyg. B.* 185, 427-429.

Mortensen, A. and Ladefoged, O. (1992). Delayed neurotoxicity of trixylenyl phosphate and a trialkyl/aryl phosphate mixture, and the modulating effect of atropine on tri-o-tolyl phosphate-induced neurotoxicity. *Neurotoxicology* 13, 347-354.

Singer, A.W., Jaax, N.K., Graham, J.S., and McLeod, C.G. (1987). Cardiomyopathy in soman and sarin intoxicated rats. *Toxicol. Lett.* 36, 243-249.

Stumpf, A.M., Tanaka Jr., D., Aulerich, R.J., and Bursian, S.J. (1989). Delayed neurotoxic effects of tri-o-tolyl phosphate in the European ferret. *J. Toxicol. Env. Health* 26, 61-73.

Varghese, R.G., Bursian, S.J., Tobias, C., and Tanaka Jr., D. (1995a). Triphenyl phosphite-induced neuropathy in the avian forebrain: A silver impregnation study of the visual and auditory systems of the Japanese quail. *Neurotoxicol.* 16, 105-114.

Varghese, R.G., Bursian, S.J., Tobias, C., and D. Tanaka Jr., D. (1995b). Organophosphorus-induced delayed neurotoxicity: A comparative study of the effects of tri-ortho-tolyl phosphate and triphenyl phosphite on the central nervous system of the Japanese quail. *Neurotoxicol.* 16, 45-54.

Veronesi, B. and Pope, C. (1990). The neurotoxicity of parathion-induced acetylcholinesterase inhibition in neonatal rats. *Neurotoxicology* 11, 609-626.

Ware, G.W. (1994). Chapter 4: Insecticides. In *The Pesticide Book, Fourth Edition* (G.W. Ware, Ed.), pp. 41-74. Thomson Publications, Fresno California.

Weiner, M.L. and Jortner, B.S. (1999). Organophosphate-induced delayed neurotoxicity of triarylphosphates. *Neurotoxicology* 20, 653-674.

Xiao, D. and Bullock, R. (1996). Effect of the novel high affinity glycine site NMDA antagonist ACEA 1021 upon ^{125}iodo-MK81 binding after subdural hematoma in the rat: an *in vivo* autoradiographic study. *J. Neurosurgery* 85, 655-661.

PART V

DISCUSSION AND CONCLUSION

Chapter 10

DISCUSSION

This dissertation detailed new information on the mode of cell death (Chapter 7), alterations in nuclear (Chapter 4, 5, and 7), mitochondrial (Chapter 5), proteolytic (Chapter 7), and cytoskeletal (Chapter 6) subcellular systems in SH-SY5Y human neuroblastoma cells exposed to six OP compounds (Fig. 0.1 and 0.2). These effects were investigated by utilizing a variety of techniques such as flow cytometry, fluorescence spectrophotometry and microscopy, colorimetric spectrophotometry, gel electrophoresis, and light and electron microscopy. Experiments revealed that OP compounds were not alike in their subcellular effects. Therefore, *in vitro* effects for each OP compound will be discussed separately in this chapter.

Information on the distribution and extent of PSP- and TPPi-induced brain and spinal cord degeneration (Chapter 8) was also generated as a prelude to assessing the mode of OP compound-induced cell death *in vivo* (Chapter 9).

Diisopropylphosphorofluoridate (DFP)

DFP did not elicit any significant changes in mitochondrial transmembrane potential, f-actin concentration, substrate adhesion, caspase activation, or nuclear fragmentation. In addition, there were no consistent trends for significant increases in protein concentration or decreases in DNA fragmentation. Later incubations did induce significant changes in the distribution of cells in the cell cycle, however. In the majority of circumstances, the proportion of G_0/G_1 and G_2/M phase cells increased at the expense of S phase cells (Table 10.1a, 10.1b, 10.1c). These changes in cell cycle status were mirrored by other OP compounds.

The relative lack of DFP-induced effects supported previous studies that have documented a lack of effect in a wide variety of subcellular systems or molecules such as ornithine decarboxylase (Pope *et al.*, 1995), inositol phosphate (Ehrich *et al.*, 1994), and catecholamine secretion or the incorporation of adenosine into ATP (Knoth-Anderson *et al.*, 1992). Cell cycle results, specifically a decrease in S phase cells, also supported observations from Hong *et al.* (1995), who documented decreases in DNA synthesis following exposure to DFP.

The lack of DFP-induced cytotoxicity contradicted data from Harvey and Sharma (1980) who observed significant death in neuroblastoma 2-A cultures following DFP exposure. Discrepancies in cytotoxic effects may relate to the culture model used. Suffys *et al.* (1988) and Sarin *et al.* (1993) reported that the use of DFP as an inhibitor of serine proteases protected two types of cells from receptor mediated cytotoxicity. Veronesi *et al.* (1997) also observed that SH-SY5Y cells were more resistant to cytotoxic effects than other neuroblastoma cell lines such as NB41A3.

(*a*)

1mM	0	7.5	15	30	60	120	240	480	960	1440	2880	4320	5760	7200
TMP	+	-	-	-	-	-	-	-	-	-	-			
FA	+	+	+	-	-	-	-	-	+	+	+			
SA	-	+	+	-	+	-	-	+	-					
CA	+									-	+			
DNA F	-	+	-	--	+	-	-	+	+	+	+	+	-	+
NUCF	+		-	+	+	+	+	+	-	+	+	+	+	
G0/G1								+	+	+	+	-	-	--
S								-	-	-	-	+	+	++
G2/M								-	+	+	+	+	+	++
PROT	+	+	--	+	+	+	++	+	+	+	-			

(*b*)

100uM	0	7.5	15	30	60	120	240	480	960	1440	2880	4320	5760	7200
TMP	+	+	-	-	-	+	-	-	-	-	-			
FA	-	-	-	-	-	-	-	-	-	-	-			
SA	-	+	-	-	+	+	-	-	-	+	+			
CA														
DNA F	-	-	-	-	-	-	-	-	-	-	-	-	--	-
NUCF	+		-	+	+	+	+	+	+	+	-	-	+	
G0/G1								+	+	+	+	+	++	+
S								-	-	-	-	-	--	+
G2/M								-	-	+	+	+	+	++
PROT	-	-	+	+	+	++	+	+	+	++	+			

(*c*)

10uM	0	7.5	15	30	60	120	240	480	960	1440	2880	4320	5760	7200
TMP														
FA														
SA														
CA														
DNA F										-	-	-	-	-
NUCF														
G0/G1										+	+	+	+	+
S										-	+	-	--	+
G2/M										+	+	+	+	++
PROT														

Table 10.1 Summary table for DFP-induced changes in mitochondrial transmembrane potential (TMP), f-actin concentration (FA), substrate adhesion (SA), caspase activation (CA), DNA fragmentation (DNAF), nuclear fragmentation (NUCF), the proportion of cells in G_0/G_1 phase of the cell cycle (G0/G1), the proportion of cells in S phase of the cell cycle (S), the proportion of cells in G_2/M phase of the cell cycle (G2/M), and the total protein concentration (PROT). Symbols represent values above (+) or below (-) controls. Cells with no symbols indicate times in which data was not gathered. Symbols also represent significantly higher (++) or significantly lower (--) values when compared to controls ($p<0.05$). Table 10.1a, 1mM DFP; Table 10.1b, 100µM DFP; Table 10.1c, 10µM DFP.

Paraoxon

Paraoxon elicited dose-dependent increases in mitochondrial hyperpolarization and then depolarization in SH-SY5Y cells immediately following exposure. Significant increases in the activation of caspase enzymes followed approximately a day later and preceded increases in DNA fragmentation and nuclear fragmentation. No significant changes were observed in substrate adhesion or protein synthesis. Combined results suggested that cytotoxic exposures to paraoxon were inducing a delayed, traditional apoptosis and eliminating SH-SY5Y human neuroblastoma cells from all phases of the cell cycle. Lower concentration exposures (100μM) also induced DNA fragmentation at longer incubation periods, but selectively increased G_0/G_1 and G_2/M while deleting S phase cells (Table 10.2a, 10.2b, 10.2c).

A variety of investigations have exhibited *in vitro* postexposure effects from paraoxon. Paraoxon has been shown to increase the sister chromatid exchange (SCE) rate (Sobti *et al.*, 1982; Herath *et al.*, 1989; Nishio and Uyeki, 1981), reduce DNA synthesis (Flaskos *et al.*, 1994), and increase RNA synthesis (Knoth-Anderson *et al.*, 1992). Accumulation of cells in either G_0/G_1 or G_2/M phase of the cell cycle as observed in this dissertation may explain the decrease in DNA synthesis observed by Flaskos *et al.* (1994). Increased DNA damage such as increases in the rate of SCE may also illustrate why cells accumulate in the G_0/G_1 or G_2 gap phases. Phase accumulation has been observed following exposure to many DNA damaging stimuli (Ko and Prives, 1996; Pellegata *et al.*, 1996). Increases in RNA synthesis may be resultant from the induction of apoptosis observed in this dissertation. This mode of cell death sometimes requires *de novo* protein production, and hence RNA synthesis (Donato and Perez, 1998). Significant increases in protein concentration following exposure to paraoxon were only observed once in this dissertation, however, and imply that other factors may be involved.

Cellular rounding and substrate detachment as reported in Nostrandt *et al.* (1992) were not observed following paraoxon exposure in this study. The results presented by Nostrandt *et al.* (1992) supported other observations reporting reduced neurite outgrowth and maintenance (Tuler and Bowen, 1989; Flaskos *et al.*, 1994) since cell attachment and filopodial (neurite) maintenance have been shown to be interrelated (Alberts *et al.*, 1994).

(*a*)

1mM	0	7.5	15	30	60	120	240	480	960	1440	2880	4320	5760	7200
TMP	+	+	++	++	+	+	-	-	-					
FA														
SA	+	-	-	-	-	-	-	-	-					
CA	+									++	++			
DNA F										+	+	++	++	++
NUCF	-		+	+	+	+	+	+	+	+	+	++	++	
G0/G1										-	-	--	--	--
S										+	+	-	--	--
G2/M										-	-	-	--	--
PROT	+	+	-	-	+	+	+	+	+	+	-			

(*b*)

100uM	0	7.5	15	30	60	120	240	480	960	1440	2880	4320	5760	7200
TMP	-	-	-	-	--	--	--	--	--					
FA														
SA	+	-	-	-	-	-	-	-	-					
CA														
DNA F										-	-	+	--	++
NUCF	+		-	+	+	+	+	-	+	+	-	++	-	
G0/G1										+	+	-	+	+
S										-	-	+	--	++
G2/M										+	-	-	+	++
PROT	+	+	+	+	+	++	+	+	+	++	+			

(*c*)

10uM	0	7.5	15	30	60	120	240	480	960	1440	2880	4320	5760	7200
TMP	-	+	+	+	+	+	+	-	+					
FA														
SA	+	-	+	-	-	+	+	+	-					
CA														
DNA F										-	-	+	-	+
NUCF														
G0/G1										-	-	+	+	++
S										-	+	-	--	+
G2/M										+	+	+	-	+
PROT														

Table 10.2 Summary table for paraoxon-induced changes in mitochondrial transmembrane potential (TMP), f-actin concentration (FA), substrate adhesion (SA), caspase activation (CA), DNA fragmentation (DNAF), nuclear fragmentation (NUCF), the proportion of cells in G_0/G_1 phase of the cell cycle (G0/G1), the proportion of cells in S phase of the cell cycle (S), the proportion of cells in G_2/M phase of the cell cycle (G2/M), and the total protein concentration (PROT). Symbols represent values above (+) or below (-) controls. Cells with no symbols indicate times in which data was not gathered. Symbols also represent significantly higher (++) or significantly lower (--) values when compared to controls ($p<0.05$). Table 10.2a, 1mM paraoxon; Table 10.2b, 100μM paraoxon; Table 10.2c, 10μM paraoxon.

Parathion

Parathion also elicited a dose-dependent increase in mitochondrial hyperpolarization in SH-SY5Y cells immediately following exposure. Cytotoxic concentrations (1mM) induced significant increases in nuclear fragmentation 16 hours later. This was followed by a significant decrease in the concentration of f-actin and an increase in the activation of caspase enzymes. A large but insignificant increase in DNA fragmentation occurred next. Unlike paraoxon, parathion induced significant increases in protein concentration over time. Like paraoxon, results suggested that cytotoxic exposures to parathion were inducing a delayed, traditional apoptosis. Parathion also induced the elimination of G_0/G_1 phase cells and a corresponding increase in S and G_2/M phase cells. This occurred more rapidly with parathion than with its esterase-inhibiting oxygen analog, paraoxon. Lower concentration parathion exposures (100μM) contrasted those with cytotoxic potential in that they increased the concentration of f-actin and G_0/G_1 phase cells and reduced the proportion of S phase cells. Nuclear fragmentation also occurred later with this concentration (Table 10.3a, 10.3b, 10.3c).

Parathion-induced increases in SCE frequency have been reported following noncytotoxic exposures (Chen *et al.*, 1981; Sobti *et al.*, 1982; Sobti *et al.*, 1982; Herath *et al.*, 1989; Nishio and Uyeki, 1981). The ability to induce SCE was greater with parathion alone than when it was co-incubated with a metabolic activating system (Chen *et al.*, 1982). Paraoxon has been shown to be the activated form of parathion and possesses less cytotoxic potential as determined in this dissertation. This fact implied that SCE rates and apoptosis were correlated. As mentioned with paraoxon, DNA damage (SCE) may have forced the cells exposed to parathion to accumulate in G_0/G_1 and decrease in S phase of the cell cycle. Similarly, increased SCE rates (DNA damage) may also account for the increased rates of apoptosis (Ko and Prives, 1996; Pellegata *et al.*, 1996) when compared to paraoxon. Parathion-induced significant increases in protein concentration may also be related to the execution of apoptosis as described earlier.

Antunes-Madeira *et al.* (1980) reported that parathion interferes with membrane lipid interactions and increases membrane permeability to noneletrolytes. Parathion-induced membrane alterations could have induced the inhibition of membrane depolarization and decreases in carbachol stimulated Ca^{2+} influx (Liu *et al.*, 1994) or increased receptor mediated ion currents (Veronesi *et al.*, 1997), since these factors are tightly regulated by plasma membrane status. Decreases in depolarization ability complemented observations of mitochondrial hyperpolarization in the dissertation. This factor, in addition to ionic dysregulation may have induced cytotoxic events leading to apoptosis (Fig. 0.4).

(*a*)

1mM	0	7.5	15	30	60	120	240	480	960	1440	2880	4320	5760	7200
TMP	+	+	++	++	++	++	++	++	++					
FA	+	-	-	-	-	+	+	-	-	--	--			
SA	-	-	+	-	+	+	+	-	-					
CA	+							+	+	-	++	++		
DNA F	-	+	-	--	+	-	-	+	+	+	+	+		
NUCF	+		-	+	+	+	+	+	++	++	++	++	+	
G0/G1								-	+	+	-	--		
S								+	-	-	+	++		
G2/M								-	+	+	+	+		
PROT	+	+	+	+	++	+	++	++	++	+	++			

(*b*)

100uM	0	7.5	15	30	60	120	240	480	960	1440	2880	4320	5760	7200
TMP	+	+	++	++	++	++	++	++	++					
FA	+	+	+	-	+	+	+	+	+	+	++			
SA	-	-	+	+	-	+	+	-	-					
CA	+									+	++			
DNA F	-	-	-	-	-	-	-	-	-	-	+			
NUCF	+		-	+	+	+	+	+	+	+	++	+	+	
G0/G1								+	+	+	+			
S								-	-	-	-			
G2/M								-	+	+	+			
PROT	++	+	+	+	++	++	+	++	+	++	+			

(*c*)

10uM	0	7.5	15	30	60	120	240	480	960	1440	2880	4320	5760	7200
TMP	-	-	+	+	-	+	+	-	+					
FA														
SA	+	-	-	+	+	+	+	-	+					
CA														
DNA F														
NUCF														
G0/G1														
S														
G2/M														
PROT														

Table 10.3 Summary table for parathion-induced changes in mitochondrial transmembrane potential (TMP), f-actin concentration (FA), substrate adhesion (SA), caspase activation (CA), DNA fragmentation (DNAF), nuclear fragmentation (NUCF), the proportion of cells in G_0/G_1 phase of the cell cycle (G0/G1), the proportion of cells in S phase of the cell cycle (S), the proportion of cells in G_2/M phase of the cell cycle (G2/M), and the total protein concentration (PROT). Symbols represent values above (+) or below (-) controls. Cells with no symbols indicate times in which data was not gathered. Symbols also represent significantly higher (++) or significantly lower (--) values when compared to controls ($p<0.05$). Table 10.3a, 1mM parathion; Table 10.3b, 100µM parathion; Table 10.3c, 10µM parathion.

Phenyl Saligenin Phosphate (PSP)

Exposure to the highest concentration of PSP (1mM) induced an immediate hyperpolarization in mitochondria and decreased the concentration of cytoskeletal f-actin. Substrate adhesion was then lost, cells started floating up into the media, and the relative amount of protein started to decrease. Apoptotic caspase activation and DNA fragmentation soon followed. Nuclear fragmentation or budding characteristic of traditional apoptosis was not seen in these exposures and suggested that an initiated apoptotic program had halted prior to completion. This led to the designation of this form of cytotoxicity as a Type II apoptosis or an apoptotic-necrosis. The intense cytotoxicity generated by this exposure led to a non-selective deletion of all cells without regard to cell cycle phase. Exposure to a lower concentration of PSP (100μM) induced a significant decrease in f-actin concentration followed by a loss of substrate adhesion and mitochondrial hyperpolarization. Significantly increased nuclear fragmentation and a decrease in total protein concentration occurred next and were followed by increases in the activation of caspases proteases and DNA fragmentation. As with 1mM exposures, the cytotoxic response led to a non-selective deletion of all cells without regard to cell cycle phase. Nuclear fragmentation into characteristic apoptotic particles indicated that the intensity of the cytotoxic exposure was less with lower concentrations. The lowest test concentration of PSP (10μM) also induced a cytotoxic response in SH-SY5Y cells. As with the other concentrations, mitochondrial hyperpolarization was observed immediately following exposure. Significant caspase activation and nuclear fragmentation was delayed until three days later and was followed by significant increases in DNA fragmentation. As with 100μM exposures, 10μM PSP exposures predominately induced an apoptotic form of cell death (Table 10.4a, 10.4b, 10.4c).

PSP-induced *in vitro* effects have not been extensively documented. Within the scope of the dissertation, PSP proved to be the most cytotoxic of all OP compounds. The intense cytotoxicity of PSP may relate to its ability to damage DNA. Tricresyl phosphate, a structural analog of PSP, has been shown to induce the formation of DNA adducts (Mentzschel *et al.*, 1993). As mentioned, DNA damage is directly related to the induction of apoptosis or phase accumulation. Since high concentrations of PSP induced rapid death that was not traditionally apoptotic, other factors, as yet unidentified, were probably involved. Significant selective depletion of G_0/G_1 phase cells by the least cytotoxic PSP exposure (10μM) also suggested that this compound was acting mechanistically different than others such as DFP, paraoxon, and parathion. Activation of receptor mediated ion currents (Veronesi *et al.*, 1997) may have contributed to PSP-induced mitochondrial hyperpolarization seen in this dissertation, but was unlikely to affect cytotoxicity caused by higher concentration exposures.

(*a*)

1mM	0	7.5	15	30	60	120	240	480	960	1440	2880	4320	5760	7200
TMP	-	+	++	++	++	++	++	++	++					
FA	-		--	--	--	--	--	--	--					
SA	+	-	-	-	-	--	--	--	--					
CA	+				+	+	+	+	+	++				
DNA F	-		-	--	-	--	+	+	-	++	++	++	++	++
NUCF	+		-	+	-	+	+	-	+	+	-	-	-	
G0/G1								--	--	-	--	--	--	--
S								-	-	+	--	--	--	--
G2/M								--	--	-	+	--	--	--
PROT	+	+	-	+	+	-	-	--	--	-	--			

(*b*)

100uM	0	7.5	15	30	60	120	240	480	960	1440	2880	4320	5760	7200
TMP	-	-	-	-	-	+	+	++	++					
FA	+		-	--	--	--	--	--	--					
SA	+	-	+	-	-	-	--	--	--					
CA	+							-		++	+	++		
DNA F	-		-	--	--	--	-	-	-	++	++	++	++	++
NUCF	+		-	+	+	+	+	++	++	+	-	-	-	
G0/G1								-	--	-	--	--	--	--
S								-	--	++		-	--	-
G2/M								--	--	-		--	-	--
PROT	+	-	+	+	+	+	-	--	--	--	--			

(*c*)

10uM	0	7.5	15	30	60	120	240	480	960	1440	2880	4320	5760	7200
TMP	-	-	+	+	++	+	+	+	+					
FA														
SA	+	-	+	-	-	-	-	-	--					
CA	+							-		+	+	++		
DNA F	-							+		+	+	+	+	++
NUCF												++	++	
G0/G1	+							+		-	-	--	-	--
S	-									+		+	-	+
G2/M	+									-		++	+	++
PROT														

Table 10.4 Summary table for PSP-induced changes in mitochondrial transmembrane potential (TMP), f-actin concentration (FA), substrate adhesion (SA), caspase activation (CA), DNA fragmentation (DNAF), nuclear fragmentation (NUCF), the proportion of cells in G_0/G_1 phase of the cell cycle (G0/G1), the proportion of cells in S phase of the cell cycle (S), the proportion of cells in G_2/M phase of the cell cycle (G2/M), and the total protein concentration (PROT). Symbols represent values above (+) or below (-) controls. Cells with no symbols indicate times in which data was not gathered. Symbols also represent significantly higher (++) or significantly lower (--) values when compared to controls ($p<0.05$). Table 10.4a, 1mM PSP; Table 10.4b, 100µM PSP; Table 10.4c, 10µM PSP.

Tri-ortho-tolyl Phosphate (TOTP)

Exposure to the highest concentration of TOTP (1mM) induced many effects similar to those seen with PSP. An immediate hyperpolarization in mitochondria and decreased the concentration of cytoskeletal f-actin followed administration of this compound. Apoptotic caspase activation occurred next and was followed by DNA fragmentation and then nuclear fragmentation. Unlike PSP, however, 1mM TOTP exposures did not induce a loss of substrate adhesion or protein concentration. Early cell death in these cultures was characterized by similar morphological and biochemical features as PSP, and suggested that an intrinsic apoptotic program had been forced to stop prior to completion. Remaining cells less affected by 1mM TOTP exposures, however, underwent traditional apoptosis in later incubation periods. As with PSP, 1mM TOTP non-selectively deleted cells without regard to cell cycle phase. Exposure to a lower concentration of TOTP (100μM) induced many of the same effects but at later incubation periods. Significant mitochondrial hyperpolarization was observed after 60 min of incubation. This was followed by a decrease in f-actin, caspase activation, nuclear fragmentation, and DNA fragmentation. Most cells at this concentration of exposure displayed traditionally apoptotic characteristics when dying. One hundred micromolar TOTP exposures also non-selectively deleted cells without regard to cell cycle phase (Table 10.5a, 10.5b, 10.5c).

TOTP was the second-most lethal OP compound utilized in this dissertation. Investigators have documented a variety of *in vitro* alterations following TOTP exposures. Morphological changes such as reduced neurite outgrowth were observed by Harvey and Sharma (1980) and Flaskos *et al.* (1994). Since f-actin is the primary constituent of filopodial (neuritic) extensions (Zigmond, 1996; Hall, 1998), it follows that any changes in neurite quality would be reflected in f-actin concentration. Decreased f-actin concentrations following TOTP exposures were observed in this dissertation and may account for neurite reduction seen by these authors. Cell substrate attachment and filopodial (neurite) maintenance have also been shown to be interrelated (Alberts *et al.*, 1994). Oddly enough, substrate attachment was not affected by TOTP-induced decreases in f-actin concentration. TOTP-induced neurite reduction has also been correlated to a decrease in metabolic activity and protein synthesis (Harvey and Sharma, 1980) and decreased synthesis of DNA (Flaskos *et al.*, 1994). Decreased protein levels were not, however, observed in this dissertation. Decreased DNA synthesis may have resulted from TOTP-induced DNA damage. Mentzschel *et al.* (1993) observed that TOTP was mutagenic following metabolic activation. As with PSP, TOTP-induced DNA damage may have contributed to the intensely cytotoxic reactions but probably were not wholly responsible for their initiation.

(*a*)

1mM	0	7.5	15	30	60	120	240	480	960	1440	2880	4320	5760	7200
TMP	+	+	++	++	++	++	++	++	+					
FA	+		--	--	--	--	--	--	--					
SA	-	-	-	-	-	-	-	-	-					
CA	+							++	++	++	++	++		
DNA F	-		-	-	-	-	-	+	++	+	+	++	++	++
NUCF	+		+	-	+	+	+	+	+	++	++	++	++	
G0/G1								-	--	-	--	--	--	--
S								+	-	+	++	++	--	-
G2/M								-	--	-	-	--	-	--
PROT	+	+	+	+	+	++	+	+	+	+	-			

(*b*)

100uM	0	7.5	15	30	60	120	240	480	960	1440	2880	4320	5760	7200
TMP	-	+	+	+	++	++	++	++	++					
FA	+		+	+	-	-	+	-	--					
SA	+	-	-	-	-	-	-	-	-					
CA	-									++	++			
DNA F	+		+	+	-	-	+	-	-	+	+	++	++	++
NUCF	+		-	+	+	+	+	+	+	+	++	++	+	
G0/G1								-	--	-	-	--	--	--
S								-	-	-	+	-	--	-
G2/M								-	-	-	-	-	--	--
PROT	+	+	+	+	+	++	+	+	+	+	+			

(*c*)

10uM	0	7.5	15	30	60	120	240	480	960	1440	2880	4320	5760	7200
TMP	-	-	-	-	-	-	-	-	+					
FA														
SA	-	-	-	-	-	-	-	-	-					
CA														
DNA F										-	-	-	-	+
NUCF												+	+	
G0/G1										-	+	+	++	+
S										-	+	+	-	-
G2/M										+	-	-	-	-
PROT														

Table 10.5 Summary table for TOTP-induced changes in mitochondrial transmembrane potential (TMP), f-actin concentration (FA), substrate adhesion (SA), caspase activation (CA), DNA fragmentation (DNAF), nuclear fragmentation (NUCF), the proportion of cells in G_0/G_1 phase of the cell cycle (G0/G1), the proportion of cells in S phase of the cell cycle (S), the proportion of cells in G_2/M phase of the cell cycle (G2/M), and the total protein concentration (PROT). Symbols represent values above (+) or below (-) controls. Cells with no symbols indicate times in which data was not gathered. Symbols also represent significantly higher (++) or significantly lower (--) values when compared to controls ($p<0.05$). Table 10.5a, 1mM TOTP; Table 10.5b, 100µM TOTP; Table 10.5c, 10µM TOTP.

Triphenyl Phosphite (TPPi)

Exposure to the highest concentration of TPPi (1mM) induced an immediate hyperpolarization in mitochondria which preceded a decrease in the concentration of cytoskeletal f-actin. Increased nuclear fragmentation was later observed and followed by a loss of substrate adhesion and protein concentration, activation of caspase proteases, and an increase in DNA fragmentation. Cells in the G_0/G_1 phase of the cell cycle were selectively eliminated by apoptotic death following exposure to 1mM TPPi. Exposure to a lower concentration of TPPi (100µM) also induced immediate mitochondrial hyperpolarization and a subsequent decrease in f-actin. This preceded delayed increases in DNA fragmentation which occurred 4 days later. The mode of cell death induced by 100µM TPPi was also apoptotic in nature. This concentration, however, induced the eradication of S and G_2/M phase cells (Table 10.6a, 10.6b, 10.6c).

TPPi-induced alterations in *in vitro* culture systems have been described in limited fashion. Knoth-Anderson *et al.* (1992) disclosed that TPPi elicited damage to the cell soma and caused mitochondrial impairment and a retraction of filopodial extensions over time. A reduction in neurites (filopodia) was also reported by Flaskos *et al.* (1994). As explained previously, a loss of neuritic extensions may be due to decreases in f-actin concentration. Retraction of the neuritic extensions may also have induced decreases in substrate adhesion reported in this dissertation. Damage to the cell soma correlated well to the induction of delayed apoptosis by TPPi in this dissertation and may also have accounted for the reductions in DNA synthesis observed by Flaskos *et al.* (1994). TPPi-induced damage to DNA synthetic machinery is not supported by dissertation results from investigations into OP compound-induced changes in the cell cycle. The proportion of cells in S phase of the cycle actually increased following cytotoxic (1mM) exposures.

Decreased catecholamine secretion was observed following exposure to TPPi in bovine adrenomedullary cells (Knoth-Anderson *et al.*, 1992; Knoth-Anderson and Abou-Donia, 1993). These observations refute suppositions that neurosecretion is modulated by the depolymerization of f-actin filaments (Viviani *et al.*, 1996). A loss of f-actin concentration, as observed in the dissertation, should have resulted in increased neurosecretion. Differences in response may have to do with particular neurosecretory characteristics of the bovine chromaffin cells.

(*a*)

1mM	0	7.5	15	30	60	120	240	480	960	1440	2880	4320	5760	7200
TMP	-	++	++	++	++	++	++	++	--	--	-			
FA	-	-	-	-	-	-	--	--	--	--	--			
SA	-	+	+	+	+	+	-	-	-	-	--			
CA	+							+	+	+	++	++		
DNA F	-	-	-	-	+	-	+	+	+	+	++	++	++	++
NUCF	+		+	+	-	+	+	+	+	++	+	++	++	
G0/G1								-	-	-	-	--	--	--
S								+	+	+	+	++	--	-
G2/M								-	-	+	+	++	+	-
PROT	+	+	+	+	++	+	+	+	+	+	--			

(*b*)

100uM	0	7.5	15	30	60	120	240	480	960	1440	2880	4320	5760	7200
TMP	-	+	++	++	++	++	++	+	--	--	-			
FA	-	-	-	-	-	-	--	-	-	-	-			
SA	+	-	-	-	+	-	-	-	+	+	-			
CA														
DNA F	-	-	-	-	-	-	-	-	-	+	+	-	--	+
NUCF	+		-	+	+	+	+	+	+	+	-	+	+	
G0/G1								+	+	+	+	+	++	-
S								-	-	-	-	+	-	-
G2/M								-	-	-	+	-	-	+
PROT	++	+	+	++	+	++	+	+	+	++	+			

(*c*)

10uM	0	7.5	15	30	60	120	240	480	960	1440	2880	4320	5760	7200
TMP														
FA														
SA														
CA														
DNA F										-	-	-	-	-
NUCF												-	+	
G0/G1										+	+	+	+	-
S										-	+	-	-	+
G2/M										-	-	+	-	+
PROT														

Table 10.6 Summary table for TPPi-induced changes in mitochondrial transmembrane potential (TMP), f-actin concentration (FA), substrate adhesion (SA), caspase activation (CA), DNA fragmentation (DNAF), nuclear fragmentation (NUCF), the proportion of cells in G_0/G_1 phase of the cell cycle (G0/G1), the proportion of cells in S phase of the cell cycle (S), the proportion of cells in G_2/M phase of the cell cycle (G2/M), and the total protein concentration (PROT). Symbols represent values above (+) or below (-) controls. Cells with no symbols indicate times in which data was not gathered. Symbols also represent significantly higher (++) or significantly lower (--) values when compared to controls ($p<0.05$). Table 10.6a, 1mM TPPi; Table 10.6b, 100µM TPPi; Table 10.6c, 10µM TPPi.

CONCLUSIONS

The hypotheses put forth was designed to evaluate the mode of cell death (apoptosis versus oncotic necrosis), two potential initiation sites for cytotoxicity (nucleus and mitochondria), proteolytic effector activation (caspase), and cytoskeletal (f-actin) proteolysis following exposure to OP compounds. Six OP compounds were chosen for this study because they represented a spectrum of toxic and neuropathic effects following *in vivo* exposure.

Overall, our *in vitro* model supported primary hypotheses that cytotoxic concentrations of OP compounds elicited a predominately apoptotic response. Investigations also supported the secondary hypotheses that mitochondria were potential cytotoxic initiation sites and that proteolytic (caspase) activation would occur midway through the cytotoxic process. In contrast, experiments did not support the secondary hypotheses that nuclear changes could initiate cytotoxicity or that cytoskeletal f-actin degradation would occur late in the cytotoxic process.

In vitro subcellular alterations induced by non-neuropathic (paraoxon and parathion) and neuropathic (DFP, PSP, TOTP, TPPi) OP compounds could not be correlated to the *in vivo* development of OPIDN or their ability to inhibit NTE. Apoptosis, mitochondrial hyperpolarization followed by depolarization, and f-actin degradation induced by paraoxon and parathion was similar in onset and duration to those induced by PSP, TOTP, and TPPi. In addition, DFP, induced different subcellular effects *in vitro* than paraoxon and parathion, or PSP, TOTP, and TPPi in most circumstances. The distribution of cell cycle events (nuclear function) was the only subcellular parameter uniformly changed by all OP compounds capable of inducing OPIDN. These events were also changed by the non-neuropathic OP compounds, paraoxon and parathion. These results suggested that factors other than those directly involved in cell death (e.g. metabolism, systemic distribution of OP compounds) may have played an additional role in the etiology of OPIDN.

In addition, *in vitro* subcellular alterations induced by OP compounds could not be correlated to cholinergic effects seen *in vivo*. Subcellular changes induced by protoxicant OP compounds such as TOTP and parathion were greater than those elicited by active AChE inhibitors (PSP and paraoxon) in many cases. Similarly, DFP, an acute inhibitor of AChE *in vivo*, elicited subcellular effects different from all other compounds, regardless of their ability to inhibit AChE. This suggested that factors involved in the accumulation and distribution of neurotransmitters such as acetylcholine were not involved in OP compound-induced cell death.

Investigations designed to clarify the mode of OP compound-induced cell death *in vivo* revealed discrete neuronal degenerative patterns in excess of that previously recorded. These results did not unequivocally determine the mode of cell death involved, but provided an initiation point for further investigations.

This dissertation created many avenues for future research since it combined the fields of pesticide exposure with that of cell death. In the dissertation, OP compounds induced cells to undergo *in vitro* apoptosis. Similar results were not generated in *in vivo* studies and need to be repeated by

others in different manners to conclude that cell death does not occur in OPIDN. The *in vitro* apoptotic response was modulated by compounds that affected receptor signaling, mitochondrial function, and proteolytic activity. These responses were not explored in depth and merit more investigation. Other potential cell death pathways such as those initiated through plasma membrane or cytoskeletal disturbances and perturbations in basic cellular functions such as metabolism, calcium flux, and plasma membrane permeability also need to be investigated, since these impact the mode and extent of cell death. Future investigations could also be designed to clarify *in vitro* responses of cell models to controls or metabolites (fluorine, para-nitrophenol) not used in these studies. This would clarify whether the cells were responding to the OP compounds or other factors.

Once basic cellular events following OP compound exposure have been delineated, investigations into molecular markers of cell death, such as p53, p21, Bcl-2, Bax, pRb, c-Jun, c-Fos, c-Myc could be initiated. This would fine tune the temporal sequence of events following OP compound exposure. In addition, if *in vivo* studies also demonstrated cell death and such changes, this would provide potential molecular sites for therapeutic intervention and amelioration of OPIDN.

PART VI

GENERAL REFERENCES

REFERENCES

Abou-Donia, M.B., Makkawy, H.-A., and Graham, D.G. (1982). Coumaphos: Delayed neurotoxic effect following dermal administration in hens. *J. Toxicol. Environ. Health* 10, 87-99.

Abou-Donia, M.B, Graham, D.G., Makkawy, H.-A., and Abdo, K.M. (1983). Effect of subchronic dermal application of O-ethyl O-4-nitrophenyl phenylphosphonothioate on producing delayed neurotoxicity in hens. *Neurotoxicol.* 4, 247-260.

Abou-Donia, M.B. (1993). The cytoskeleton as a target for organophosphorus ester-induced delayed neurotoxicity (OPIDN). *Chem. Biol. Int.* 87. 383-393.

Abou-Donia, M.B. (1995). Chapter 13 Organophosphorus pesticides. In *Handbook of Toxicology*. Chang, L.W. and Dyer, R.S. (eds). pp419-473. Marcel Dekker, Inc., New York.

Alberts, B., Bray, D., Lewis, J., Raff, M., Roberts, K., and Watson, J.D. (1994). Chapter 16: The cytoskeleton. In *Molecular Biology of the Cell*, pp. 821-861. Garland Publishing, Inc., New York.

Al-Shatti, A.K.S., El-Desouky, M., Zaki, R., Al-Azem, M.A., and Al-Lagani, M. (1997). Health care for pesticide applicators in a locust eradication campaign in Kuwait (1988-1989). *Environ. Res.* 73, 219-226.

Antunes-Madeira, M.C., Carvalho, A.P., and Madeira, V.M.C. (1980). Effects of insecticides on thermotropic lipid phase transitions. *Pest. Biochem. Physiol.* 14, 161-169.

Aspelin, A.L. (1997). Pesticides industry sales and usage: 1994 and 1995 market estimates. Biological and Economic Analysis Division, Office of Pesticide Programs, Office of Prevention, Pesticides and Toxic Substances. pp1-35. *U.S. Environmental Protection Agency*. Washington D.C.

Baker, D.L., Reddy, U.R., Pleasure, D., Thorpe, C.L., Evans, A.E., Cohen, P.S., and Ross, A.H. (1989). Analysis of nerve growth factor receptor expression in human neuroblastoma and neuroepithelioma cell lines. *Cancer Res.* 49, 4142-4146.

Barber, J.R. and Verma, I.M. (1987). Modification of fos proteins: Phosphorylation of c-fos, but not v-fos, is stimulated by 12-tetradecanoyl-phorbol-13-acetate and serum. *Mol. Cell Biol.* 7, 2201-2211.

Barkett, M., Xue, D., Horvitz, H.R., and Gilmore, T.D. (1997). Phosphorylation of IκB-α inhibits its cleavage by caspase CPP32 *in vitro*. *J. Biol. Chem.* 272, 29419-29422.

Barnes, J.M. and Denz, F.A. (1953). Experimental demyelination with organo-phosphorus compounds. *J. Pathol. Bact.* 65, 597-605.

Biedler, J.L. and Spengler, B.A. (1976). Metaphase chromosome anomaly: Association with drug resistance and cell-specific products. *Science.* 191, 185-187.

Biedler, J.L., Spengler, B.A., Chang, T.-D., and Ross, R.A. (1988). Transdifferentiation of human neuroblastoma cells results in coordinate loss of neuronal and malignant properties. *Adv. Neuroblastoma Res.* 2, 265-276.

Booth, N.H. and McDonald, L.E. (eds)(1982). *Veterinary Pharmacology and Therapeutics*. pp1-1021. The Iowa State University Press. Ames, Iowa.

Bouldin, T.W. and Cavanagh, J.B. (1979a). Organophosphorus neuropathy: I. A teased-fiber study of the spatio-temporal spread of axonal degeneration. *Am. J. Pathol.* 94, 240-251.

Bouldin, T.W. and Cavanagh, J.B. (1979b). Organophosphorus neuropathy: II. A fine-structural study of the early stages of axonal degeneration. *Am. J. Pathol.* 94, 253-270.

Bursian, S., Flaga, C., and Ringer, R. (1982). The injection of the delayed neurotoxin tri-o-tolyl phosphate into embryonating chicken eggs and its effects on subsequent chick development. *J. Toxicol. Environ. Health* 10, 101-109.

Bursian, S.J., Brewster, J.S., and Ringer, R.K. (1983). Differential sensitivity to the delayed neurotoxin tri-o-tolyl phosphate in several avian species. *J. Toxicol. Environ. Health* 11, 907-916.

Carrington, C.D., Brown, H.R., and Abou-Donia, M.B. (1988). Histopathological assessment of triphenyl phosphite neurotoxicity in the hen. *Neurotoxicol.* 2, 223-234.

Cavalleri, A. and Cosi, V. (1980). Polyneuropathies in shoe factory workers. In Advances in Neurotoxicity, *Proceedings of the International Congress on Neurotoxicology*, Varese, Italy, 27-30 September 1979. Manzo, L., Léry, N., Lacasse, Y., and L. Roche (eds). pp193-200. Pergamon Press, Oxford.

Cece, R., Barajon, I., and Tredici, G. (1995). Cisplatin induces apoptosis in SH-SY5Y human neuroblastoma cell line. *Anticancer Res.* 15, 777-782.

Cengel, K.A., Godbout, J.P., and Freund, G.G. (1998). Phosphatidylinositol 3'-kinase is associated with a serine kinase that is activated by okadaic acid. *Biochem. Biophy. Res. Comm.* 242, 513-517.

Chemnitius, J.M., Hölling, M., Meyer, J.H., Schmidt, P.F., Schomburg, E.D., Steffens, H., and Zech, R. (1989). Influence of the organophosphorus compound DFP on inhibitory motor systems and esterase activity in the spinal cord of cats. *Neurosci. Res.* 6, 257-263.

Chen, H.H., Hsueh, J.L., Sirianni, S.R., and Huang, C.C. (1981). Induction of sister-chromatid exchanges and cell cycle delay in cultured mammalian cells treated with eight organophosphorous pesticides. *Mutat. Res.* 88, 307-316.

Cohen, P. (1982). The role of protein phosphorylation in neural and hormonal control of cellular activity. *Nature* 296, 613-620.

Copani, A., Bruno, V., Battaglia, G., Leanza, G., Pellitteri, R., Russo, A., Stanzani, S., and Nicoletti, F. (1995). Activation of metabotrophic glutamate receptors protects cultured neurons against apoptosis induced by β-amyloid peptide. *Mol. Pharmacol.* 47, 890-897.

Davidoff, A.M., Pence, J.C., Shorter, N.A., Iglehart, J.D., and Marks, J.R. (1992). Expression of p53 in human neuroblastoma- and neuroepithelioma-derived cell lines. *Oncogene.* 7, 127-133.

Davis, C.S. and Richardson, R.J. (1980). Organophosphorus compounds. In *Experimental and Clinical Neurotoxicology*. Spencer, P.S. and H.H. Schaumburg (eds) The Williams and Wilkins Company, Baltimore. pp532-533.

de Raat, W.K., Stevenson, H., Hakkert, B.C., and van Hemmen, J.J. (1997). Toxicological risk assessment of worker exposure to pesticides: Some general principles. *Reg. Toxicol. Pharmacol.* 25, 204-210.

Dunnington, E.A., Siegel, P.B., and Ehrich, M. (1989). Differences in response of chickens from two genetic lines to diisopropyl phosphorofluoridate. *Neurotoxicol.* 10, 71-78.

Dyer, K.R., Jortner, B.S., Shell, L.G., and Ehrich, M. (1992). Comparative dose-response studies of organophosphorus ester-induced delayed neuropathy in rats and hens administered mipafox. *Neurotoxicol.* 13, 745-756.

Ehrich, M., Briles, R.W., Briles, W.E., Dunnington, E.A., Martin, A., Siegel, P.B., and Gross, W.B. (1986). Neurotoxicity of triorthotolyl phosphate in chickens of different genotypes in the presence and absence of deoxycorticosterone. *Poultry Sci.* 65, 375-379.

Ehrich, M., Jortner, B.S., Taylor, D., Dunnington, E.A., and Siegel, P.B. (1993). Differences between genetic stocks of chickens in response to acute and delayed effects of an organophosphorus compound. *J. Toxicol. Environ. Health.* 39, 539-553.

Ehrich, M., Correll, L., and Veronesi, B. (1994). Neuropathy target esterase inhibition by organophosphorus esters in human neuroblastoma cells. *Neurotoxicol.* 15, 309-314.

Ehrich, M., Jortner, B.S., and Padilla, S. (1995a). Comparison of the relative inhibition of acetylcholinesterase and neuropathy target esterase in rats and hens given cholinesterase inhibitors. *Fundam. Appl. Toxicol.* 24, 94-101.

Ehrich, M., Correll, L., Carlson, K., Wilcke, J., and Veronesi, B. (1995b). Examination of culture conditions on esterase activities in human and mouse neuroblastoma cells. *In Vitro Toxicol.* 8, 199-207.

Ehrich, M. (1996). Neurotoxic esterase inhibition: Predictor of potential for organophosphorus-induced delayed neuropathy. Biomarkers for Agrochemicals and Toxic Substances. *ACS Symp. Ser.* 643, 79-93.

Ehrich, M., Correll, L., and Veronesi, B. (1997). Acetylcholinesterase and neuropathy target esterase inhibitions in neuroblastoma cells to distinguish organophosphorus compounds causing acute and delayed neurotoxicity. *Fundam. Appl. Toxicol.* 38, 1-9.

Ehrich, M. and Correll, L. (1998). Inhibition of carboxylesterases in SH-SY5Y human and NB41A3 mouse neuroblastoma cells by organophosphorus esters. *J. Toxicol. Environ. Health, Part A*. 53, 101-115.

El-Sebae, A.H., Soliman, S.A, Abo Elamayem, M., and Ahmed, N.S. (1977). Neurotoxicity of organophosphorus insecticides leptophos and EPN. *J. Environ. Sci. Health.* B12, 269-288.

EPA, (1996). Delayed neurotoxicity of organophosphorus substances following acute and 28-day exposure "Public Draft". United States Environmental Protection Agency Prevention, Pesticides and Toxic Substances (7101) EPA 712-C-96-237, Health Effects Test Guidelines. pp1-6.

Escartín, E. and Porte, C. (1996). Acetylcholinesterase inhibition in the crayfish *Procambarus clarkii* exposed to fenitrothion. *Ecotoxicol. Environ. Safety* 34, 160-164.

Fahraeus, R., Paramio, J.M., Ball, K.L., Lain, S., and Lane, D.P. (1996). Inhibition of pRb phosphorylation and cell-cycle progression by a 20-residue peptide derived from $p16^{CDKN2/INK4A}$. *Curr. Biol.* 6, 84-91.

Farage-Elawar, M., Duffy, J.S., and Francis, B.M. (1991). Developmental toxicity of desbromoleptophos in chicks: enzyme inhibition, malformations and functional deficits. *Neurotoxicol. Teratol.* 13, 91-97.

Fedalei, A. and Nardone, R.M. (1983). Volume 1: Product Safety Evaluation. Chapter 15. An *in vitro* alternative for testing the effect of organophosphates on neurotoxic esterase activity. In Alternative Methods in Toxicology. Goldberg, A.M. (ed). pp. 252-269. Mary Ann Liebert Inc., New York.

Fernando, J.C.R., Lim, D.K., Hoskins, B., and Ho, I.K. (1985). Variability of neurotoxicity of and lack of tolerance to the anticholinesterases soman and sarin in the rat. *Res. Comm. Chem. Pathol. Pharmacol.* 48, 415-430.

Flaskos, J., McLean, W.G., and Hargreaves, A.J. (1994). The toxicity of organophosphate compounds towards cultured PC12 cells. *Toxicol. Lett.* 70, 71-76.

Forsythe, I.D., Lambert, D.G., Nahorski, S.R., and Linsdell, P. (1992). Elevation of cytosolic calcium by cholinoceptor agaonists in SH-SY5Y human neuroblastoma cells: estimation of the contribution of voltage-dependent currents. *Br. J. Pharmacol.* 107, 207-214.

Funk, K.A., Henderson, J.D., Liu, C.-H., Higgins, R.J., and Wilson, B.W. (1994a). Neuropathology of organophosphate-induced delayed neuropathy (OPIDN) in young chicks. *Arch. Toxicol.* 68, 308-316.

Gilot-Delhalle, J., Colizzi, A., Moutschen, J., and Moutschen-Dahmen, M. (1983). Mutagenicity of some organophosphorus compounds at the *ade6* locus of *Schizosaccharomyces pombe*. *Mutat. Res.* 117, 139-148.

Greenman, S.B., Rutten, M.J., Fowler, W.M., Scheffler, L., Shortridge, L.A., Brown, B., Sheppard, B.C., Deveney, K.E., Deveney, C.W., and Trunkey, D.D. (1997). Herbicide/pesticide effects on intestinal epithelial growth. *Environ. Res.* 75, 85-93.

Haldar, S., Jena, N., and C.M. Croce, C.M. (1995). Inactivation of Bcl-2 by phosphorylation. *Proc. Nat. Acad. Sci. USA.* 92, 4507-4511.

Hammerling, U., Bjelfman, C., and Påhlman, S. (1987). Different regulation of N- and c-myc expression during phorbol ester-induced maturation of human SH-SY5Y neuroblastoma cells. *Oncogene.* 2, 73-77.

Hartley, C.L., Johnston, H.B., Nicol, S., Chan, K.M., Baines, A.J., Anderton, B.H., and Thomas, S.M. (1996). Phenotypic morphology and the expression of cytoskeletal markers during long-term differentiation of human SH-SY5Y neuroblastoma cells. *In Vitro Toxicol.* 10, 539-550.

Harvey, M.J. and Sharma, R.P. (1980). Organophosphate cytotoxicity: the effects on protein metabolism in cultured neuroblastoma cells. *J. Environ. Pathol. Toxicol.* 3, 423-436.

Hatch, R.C. (1982). Chapter 61: Poisons causing nervous stimulation or depression. In *Veterinary Pharmacology and Therapeutics.* Booth, N.H. and L.E. McDonald (eds). pp976-1021. The Iowa State University Press. Ames, Iowa.

Henschler, D., Schmuck, G., van Aerssen, M., and Schiffmann, D. (1992). The inhibitory effect of neuropathic organophosphate esters on neurite outgrowth in cell cultures: A basis for screening for delayed neurotoxicity. *In Vitro Toxicol.* 6, 327-335.

Herath, J.F., Jalai, S.M., Ebertz, M.J., and Martsolf, J.T. (1989). Genotoxicity of the organophosphorus insecticide malathion based on human lymphocytes in culture. *Cytologia.* 54, 191-195.

Hockenberry, D., Nuñez, G., Milliman, C., Schreiber, R.D., and Korsmeyer, S.J. (1990). Bcl-2 is an inner mitochondrial membrane protein that blocks programmed cell death. *Nature.* 348, 334-336.

Holmuhamedov, E.L., Kholmoukhamedova, G.L., and Baimuradov, T.B. (1996). Non-cholinergic toxicity of organophosphates in mammals: Interaction of ethaphos with mitochondrial functions. *J. Appl. Toxicol.* 16, 475-481.

Hong, S.-J., Rohde, B.H., and Chiou, G.C.Y. (1995). Use of C1300 neuroblastoma cells to evaluate the protective value of hexamethonium, trimethaphan, hemicholinium, and triethylcholine against diisopropyl phosphorofluoridate toxicity. *J. Pharmaceut. Sci.* 84, 65-70.

Itano, Y. and Nomura, Y. (1995). 1-methyl-4-phenyl-pyridinium ion (MPP+) causes DNA fragmentation and increases the Bcl-2 expression in human neuroblastoma, SH-SY5Y cells, through different mechanisms. *Brain Res.* 704, 240-245.

Itano, Y., Ito, A., Uehara, T., and Nomura, Y. (1996). Regulation of Bcl-2 protein expression in human neuroblastoma SH-SY5Y cells: Positive and negative effects of protein kinases C and A, respectively. *Journal of Neurochem.* 67, 131-137.

Jensen, L.M., Zhang, Y., and Shooter, E.M. (1992). Steady-state polypeptide modulations associated with nerve growth factor (NGF)-induced terminal differentiation and NGF deprivation-induced apoptosis in human neuroblastoma cells. *J. Biological Chem.* 267, 19325-19333.

Joksic, G., Vidakovic, A., and Spasojevic-Tisma, V. (1997). Cytogenetic monitoring of pesticide sprayers. *Environ. Res.* 75, 113-118.

Jortner, B.S. and Ehrich, M. (1987). Neuropathological effects of phenyl saligenin phosphate in chickens. *Neurotoxicol.* 8, 303-314.

Katoh, K., Konno, N., Yamauchi, T., and Fukushima, M. (1990). Effects of age on susceptibility of chickens to delayed neurotoxicity due to triphenyl phosphite. *Pharmacol. Toxicol.* 66, 387-392.

Kauffman, F.C., Davis, L.H., and Whittaker, M. (1990). Activation of glycogen phosphorylase in rat pheochromocytoma PC12 cells and isolated hepatocytes by organophosphates. *Biochem. Pharmacol.* 39, 347-354.

Kinebushi, H., Shiraishi, N., and Konishi, Y. (1993). Delayed neuropathy caused by organophosphates in Japanese quails. *Proc. Int. Conf. on Periph. Nerve Tox.* 33-35.

Knoth-Anderson, J., Veronesi, B., Jones, K., Lapadula, D.M., and Abou-Donia, M.B. (1992). Triphenyl phosphite-induced ultrastructural changes in bovine adrenomedullary chromaffin cells. *Toxicol. Appl. Pharmacol.* 112, 110-119.

Knoth-Anderson, J. and Abou-Donia, M.B. (1993). Differential effects of triphenylphosphite and diisopropyl phosphorofluoridate on catecholamine secretion from bovine adrenomedullary chromaffin cells. J. Toxicol. Environ. Health. 38, 103-114.

Ko, L.J. and Prives, C. (1996). p53:Puzzle and paradigm. *Genes and Dev.* 10, 1054-1072.

Koelle, G.B. (1994). Pharmacology of organophosphates. *J. Appl. Toxicol.* 14, 105-109.

Kromer, G. (1997). The proto-oncogene Bcl-2 and its role in regulating apoptosis. *Nature Med.* 3, 614.

Kunimatsu, T., Kamita, Y., Isobe, N., and Kawasaki, H. (1996). Immunotoxicological insignificance of fenitrothion in mice and rats. *Fundam. Appl. Toxicol.* 33, 246-253.

Lai, C.-T. and Yu, P.H. (1997). R(-)-deprenyl potentiates dopamine-induced cytotoxicity toward catecholaminergic neuroblastoma SH-SY5Y cells. *Toxicol. Appl. Pharmacol.* 142, 186-191.

Lallemont, G., Mestries, J.C., Privat, A., Brochier, G., Baubichon, D., Carpentier, P., Kamenka, J.M., Sentenac-Roumanou, H., Burckhart, M.-F., and Peoc'h, M. (1997). GK11: Promising additional neuroprotective therapy for organophosphate poisoning. *Neurotoxicol.* 18, 851-856.

Lambert, M.P., Stevens, G., Sabo, S., Barber, K., Wang, G., Wade, W., Krafft, G., Snyder, S., Holzman, T.F., and Klein, W.L. (1994). β/A4-evoked degeneration of differentiated SH-SY5Y human neuroblastoma cells. *J. Neurosci. Res.* 39, 377-385.

Langenberg, J.P., De Jong, L.P.A., Benschop, H.P. (1996). Protection of guinea pigs against soman poisoning by pretreatment with p-nitrophenyl phosphoramidates. *Toxicol. Appl. Pharmacol.* 140, 444-450.

Lasorella, A., Iavarone, A., and Israel, M.A. (1995). Differentiation of neuroblastoma enhances Bcl-2 expression and induces alterations of apoptosis and drug resistance. *Cancer Res.* 52, 4711-4716.

Li, Y.-P., Bushnell, A.F., Lee, C.-M., Perlmutter, L.S., and Wong, S.K.F. (1996). β-amyloid induces apoptosis in human-derived neurotypic SH-SY5Y cells. *Brain Res.* 738, 196-204.

Liu, Y. and Storm, D.R. (1989). Dephosphorylation of neuromodulin by calcineurin. *J. Biol. Chem.* 264, 12800-12804.

Martin, D.M., Yee, D., Carlson, R.O., and Feldman, E.L. (1992). Gene expression of the insulin-like growth factors and their receptors in human neuroblastoma cell lines. *Mol. Brain Res.* 15, 241-246.

Martin, D.M. and Feldman, E.L. (1993). Regulation of insulin-like growth factor-II expression and its role in autocrine growth of human neuroblastoma cells. *J. Cell. Physiol.* 155, 290-300.

Matthews, C.C. and Feldman, E.L. (1996). Insulin-like growth factor I rescues SH-SY5Y human neuroblastoma cells from hyperosmotic induced programmed cell death. *J. Cell Biol.* 102, 323-331.

Mattsson, M.E.K., Enberg, G., Ruusala, A.-I., Hall, K., and Påhlman, S. (1986). Mitogenic response of human SH-SY5Y neuroblastoma cells to insulin-like growth factor I and II is dependent on the stage of differentiation. *J. Cell Biol.* 102, 1949-1954.

Maxwell, D.M. and Koplovitz, I. (1990). Effect of endogenous carboxylesterase on HI-6 protection against soman toxicity. *J. Pharmacol. Exper. Ther.* 254, 440-444.

McCain, W.C., Flaherty, D.M., Correll, L., Jortner, B., and Ehrich, M. (1996). Catecholamine concentrations and contractile responses of isolated vessels from hens treated with cyclic phenyl saligenin phosphate or paraoxon in the presence or absence of verapamil. *J. Toxicol. Environ. Health* 48, 397-411.

Mentzschel, A., Schmuck, G., DeKant, W., and Henschler, D. (1993). Genotoxicity of neurotoxic triaryl phosphates: Identification of DNA adducts of the ultimate metabolites, saligenin phosphates. *Chem. Res. Toxicol.* 6, 294-301.

Mileson, B.E., Chambers, J.E., Chen, W.L., Dettbarn, W., Ehrich, M., Eldefrawi, A.T., Gaylor, D.W., Hamernik, K., Hodgson, E., Karczmar, A.G., Padilla, S., Pope, C.N., Richardson, R.J., Saunders, D.R., Sheets, L.P., Sultatos, L.G., and Wallace, K.B. (1998). Common mechanism of toxicity: A case study of organophosphorus pesticides. *Toxicol. Sci.* 41, 8-20.

Mochida, K., Gomyoda, M., Fujita, T., and Yamagata, K. (1988). Tricresyl phosphate and triphenyl phosphate are toxic to cultured human, monkey and dog cells. *Zbl. Bakt. Hyg. B.* 185, 427-429.

Mortensen, A. and Ladefoged, O. (1992). Delayed neurotoxicity of trixylenyl phosphate and a trialkyl/aryl phosphate mixture, and the modulating effect of atropine on tri-o-tolyl phosphate-induced neurotoxicity. *Neurotoxicol.* 13, 347-354.

Nakagawa-Yagi, Y. (1994). Induction of apoptotic cell death in differentiating neuroblastoma SH-SY5Y cells by colchicine. *Biochem. Biophys. Res. Comm.* 199, 807-817.

Nakagawa-Yagi, Y., Ogane, N., Inoki, Y., and Kitoh, N. (1996). The endogenous estrogen metabolite 2-methoxyestradiol induces apoptotic neuronal cell death *in vitro*. *Life Sci.* 58, 1461-1467.

Nishio, A. and Uyeki, E.M. (1981). Induction of sister chromatid exchanges in Chinese hamster ovary cells by organophosphate insecticides and their oxygen analogs. *J. Toxicol. Environ. Health* 8, 939-946.

Nostrandt, A.C. and Ehrich, M. (1992). Development of a model cell culture system in which to study early effects of neuropathy-inducing organophosphorus esters. *Toxicol. Lett.* 60, 107-114.

Nostrandt, A.C. and Ehrich, M. (1993). Modification of mipafox-induced inhibition of neuropathy target esterase in neuroblastoma cells of human origin. Toxicol. Appl. Pharmacol. 121, 36-42.

Oh, E.-S., Couchman, J.R., and Woods, A. (1997). Serine phosphorylation of syndecan-2 proteoglycan cytoplasmic domain. Arch. Biochem. Biophys. 344, 67-74.

Påhlman, S., Odelstad, L., Larsson, E., Grotte, G., and Nilsson, K. (1981). Phenotypic changes of human neuroblastoma cells in culture induced by 12-O-tetradecanoyl-phorbol-13-acetate. *Int. J. Cancer* 28, 583-589.

Peraica, M., Capodicasa, E., Moretto, A., and Lotti, M. (1993). Organophosphate polyneuropathy in chicks. *Biochemical Pharmacol.* 45, 131-135.

Perez-Polo, J.R., Werrbach-Perez, K., and Tiffany-Castiglioni, E. (1979). A human clonal cell line model of differentiating neurons. *Devel. Biol.* 71, 341-355.

Poluha, W., Poluha, D.K., Chang, B., Crosbie, N.E., Schonhoff, C.M., Kilpatrick, D.L., and Ross, A.H. (1996). The cyclin-dependent kinase inhibitor $p21^{Waf1}$ is required for survival of differentiating neuroblastoma cells. *Mol. Cell. Biol.* 16, 1335-1341.

Pope, C.N., diLorenzo, K., and Ehrich, M. (1995). Possible involvement of a neurotrophic factor during the early stages of organophosphate-induced delayed neurotoxicity. *Toxicol. Lett.* 75, 111-117.

Preston, R.J., Au, W., Bender, M.A., Brewen, J.G., Carrano, A.V., Heddle, J.A., McFee, A.F., Wolff, S., and Wassom, J.S. (1981). Mammalian *in vivo* and *in vitro* cytogenetic assays: A report of the U.S. EPA's Gene-Tox Program. *Mutat. Res.* 87, 143-188.

Pulverer, B.J., Kyriakis, J.M., Avruch, J., Nikolakaki, E., and Woodgett, J.R. (1991). Phosphorylation of c-Jun mediated by MAP kinases. *Nature.* 353, 345-349.

Rabizadeh, S., Bitler, C.M., Butcher, L.L., and Bredesen, D.E. (1994). Expression of the low-affinity nerve growth factor receptor enhances β-amyloid peptide toxicity. *Proc. Nat. Acad. Sci. USA.* 91, 10703-10706.

Raveh, L., Grauer, E., Grunwald, J., Cohen, E., and Ashani, Y. (1997). The stoichiometry of protection against soman and VX toxicity in monkeys pretreated with human butyrylcholinesterase. *Toxicol. Appl. Pharmacol.* 145, 43-53.

Riccardi, A., Servidei, T., Tornesello, A., Puggioni, P., Mastrangelo, S., Rumi, C., and Riccardi, R. (1995). Cytotoxicity of paclitaxel and docetaxel in human neuroblastoma cell lines. *Eur. J. Cancer.* 31A, 494-499.

Ronca, F., Chan, S.-L., and Yu, V.C. (1997). 1-(5-isoquinolinesulfonyl)-2-methylpiperazine induces apoptosis in human neuroblastoma cells, SH-SY5Y, through a p53-dependent pathway. *J. Biol. Chem.* 272, 4252-4260.

Ross, R.A., Spengler, B.A., and Biedler, J.L. (1983). Coordinate morphological and biochemical interconversion of human neuroblastoma cells. *JNCI* 71, 741-749.

Rowles, T.K., Song, X., and Ehrich, M. (1995). Identification of endpoints affected by exposure of human neuroblastoma cells to neurotoxicants at concentrations below those that affect cell viability. *In Vitro Toxicol.* 8, 3-13.

Sadée, W., Yu, V.C., Richards, M.L., Preis, P.N., Schwab, M.R., Brodsky, F.M., and Beidler, J.L. (1987). Expression of neurotransmitter receptors and *myc* protooncogenes in subclones of a human neuroblastoma cell line. *Cancer Res.* 47, 5207-5212.

Saunders, D.S and Harper, C. (1994). Chapter 11. Pesticides. In *Principles and Methods of Toxicology*, Hayes, W. (ed). Thrid Edition. Raven Press, New York, New York. pp389-415.

Sawyer, T.W., Weiss, M.T., Boulet, C.A., and Hansen, A.S. (1991). Toxicity of organophosphate nerve agents and related phosphonylated oximes compared to their anticholinesterase activity in neuron cultures. *Fundam. Appl. Toxicol.* 17, 208-214.

Schilter, B., Renwick, A.G., and Huggett, A.C. (1996). Limits for pesticide residues in infant foods: A safety based proposal. *Reg. Toxicol. Pharmacol.* 24, 126-140.

Shea, T.B., Cressman, C.M., Spencer, M.J., Beermann, M.L., and Nixon, R.A. (1995). Enhancement of neurite outgrowth following calpain inhibition is mediated by protein kinase C. *J. Neurochem.* 65, 517-527.

Sheets, L. and Norton, S. (1985). Morphologic alterations in leg muscles of chicks treated with triorthocresyl phosphate *in ovo*. *Toxicol. Appl. Pharmacol.* 79, 39-46.

Sheets, L., Hassanein, R.S., and Norton, S. (1987). Gait analysis of chicks following treatment with tri-ortho-cresyl phosphate *in ovo*. *J. Toxicol. Environ. Health* 21, 445-453.

Sheets, L.P., Hamilton, B.F., Sangha, G.K., and Thyssen, J.H. (1997). Subchronic neurotoxicity screening studies with six organophosphate insecticides: An assessment of behavior and morphology relative to cholinesterase inhibition. *Fundam. Appl. Toxicol.* 35, 101-109.

Sidell, F.R. (1994). Clinical effects of organophosphorus cholinesterase inhibitors. *J. Appl. Toxicol.* 14, 111-113.

Silveira, C.L.P., Eldefrawi, A.T., and Eldefrawi, M. (1990). Putative M2 muscarinic receptors of rat heart have high affinity for organophosphorus anticholinesterases. *Toxicol. Appl. Pharmacol.* 103, 474-481.

Singleton, J.R., Randolph, A.E., and Feldman, E.L. (1996). Insulin-like growth factor I receptor prevents apoptosis and enhances neuroblastoma tumorigenesis. *Cancer Res.* 56, 4522-4529.

Sitkiewicz, D., Skonieczna, M., Krzywicka, K., Dziedzic, E., Staniszewska, K., and Bicz, W. (1980). Effect of organophosphorus insecticides on the oxidative processes in rat brain synaptosomes. *J. Neurochem.* 34, 619-626.

Skonieczna, M., Sitkiewicz, D., and Bicz, W. (1980). Modification of oxidative phosphorylation in brain mitochondria during development and aging by the oxygen analog of Ronnel. *Pest. Biochem. Physiol.* 14, 314-318.

Sobti, R.C., Krishan, A., and Pfaffenberger, C.D. (1982). Cytokinetic and cytogenetic effects of some agricultural chemicals on human lymphoid cells *in vitro*: Organophosphates. *Mutat. Res.* 102, 89-102.

Song, X. and Ehrich, M. (1997). Alterations of cytoskeletal tau protein of SH-SY5Y human neuroblastoma cells after exposure to MPTP. *Neurotoxicol.* 19, 73-82.

Sorensen, S.D., McEwen, E.L., Linseman, D.A., and Fisher, S.K. (1997). Agonist-induced endocytosis of muscarinic cholinergic receptors: Relationship to stimulated phosphoinositide turnover. *J. Neurochem.* 68, 1473-1483.

Strack, V., Stoyanov, B., Bossenmaier, B., Mosthaf, L., Kellerer, M., and Häring, H.-U. (1997). Impact of mutations at different serine residues on the tyrosine kinase activity of the insulin receptor. *Biochem Biophys Res Comm.* 239, 235-239.

Sumantran, V.N. and Feldman, E.L. (1993). Insulin-like growth factor I regulates *c-myc* and GAP-43 messenger ribonucleic acid expression in SH-SY5Y human neuroblastoma cells. *Endocrinol.* 132, 2017-2023.

Takai, Y., Inagaki, N., Tsutsumi, O., and Inagaki, M. (1996). Visualization and regulation of intermediate filament kinase activities. *Cell Dev. Biol.* 7, 741-749.

Tanaka Jr., D., Bursian, S.J., and Lehning, E. (1990). Selective axonal and terminal degeneration in the chicken brainstem and cerebellum following exposure to *bis*(1-methylethyl)phosphorofluoridate (DFP). *Brain Res.* 519, 200-208.

Tanaka Jr., D., Bursian, S.J., and Lehning, E.J. (1992). Neuropathological effects of triphenyl phosphite on the central nervous system of the hen (*Gallus domesticus*). *Fundam. Appl. Toxicol.* 18, 72-78.

Taylor, D.D., Jortner, B.S., Walton, A., and Ehrich, M. (1995). An immunohistochemical study of the cytoskeleton of SH-SY5Y human neuroblastoma cells, and the effects of acrylamide. *In Vitro Toxicol.* 8, 323-333.

Tredici, G., Petruccioli, M.G., Tarelli, L.T., Cece, R., and Pizzini, G. (1995). Ultrastructural and confocal laser scanning microscopical aspects of apoptosis in cultured human neuroblastoma SH-SY5Y cells. *It. J. Anat. Embryol.* 100, 47-53.

Tuler, S.M. and Bowen, J.M. (1989). Toxic effect of organophosphates on nerve cell growth and ultrastructure in culture. *J. Toxicol. Environ. Health* 27, 209-223.

Varghese, R.G., Bursian, S.J., Tobias, C., and Tanaka Jr., D. (1995a). Triphenyl phosphite-induced neuropathy in the avian forebrain: A silver impregnation study of the visual and auditory systems of the Japanese quail. *Neurotoxicol.* 16, 105-114.

Varghese, R.G., Bursian, S.J., Tobias, C., and Tanaka Jr., D. (1995b). Organophosphorus-induced delayed neurotoxicity: A comparative study of the effects of tri-ortho-tolyl phosphate and triphenyl phosphite on the central nervous system of the Japanese quail. *Neurotoxicol.* 16, 45-54.

Veronesi, B. and Ehrich, M. (1993a). Differential cytotoxic sensitivity in mouse and human cell lines exposed to organophosphate insecticides. *Toxicol. Appl. Pharmacol.* 120, 240-246.

Veronesi, B. and Ehrich, M. (1993b). Using neuroblastoma cell lines to examine organophosphate neurotoxicity. *In Vitro Toxicol.* 6, 57-65.

Veronesi, B., Ehrich, M., Blusztajn, J.K., Oortgiesen, M., and Durham, H. (1997). Cell culture model of interspecies selectivity to organophosphorus insecticides. *Neurotoxicol.* 18, 283-298.

Walter, Z., Czajkowska, A., and Lipecka, K. (1980). Effect of malathion on the genetic material of human lymphocytes stimulated by phytohemagglutinin (PHA). *Hum. Genet.* 53, 375-381.

Ware, G.W. (1994). Chapter 4: Insecticides. In *The Pesticide Book*: 4th edition. Ware G.W. (ed) Thomson Publications. Fresno, California. pp41-74.

Waring, P., Khan, T., and Sjaarda, A. (1997). Apoptosis induced by gliotoxin is preceeded by phosphorylation of histone H3 and enhanced sensitivity of chromatin to nuclease digestion. *J. Biol. Chem.* 272, 17929-17936.

Whiteside, S.T. and Israël, A. (1997). IκB proteins: Structure, function and regulation. *Sem. Cancer Biol.* 8, 75-82.

Wilcox, R.A., Strupish, J., and Nahorski, S.R. (1996). Quantal calcium release in electropermeabilized SH-SY5Y neuroblastoma cells perfused with myo-inositol 1,4,5-trisphosphate. *Cell Calcium* 20, 243-255.

Yourick, J.J., Eklo, P.A., McCluskey, M.P., and Ray, R. (1991). Regeneration of acetylcholinesterase in clonal neuroblastoma-glioma hybrid NG108-15 cells after soman inhibition: Effect of glycyl-l-glutamine. *Cell Biol. Toxicol.* 7, 229-236.

PART VII

APPENDICES AND VITA

Appendix A - Representative flow cytometry histograms for propidium iodide labeling of DNA content

Representative flow cytometry histograms for propidium iodide labeling of DNA content (From Figures 3.4, 3.5, 3.6, and 3.7). These histograms were generated in Multicycle DNA Cell Cycle Analysis Software (version 3.11, Phoenix Flow Systems, San Diego, CA). G_0/G_1, S, and G_2/M = the % of cells in respective phase of the cell cycle; $subG_1$ = the % of cells with fragmented DNA; 38400, 19200, 9600, and 4800 = seeding densities (cells/cm^2); w/o = without media change. Numbers at the bottom of each histogram are assigned by the flow cytometer for archiving purposes.

Time	38400 cells/cm^2	38400 cells/cm^2 w/o	19200 cells/cm^2	19200 cells/cm^2 w/o
1440 min	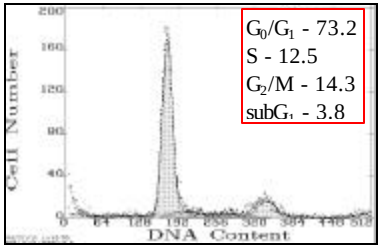 33763	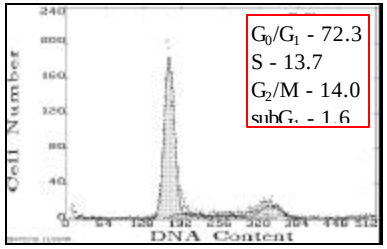 33738	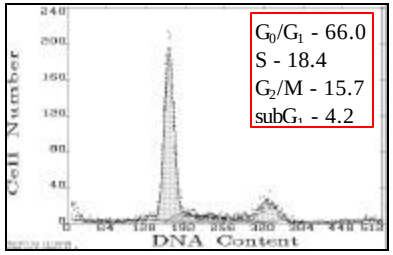 33757	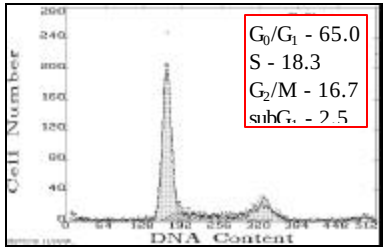 33732
2880 min	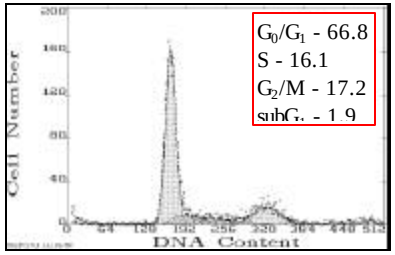 33811	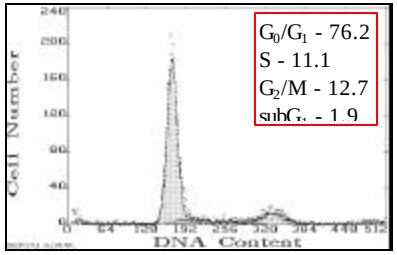 33787	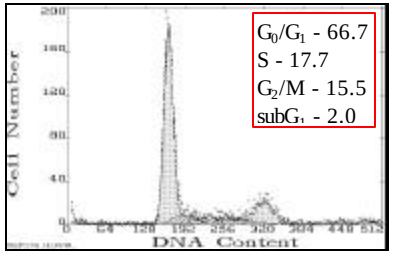 33806	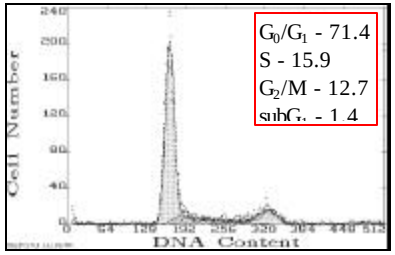 33781
4320 min	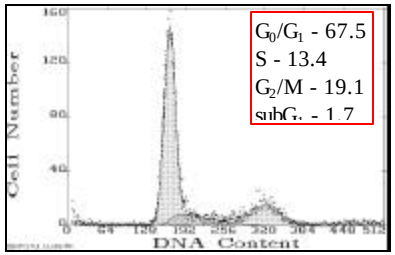 33859	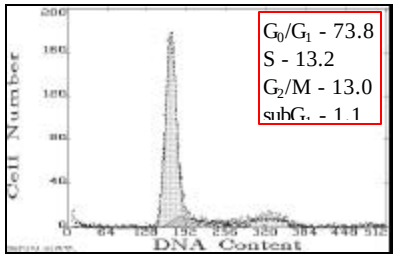 33836	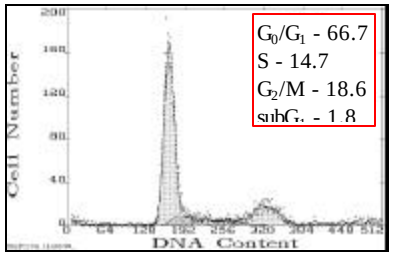 33854	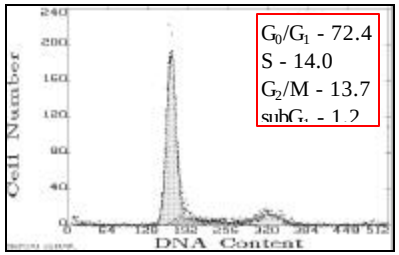 33830

Time	38400 cells/cm^2	38400 cells/cm^2 w/o	19200 cells/cm^2	19200 cells/cm^2 w/o
5760 min	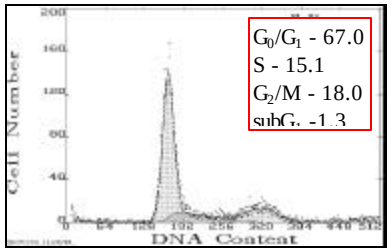 34152	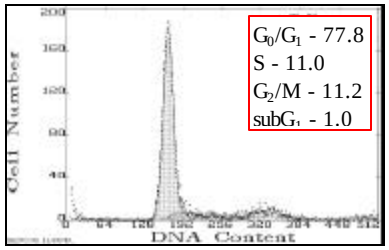 34132	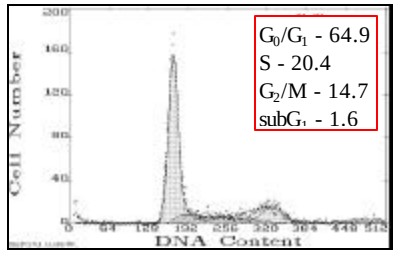 34149	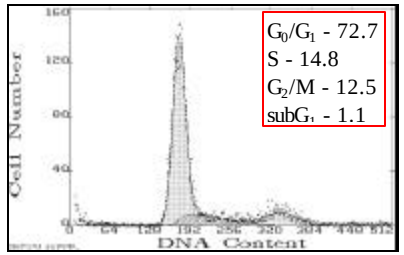 34124
7200 min	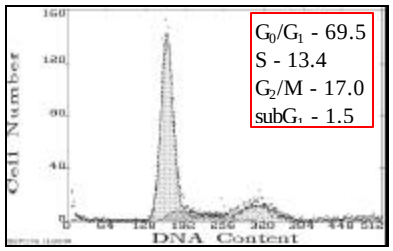 34201	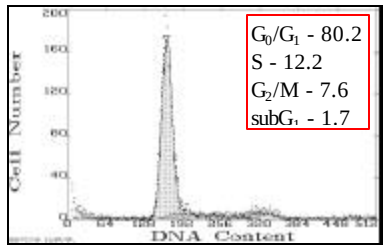 34180	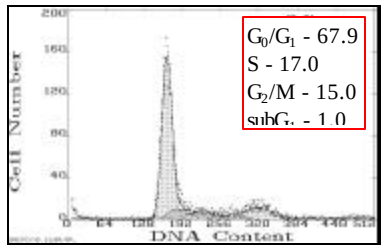 34197	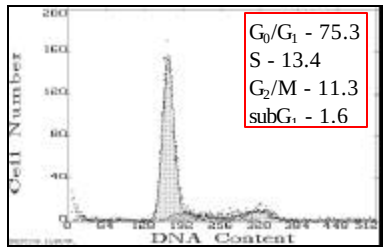 34172
8640 min	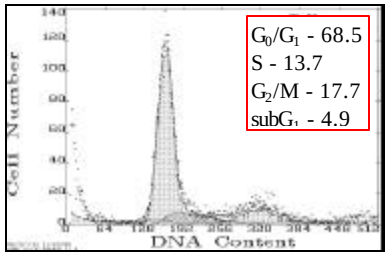 34752	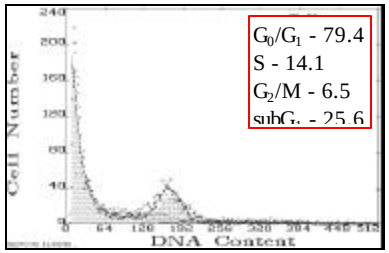 34728	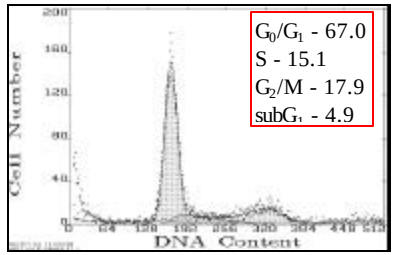 34748	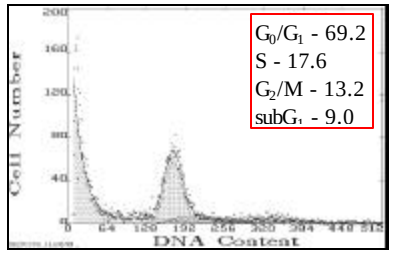 34725

Time	38400 cells/cm^2	38400 cells/cm^2 w/o	19200 cells/cm^2	19200 cells/cm^2 w/o
10080 min	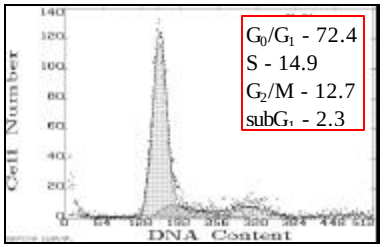 34707	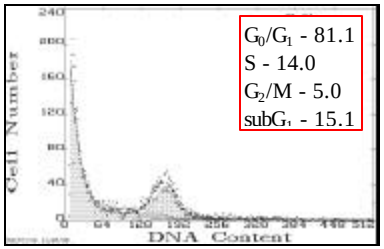 34682	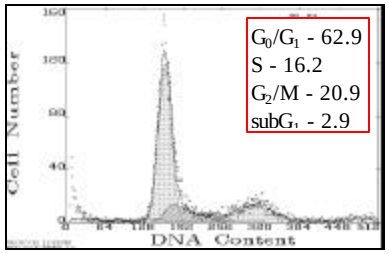 34699	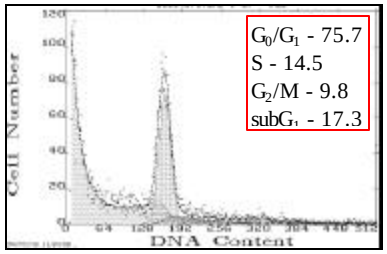 34676

Time	9600 cells/cm^2	9600 cells/cm^2 w/o	4800 cells/cm^2	4800 cells/cm^2 w/o
1440 min	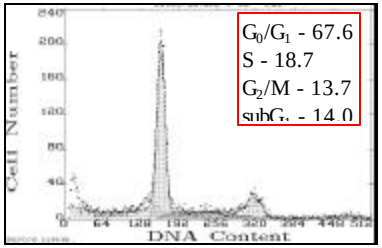 33752	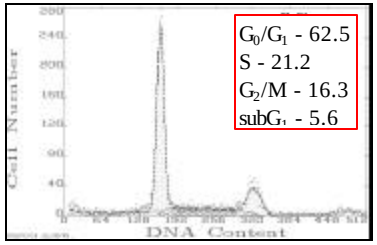 33727	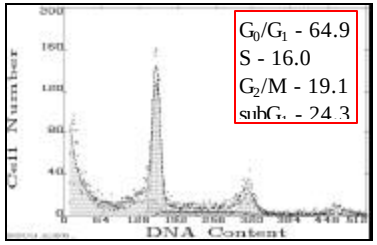 33746	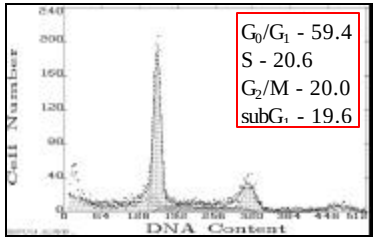 33721
2880 min	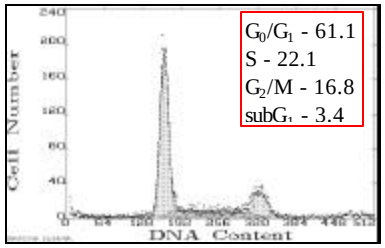 33799	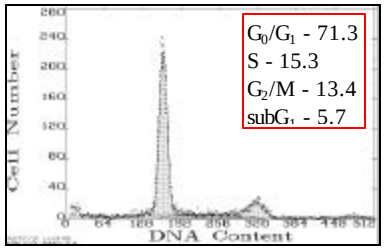 33775	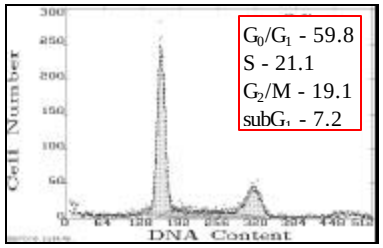 33793	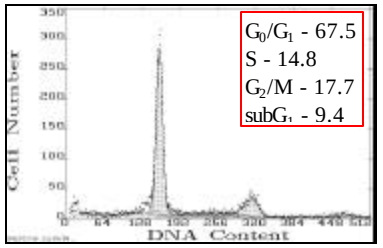 33769
4320 min	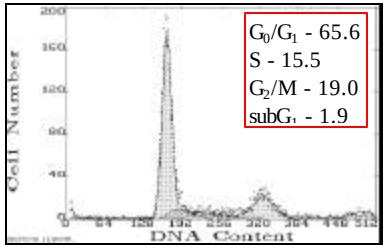 33848	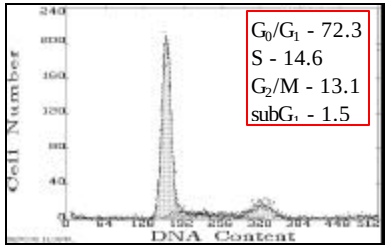 33823	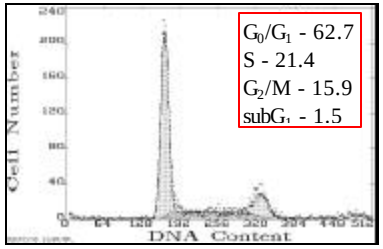 33843	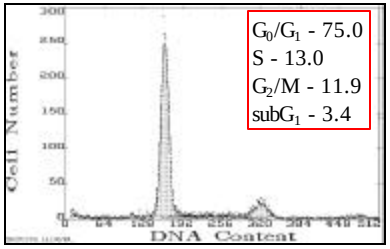 33817

Time	9600 cells/cm^2	9600 cells/cm^2 w/o	4800 cells/cm^2	4800 cells/cm^2 w/o
5760 min	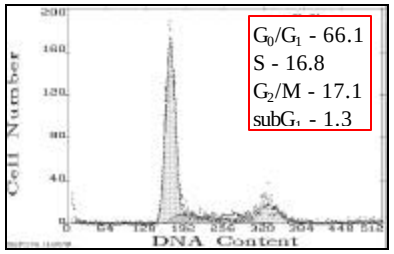 34145	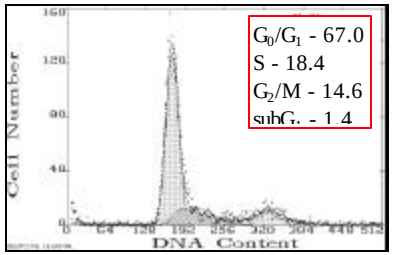 34117	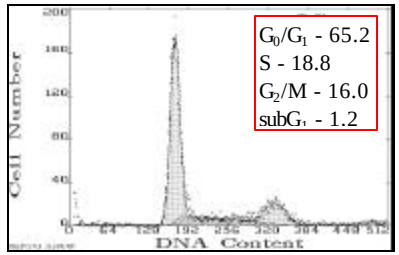 34139	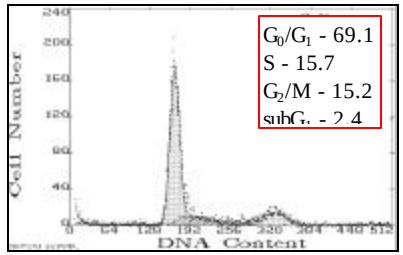 34111
7200 min	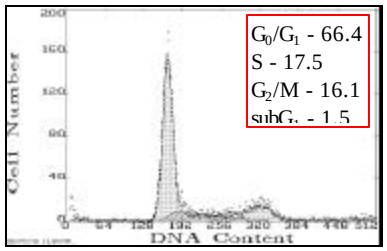 34189	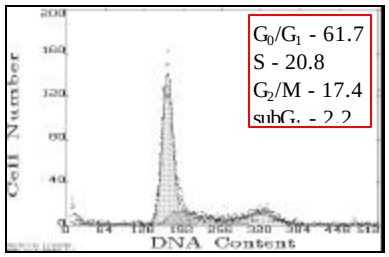 34164	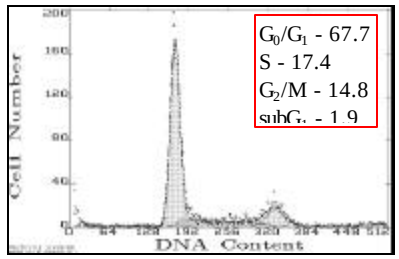 34186	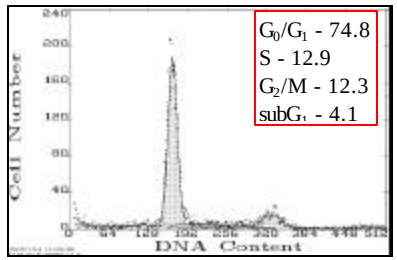 34158
8640 min	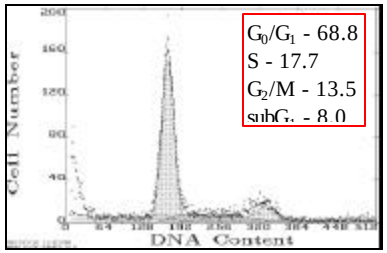 34740	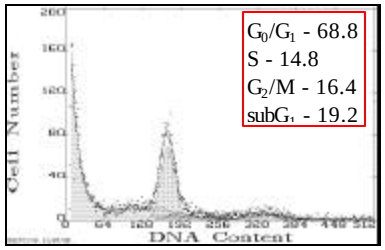 34714	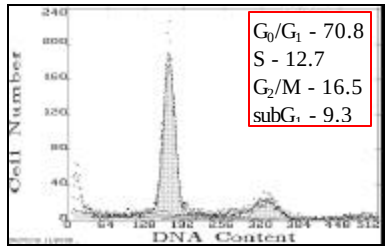 34734	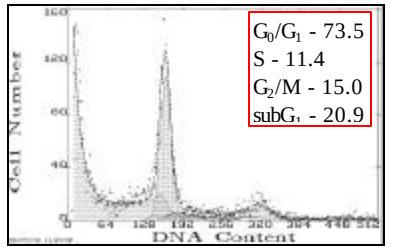 34709

Time	9600 cells/cm^2	9600 cells/cm^2 w/o	4800 cells/cm^2	4800 cells/cm^2 w/o
10080 min	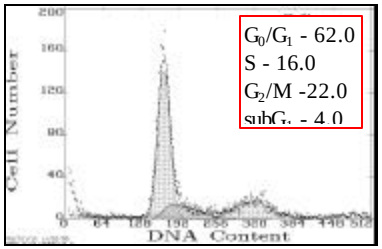 34693	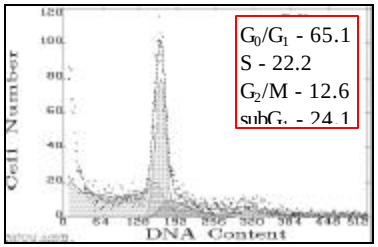 34668	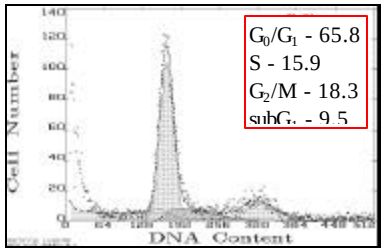 34685	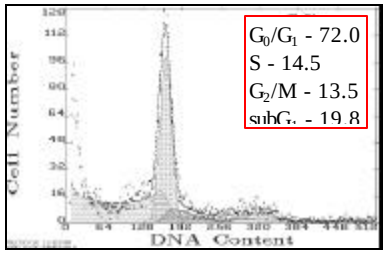 34662

Appendix B - Representative flow cytometry histograms for rhodamine 123 labeling of mitochondrial DY

Representative flow cytometry histograms for rhodamine 123 labeling of mitochondrial transmembrane potential (From Figure 5.3). These histograms were generated in Epics XL Flow Cytometry Workstation software (version 1.5, Beckman-Coulter Corp., Opa Locka, FL). Individual histograms (solvent control and treated) lie to the left of histogram overlays. Individual histograms used mean fluorescence intensities (M.F.I.) to generate percent of controls for this dissertation. For individual histograms; Y-axis = Cell Count, X-axis = Fluorescence Intensity, M.F.I. = mean fluorescence intensity of the "A" gate, and the number at bottom center is the archive histogram datum number generated by the flow cytometer. Histogram overlays are another method for observing changes in fluorescence within cells (not used in this dissertation). For overlays, ID = identification of cells as positive (+) or negative (-), % = percent of cells within a (+) or (-) grouping, M.F.I. = mean fluorescence intensity within a grouping, Y-axis = Cell Count, and the X-axis = Fluorescence.

Figure 5.3 - Left Panel

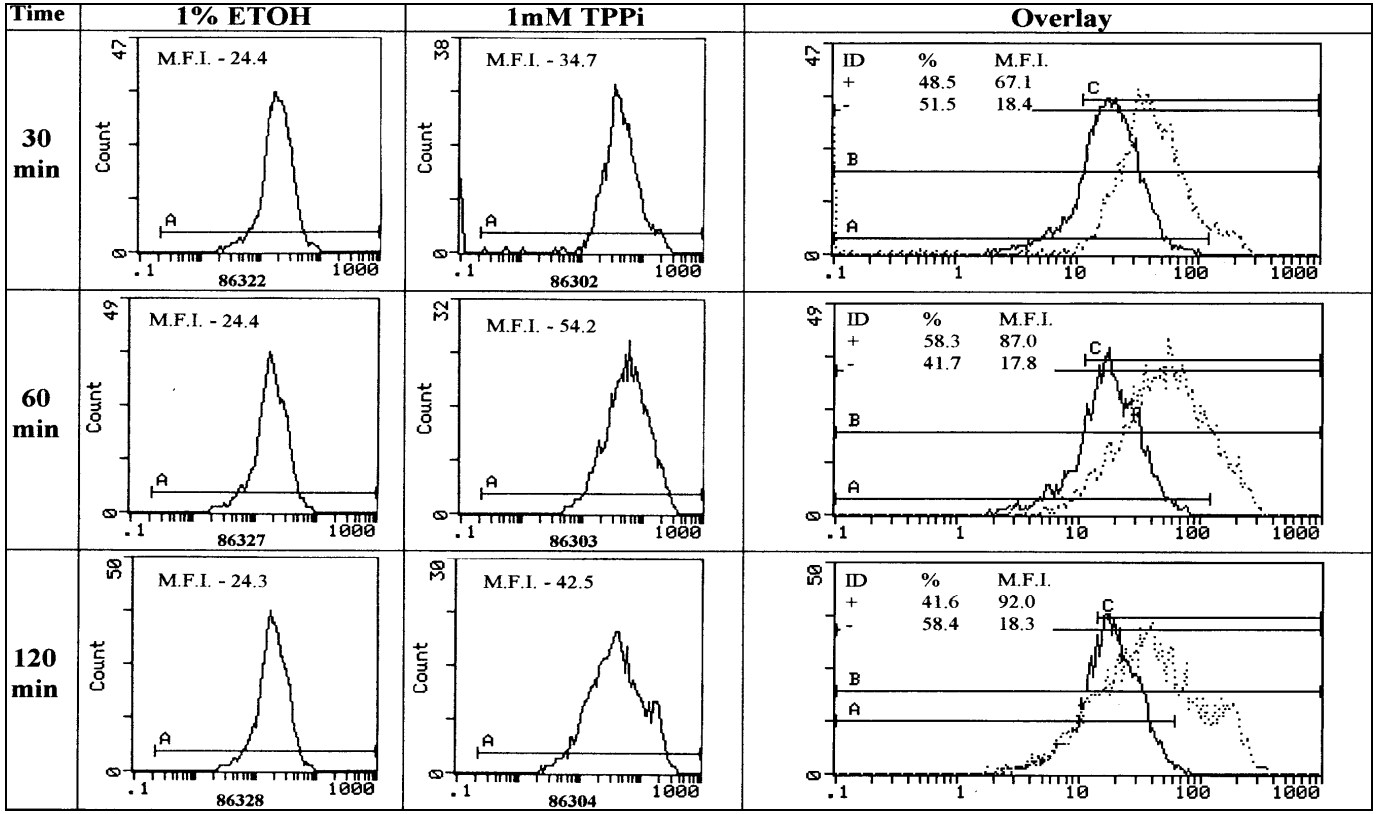

Time	1% ETOH	1mM TPPi	Overlay
240 min	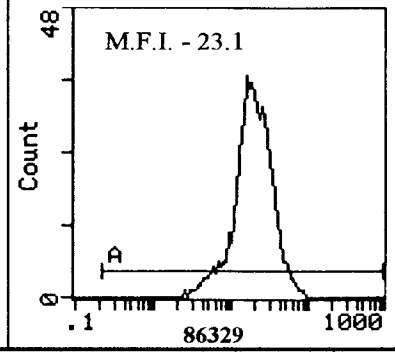	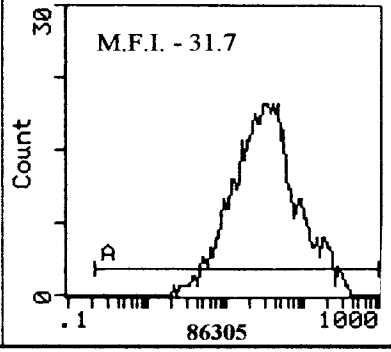	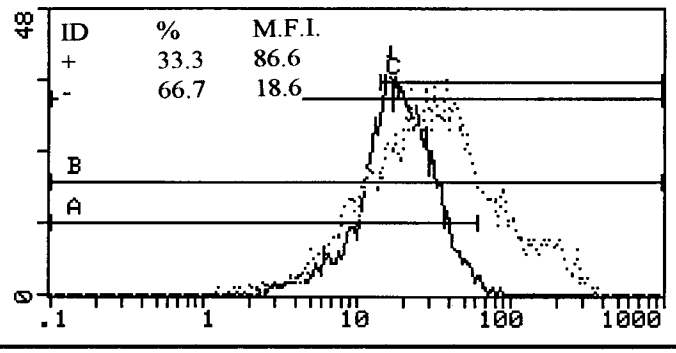

Time	0.1% ETOH	100μM TPPi	Overlay
30 min	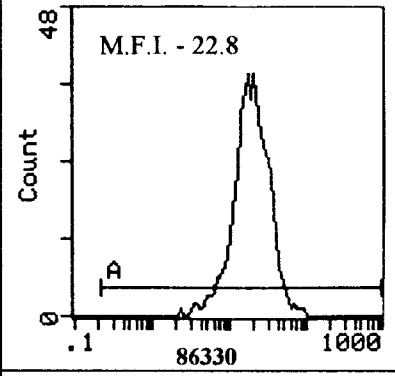	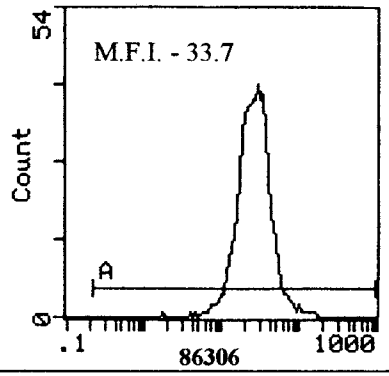	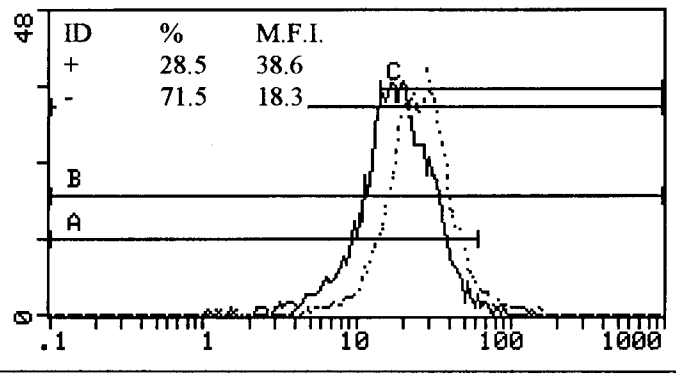
60 min	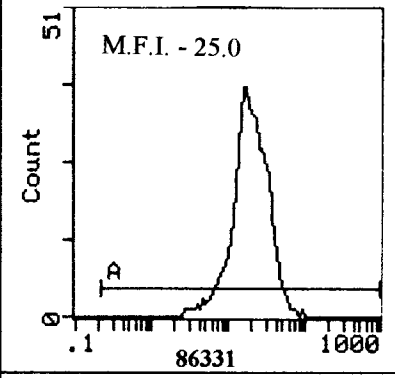	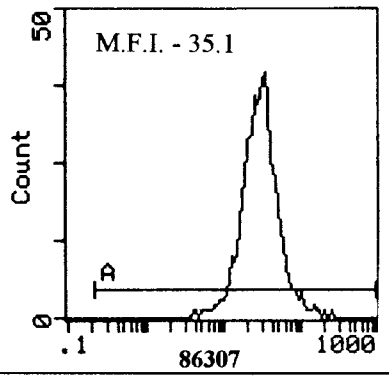	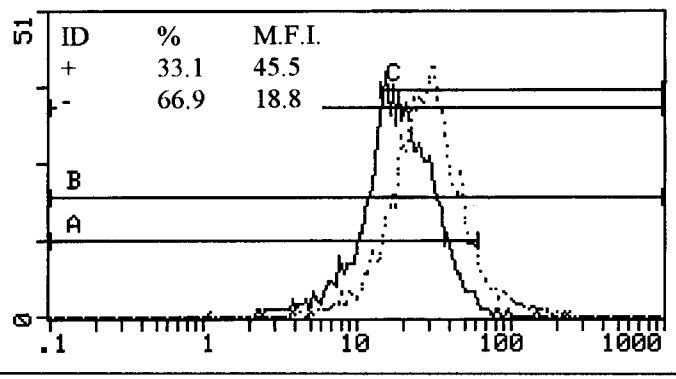
120 min	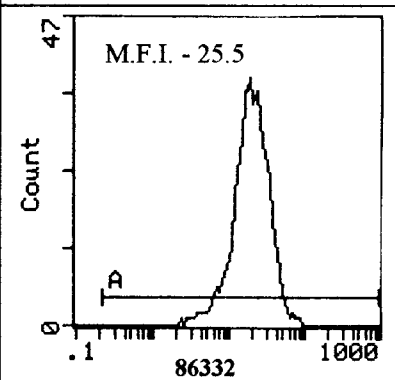	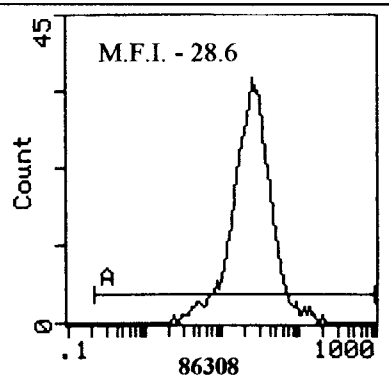	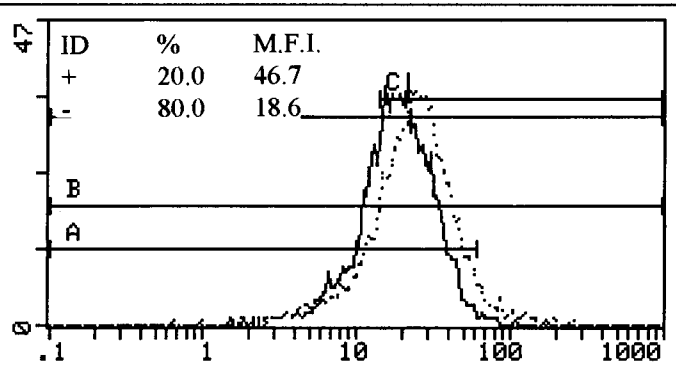

Time	0.1% ETOH	100μM TPPi	Overlay
240 min	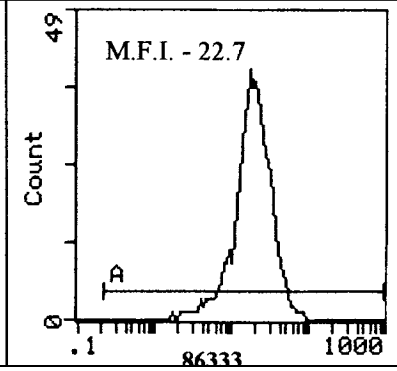	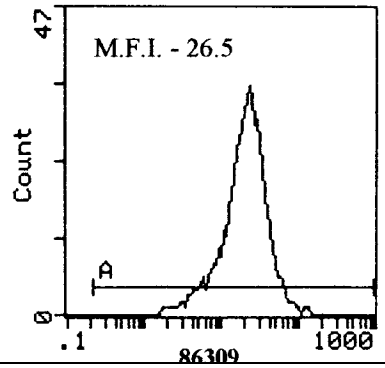	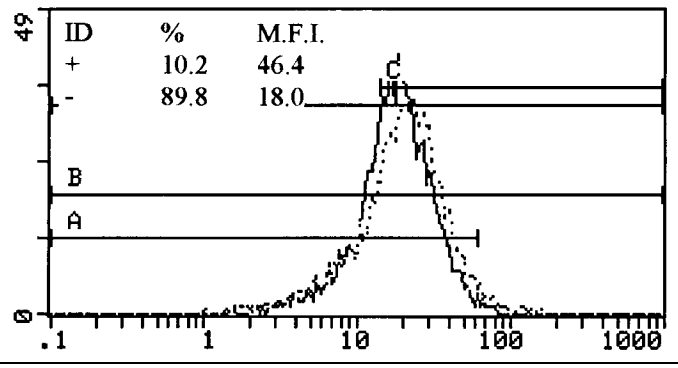

Figure 5.3 - Right Panel

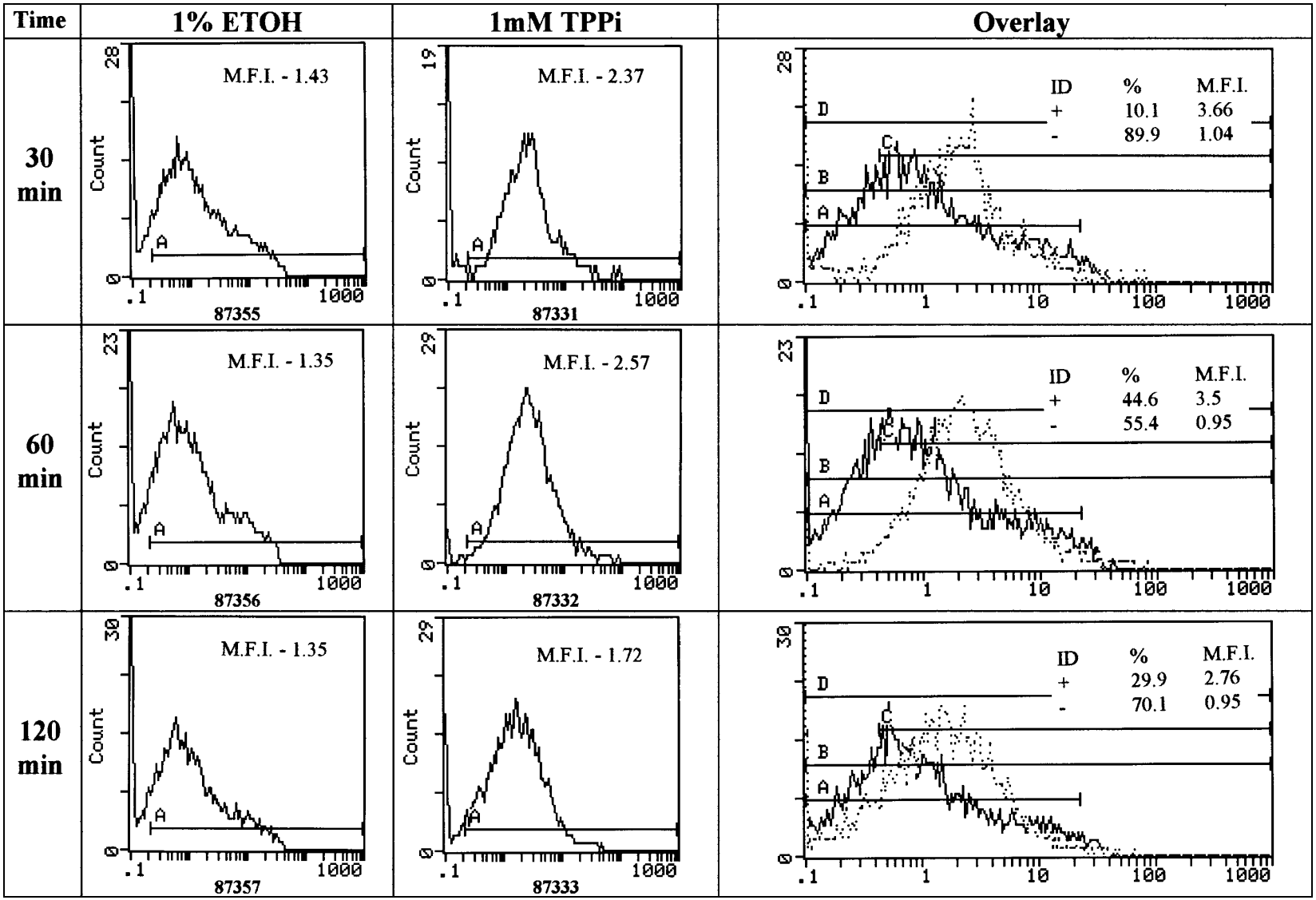

Time	1% ETOH	1mM TPPi	Overlay
240 min	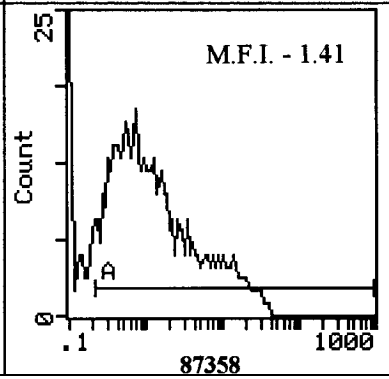	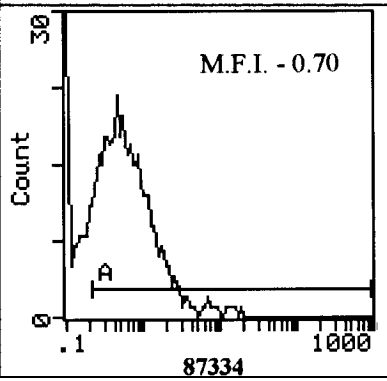	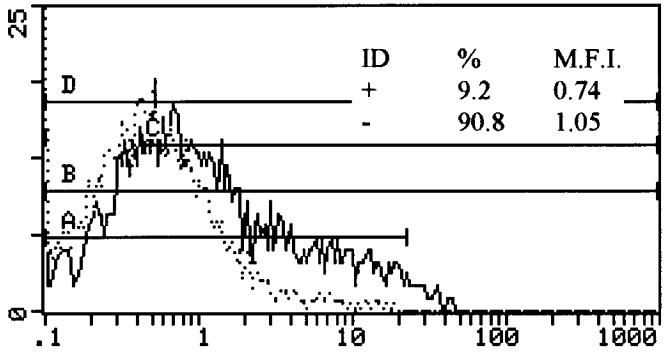

Time	0.1% ETOH	100μM TPPi	Overlay
30 min	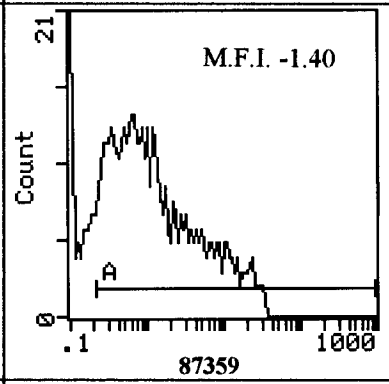	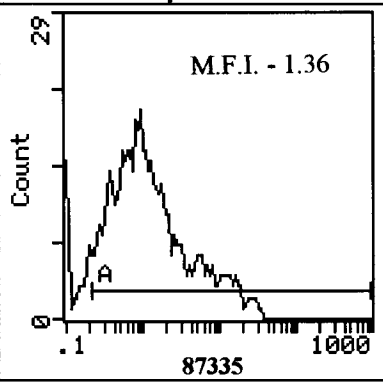	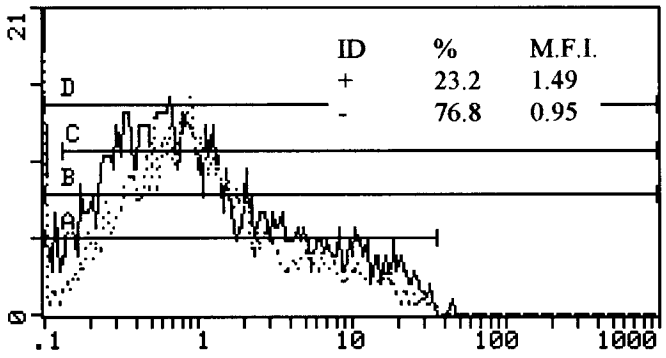
60 min	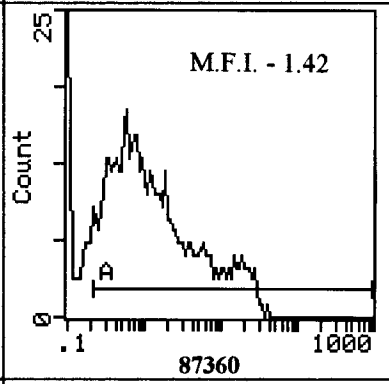	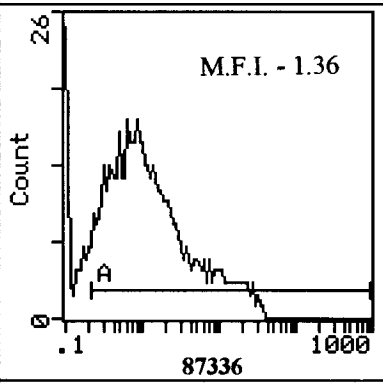	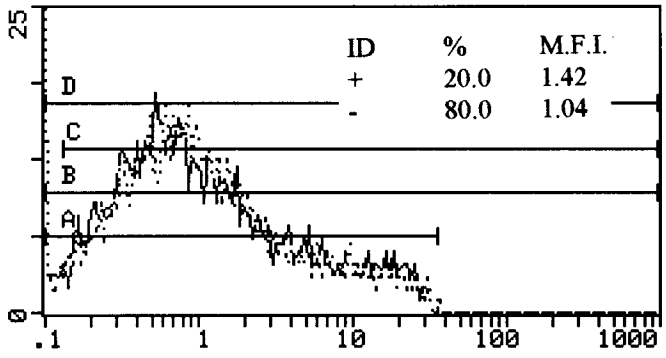
120 min	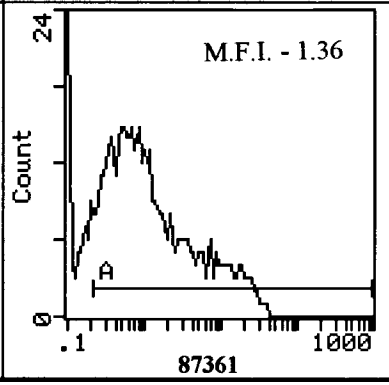	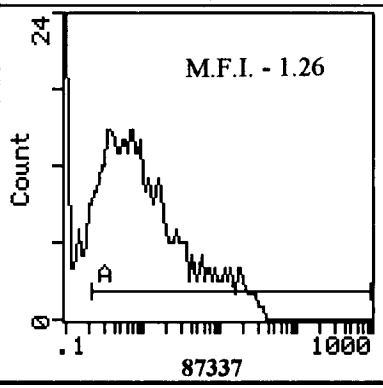	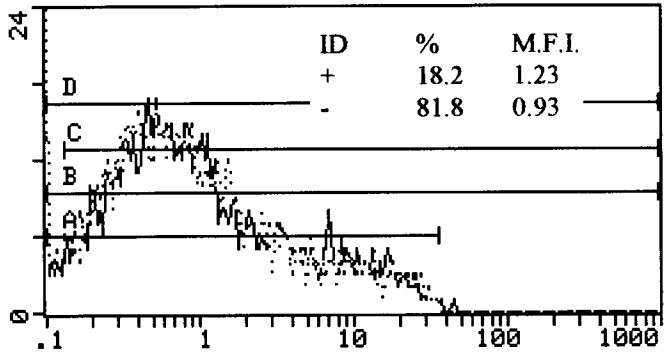

Time	0.1% ETOH	100μM TPPi	Overlay
240 min	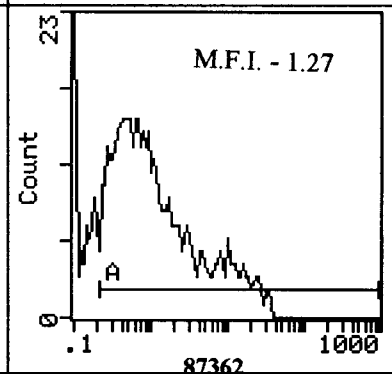	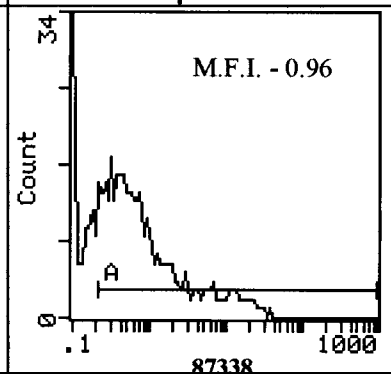	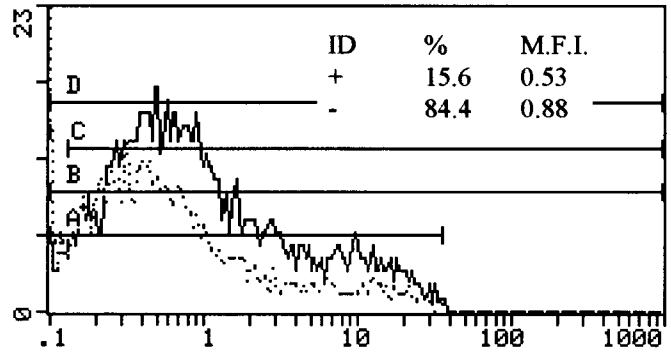

Appendix C - Representative flow cytometry histograms for FITC labeling of f-actin content

Representative flow cytometry histograms for FITC labeling of f-actin content (From Figure 6.2a). These histograms were generated in Epics XL Flow Cytometry Workstation software (version 1.5, Beckman-Coulter Corp., Opa Locka, FL). Individual histograms (solvent control and treated) lie to the left of histogram overlays. Individual histograms used mean fluorescence intensities (M.F.I.) to generate percent of controls for this dissertation. For individual histograms; Y-axis = Cell Count, X-axis = Fluorescence Intensity, M.F.I. = mean fluorescence intensity of the "J" gate, and the number at bottom center is the archive histogram datum number generated by the flow cytometer. Histogram overlays are another method for observing changes in fluorescence within cells (not used in this dissertation). For overlays, ID = identification of cells as positive (+) or negative (-), % = percent of cells within a (+) or (-) grouping, M.F.I. = mean fluorescence intensity within a grouping, Y-axis = Cell Count, and the X-axis = Fluorescence.

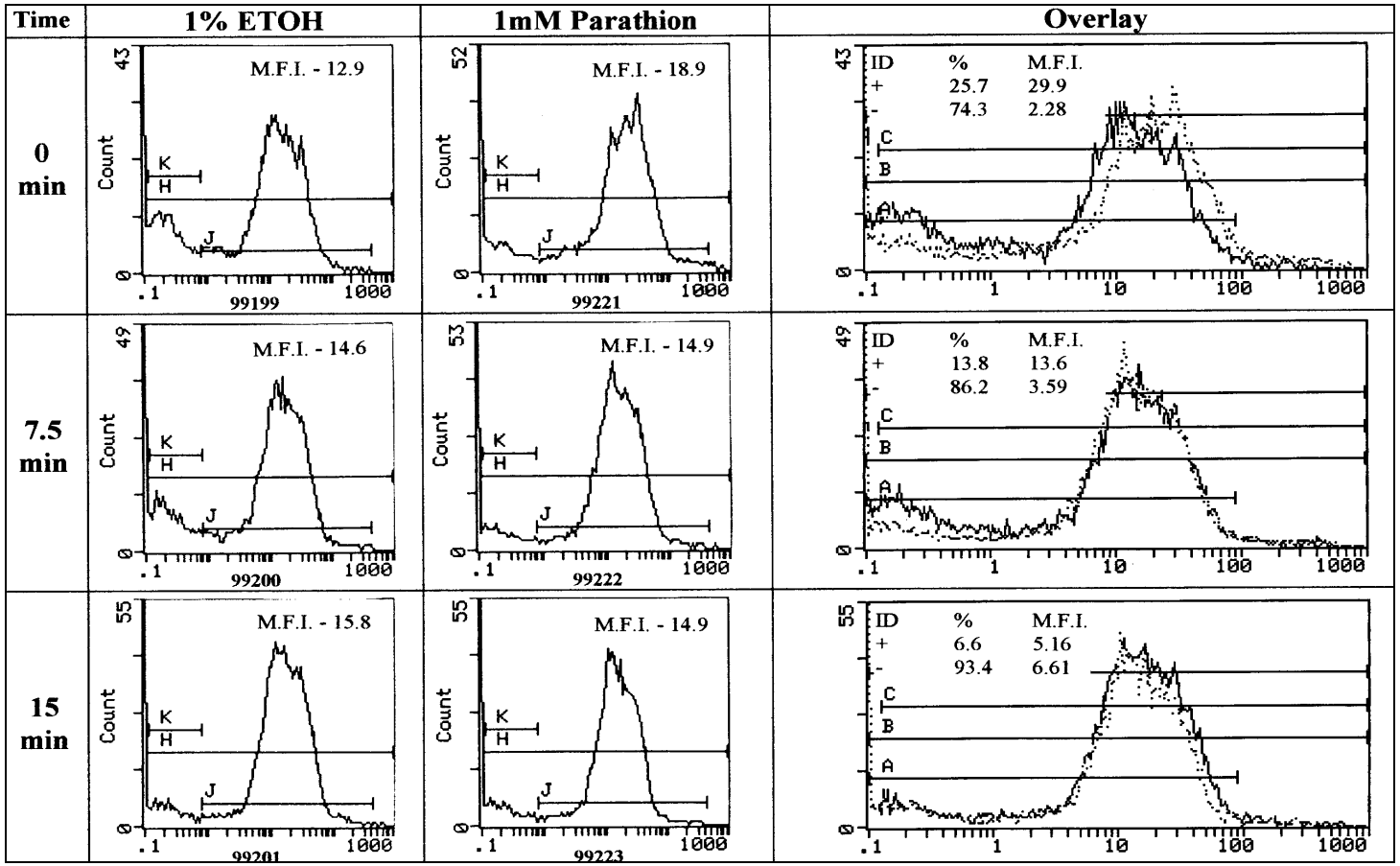

Time	1% ETOH	1mM Parathion	Overlay
30 min	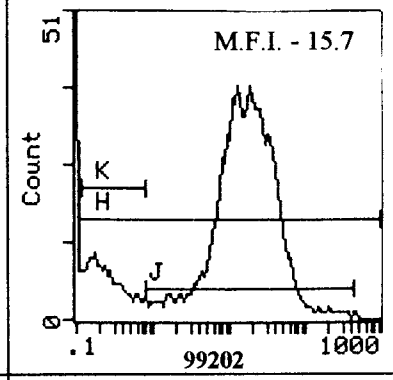	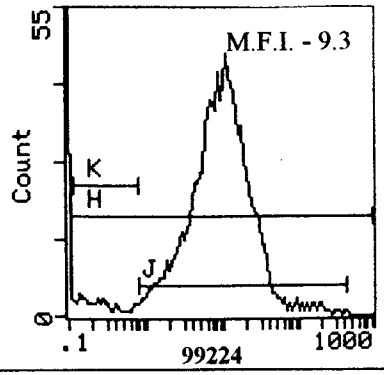	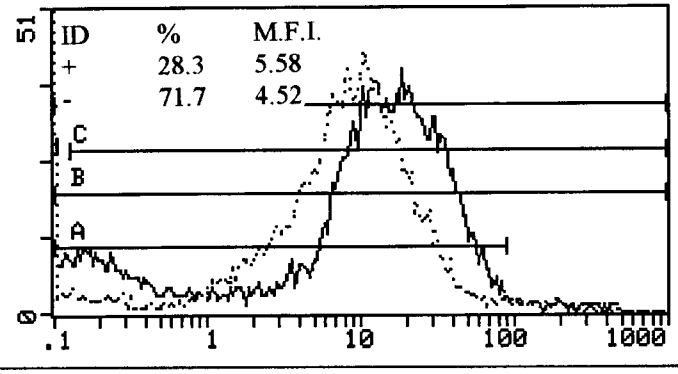
60 min	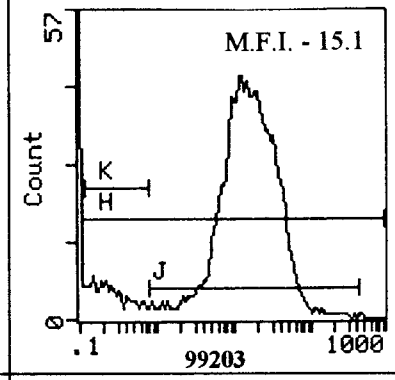	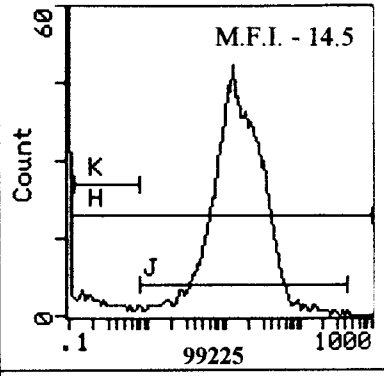	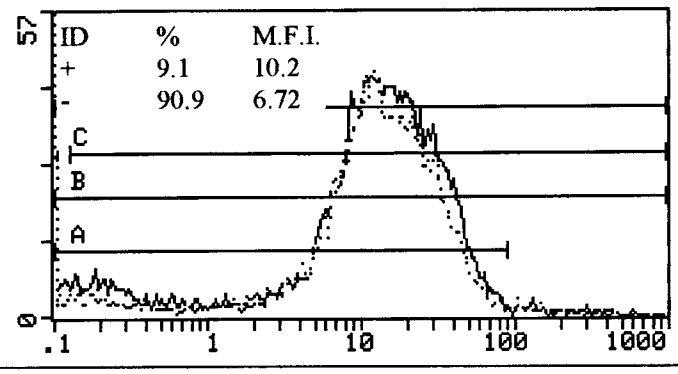
120 min	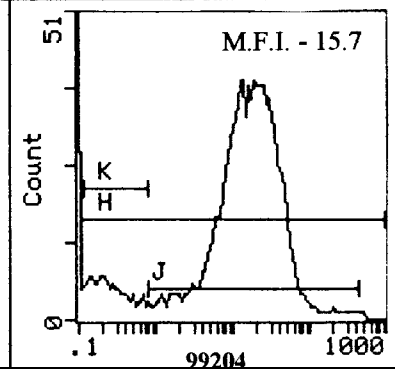	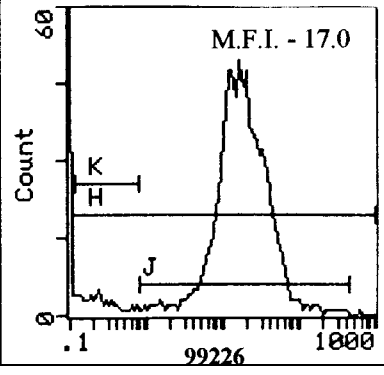	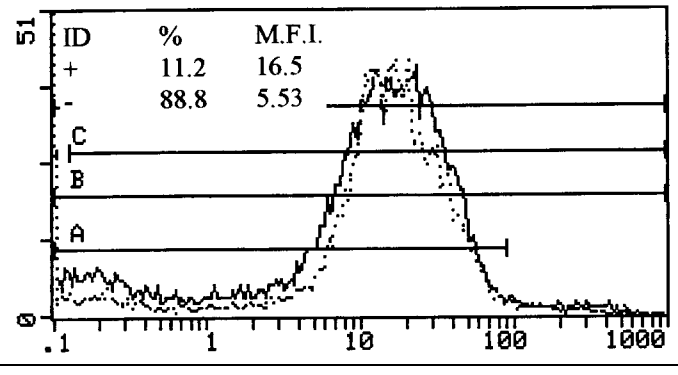

Time	1% ETOH	1mM Parathion	Overlay
240 min	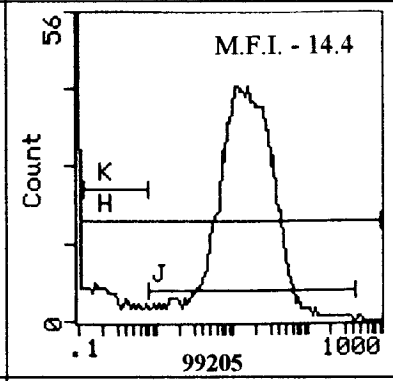	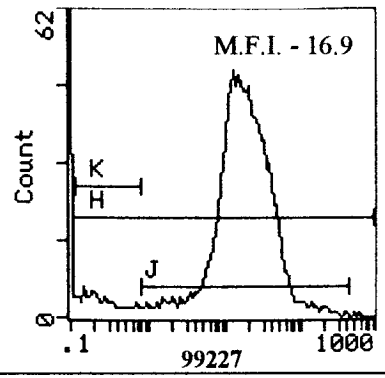	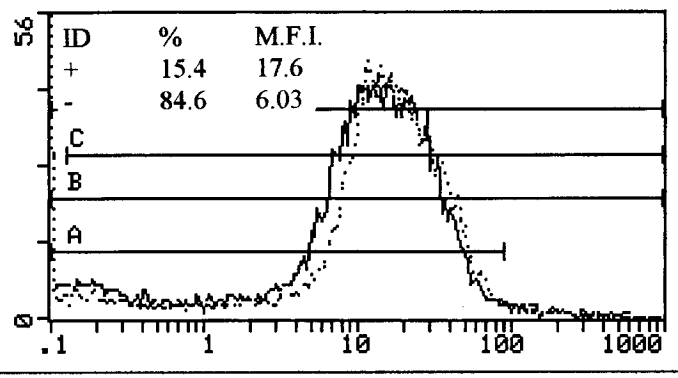
480 min	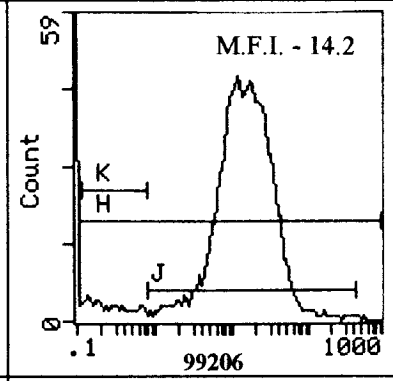	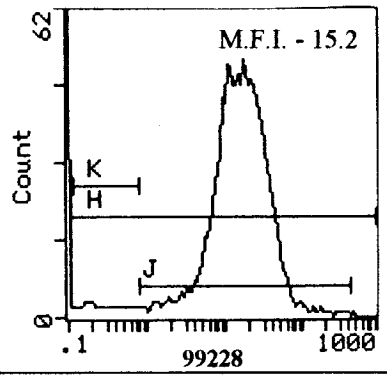	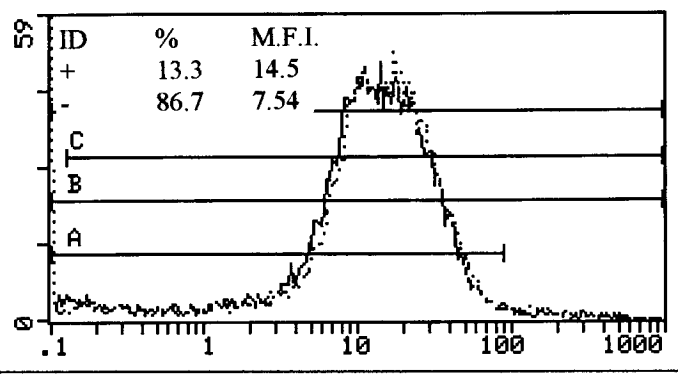
960 min	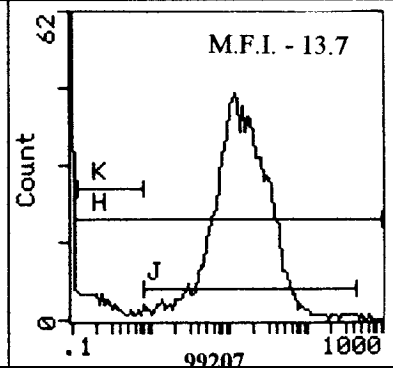	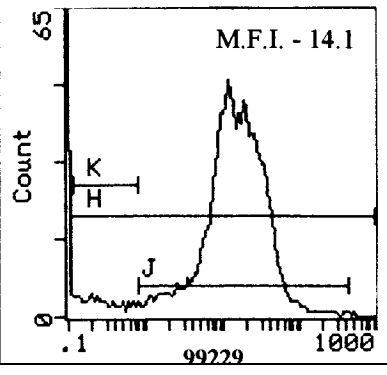	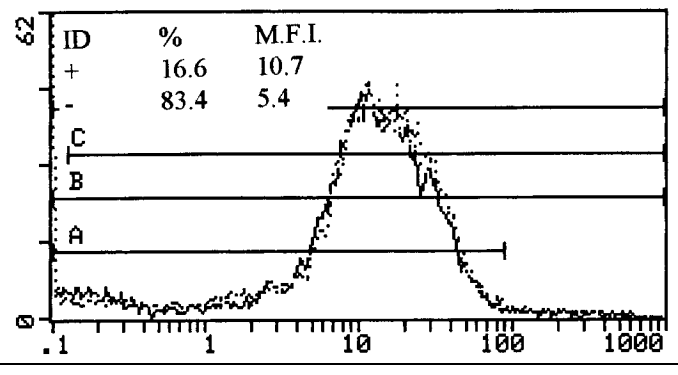

Time	1% ETOH	1mM Parathion	Overlay
1440 min	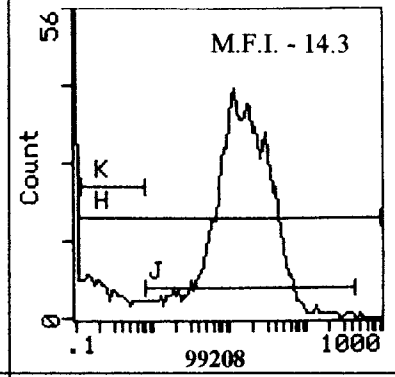	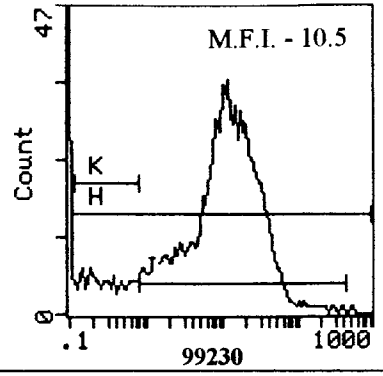	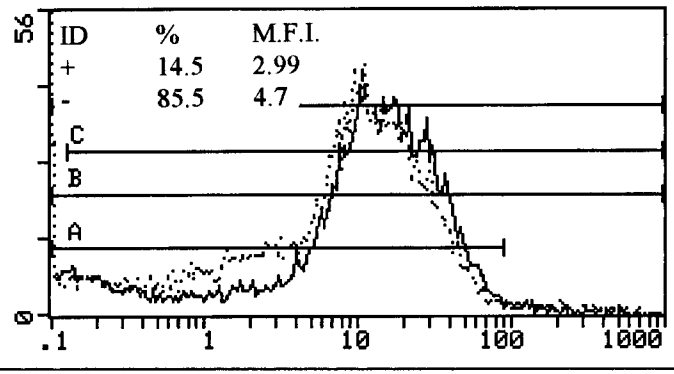
2880 min	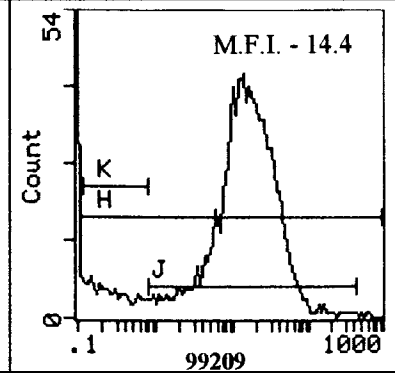	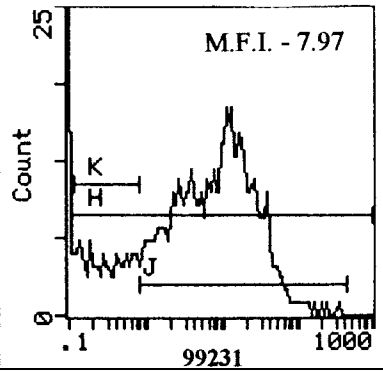	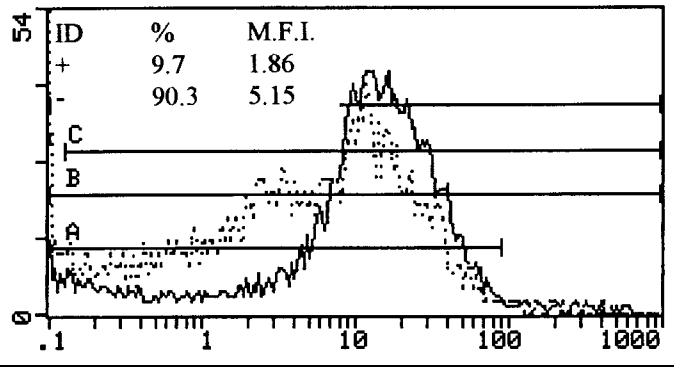

Time	0.1% ETOH	100μM Parathion	Overlay
0 min	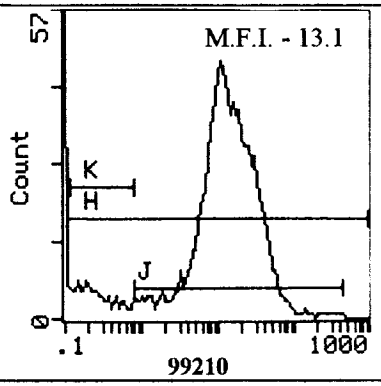	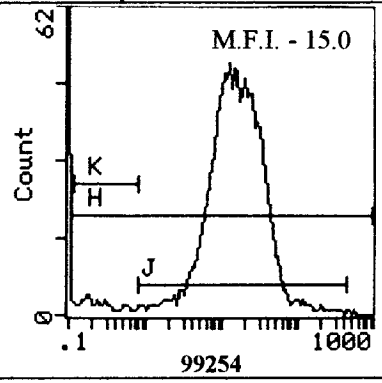	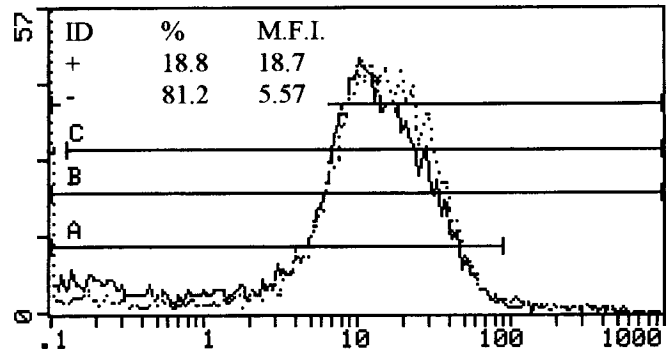
7.5 min	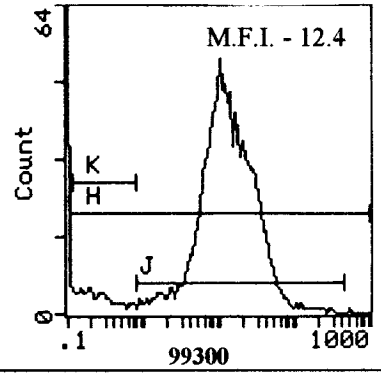	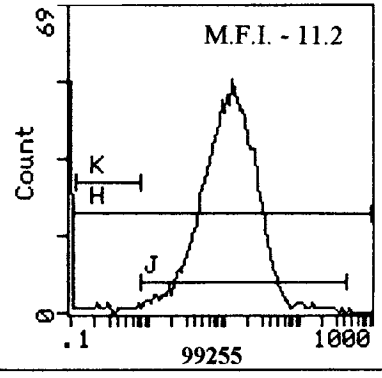	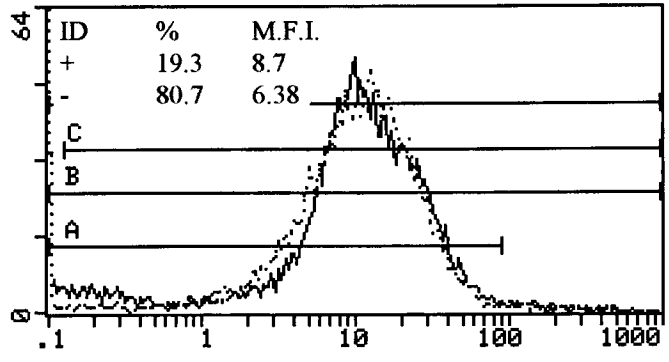
15 min	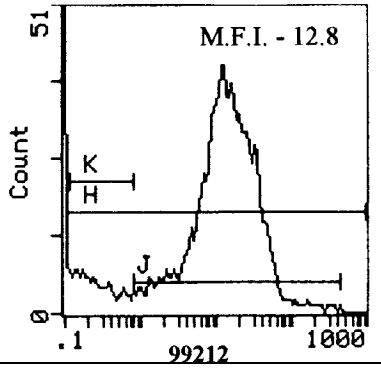	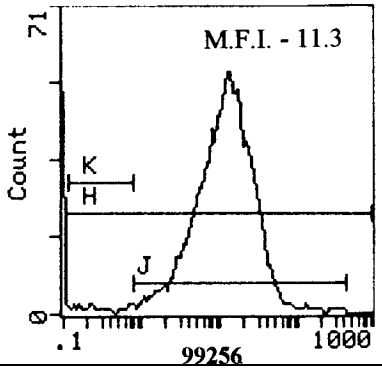	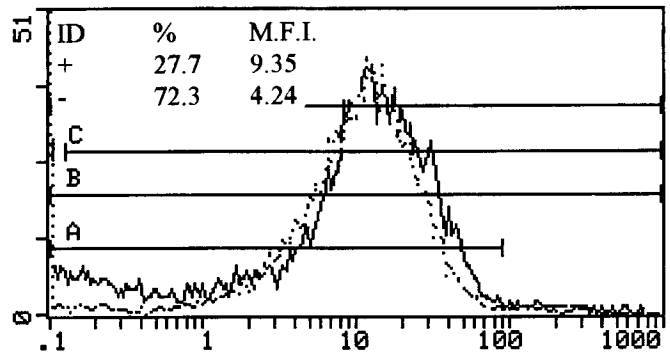

Time	0.1% ETOH	100μM Parathion	Overlay
30 min	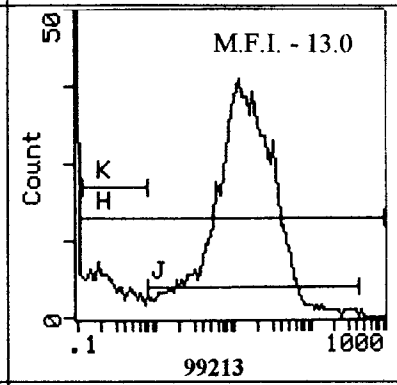	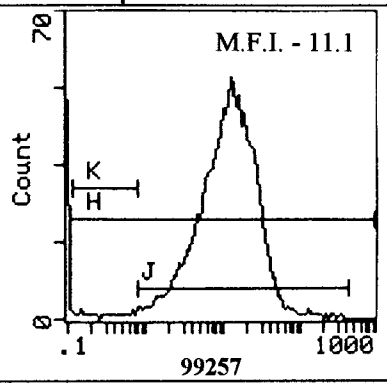	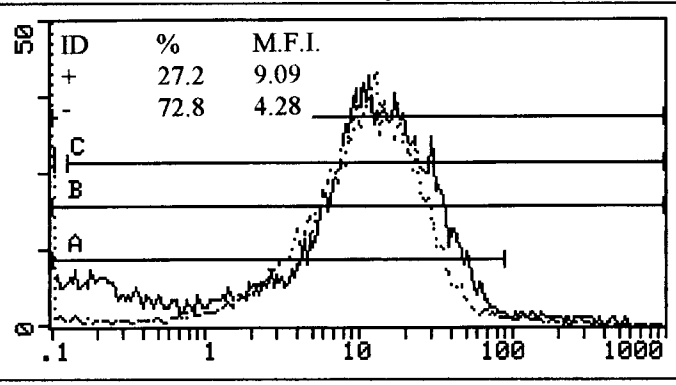
60 min	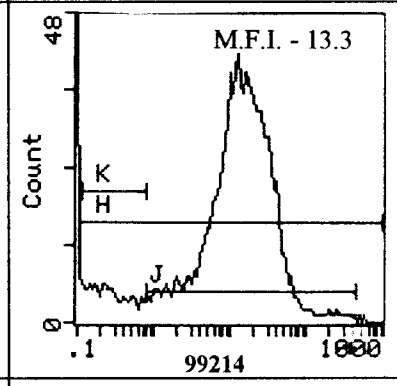	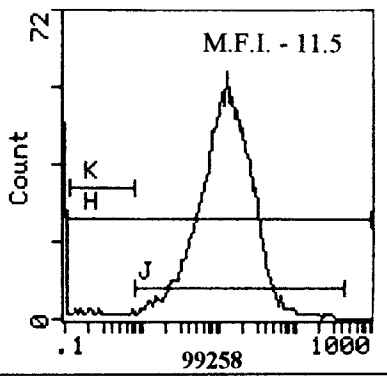	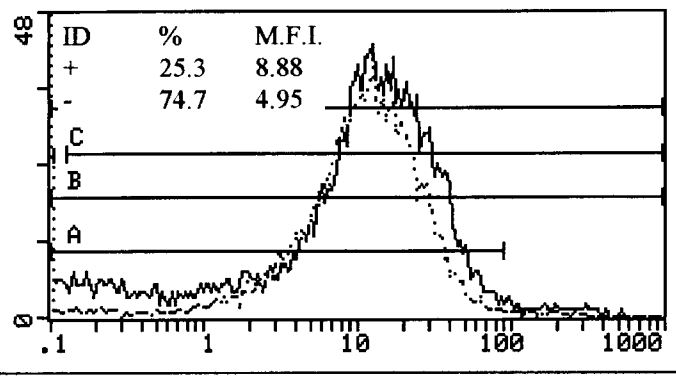
120 min	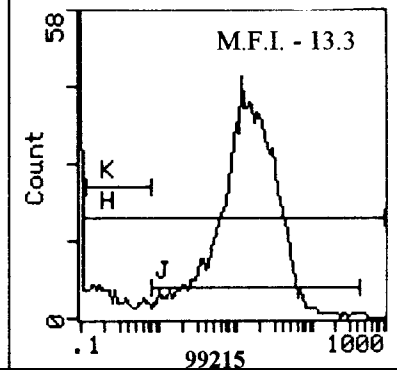	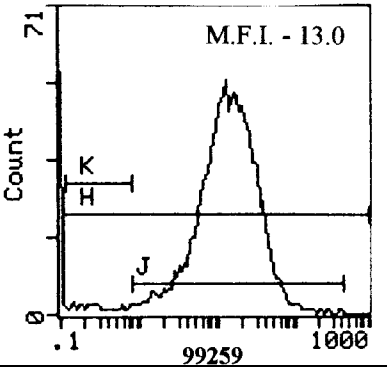	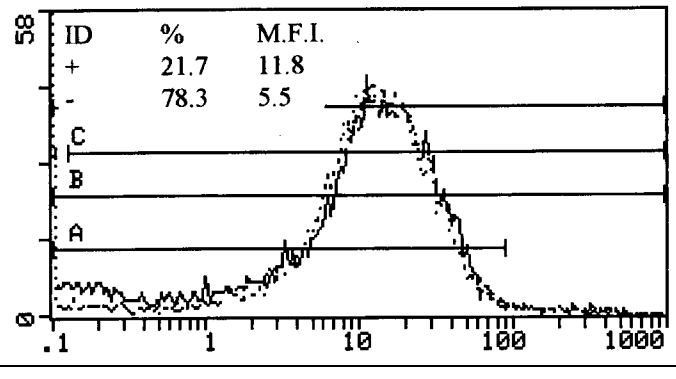

Time	0.1% ETOH	100μM Parathion	Overlay
240 min	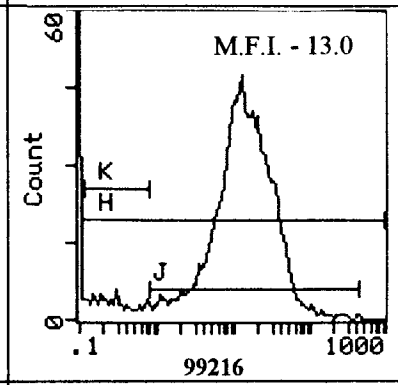	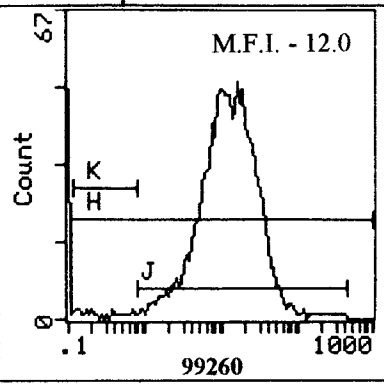	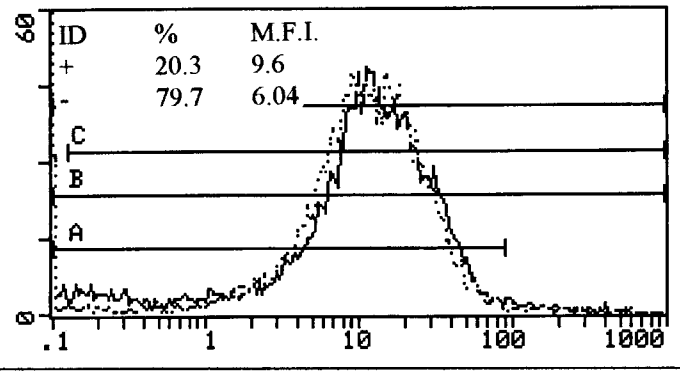
480 min	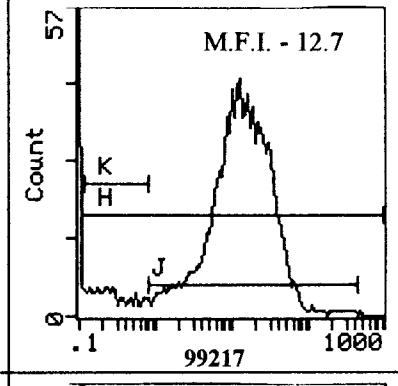	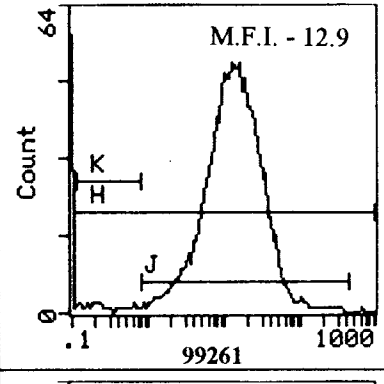	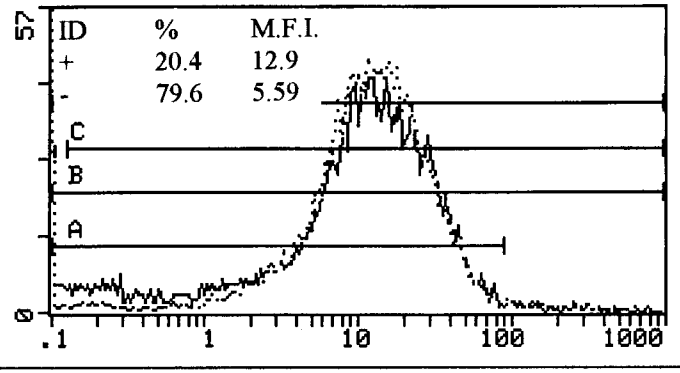
960 min	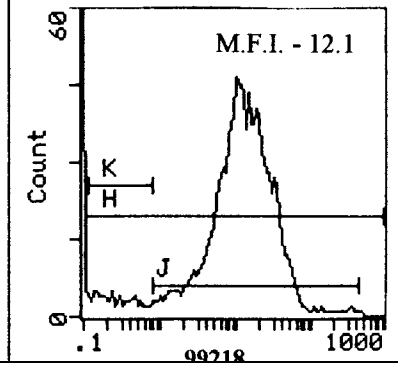	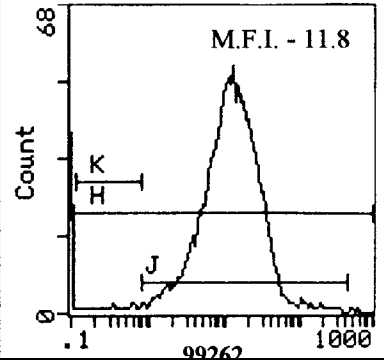	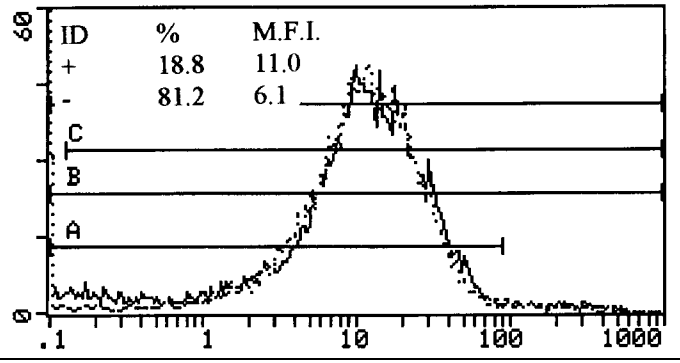

Time	0.1% ETOH	100μM Parathion	Overlay
1440 min	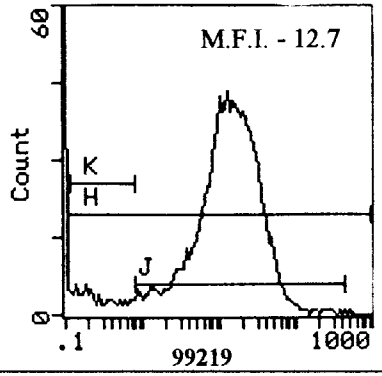	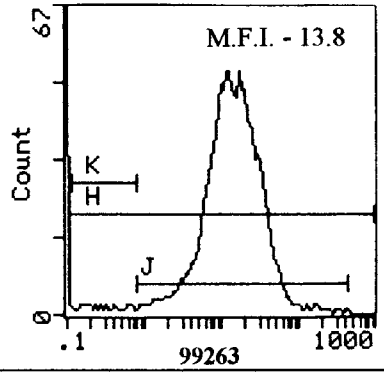	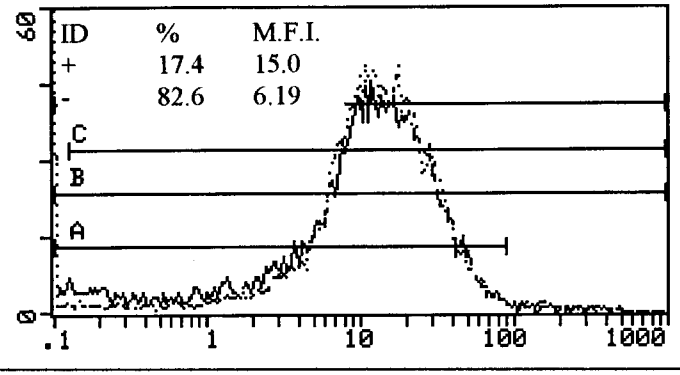
2880 min	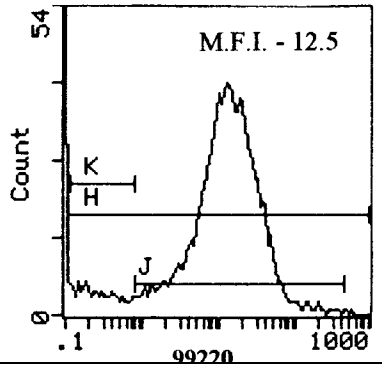	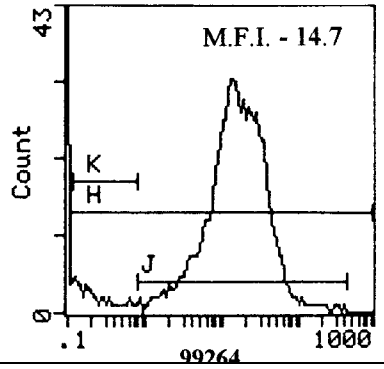	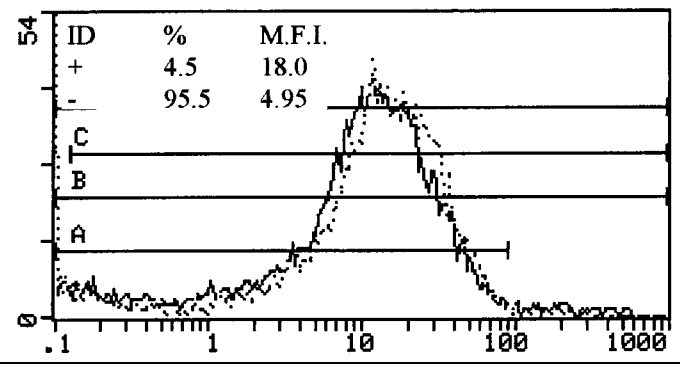

Appendix D - Representative flow cytometry histograms for phycoerythrin labeling of active caspase-3

Representative flow cytometry histograms for phycoerythrin labeling of active caspase-3 (From Figure 7.5a). These histograms were generated in Epics XL Flow Cytometry Workstation software (version 1.5, Beckman-Coulter Corp., Opa Locka, FL). Individual histograms (solvent control and treated) lie to the left of histogram overlays. Individual histograms used mean fluorescence intensities (M.F.I.) to generate percent of controls for this dissertation. For individual histograms; Y-axis = Cell Count, X-axis = Fluorescence Intensity, M.F.I. = mean fluorescence intensity of the entire field, and the number at bottom center is the archive histogram datum number generated by the flow cytometer. Histogram overlays are another method for observing changes in fluorescence within cells (not used in this dissertation). For overlays, ID = identification of cells as positive (+) or negative (-), % = percent of cells within a (+) or (-) grouping, M.F.I. = mean fluorescence intensity within a grouping, Y-axis = Cell Count, and the X-axis = Fluorescence.

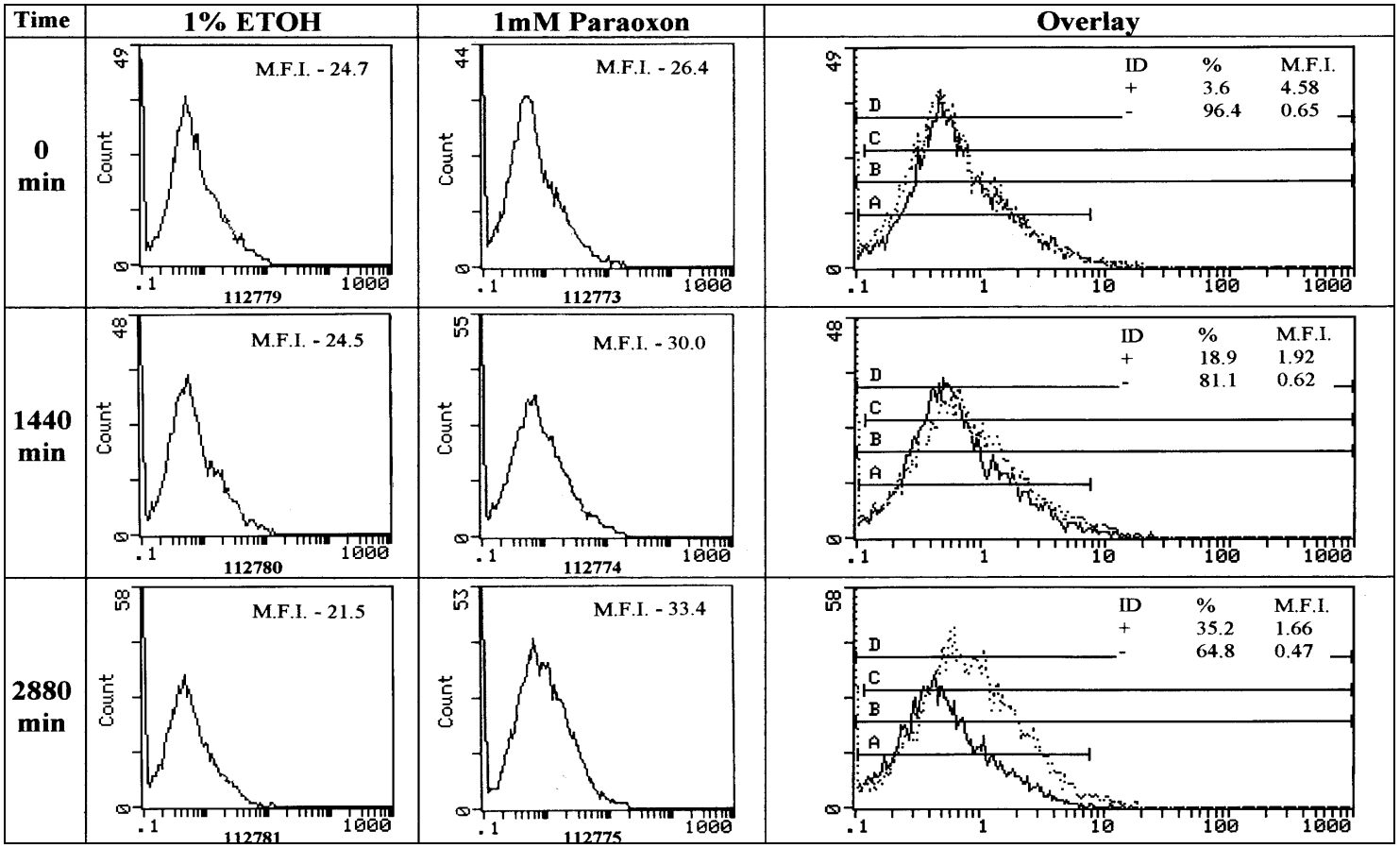

Time	1% ETOH	1mM Parathion	Overlay
0 min	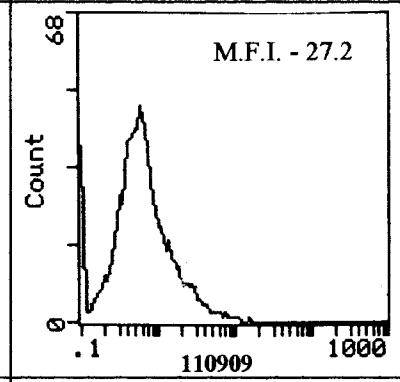	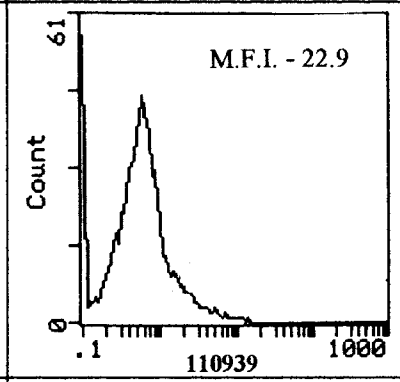	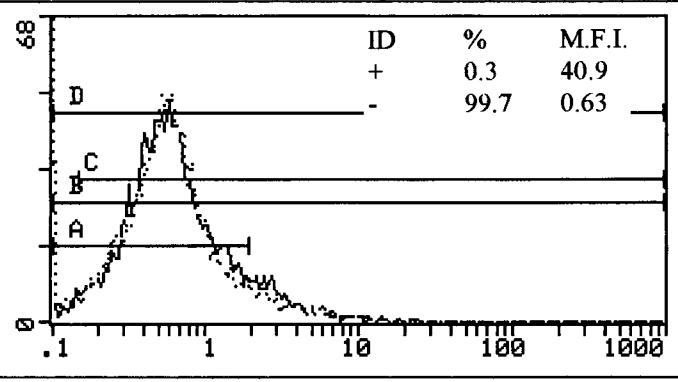
480 min	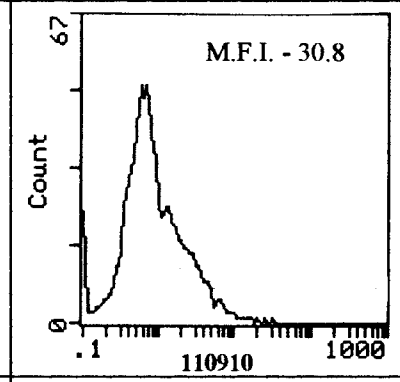	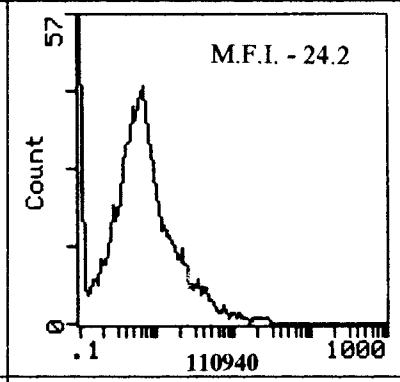	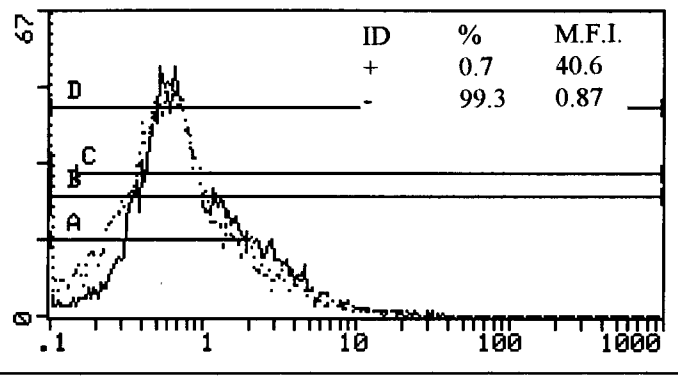
960 min	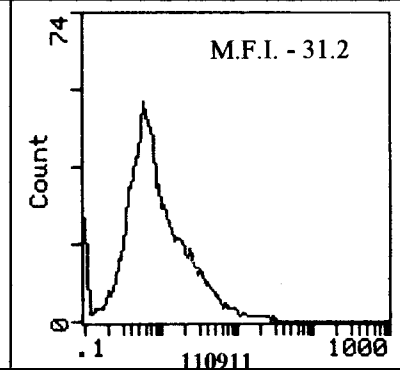	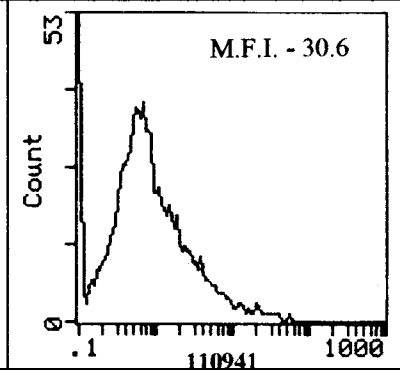	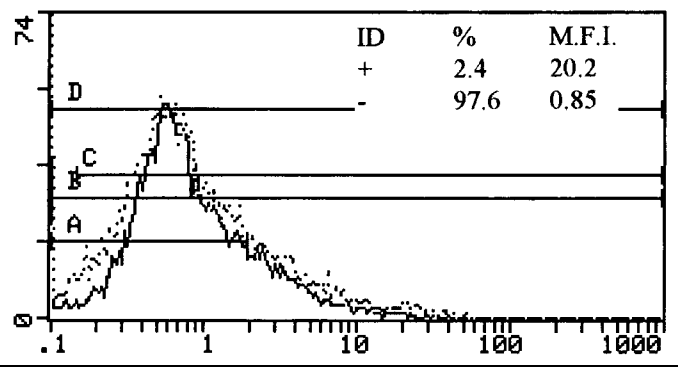

Time	1% ETOH	1mM Parathion	Overlay
1440 min	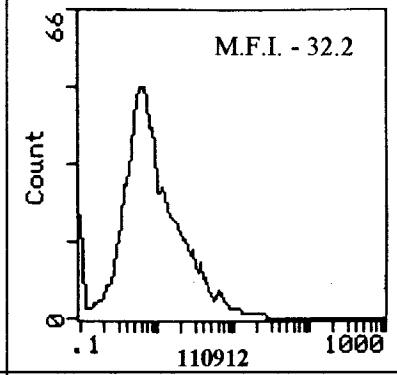	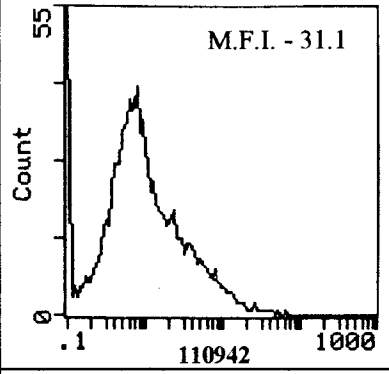	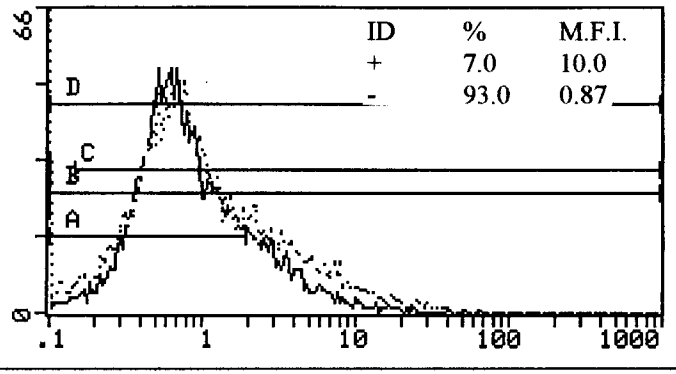
2880 min	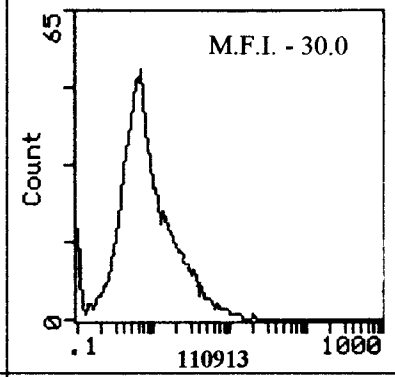	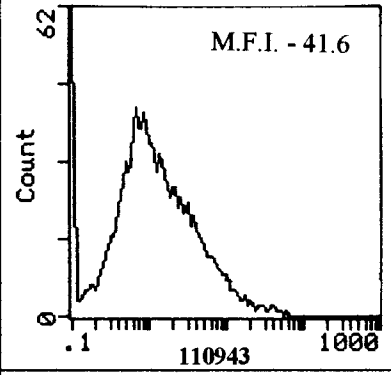	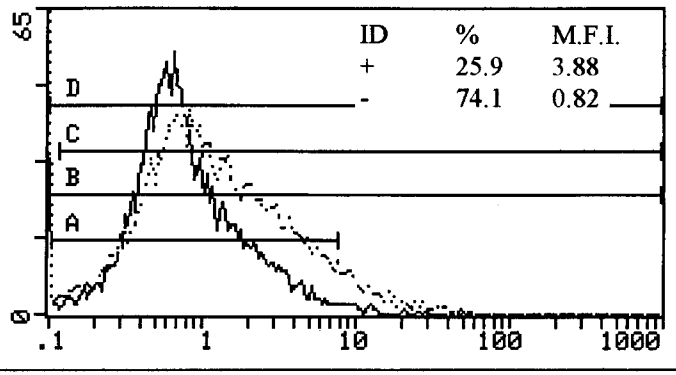
4320 min	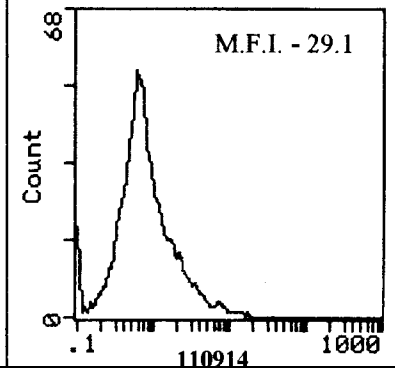	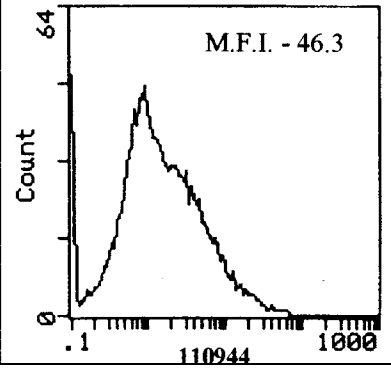	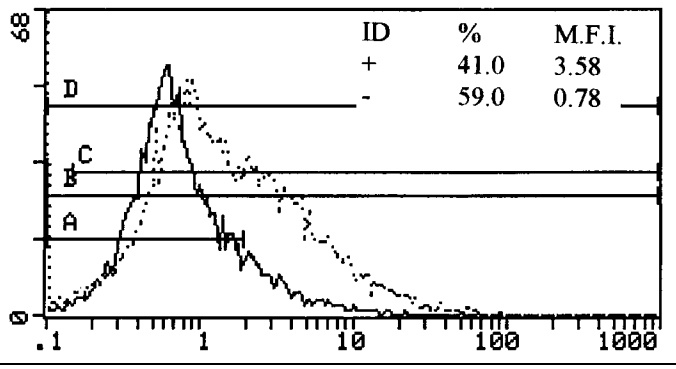

VITA

Kent Richard Carlson

The author, Kent Richard Carlson, was born on December 7th, 1964 in Cooperstown, New York. After a lengthy adolescence, he attended undergraduate school at Virginia Polytechnic Institute and State University. Five years later he graduated Sine Pecunia with a B.S. degree in Biology. In 1989 he continued studies in ecology and evolution at American University. The M.S. program in Biology was formally completed in 1994 after taking a few years off to become a biospeleologist and HIV research associate. He joined the doctoral program at the Virginia-Maryland Regional College of Veterinary Medicine in 1995. In 1998 he received a Society of Toxicology - Novartis Predoctoral Fellowship, which assisted his investigations into organophosphorus compound-induced neurotoxicology, the material of which this dissertation is made.